NASA Technical Memorandum 80076

NASA-TM-80076 19790013470

SAGE GROUND TRUTH PLAN - CORRELATIVE MEASUREMENTS FOR THE STRATOSPHERIC AEROSOL AND GAS EXPERIMENT (SAGE) ON THE AEM-B SATELLITE

EDITED BY P. B. RUSSELL

MARCH 1979

National Aeronautics and
Space Administration

Langley Research Center
Hampton, Virginia 23665

1 Report No	2 Government Accession No	3 Recipient's Catalog No
NASA TM-80076		

4 Title and Subtitle	5 Report Date / 6 Performing Organization Code
SAGE GROUND TRUTH PLAN - CORRELATIVE MEASUREMENTS FOR THE STRATOSPHERIC AEROSOL AND GAS EXPERIMENT (SAGE) ON THE AEM-B SATELLITE	5 Report Date: March 1979 6 Performing Organization Code:
7 Author(s) D. Bruton, D. M. Cunnold, G. W. Grams, J. Laver, M. P. McCormick, L. R. McMaster, D. G. Murcray, T. J. Pepin, T. W. Perry, W. G. Planet, and P. B. Russell	8 Performing Organization Report No
9 Performing Organization Name and Address NASA Langley Research Center Hampton, VA 23665	10 Work Unit No 659-12-10-02 11 Contract or Grant No
12 Sponsoring Agency Name and Address National Aeronautics and Space Administration Washington, DC 20546	13 Type of Report and Period Covered Technical Memorandum 14 Sponsoring Agency Code

15 Supplementary Notes P. B. Russell, Editor, SRI International, Menlo Park, CA; D. Bruton and T. W. Perry, Wallops Flight Center; D. M. Cunnold, MIT, Cambridge, MA; G. W. Grams, Georgia Tech., Atlanta, GA; J. Laver, NOAA, Washington, DC; M. P. McCormick and L. R. McMaster, Langley Research Center; D. G. Murcray, Denver Univ., Denver, CO;*

16 Abstract

This document describes the ground truth plan for correlative measurements to validate the Stratospheric Aerosol and Gas Experiment (SAGE) sensor data. SAGE will fly aboard the Applications Explorer Mission-B satellite scheduled for launch in early 1979 and measure stratospheric vertical profiles of aerosol, ozone, nitrogen dioxide, and molecular extinction between 79° N. and 79° S. latitude. The plan gives details of the location and times for the simultaneous satellite/correlative measurements for the nominal launch time, the rationale and choice of the correlative sensors, their characteristics and expected accuracies, and the conversion of their data to extinction profiles. In addition, an overview of the SAGE expected instrument performance and data inversion results are presented. Various atmospheric models representative of stratospheric aerosols and ozone are used in the SAGE and correlative sensor analyses.

*T. J. Pepin, Univ. of Wyoming, Laramie, WY; W. G. Planet, Nat. Environ. Satellite Service, Washington, DC.

17 Key Words (Suggested by Author(s))	18 Distribution Statement
Stratospheric Aerosol, Stratospheric Ozone, Satellite Measurements, Ground Truth, Stratospheric Nitrogen Dioxide	Unclassified - Unlimited Subject Category 45

19 Security Classif (of this report)	20 Security Classif (of this page)	21 No of Pages	22 Price*
Unclassified	Unclassified	166	$8.00

* For sale by the National Technical Information Service, Springfield, Virginia 22161

CONTRIBUTING AUTHORS

Dempsey Bruton
NASA Wallops Flight Center
Wallops Island, VA 23337

Derek M Cunnold*
Department of Meteorology
Massachusetts Institute of Technology
Cambridge, MA 01239

Gerald W Grams*
School of Geophysical Sciences
Georgia Institute of Technology
Atlanta, GA 30332

James Laver
NOAA National Meteorological Center
Washington, D C 20333

M Patrick McCormick*†
NASA Langley Research Center
Hampton, VA 23365

Leonard R McMaster
NASA Langley Research Center
Hampton, VA 23365

David G Murcray*
Department of Physics
Denver University
Denver, CO 80202

Theodore J Pepin*
Department of Physics and Astronomy
University of Wyoming
Laramie, WY 82070

Thomas W Perry
NASA Wallops Flight Center
Wallops Island, VA 23337

Walter G Planet*
National Environmental Satellite Service
Washington, D C 20233

Philip B Russell*
SRI International
Menlo Park, CA 94025

*Member, SAGE Experiment Team
†SAGE Sensor Scientist and Leader, SAGE Experiment Team

This Page Intentionally Left Blank

A FOREWORD ON LAUNCH AND EXPERIMENT DATES

When this Plan was written, the launch of SAGE was scheduled for January 25, 1979 However, because of weather and spacecraft difficulties, the launch was delayed until February 18, 1979 (1118 Eastern Standard Time) At that time the text of this Plan was already typeset, and therefore only minor changes have been made to the launch and correlative experiment dates stated in the body of this Plan

At this time (February 20, 1979) the following guidelines on experiment dates can be given Correlative Experiment 2, originally scheduled for February 12-16 at White Sands, is now planned for March 11-12, with April 5-6 as backup dates Correlative Experiment 1, originally scheduled for February 9 at Wallops Island, will also be rescheduled Although exact dates have not been set, Experiment 1 is now expected to occur after Experiment 2 (i e , after March 12)

The dates of Correlative Experiments 3-6 are also subject to change, but specific plans have not yet been made

This Page Intentionally Left Blank

ACKNOWLEDGMENTS

We are grateful to the following individuals who have contributed to the planning for SAGE correlative measurements Friedrich Geiss and Robert Fantechi of the Commission of the European Communities, for coordinating European efforts, Motokazu Hirono of Kyushu University, for coordinating Japanese efforts, Thomas Danaher of the Air Force Geophysics Laboratory, for coordinating efforts at Holloman Air Force Base, Roderick Quiroz, James Leinisch, and Frederick Finger of the National Oceanic and Atmospheric Administration, for advice on meteorological measurements, Edwin Harrison of NASA Langley Research Center, for calculations of SAGE measurement locations and times, James Rosen and David Hofmann of the University of Wyoming, David Woods of Langley Research Center, Ernest Hilsenrath of Goddard Space Flight Center, and Al Holland of Wallops Flight Center, for advice on aerosol and ozone measurements, Derek Miller of the British Meteorological Office and the SAGE Experiment Team, for both coordination and scientific guidance, Thomas Swissler of Systems and Applied Sciences Corporation, for advice on data handling, William Chu of Langley Research Center and Benjamin Herman of the University of Arizona, for advice on SAGE measurement uncertainties, James Pleasants of Langley Research Center, for information on the SAGE instrument, and John Livingston of SRI International, for scientific editing and report coordination

We are especially indebted to the late Dr Richard Craig of Florida State University for his insight on the behavior of stratospheric ozone and its implications for correlative measurement strategies His early efforts and counsel as a member of the SAGE Experiment Team are reflected in many aspects of this Plan

This Page Intentionally Left Blank

CONTENTS

ILLUSTRATIONS

This Page Intentionally Left Blank

TABLES

1. INTRODUCTION

1.1 SAGE Measurements and Ground Truth Requirements

The Stratospheric Aerosol and Gas Experiment (SAGE) is scheduled for launch in mid-February 1979 aboard the Applications Explorer Mission B (AEM-B) satellite of the National Aeronautics and Space Administration SAGE's mission is to map vertical profiles of ozone, aerosol, nitrogen dioxide, and Rayleigh molecular extinction around the globe The ozone data are expected to extend from about 10-45 km, the aerosol data from cloud tops to about 35 km (plus occasional strong layers in the mesosphere), the nitrogen dioxide data from about 25-40 km, and the Rayleigh molecular extinction data from about 15-40 km

The SAGE instrument is a four-channel photometer that measures the intensity of sunlight (centered at wavelengths 0 385, 0 45, 0 60 and 1 0 μm) traversing the earth's limb during spacecraft sunrise and sunset (See Appendix A for a description of the instrument) In this manner it will measure vertical profiles of four-wavelength extinction, at the rate of about 30 profiles per day Spatial coverage will extend from about 79° N to 79° S latitude (with some seasonal variation) and thus will complement the coverage (64° - 80° N and S) of the SAM-II stratospheric aerosol sensor on the Nimbus 7 satellite Figure 1 shows an example of latitude coverage versus time for a probable set of launch parameters

SAGE's four-channel extinction measurements will be numerically inverted to yield vertical profiles of ozone concentration, aerosol extinction (and inferred number density), nitrogen dioxide concentration, and total molecular density (When available, molecular density may be derived from the rawinsonde network and other sources, and then used as an input to the four-channel inversion process--if doing this improves the accuracy of the other derived parameters) The derived data will be archived and made available to the scientific community for use in a variety of studies However, before being released the data must be validated by comparisons with correlative measurements made by other sensors of appropriate accuracy, resolution, and reliability To avoid confusion and the compromising of SAGE data integrity, the accuracy and resolution of correlative sensors should be well understood, if possible, they should be equal to or better than those expected from SAGE

The anticipated performance of SAGE is indicated by Figure 2, which shows results of inversions using a typical SAGE inversion algorithm with simulated radiance data and simulated errors of the magnitude expected for a typical measurement cycle (Chu and McCormick, 1979) Although the accuracy and resolution achieved by SAGE are to a certain extent affected by latitude and by constituent concentrations, the models shown in Figure 2 give results that are representative of a broad range of conditions to be encountered by SAGE

Note that the vertical resolution of each inverted profile is about 1 km This resolution is achieved by virtue of two factors (1) the radiometer's narrow field of view, and (2) the sharply-peaked weighting functions for the limb-viewing geometry The limb weighting functions do in fact depend on constituent profiles, which can produce significantly poorer vertical resolution for certain conditions and heights Nevertheless, a vertical resolution of 1 km is a useful target specification for ground truth measurements

Note also the error bars in Figure 2 These bars were derived by performing the inversion for ten different cases of simulated random errors and taking the standard deviation of the resulting set of solutions (The simulated random errors are based on SAGE expected

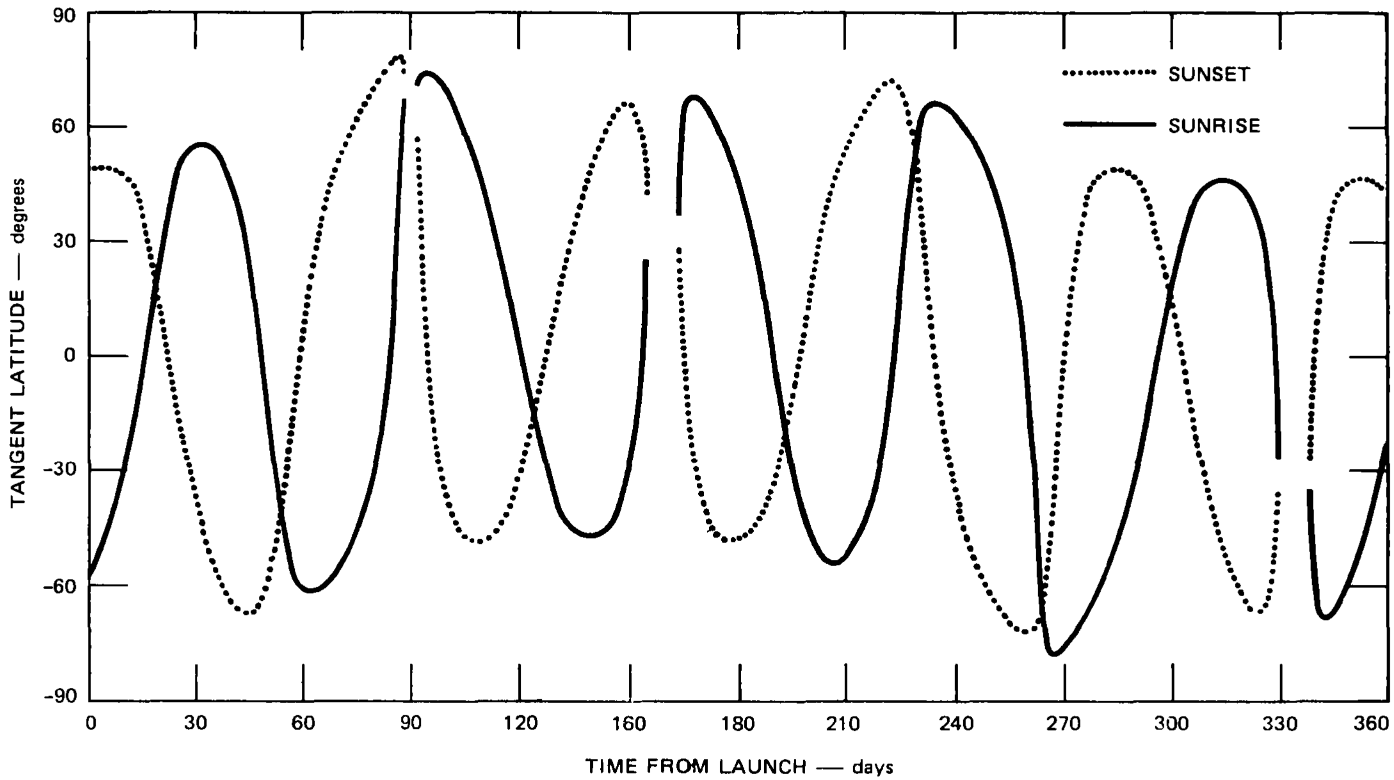

FIGURE 1 SAGE LATITUDE COVERAGE AS A FUNCTION OF MISSION TIME

Calculations assume an orbit inclination of 55°, a height of 600 km, and a launch time of 1030 EST, 25 January 1979

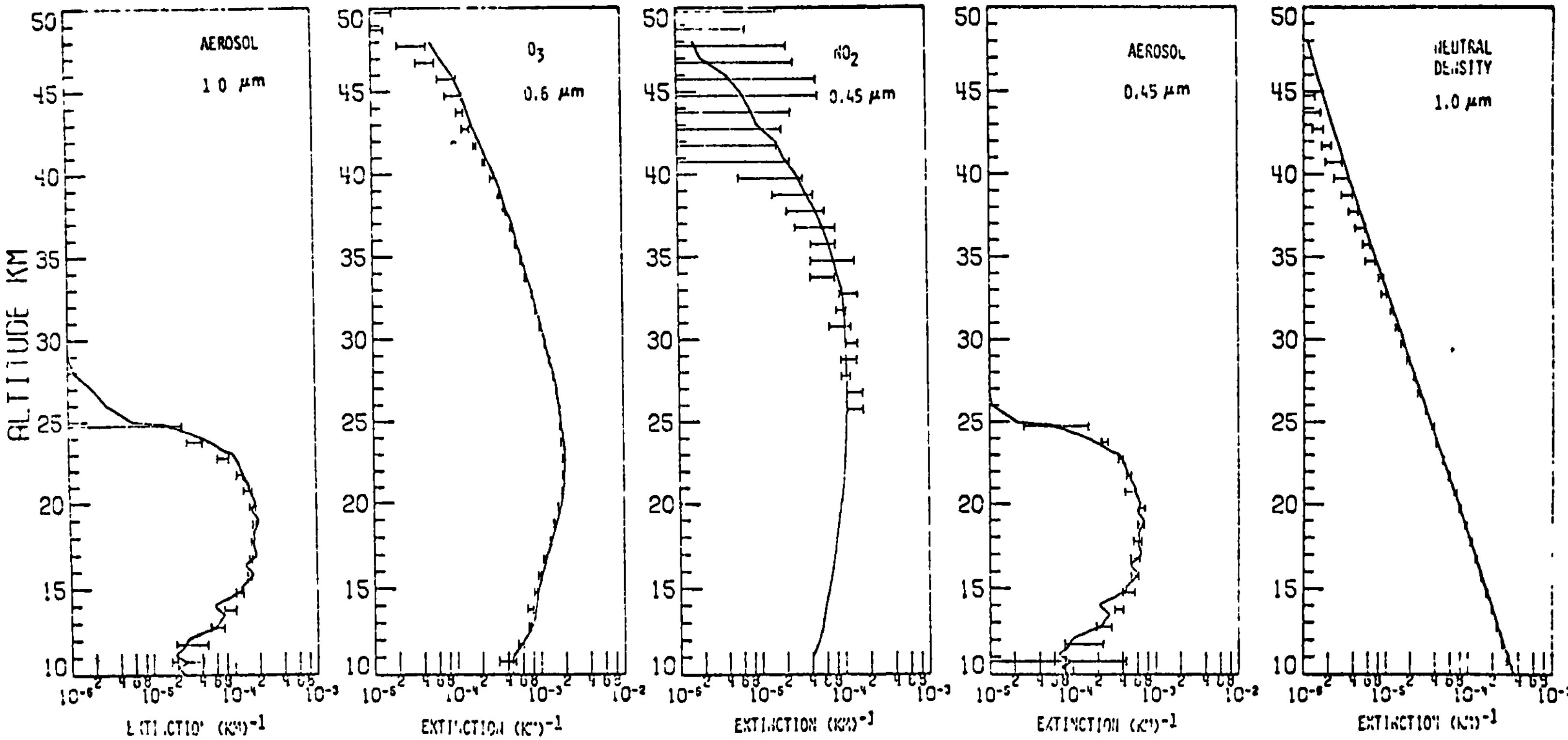

FIGURE 2 COMPARISON OF MODEL EXTINCTION PROFILES WITH RESULTS INVERTED FROM SIMULATED SAGE RADIANCE DATA

Error bars show ± one standard deviation about the mean of inverted solutions for independent simulations with different random errors All simulations assumed probable errors of 3 arc seconds for pointing, and 0 5% (of signal) for radiometric measurement All radiometric data were quantized to 10-bit A/D accuracy performance, see Appendix A) Hence, the error bars and the differences between model and inverted profiles denote the expected accuracy of SAGE-inferred constituent profiles and, therefore, the desired accuracy for correlative measurements These desired accuracies are summarized in Table 1

Table 1

DESIRED ACCURACIES OF CORRELATIVE MEASUREMENTS
(Based on SAGE Simulations)

Ozone	NO_2	Aerosol	Molecular Density
5%, 25—40 km 10%, 10—25 km 30%, 40—50 km	30%, 25—40 km factor 3, 40—50 km	10%, tropopause—25 km 30%, 25—35 km Plus noctilucent cloud occurrences	5%, tropopause—35 km 10%, 35—45 km

1.2 Overview of Ground Truth Plan

A SAGE ground truth program has been developed on the basis of the above prerequisites The program is designed to take advantage of established measurement capabilities and expertise at a number of worldwide locations At the same time it includes the development and use of sensors with needed measurement capabilities that cannot be provided by existing sensors

A schedule of SAGE ground truth experiments to be supported by U S organizations is shown in Table 2 The sites for these experiments were selected because they permit a number of sensors for the SAGE constituents to be operated simultaneously from a single location or a tight cluster of sites Table 3 gives more information on the clustered sites that were considered in developing the schedule of Table 2 Figure 3 shows the locations of the various clusters

The intent of the schedule in Table 2 is to provide

- A reasonably complete check of SAGE performance early in the mission (via the February-March 1979 experiments)
- A check of any possible differences in SAGE sunrise and sunset performance (via the White Sands-Hollman experiment)
- Ground truth support for a SAM-II/SAGE comparison (by means of the late spring or early summer 1979 Sondrestrom experiment)

Table 2

SAGE GROUND TRUTH EXPERIMENTS SUPPORTED BY U S ORGANIZATIONS
(To be supplemented by non-U S ground truth groups and others, as appropriate)

Experiment	1	2*	3	4†	5	6
Schedule (approximate)	April 1979	March 11 (sunset) March 12 (sunrise) 1979	April 1979	Spring or Summer 1979	Fall 1979	Winter 1979
Cluster	C1	C2	C4	C3	C1	C1
Sites	Wallops I Hampton	Boulder White Sands Holloman AFB	Fortaleza Natal	Sondrestrom or Poker Flat	Wallops I Hampton	Wallops I Hampton
Latitude Longitude	37 - 38 N 75 - 76 W	33 - 40 N 105 -107 W	3 - 5 S 35 - 38 W	65 - 68 N 51 or 148 W	37 - 38 N 75 - 76 W	37 - 38 N 75 - 76 W
P-3 Lidar	x	x	x	x	x	x
P-3 Spectrometer	x	x	x	x	x	x
Langley 48" Lidar	x				x	x
NCAR Lidar		x				
Dustsonde		x	x	x	x	x
O_3 Balloon	x	x	x	x	x	x
O_3 Rocket	K	K(2),H(2)	K	K	K	K
Datasonde	x	xxxx	x	x	x	x
Murcray Balloon Interferometer		x				
Pepin Balloon (photometer and spectrometer)		x		x		
LIP‡ Noxon Spectrometer		x				
Dobson/Canterbury	x	x	x	x	x	x
NCAR Sabreliner§				x		
Ames U-2**		x				

*Includes correlative measurements for both a sunrise and a sunset SAGE scan

†Combined SAM-II/SAGE correlative experiment

‡LIP (LIMS Instrument Package) is not formally a part of the SAGE Ground Truth Plan However, when LIP and SAGE measurements are sufficiently close in space and time, comparisons will be made A possible overlap may occur in Cold Lake, Alberta (55 N, 110 W) in February 1979

§Includes polar nephelometer, quartz crystal microbalance, Knollenberg optical particle counter, and possibly Dasibi O_3 sensor

**Includes Ames aerosol impactor, Ames O_3 and NO sensors, Langley quartz crystal microbalance (planned), and possibly a Lazrus multifilter sampler

K= Kruger optical rocket-borne O_3 sensor

H= Hilsenrath chemiluminescent rocket-borne O_3 sensor

NOTE Experiment dates are as scheduled on February 20, 1979 See also the *Foreword on Launch and Experiment Dates*

Table 3

PRIME CANDIDATES FOR CLUSTERED SAGE GROUND TRUTH OBSERVATIONS

Cluster Number	Instrument	Investigator	Agency or Institution	Location	Lat	Long	Parameter
1	Dobson (Umkehr)	Bruton, Perry	NASA WFC	Wallops I	38 N	75 W	O_3
1	Ozone Balloon	Perry, Bruton	NASA WFC	Wallops I	38 N	75 W	O_3, T,W
1	Ozone Rocket	Perry, Bruton	NASA WFC	Wallops I	38 N	75W	O_3
1	Datasonde	Perry, Bruton	NASA WFC	Wallops I	38 N	75 W	T,P,W
1	Airborne Lidar	Fuller, McCormick	NASA LaRC	Wallops I *	38 N*	75 W*	A
1	Ground Lidar	Fuller, McCormick	NASA LaRC	Hampton†	37 N†	76 W†	A
2	Dobson (Umkehr)			Albuquerque	35 N	107 W	O_3
2	Balloon Interferometer	Murcray	Denver U	Holloman AFB	33 N	106 W	O_3,NO_2
2	Balloon Photometer	Pepin	U Wyoming	Holloman AFB	33 N	106 W	A,O_3,NO_2,D
2	Dustsonde + O_3 Sensor	Rosen, Hofmann	U Wyoming	Holloman AFB	33 N	106 W	O_3,A,T
		Hofmann	U Wyoming	Holloman AFB	33 N	106 W	O_3,A,T
2	Balloon Spectrometer	Pepin	U Wyoming	Holloman AFB	33 N	106 W	O_3,A,T
2	Ground-Based Lidar	Fernald, Frush	NCAR	Boulder	40 N	105 W	A
2	Balloon	Noxon	NOAA-ERL	Boulder	40 N	105 W	NO_2
2	LIP Balloon	LIMS Team	(NCAR)	Palestine	32 N	96 W	O_3,NO_2, T
2	Airborne Lidar	Fuller, McCormick	NASA LaRC	Holloman AFB	33 N*	106 W*	A
2	Rocket Ozonesonde	Perry, Bruton	NASA WFC	White Sands	33 N	106 W	O_3
2	Datasonde	Perry, Bruton	NASA WFC	White Sands	33 N	106 W	T,P,W
2	Balloon Ozonesonde	Perry, Bruton	NASA WFC	White Sands	33 N	106 W	O_3
2	U-2 Quartz Microbalance	Woods, McCormick	NASA LaRC/ARC	White Sands	33 N*	106 W*	A
2	U-2 Impactor	Farlow	NASA Ames	White Sands	33 N*	106 W*	A
2	U-2 Multifilter Sampler	Lazrus	NCAR	White Sands	33 N	106 W	A
2	U-2 O_3 NO, T, Sensor	Starr	NASA Ames	White Sands	33 N	106 W	O_3
3	Dustsonde	Rosen, Hofmann	U Wyoming	Sondrestrom	67 N	51 W	A,T,O_3,?
3	Airborne Lidar	Fuller, McCormick	NASA LaRC	Sondrestrom*	67 N*	51 W*	A
3	Balloon Photometer	Pepin	U Wyoming	Sondrestrom	67 N	51 W	A,O_3,NO_2,D
3	Ozone Balloon	Perry, Bruton	NASA WFC	Sondrestrom	67 N	51 W	O_3,T
3	Datasonde	Perry, Bruton	NASA WFC	Sondrestrom	67 N	51 W	T,P,N
3	Ozone Rocket	Perry, Bruton	NASA WFC	Sondrestrom	67 N	51 W	O_3,T

Table 3 (Continued)

Cluster Number	Instrument	Investigator	Agency or Institution	Location	Lat	Long	Parameter
3	Polar Nephelometer§	Grams	Georgia Tech	Sondrestrom*	67 N*	51 W*	A
3	Optical Particle Counter§	Grams	Georgia Tech	Sondrestrom	67 N*	51 W*	A
3	Quartz Microbalance§	Woods, McCormick	NASA LaRC	Sondrestrom*	67 N*	51 W*	A
4	Ozone Balloon	Perry, Bruton	NASA WFC	Natal	5 S	35 W	O_3,T
4	Ozone Rocket	Perry, Bruton	NASA WFC	Natal	5 S	35 W	O_3,T
4	Datasonde	Perry, Bruton	NASA WFC	Natal	5 S	35 W	T,P,W
4	Airborne Lidar*	Fuller, McCormick	NASA LaRC	Natal*	5 S*	35 W*	A
4	Dustsonde + O_3 Sensor	Rosen, Hofmann	U Wyoming	Fortaleza	3 S	38 W	A,O_3,T
5	Dobson (Umkehr)	Dutsch		Arosa	47 N	10 E	O_3
5	Ozone Balloon	Atmanspacher		Hohenpeissen berg	48 N	11 E	O_3
5	Ground Lidar	Reiter	IAUFG	Garmisch-Partenkirchen	47 N	11 E	A
5	Ozone Balloon	Reiter	IAUFG	Garmisch-Partenkirchen	47 N	11 E	O_3
5	Mathews (Umkehr)	Reiter	IAUFG	Garmisch-Partenkirchen	47 N	11 E	O_3
5	Balloon Spectrometer	Laurent, Girard	ONERA	Aire sur l'Adour	44 N	0 W	O_3 NO_2 H_2O
5	Ground Lidar	Chanin	Service d'Aeronomie	St Michel	44N	6 E	O_3
6	Dobson (Umkehr)			Kagoshima	31 N	130 E	O_3
6	Ozone Balloon			Kagoshima	31 N	130 E	O_3
6	Aerosol Lidar	Hirono	Kyushu U	Fukuoka	34 N	131 E	A
7	Dobson (Umkehr)			Tateno	34 N	140 E	O_3
7	Ozone Balloon			Tateno	34 N	140 E	O_3
7	Aerosol Lidar	Iwasaka	Nagoya U	Nagoya	35 N	137 E	A
7	Aerosol Lidar	Igarashi	Radio Research Lab	Tokyo	36 N	140 E	A
7	Aerosol Lidar	Kamiyama	Tohoku U	Zao	38 N	141 E	A
8	Airborne Lidar	Fuller, McCormick	NASA LaRC	Palmer*	65 S*	64 W*	A
8	Quartz Microbalance	Woods, McCormick	NASA LaRC	Palmer*	65 S*	64 W*	A

Table 3 (Concluded)

Cluster Number	Instrument	Investigator	Agency or Institution	Location	Lat	Long	Parameter
8	Ozone Rocket						
8	Ozone Balloon						
8	Spectrometer	Murcray	Denver U	Palmer*	65 S*	64 W*	O_3,NO_2
8	Dustsondes	Rosen, Hofmann	U Wyoming	McMurdo	77 S	165 E	A, O_3
9	Ozone Balloon	Kulkarni	CSIRO	Aspendale	38 S	145 E	O_3
9	Dobson (Umehr)	Kulkarni	CSIRO				
9	Aerosol Lidar	Dilley	CSIRO	Aspendale	38 S	145 E	A
9	Dustsonde	Rosen, Hofmann	U Wyoming	Mildura	34 S	142 E	A,T
9	Chemiluminescent Balloonsonde	Galbally	CSIRO	Mildura	34 S	142 E	NO, NO_2 O_3
9	Infrared Spectrometer	Galbally	CSIRO	Mildura	34 S	142 E	NO, NO_2 O_3

*Air-mobile

†Ground-mobile

††5/78, 10/78, 12/78, 2/79 Scheduled for LIMS verification (Dates listed in order of priority)

§On NCAR Sabreliner

NOTE A = Aerosol, D = Density, NO_2 = Nitrogen dioxide, O_3 = Ozone, P = Pressure, T = Temperature, W = Winds

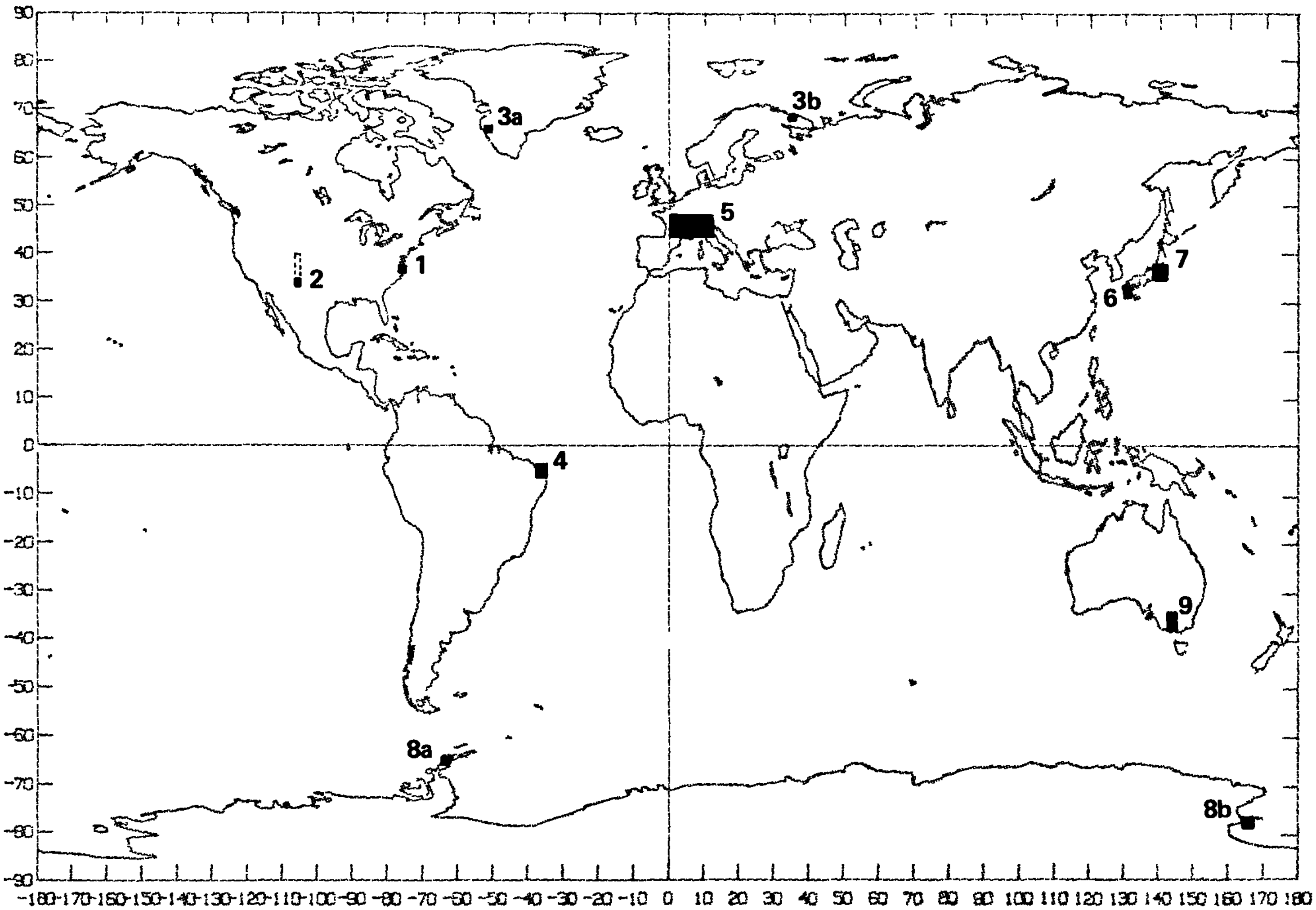

FIGURE 3 LOCATIONS OF SOME POSSIBLE SAGE GROUND TRUTH CLUSTERS

Sites 3a and 8a are also SAM II ground-truth sites (See, e g, Russell et al, 1978)

- Midlatitude, high-latitude, and low-latitude correlative measurements

- Continuing checks of SAGE performance in different seasons

Section 2 describes the sensors to be used in the United States-supported ground truth experiments Section 3 provides additional detail on scheduling and logistics, and Section 4 describes data-handling procedures

Besides the U S -sponsored activities, both Japanese and European ad hoc ground truth groups have been formed, and efforts are being made to coordinate with Australian and Russian measurement teams These ad hoc groups include many established teams with a wide range of expertise in stratospheric constituent measurements The teams and their capabilities are described in Section 2 1

2. GROUND TRUTH SENSORS AND PROGRAMS

2.1. SAGE Ad Hoc Ground Truth Groups

A Japanese and a European SAGE ad hoc ground truth group have been formed. The Japanese group is being coordinated by Professor Motokazu Hirono of Kyushu University in Fukuoka; the European group is being coordinated by Dr. Robert Fantechi of the Commission of European Communities in Brussels. Tables 4 and 5 show teams and sensors for each group. There is also the possibility of establishing an Australian ground truth group, centered around the capabilities of CSIRO described in Table B-1 of Appendix B, and possibly also a Soviet group under Professor K. Ya. Kondratyev of the Main Geophysical Observatory, Leningrad.

Each ad hoc group is now developing its own experiment schedule. The role of the SAGE Experiment Team (SET)[1] in coordinating these activities will be limited; specifically, the SET will provide mission analysis data (i.e., SAGE measurement times and locations), specify desired data formats (see Section 4.2), and disseminate U.S. ground truth experiment schedules. In addition to this coordination activity, however, the SET will participate fully in making use of Japanese, European, Australian, and Russian correlative data to validate the SAGE data.

2.2. Ozone Sensors

2.2.1. Dobson Spectrophotometer

A Dobson spectrophotometer[2] will be used to make ozone measurements at several ground truth sites (see Tables 2, 4, and 5). This instrument (Figure 4), by measuring selected ultraviolet wavelengths radiated by the sun, moon, or the zenith sky can be used to infer the quantity of ozone within the total air column above the instrument. The result is expressed as a thickness of a layer of pure ozone at standard temperature and pressure.

Normally a Dobson station performs observations three times a day--in the midmorning, near local noon, and in the midafternoon. At high-latitude stations fewer observations are called for during certain times of the year. This will also be the case during any of the planned in situ ozone soundings from the various participating sites. Because the accuracy of Dobson data deteriorates rapidly as the sun elevation angle decreases, twilight measurements are not practical.

Umkehr data (low-resolution vertical ozone profiles) will be obtained from certain Dobson sites. Efforts will be made to extrapolate data obtained at reasonable sun elevation angles to twilight points of tangency.

---

[1]SET members are Dr. M. P. McCormick (leader), NASA Langley Research Center; Dr. R. A. Craig, Florida State University (deceased); Dr. Derek M. Cunnold, Massachusetts Institute of Technology; Dr. Gerald W. Grams, Georgia Institute of Technology; Dr. Benjamin M. Herman, University of Arizona; Dr. D. E. Miller, British Meteorological Office; Dr. D. G. Murcray, University of Denver; Dr. T. J. Pepin, University of Wyoming; Dr. Walter G. Planet, National Environmental Satellite Service; and Dr. Philip B. Russell, SRI International.

[2]U.S. Department of Commerce, National Weather Service: *Observer's Manual Dobson Ozone Spectrophotometer*. Revised November 1, 1972.

Table 4

SAGE JAPANESE AD HOC GROUND TRUTH GROUP

A Lidar Observation

Team	Objective	Laser	Site
Department of Physics, Kyushu University (M Hirono)	Aerosol Scattering 10 - 40 km	Ruby, Nd YAG	Fukuoka* (33°37'N,130°26'E)
Water Research Institute, Nagoya University (Y Iwasaka)	Aerosol Scattering 10 - 40 km	Ruby, Nd YAG	Nagoya† (35°10'N,136°50'E)
Department of Geophysics, Tohoku University (H Kamiyama)	Aerosol Scattering 10 - 40 km	Ruby	Zeo‡ (38°8'N,140°32'E)

B Balloon and Spectrometer Observation (on Aircraft or Ground)

Team	Objective	Instrument	Site
Upper Atmosphere Division Meteorological Research Institute (M Misaki)	1 NO_2, NO, N_2O, HNO_3 $CFCl_3$, CF_2Cl_2, CCl_4	1 Interference Spectrometer on Aircraft	Tateno (36°3'N,140°8'E)
	2 Aitken Particles, HCl, CH_4	2 Balloon Sampling	
Atmospheric Research Institute Nagoya University (H Ishikawa)	1 Aerosol Profile	1 Balloon Solar Occultation, Balloon Optical Particle Counter	Sanriku (39°8'N,141°49'E)
	2 Ozone Profile	2 Balloon Solar Occultation	
Aerological Division Department of Observation Japanese Meteorological Agency (K Nyui)	1 Ozone Profile	1 Ozone Balloon	1 Kagoshima (31°38'N,130°36'E) Tateno (36°3'N,140°8'E)
	2 Ozone Column Content	2 Dobson Spectrophotometer	2 Tateno (36°3'N,140°8'E)
Niigato University	NO_2	Ground-Based Spectrometer	Niigata (37°55'N,139°2'E)

*Ruby observations made since October 1974, Nd-YAG observations expected to start in February 1979

†Observations suspended at present, to be restored in 1979

‡Observations suspended at present, probably to be restored in 1979

Table 5

SAGE EUROPEAN AD HOC GROUND TRUTH GROUP

Team	Objective	Instrument	Site
ETH-Zurich (H Dutsch)	1 O_3 profiles, 0-35 km	1 O_3 sondes*	1 Hohenpeissenberg (47°48'N,11°00'E) Payerne (46°49'N,6°57'E) Brussels (50°50'N,4°21'E) Elnas, Cagliari (39°13'N,9°08'E)
	2 O_3 profiles (higher but coarser)	2 Dobson-Umkehr	2 Arosa (46°47'N, 9°41'E)
	3 Total O_3	3 Dobson	3 Arosa (46°47'N, 9°41'E)
Service d'Aèronomie, CNRS (M L Chanin, J Blamont, G Megie, P Aimedieu)	1 O_3,H_2O profiles 0-40 km, noctilucent clouds	1 Dye lidars	1 St Michel (44°N, 6° E) Verrières-le-Buisson (48°45'N,21°7'E) Heyss Island (80°5'N, E)
	2 O_3, neutral density, aerosol profiles 15-20 km (night) 15-28 km (day)	2 Long-life (~9 mos) variable-height balloon with chemiluminescent O_3 sensor, T,P sensors, plus U Wyo dustsonde or LRC aerosol sampler (possibly)	2 Launch Praetoria (25°45'N,28°12'E) or Christchurch (43°33'S,172°40'E) drifts over wide area
	3 O_3,OH profiles	3 Rocket (Franco-Russian Program)	3 Russia, India
	4 O_3 profiles, 0-48 km	4 Chemiluminescent balloonsonde	4 Aire sur l'Adour (43°42'N,0°15'W) and others
Inst d'Aèronomie Spatiale Brussels (P Simon)	1 O_3 profiles 25-60 km	1 Dropsonde solar integrating radiometer (Balloon [25-40 km] or rocket [>40 km] launch)	1 UK Met Office rocket Possible rocket South Uist (57°N, 7°W)
ONERA (J Laurent, A Girard)	1 O_3,NO_2,H_2O,HNO_3,CFM profiles	1 Solar IR grating spectrometer (balloon-borne)	1 Aire sur l'Adour (43°42'N, 0°15'W) Palestine (32°N,96°W)
Inst Atmos Environ Res, Garmisch-Partenkirchen (H Jaeger, W Carnuth, R Reiter)	1 Aerosol profiles 5-35 km	1 Ruby lidar, Conductivity sonde	1 Garmisch-Partenkirchen (47°30'N,11°05'E)
	2 Total O_3 and profiles	2 Matthews radiometer, O_3 sondes	2 Garmisch-Partenkirchen (47°30'N,11°05'E)

Table 5 (Concluded)

Team	Objective	Instrument	Site
AERE Harwell (A Eggleton)	1 O_3 horizontal variations near 17 5 km max 2 O_3 profiles 5-17 5 km	1 Dasibi UV absorption sensor on Concorde aircraft 2 As above	1 London-Washington DC (51°30'N, 0°10'W-38°55'N,77°00'W) 2 Points of ascent and descent
CEC, Joint Research Center, Ispra (F Geiss)	1 Aerosol profiles	1 Ruby lidar	1 Ispra (45°48'N, 8°36'E)
Meteorological Office, UK (D Miller, J Gibbs, L Simmons, John Harries, NPL)	1 O_3, H_2O profiles 2 NO_2, HNO_3 profiles 3 Aerosol profiles 10-30 km 4 O_3 5 O_3 profiles 6 Neutral density	1 IR emission sonde (J Harries, NPL) 2 SIBEX balloon package (J Harries, NPL) 3 Dye lidar 605 nm, possibly 750 nm 4 Dobson spectrophotometer 5 Dropsonde solar radiometer (P Simon, IAS, Brussels) (UK Met Office rocket launch, see IAS, above) 6 Mark III rawinsonde, Stratospheric Sounder on Tiros N for gridded analysis (with Finger, NOAA)	1 Bracknell (51°26'N, 0°46'W) or USA 2 USA Sicily 3 Bracknell (51°26'N, 0°46'W) 4 Bracknell (51°26'N, 0°46'W) Seychelles (4°36'S,55°30'W) St Helena (16°0'S,5°42'W) Lerwick, Scotland (60°09'N, 1°09'W) 5 South Uist (57°N,7'W) 6 Bracknell (51°26'N,0°46'W)
Appleton Lab, SRC, Slough (L Thomas, T Gibson)	1 Aerosol profiles 5-35 km plus noctilucent clouds	1 Dye lidar	1 Winkfield (51°27'N, 0°43'W)
Univ Koeln, FRG (A Ghazi, H Paetzold)	1 O_3H_2O profiles 2 Total O_3	1 Optical balloonsonde 2 Dobson spectrophotometer	1 Koeln 850°56'N, 6°56'E) 2 Koeln 850°56'N, 6°56'E)

*Comparison of 5 different sondes at Hohenpeissenberg scheduled for April 1978 Dobson spectrophotometers will also be compared

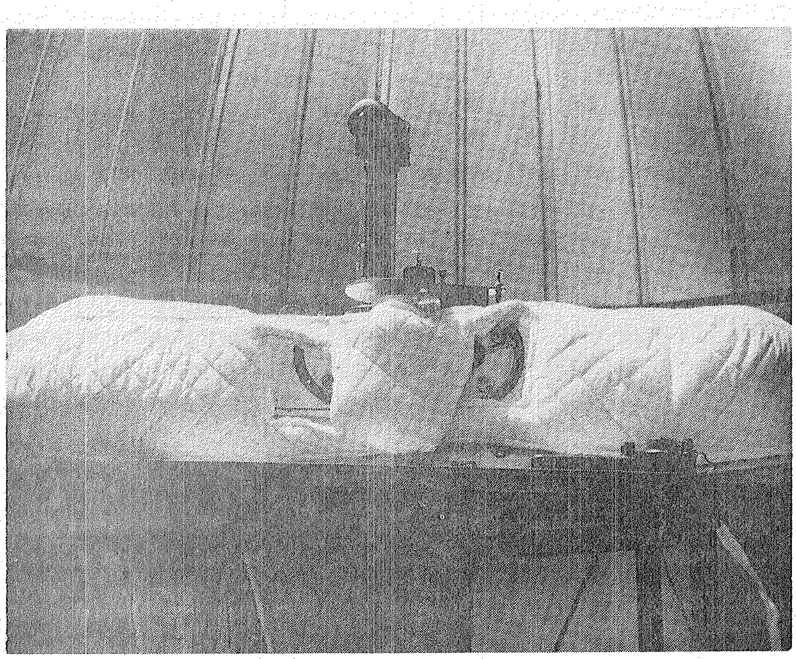

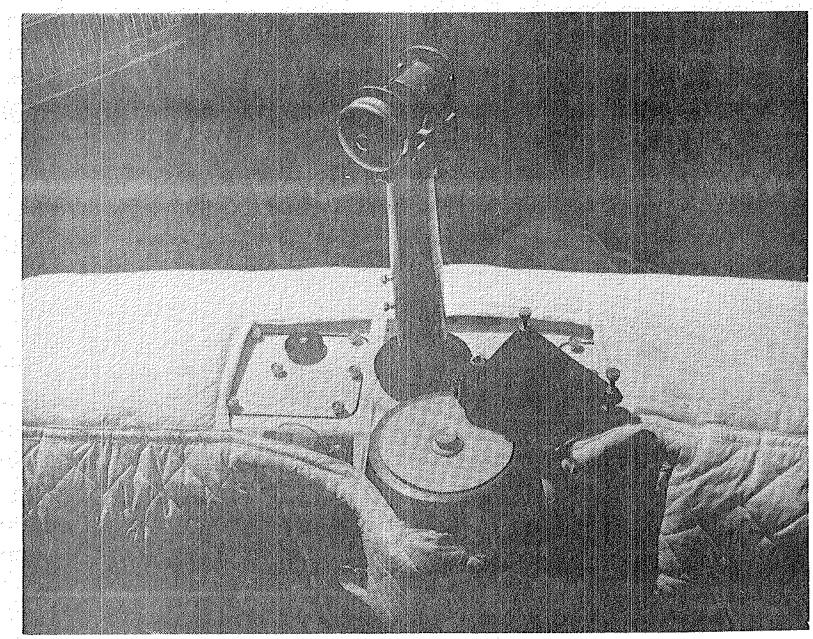

FIGURE 4 DOBSON SPECTROPHOTOMETER

2.2.2. Canterbury Photometer

The University of Canterbury (New Zealand) narrow-bandpass filter spectrometer, as the name implies, uses six narrow-bandpass interference filters to isolate wavelengths of interest These filters are sequentially rotated in front of the entrance aperture, thus allowing the photomultiplier tube detector to measure intensities at each wavelength twice a second All six wavelengths are in the ultraviolet region of the spectrum and were chosen to match the standard Dobson A, C and D wavelength pairs The radiation source can be the sun or the zenith sky The instrument design allows allowing the field of view to be changed from 2 3°, for use with the sun, to 4 6° for use with the zenith sky

The Canterbury photometer, an extremely portable instrument, is being considered for acceptance as a standard method to measure total ozone concentrations A comparison of the Wallops Flight Center Dobson and Canterbury instruments has been in progress since October 1977 The results thus far indicate that differences related to air mass and ambient temperature changes are not negligible, but that empirical corrections can potentially reduce the discrepancies to ± 2% of the Dobson values Note An extensive ozone photometer intercomparison, involving the Dobson, Canterbury, Russian M-83, and the Canadian Brewer instruments, is being conducted An early effort to secure correlative support for SAGE from all these will be made

2.2.3. Balloonborne ECC Ozonesonde

The Electrochemical Concentration Cell (ECC) balloon-borne ozonesonde is a light-weight, compact, and relatively inexpensive instrument developed for measuring the vertical distribution of atmospheric ozone [3] An interior view of the sonde is shown in Figure 5 [4] It is electronically coupled to a standard NOAA Radiosonde (Section 2 5) and thus also provides atmospheric pressure, temperature, and humidity in addition to ozone measurements The ECC ozonesonde is suspended approximately 22 meters below a 1200-gram balloon with the radiosonde suspended about one meter below the ozonesonde Figures 6 and 7 depict the flight configuration This combination, using the transmitter of the radiosonde, transmits data to the ground-based AN/GMD system

The precision of the ECC ozonesonde is currently estimated to be within 10 to 12% (1σ)

2.2.4. Super Loki Optical Ozonesonde

The Super Loki Optical Ozonesonde[5] is a rocket-launched payload, ejected at rocket apogee, that provides ozone profiles between 70 and 15 kilometers The ozone measurements are made during descent of the sensor, which is attached to a parachute The sensor provides an absolute measurement based on known values of the ozone absorption coefficients during daylight hours only Figure 8 shows the payload in the launch configuration with the standard Super Loki rocket used for the normal meteorological sounding systems The telemetry system operates on 1680 MHz, transmitting the data to a standard AN/GMD system equipped with a PCM adapter kit

---

[3] Vehicles and Sensors of the UPN 607 Applications Sounding Rocket Program, October 1977, Preliminary

[4] Instruction Manual, Electrochemical Concentration Cell Ozonesonde Model ECC-3A, January 1 1977

[5] Vehicles and Sensors of the UPN 607 Applications Sounding Rocket Program October 1977 Preliminary Instruction Manual Electrochemical Concentration Cell Ozonesonde Cell Ozonesonde Model ECC-3a January 1 1977

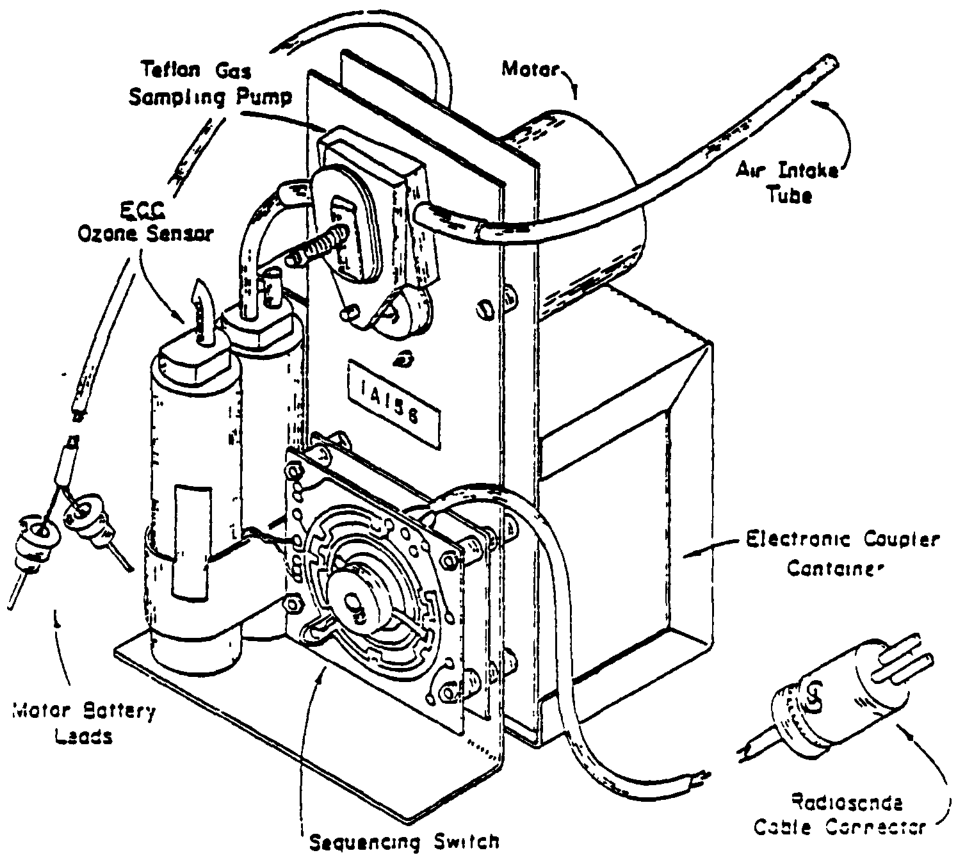

FIGURE 5 ECC OZONESONDE

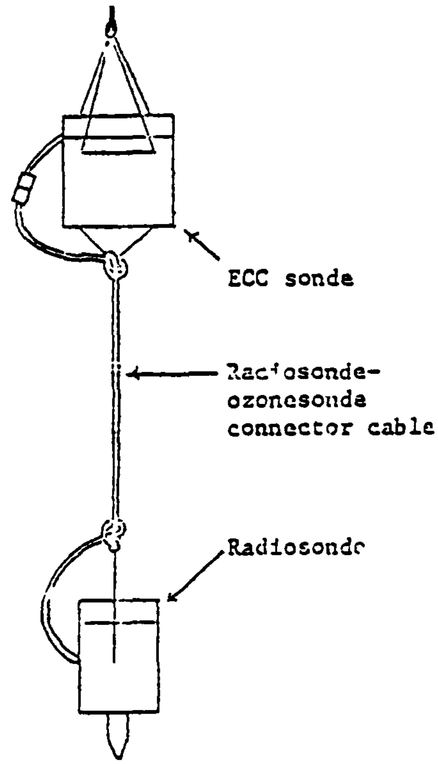

FIGURE 6 ECC OZONESONDE HOOK-UP TO RADIOSONDE

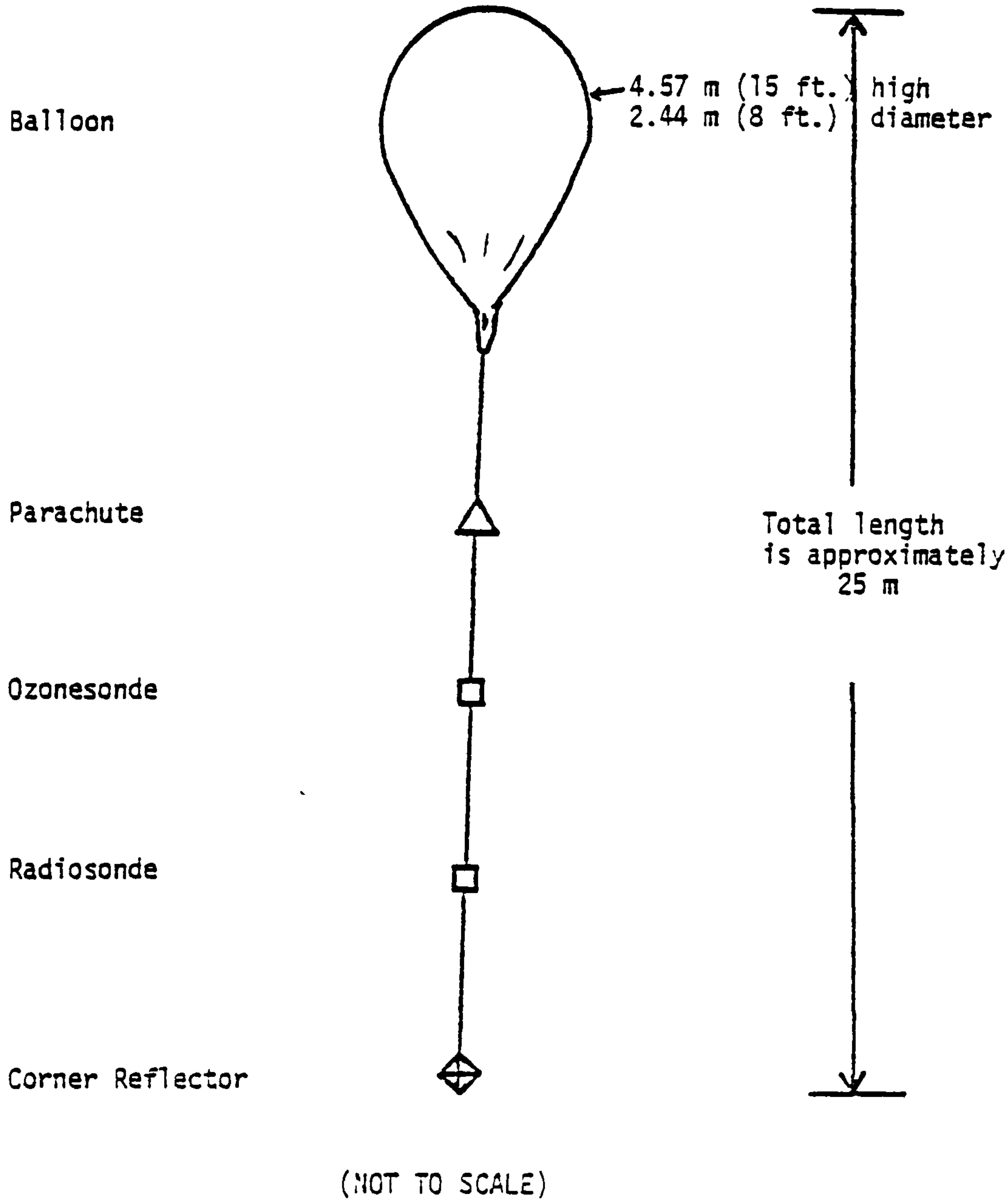

FIGURE 7 OZONESONDE BALLOON AND TRAIN

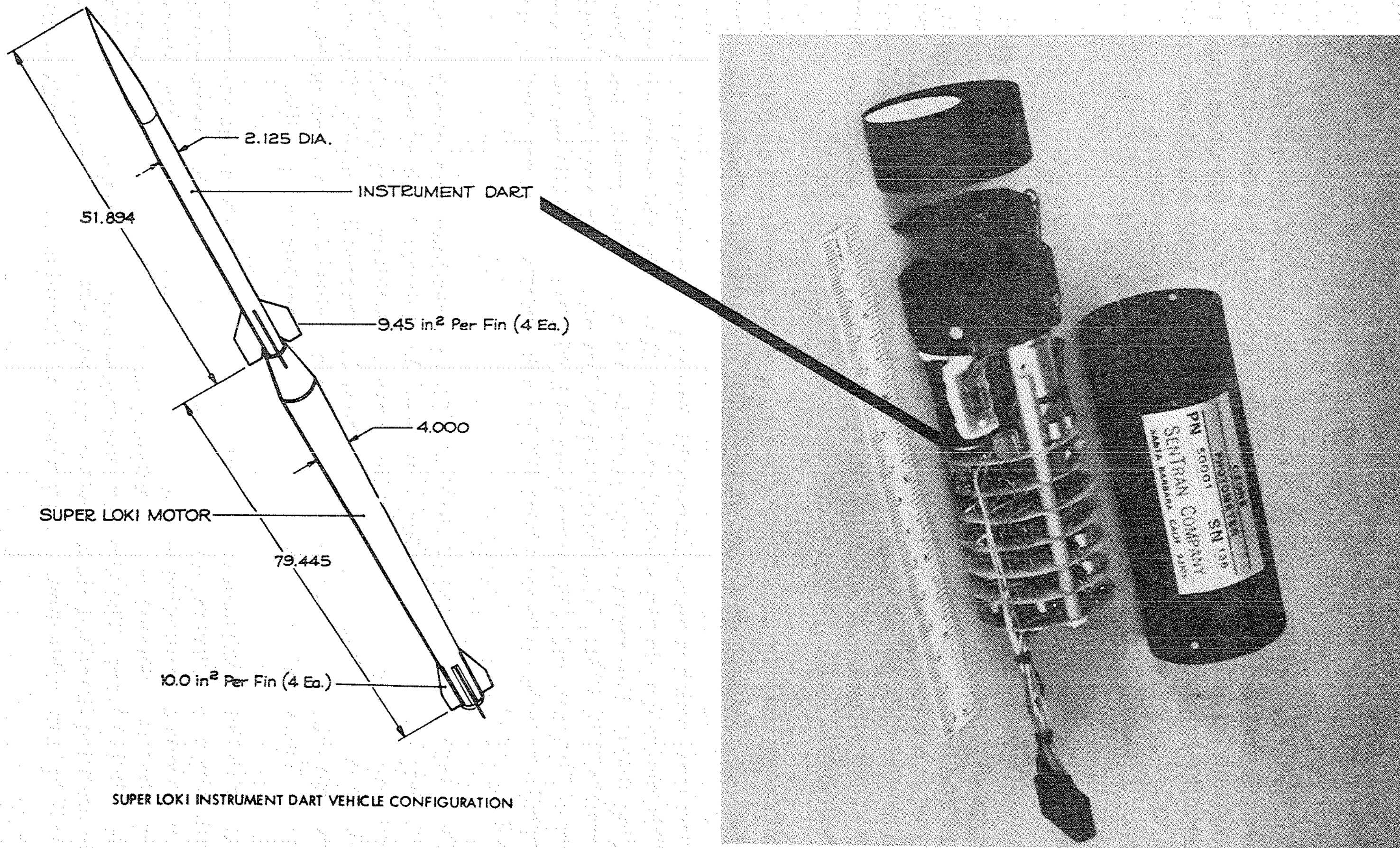

SUPER LOKI INSTRUMENT DART VEHICLE CONFIGURATION

FIGURE 8 SUPER LOKI OPTICAL OZONE ROCKET/PAYLOAD

The sensor of the Super Loki Optical Ozonesonde is a four-channel filter-wheel UV photometer A planar diffuser plate, located at the optical entrance of the sensor, intercepts incoming sunlight, while the varying solar angle of incidence is compensated for electronically The UV filters consist of interference filter elements to define the spectral bands and a common broadband UV filter that blocks unwanted radiation in the visible spectrum

The precision of the optical ozonesonde is estimated at 5% or better between 25 and 50 km This estimate is based on the properties of signal-to-noise ratios of the raw data for the ozone algorithm [6] The system accuracy is dependent on two factors (1) the error of the ozone absorption coefficient, and (2) the changes in the UV filter characteristics after calibration The accuracy is believed to be better than 10% The system can provide good data for solar zenith angles of about 80° or less, for angles exceeding 84°, the data become unusable

2.2.5. Super Arcas Chemiluminescent Ozonesonde

The Super Arcas chemiluminescent ozonesonde is a rocket-launched payload ejected at apogee, that measures the ozone distribution between 70 and 15 km as the sonde descends through the atmosphere on a parachute The ambient air is sampled by self-pumping, that is, a ballast tank, connected to the atmosphere by means of an inlet pipe, remains in pressure equilibrium with the increasing external pressure as the sonde descends The chemiluminescent detector and a photometer are oriented along the axis of the inlet pipe and enable continuous measurement of the ozone

The chemiluminescent detector is an improved version of the one carried on balloon ozonesondes several years ago Its luminescence is proportional to ozone flux, which is the ozone concentration times the flow rate It can be shown that the flow rate is proportional to the pressure rise in the ballast tank, which is measured in flight Before flight a calibration is performed for each sonde This calibration simulates actual pressures, flow rates, and ozone concentrations expected during flight The measurement principle and early flight results have been described by Hilsenrath (1969, 1971) The present system flies on a Super Arcas meteorological rocket, as shown in Figure 9, and utilizes the standard 1680-MHz AN/GMD telemetry system The sensor signals are pulse-code-modulated (PCM) and, therefore, require decommutation for data processing

An error analysis indicates precision of about 8% This is calculated from expected random errors due to "noise" and systematic errors or flight-to-flight errors Most of this error is related to the uncertainty entailed in establishing the sensor's sensitivity from the calibration procedures Two flights conducted 13 minutes apart showed a repeatability of 6% This was derived from the average difference separating the two ozone profiles from a mean profile at one-kilometer intervals This result compares favorably with the computed 8% precision

The absolute error in the experiment depends on the uncertainty of the ozone concentration in the sonde calibration, undetected ozone losses, and nonlinearities in the measurement The uncertainty of the ozone concentration depends on the ozone monitor used in the calibration This ozone monitor is calibrated at the National Bureau of Standards by measuring absorption at wavelength 253 7 nm The absolute measurement error is computed to be 12% (independent of the precision described above), which includes a 4% error associated with the ozone monitor used in the calibration Comparison of chemiluminescent rocketsonde

[6] Design of Optical Ozonesonde for the Super Loki Dart Rocket Draft Report NASA Goddard Space Flight Center Greenbelt Maryland

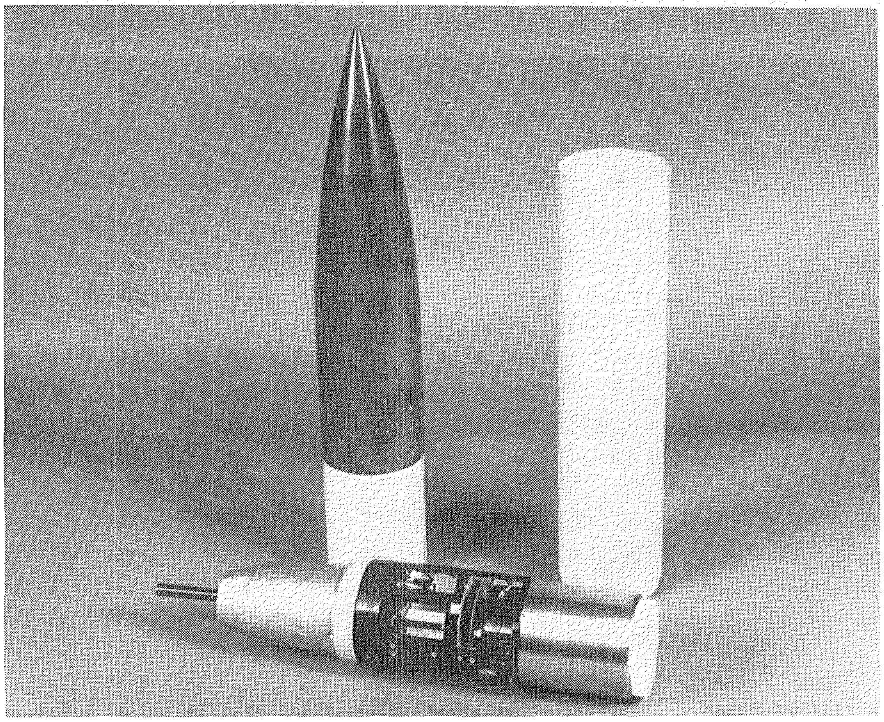

FIGURE 9 SUPER ARCAS CHEMILUMINESCENT OZONESONDE

measurements with balloon-borne and optical rocketsonde measurements shows differences no greater than 20%, usually on the order of 10%. Altitude resolution between 60 and 20 km is finer than 1/2 km. A comparison of the chemiluminescent and optical sondes with a sounding from LRIR on the Nimbus 6 satellite is shown in Figure 10.

2.2.6. Ozone Lidar

Recent work on the differential absorption lidar (DIAL) technique has led to the development of ozone lidar systems (e.g., Megie, et al., 1977). This technique uses a tunable laser to vary the output wavelength of the lidar so that it coincides with the wavelength of an ozone absorption line. The absorption of the laser radiation by ozone molecules thereby provides a method for determining the vertical profile of ozone molecules. Lidar echoes are recorded as a function of range for a wavelength corresponding to the center of an ozone absorption line, as well as for a nearby wavelength that is not absorbed by ozone or other atmospheric molecules. The system described by Megie et al. obtained ozone profiles from the 18- to 28-km altitude interval with approximately 1.2-km altitude resolution--using ultraviolet wavelengths of 308 nm and 303.7 nm generated by a frequency-doubled rhodamine-6G dye laser.

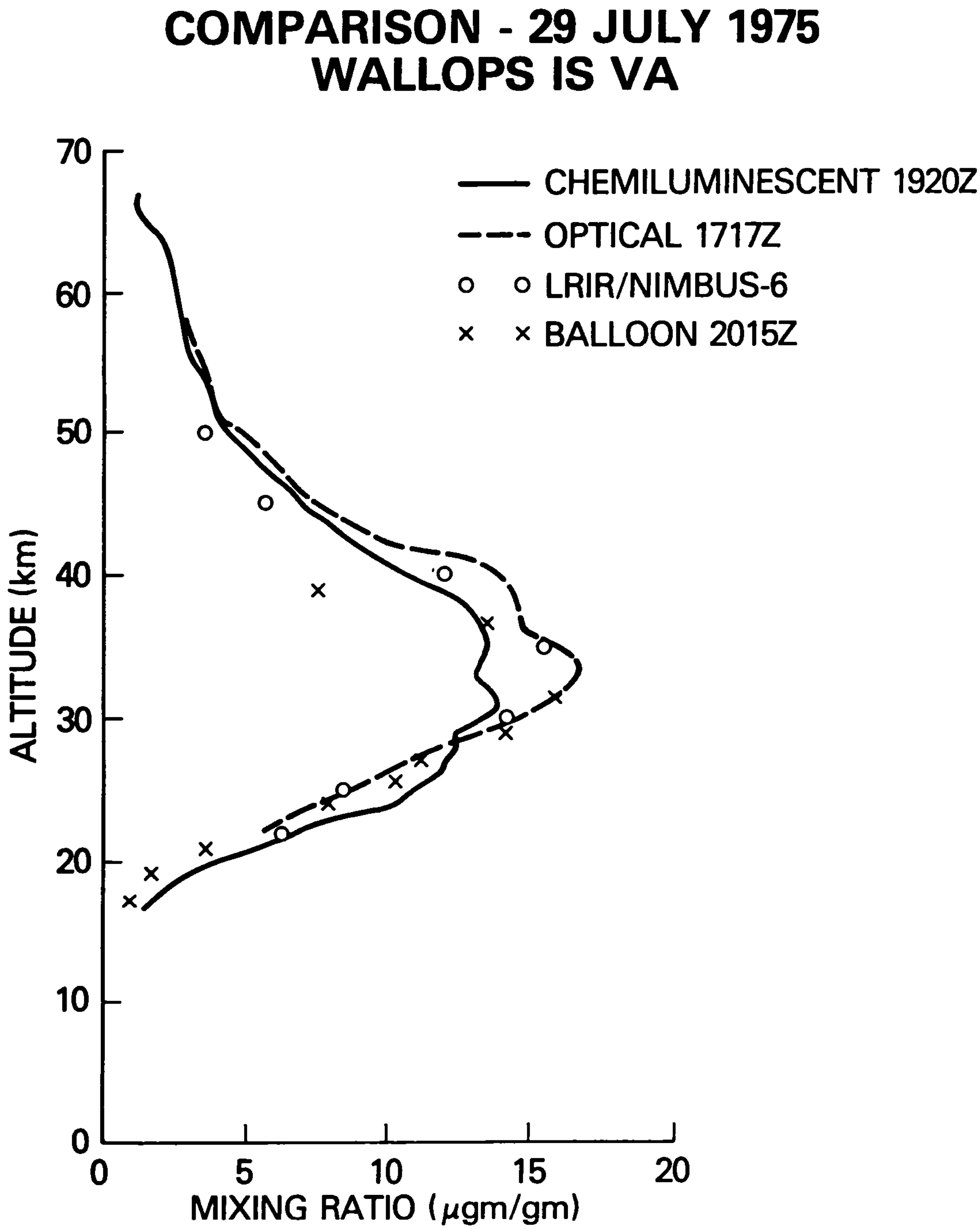

FIGURE 10 COMPARISON OF OZONE MEASUREMENTS MADE BY CHEMILUMINESCENT ROCKETSONDE, OPTICAL ROCKETSONDE, LRIR SATELLITE SENSOR, AND ECC BALLOONSONDE

2.2.7. PAM II

The PAM II (Preliminary Aerosol Experiment) experiment constructed by Dr Pepin is planned for launch on the Air Force P78-1 satellite on February 19, 1979 PAM II is a solar photometer that operates like the SAGE and SAM II experiments in that it measures solar extinction at spacecraft sunrise and sunset events However, instead of scanning the solar disk, the PAM II instrument points to the radiometric center of the disk and measures the total signal from the full disk--in a manner simlar to the measurement that was made using SAM on the ASTP flight (Pepin 1977)

PAM II has three optical channels at wavelengths of 0 43, 0 60 , and 1 0 μm Its mission is to map vertical profiles of aerosols and ozone by scanning the atmosphere during spacecraft sunrise and sunset events Because P78-1 will fly in a polar, sun-synchronous high-noon orbit, the latitude bands covered by the PAM II experiment will be restricted to 63 to 82 ° N and S latitude

Because SAGE's latitude coverage is expected to extend from the equator to 79° N and S, the coverage of the PAM II and SAGE sensors will overlap partially At the times overlap occurs there will be opportunities to compare measurements made by the two independent remote-sounding systems The PAM II ozone measurements will be available for extending the study of the SAGE vertical ozone profiles to higher latitudes

2.2.8. Other Ozone Sensors

A variety of sensors is available for in situ ozone observations on aircraft platforms It is likely that most measurements of this type will be made with the Dasibi ultraviolet absorption instrument, which monitors ozone on a continuous basis by means of a long-pass UV absorption cell The light source in this system is a 253 7-nm Hg lamp To obtain corrections for lamp or electronic drift, the instrument continuously compares the signal from the sample cell with that of an identical reference chamber The gas stream flowing through the reference cell is first scrubbed of all ozone The difference between the signal from the sample chamber and its counterpart from the reference cell then constitutes a measure of the absolute ozone concentration

2.3. Aerosol Sensors

2.3.1. Dustsonde

Figure 11 shows a schematic drawing of the University of Wyoming balloon-borne dustsonde that is planned for ground truth in the SAGE program Its mode of operation is as follows Air sampled during balloon ascent and parachute descent is pumped at approximately 0 75 l/min in a well-defined stream through the focal point of the condenser lens in the 2 5-liter scattering chamber, where the individual stratospheric aerosol particles scatter light into the microscopes The light pulses that can be observed with the microscope are detected and amplified by the photomultipliers By means of pulse height discrimination and careful laboratory calibration with aerosols of known size and index of refraction, the integral concentration of aerosol particles with radii greater than 0 15 and 0 25 μm can be determined We will refer to these integral concentrations as N_{15} and N_{25}, respectively

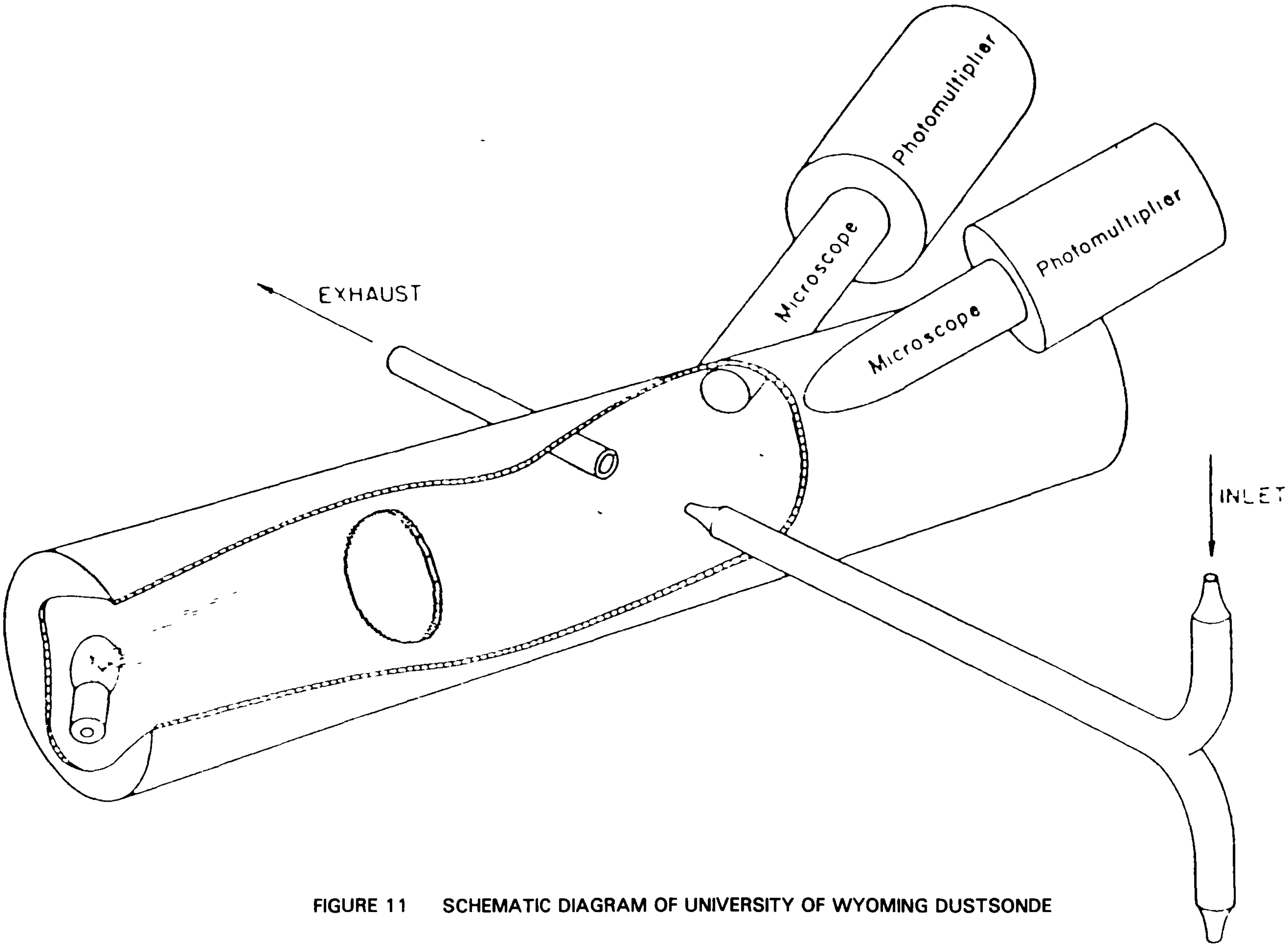

FIGURE 11 SCHEMATIC DIAGRAM OF UNIVERSITY OF WYOMING DUSTSONDE

Two photomultipliers are used to enhance the signal-to-noise ratio by counting only coincident events from the two detectors The background noise for the system is mainly due to Rayleigh scattering from air molecules in the chamber at low altitude and from cosmic ray scintillation in the photomultiplier glass at high altitude The requirement for coincidence of events from the two detectors removes the contribution due to the cosmic ray scintillation The background is measured approximately every fifteen minutes during the flight by having filtered air pass through the chamber The background produced by the Rayleigh scattering is negligible above a 10-km altitude Below this altitude the measured corrections for the background are employed The dustsonde is also equipped with rawinsonde temperature elements for recording the vertical temperature profile

Resolution and Accuracy

Figure 12 shows a typical dustsonde-measured profile of particle number density Note that below about 28 km the vertical resolution is better than 1 km in both particle size channels Professor Rosen has performed an analysis of the accuracy of dustsonde measurements (e g Hofmann et al , 1975) The major sources of error are counting statistics and possible variations in the refractive index of particles The counting method and sensor channels are designed to minimize these errors, for stratospheric heights below 25 km they result in typical uncertainties of about 8% for both Channels I and II ($r \geqslant 0$ 15 and 0 25 μm, respectively) Above 25 km these errors tend to increase significantly because of poorer counting statistics and less accurate measurement of the sampled air volume

Dustsonde measurements can be converted to an estimated particulate 1 0-μm extinction coefficient by using an assumed refractive index and a two-parameter size distribution fitted to the two-channel dustsonde data on N_{15} and N_{25} Figure 13 shows the dependence of the conversion ratio on optical model properties

[The size distribution functions and refractive indices shown have been derived from measurements by various investigators--e g Hofmann et al (1975), Toon and Pollack (1976), Harris and Rosen (1976), Swissler and Harris (1976) However, to generate the complete range of values shown for each curve, parameters were varied, sometimes beyond the range of observations Note that observations of N_{15}/N_{25} less than 2 are very rare, and average values for stratospheric layers several km thick are typically between 3 and 5]

In a given dustsonde measurement the channel ratio, N_{15}/N_{25}, is known, but the particle size model and refractive index can in general only be estimated on the basis of previous measurements Thus, the conversion ratio uncertainty is given by the vertical spread in the curves above the measured value of N_{15}/N_{25} Figure 14 shows the one-standard-deviation spread for the different aerosol compositions As can be seen, the uncertainty in converting a two-channel dustsonde measurement to 1 0-μm extinction is thus about $\pm$25% if particle composition is unknown, and about $\pm$15% if the refractive index is known to be one of the two values shown in Figure 13 (i e, either silicate or aqueous sulfuric- acid composition) A similar conclusion was obtained by Pepin and Cerni (1977)

2.3.2. Airborne Lidar

An airborne lidar for SAGE and SAM-II ground truth measurements has been developed under the direction of William Fuller at NASA Langley Research Center (LRC) The lidar design is based on a study by Evans (1977), with appropriate modifications by LRC personnel

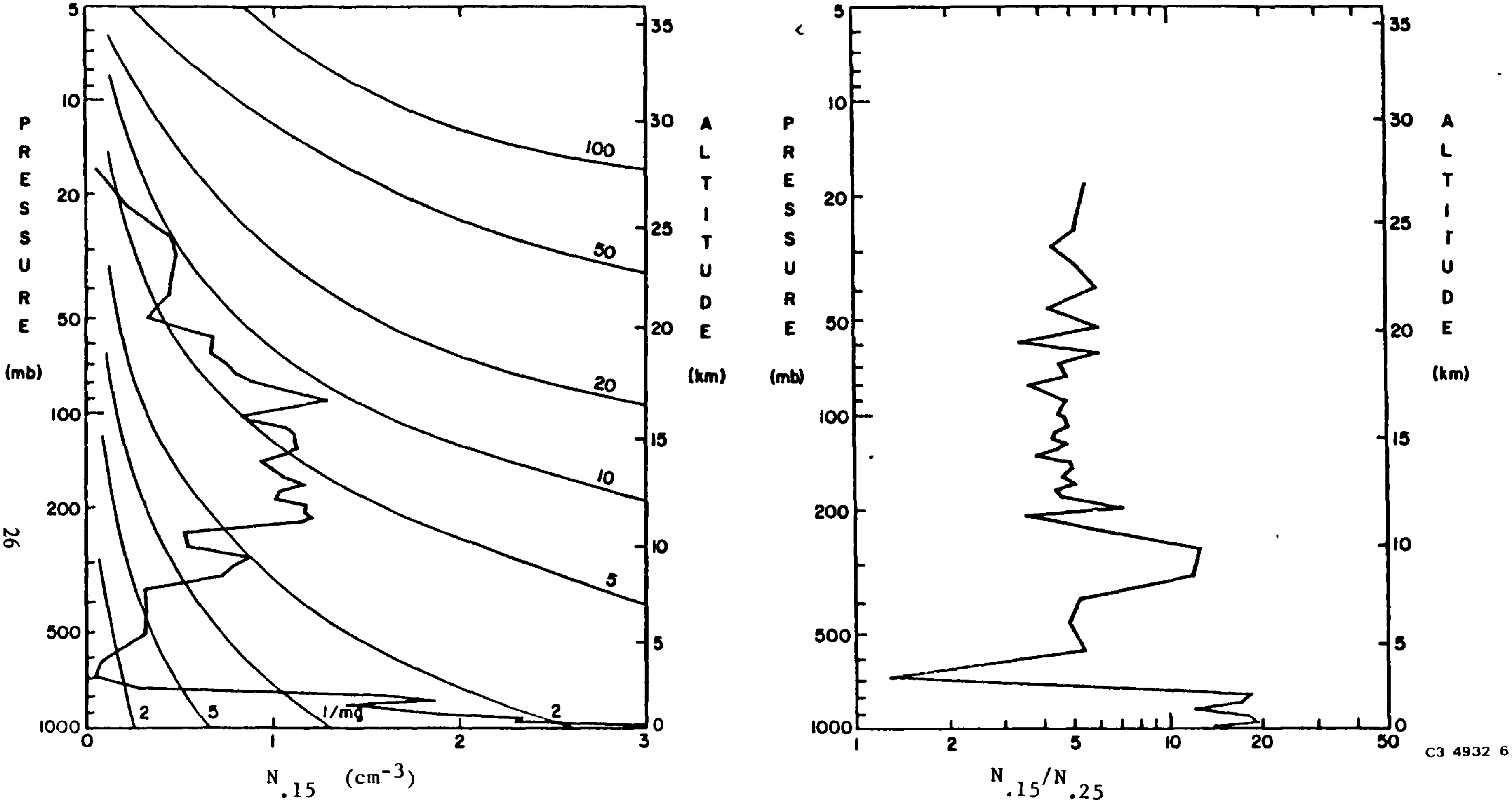

FIGURE 12 EXAMPLE OF TWO-CHANNEL DUSTSONDE MEASUREMENT OF PARTICLE NUMBER DENSITY, OBTAINED AT MCMURDO STATION (78° S, 167° E) DURING NONVOLCANIC CONDITIONS (12 JANUARY 1973)

(a) Number of particles with radius $\geqslant$0 15 μm (N_{15}, measured by channel I) Smooth curves are lines of constant mixing ratio (particle number per mg of air) (b) Ratio of numbers of particles measured by channels I and II N_{25} is number of particles with radius $\geqslant$ 0 25 μm, and is measured by Channel II Ratio data are plotted at heights where Channel II data are available N_{15} data are interpolated at these heights in computing ratios

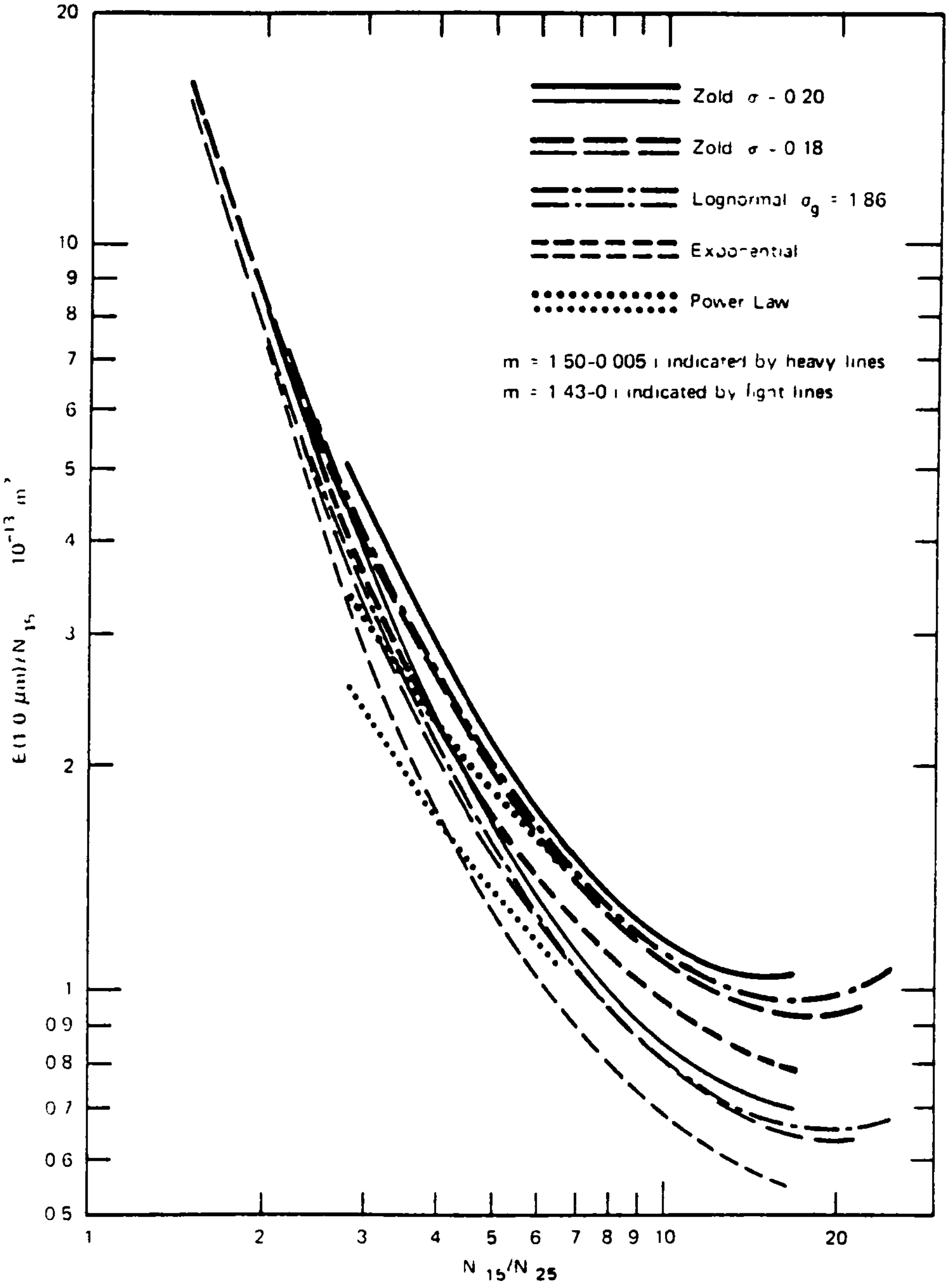

FIGURE 13 DEPENDENCE OF EXTINCTION-TO-NUMBER RATIO [E(1 0 μ)/ N_{15}] ON CHANNEL I/II RATIO (N_{15}/N_{15}) , PARTICLE SIZE MODEL, AND REFRACTIVE INDEX

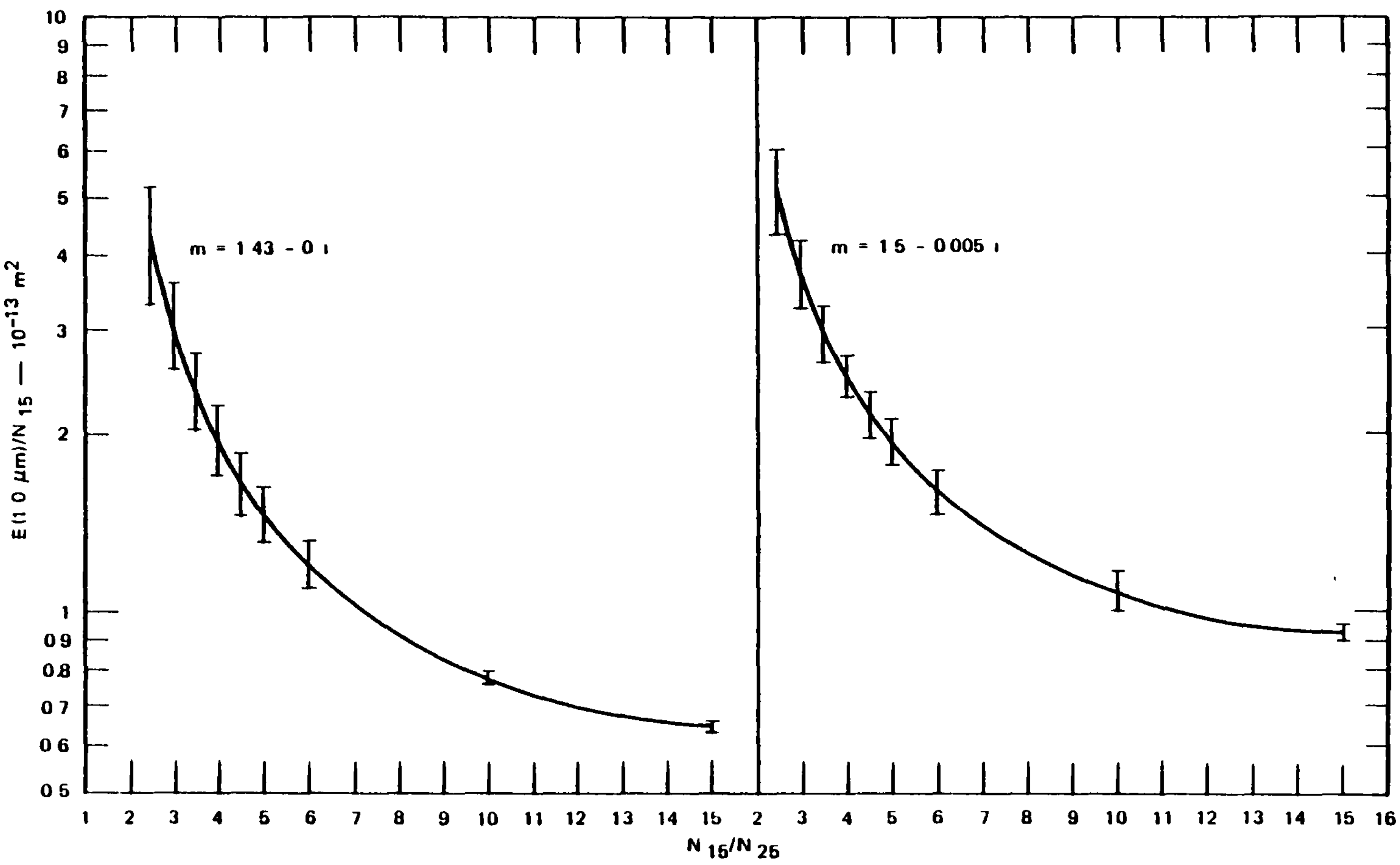

FIGURE 14 MEAN AND STANDARD DEVIATION OF COMPUTED EXTINCTION-TO-NUMBER RATIOS

Each curve is the result of Mie calculations for five different types of size distribution functions

Table 6 shows the design parameters, Figure 15 a photo of the lidar itself (Although it currently uses only a ruby laser, plans call for the Nd-YAG laser and associated detector to be added in time for at least some of the SAGE correlative measurements) Figure 16 illustrates the organization of the airborne lidar project

The platform for the airborne lidar is the P-3 aircraft of the NASA Wallops Flight Center

Resolution and Accuracy

Measurements with the NASA Langley 48" ruby lidar, the SRI 16" ruby-dye lidar, and the NCAR ruby lidar, among others, have shown that stratospheric aerosol measurements can be made with a vertical resolution of 1 km or better (up to about 30 km) by accumulating photons

Table 6

DESIGN PARAMETERS OF AIRBORNE LIDAR

Transmitter	Ruby	Nd YAG
Wavelength (μm)	0 6943	1 06
Energy per Pulse (J)	1 0	0 5
Repetition Rate (pps)	1 0	20
Pulse Width (n sec)	30	20
Beam Divergence (mr)	1 0	1 0
Beam Diameter (cm)	8	7 6
Receiver		
Diameter (cm)	36	36
Field of View (mr)	2	2
Filter Bandwidth (A)	10	10
Optical Eff to PMT	0 35	0 35
PMT Quant Eff	0 10	0 03
Skylight Background* [w/(m^2 srA)]	2×10^{-4}	$1\ 3\times10^{-5}$
Data Acquisition		
Bandwidth	1-2 5 mHz	
ADC Rate	10 mHz (max)	
ADC Resolution	10 Bit	
ADC Memory	2048 Words	
Computer Memory	32 K 16-Bit Words	
Magnetic Tape	45 IPS, 800 CPI, 9 Track	

*For zenith-viewing lidar flying above 6 km, with sun near horizon

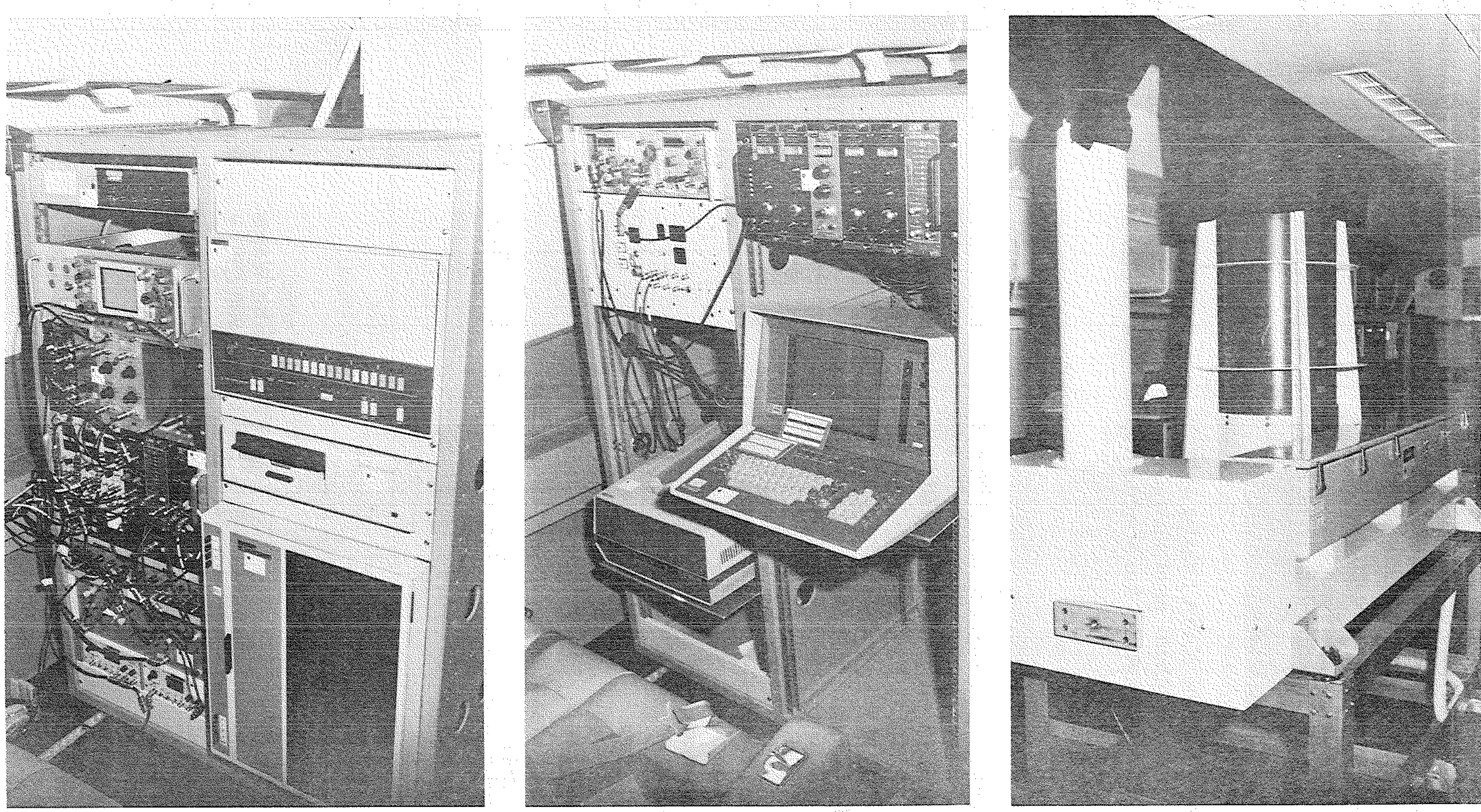

FIGURE 15 THE NASA LANGLEY AIRBORNE LIDAR SYSTEM

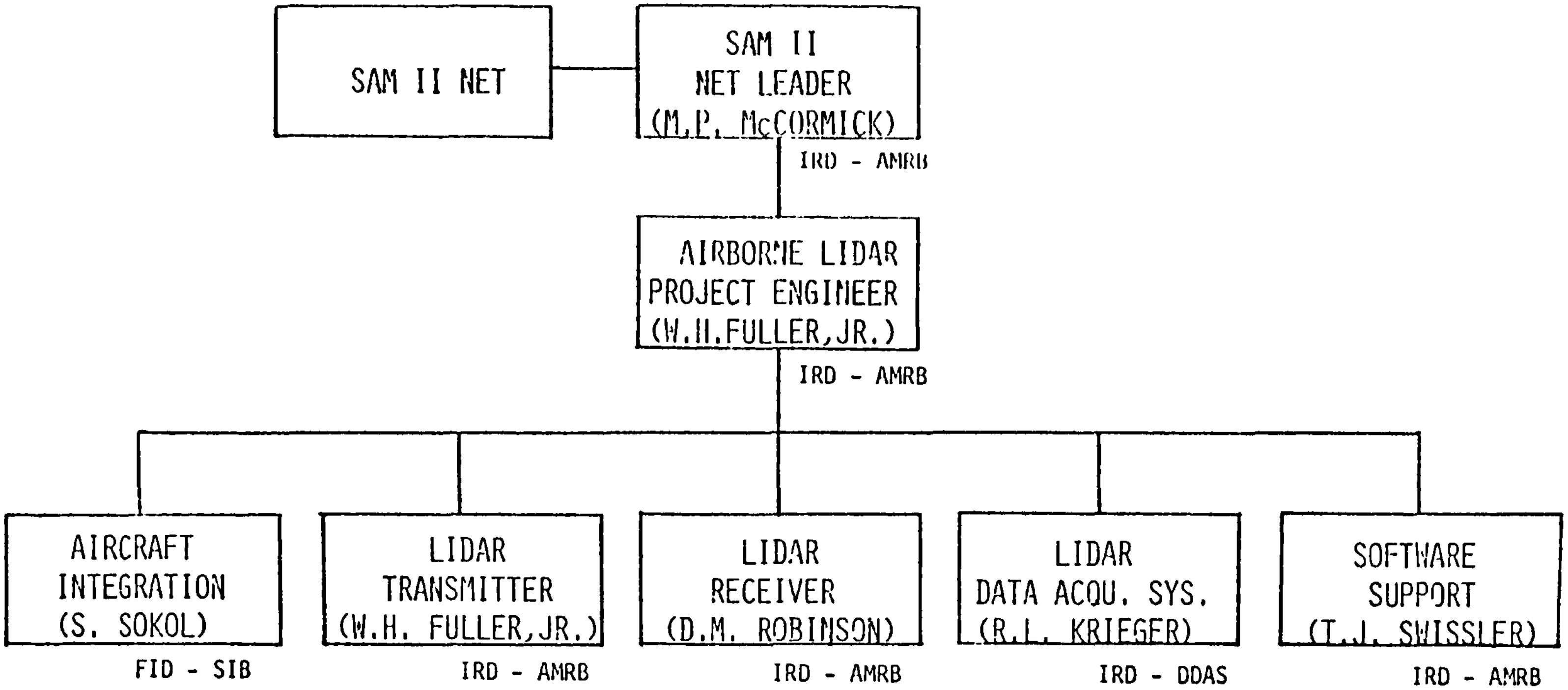

FID - FLIGHT INSTRUMENTATION DIVISION
IRD - INSTRUMENT RESEARCH DIVISION
AMRB - AEROSOL MEASUREMENTS RESEARCH BRANCH
DDAS - DIGITAL DATA ACQUISITION SECTION
SIB - SPACECRAFT INSTRUMENTATION BRANCH

FIGURE 16 ORGANIZATION OF AIRBORNE LIDAR PROJECT for reasonable amounts of time The accuracy of the particulate backscattering coefficients derived from such measurements is a strong and complicated function of the laser wavelength, other lidar parameters, skylight background, aerosol concentration, the proximity of the nearest radiosonde sounding, the validity of normalization procedures, and even the uncertainty in the ozone vertical profile To evaluate this accuracy for realistic situations we have developed a computer program that simulates the measurement and data analysis process, as shown in Figure 17 (A parameter shown in Figure 17 is the scattering ratio, R, a central quantity derived in the analysis of stratospheric lidar data It is defined as $R \equiv (B_p + B_g)/B_g$, where B_p and B_g are respectively the particulate and gaseous backscattering coefficients)

At each appropriate step of the simulation the program computes the relative uncertainty in each derived quantity by using an analytical expression The sources of error include (1) signal measurement error, (2) molecular density uncertainty, (3) aerosol and ozone transmission uncertainty, and (4) normalization uncertainty As a check on the analytical expressions for error propagation, random number generators (symbolized by circles in Figure 17) are used to inject random errors from sources (1)-(3) at appropriate points of the simulation [Error (4), normalization, affects the entire derived profile in a systematic way and should not be simulated by different random errors at each data point] Table 7 lists the sizes of the error sources used in the simulations (Justification for the chosen error sizes is given by Russell et al , 1976a,b)

Figures 18-20 show the results of using the program to simulate airborne lidar measurements for different latitudes and aerosol conditions

2.3.3. Ground-Based Lidar

2.3.3.1. NASA Langley 48" Ruby Lidar System

Shown in Figure 21 is the Langley Research Center's 48" laser radar (lidar) rystem It comprises two temperature-controlled lasers (ruby and neodymium-doped glass) mounted on either side of an f/10 Cassegrain telescope consisting of a 48-inch-diameter f/2 all-metal primary and a 10-inch diameter secondary mirror A schematic of the system is displayed in Figure 22 The detector package output is recorded by a high-speed data acquisition system Analog signals are amplified and bandwidth-limited, digitized at a 10-MHz rate with 8-bit accuracy, and then recorded on magnetic tape Pulse count data are amplified, discriminated, counted at a 200-MHz rate, and also stored on magnetic tape Altitude resolution is obtained by using the variable (1-, 5-, or 10-microsecond) bin widths that are available A 16K-word-storage computer is used to control the data acquisition system and provide data processing An X-band microwave radar, boresighted with the laser system axis, is used to ensure safe operation in the atmosphere A rotating shutter reduces laser fluorescence after Q-switching The entire system is mobile and can scan in elevation and azimuth at a slew rate of 1° per second

Presently the 48" system is being updated for simultaneous two-channel measurements and the addition of new ten-bit accuracy analog-to-digital converters In addition, a real-time graphics display system is being added

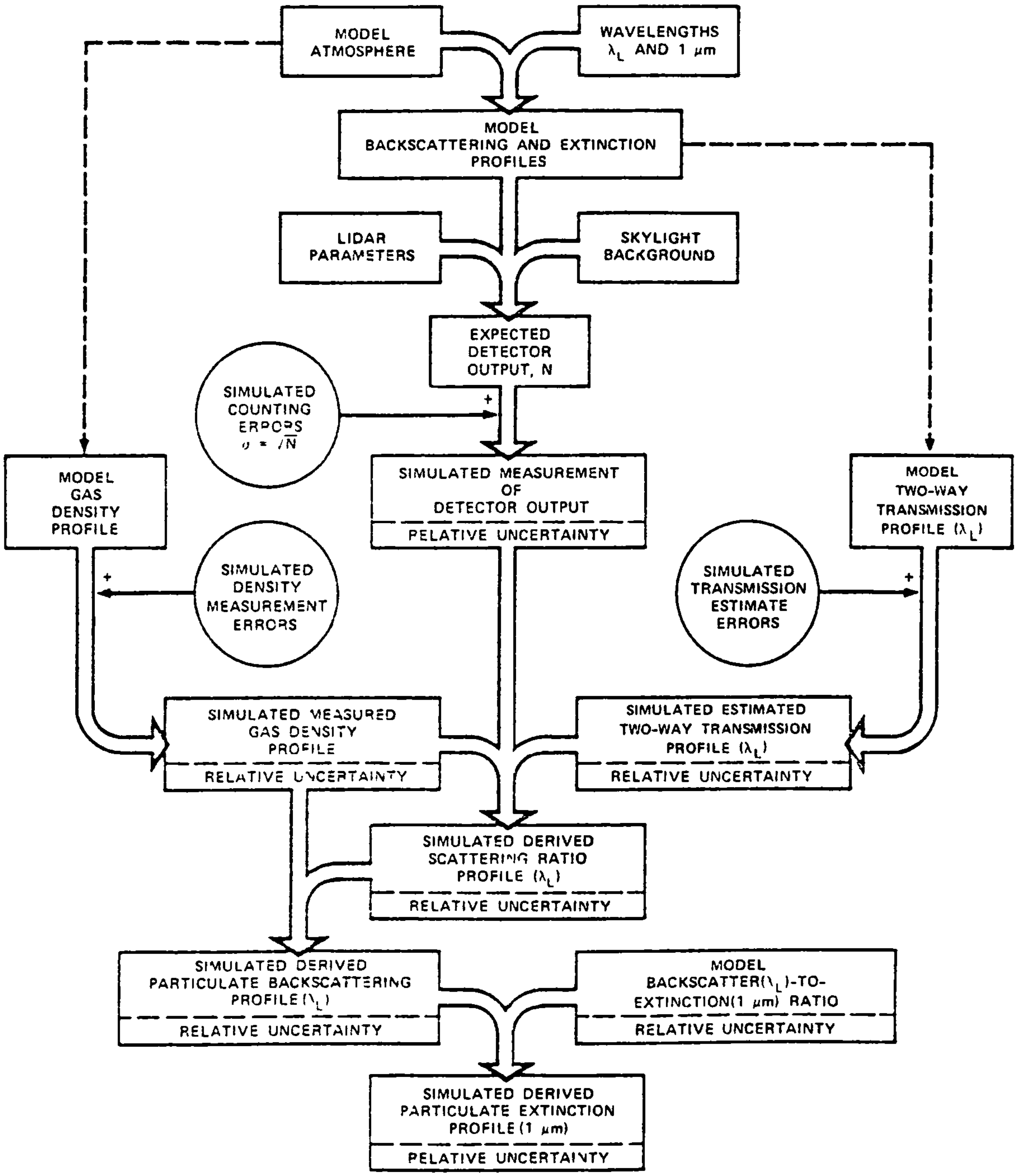

FIGURE 17 SIMULATION PROCEDURE FOR EVALUATING LIDAR MEASUREMENT ERRORS

λ_L is the lidar wavelength Each simulation is also performed for the SAM II/SAGE wavelength, 1 0 μm Circles symbolize random number generators that inject simulated errors into derived quantities at appropriate steps of the computation

Table 7

ASSUMED SIZES OF ERROR SOURCES IN LIDAR DATA ANALYSIS

Source	Relative Uncertainty
Detector Signal, S	$\frac{\sigma_S}{S} = \frac{\sqrt{S+B+I}}{S}$
Molecular Density, D	$\frac{\sigma_D}{D} =$ 1% below 30 km* 3% above 30 km
Two-Way Transmission, T^2	$\frac{\sigma_{T^2}}{T^2} = \sqrt{(0.4\tau_3)^2 + \tau_p^2}$†
Normalization Constant, K	$\frac{\sigma_K}{K} = \mathrm{Min}\ [0.05(R_{max}-1),\ 0.025(\lambda_L/0.69\mu m)^{4.08-b}]$‡

Notes

B, I = Detector output resulting from background light and internal noise, respectively

τ_3, τ_p = One way optical thickness of ozone and aerosol particles, respectively, between normalization altitude and altitude of analysis

R_{max} = Maximum scattering ratio in lidar profile being analyzed

λ_L = Lidar wavelength

b = Exponent of power-law approximation to wavelength dependence of particulate backscattering between 0.69 μm and λ_L. For most practical purposes $b \simeq 1.8$

*Assumes radiosonde density profile available within about 100 km and 6 hours of lidar measurement, and no intervening frontal activity

†Assumes ±20% uncertainty in τ_3 and ±50% uncertainty in τ_p

‡Based on typical aerosol concentration present at height of minimum mixing ratio in a long series of nonvolcanic and postvolcanic dustsonde measurements at Laramie, Wyoming, and on several ruby lidar/dustsonde comparison experiments. The error sizes shown apply to the case in which the scattering ratio profile is normalized to force its minimum to equal the value expected from previous dustsonde measurements, rather than the value 1.00 commonly used. If instead $R_{min} = 1.00$ is forced, the expected errors become asymmetric (always negative) and roughly twice as large

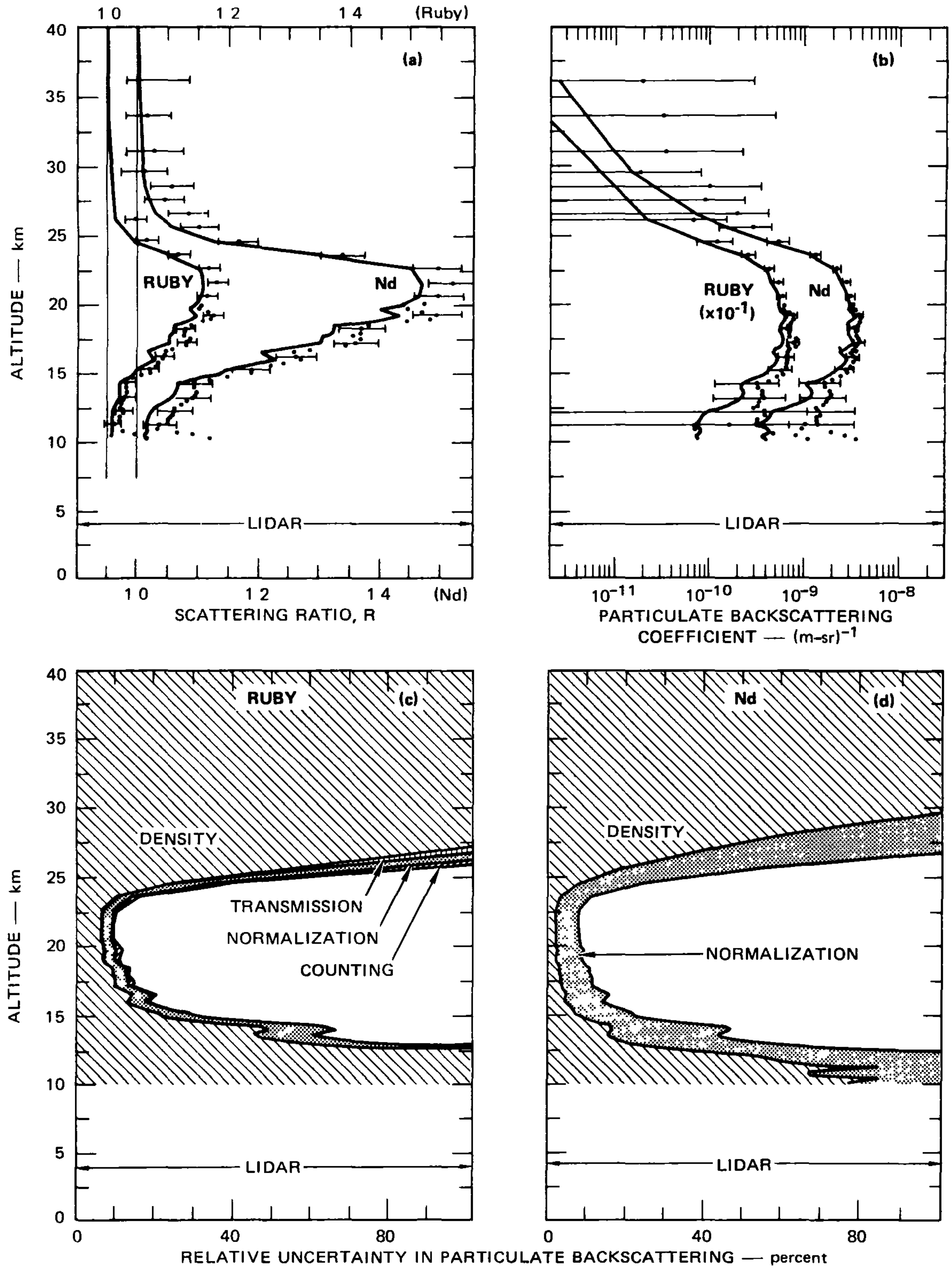

FIGURE 18 LIDAR MEASUREMENT UNCERTAINTIES AND SIMULATED MEASUREMENTS FOR THE W-48 (LARAMIE, WYOMING) MODEL ATMOSPHERE

(a) Model scattering ratios, simulated measurements (dots), and expected error bars (b) Model backscattering coefficients, simulated measurements (dots), and expected error bars (c),(d) Relative uncertainty in particulate backscattering, showing contributions by source

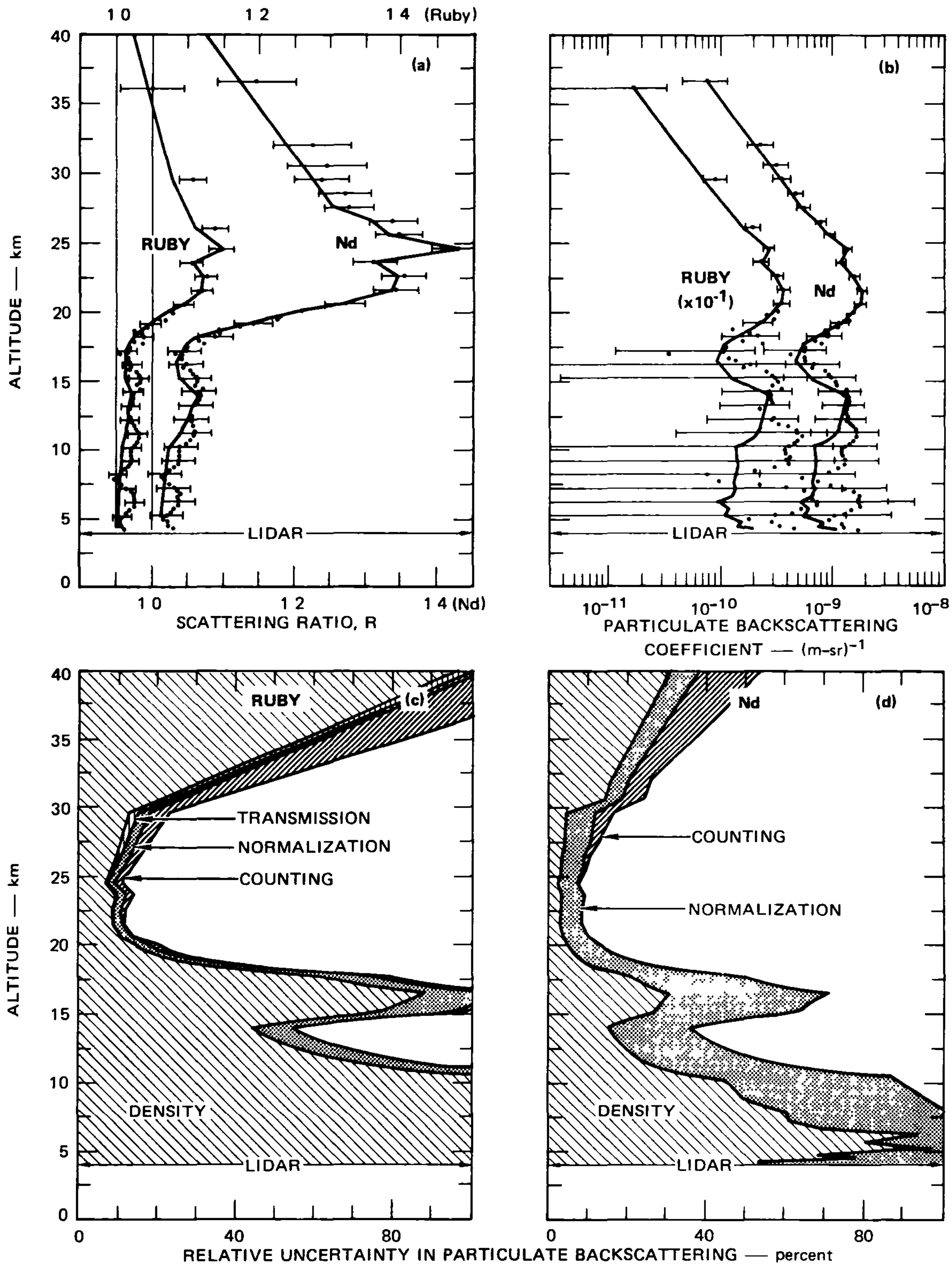

FIGURE 19 LIDAR MEASUREMENT UNCERTAINTIES AND SIMULATED MEASUREMENTS FOR THE P-10 (ALBROOK, PANAMA) MODEL ATMOSPHERE

(a) Model scattering ratios, simulated measurements (dots), and expected error bars (b) Model backscattering coefficients, simulated measurements (dots), and expected error bars (c),(d) Relative uncertainty in particulate backscattering, showing contributions by source

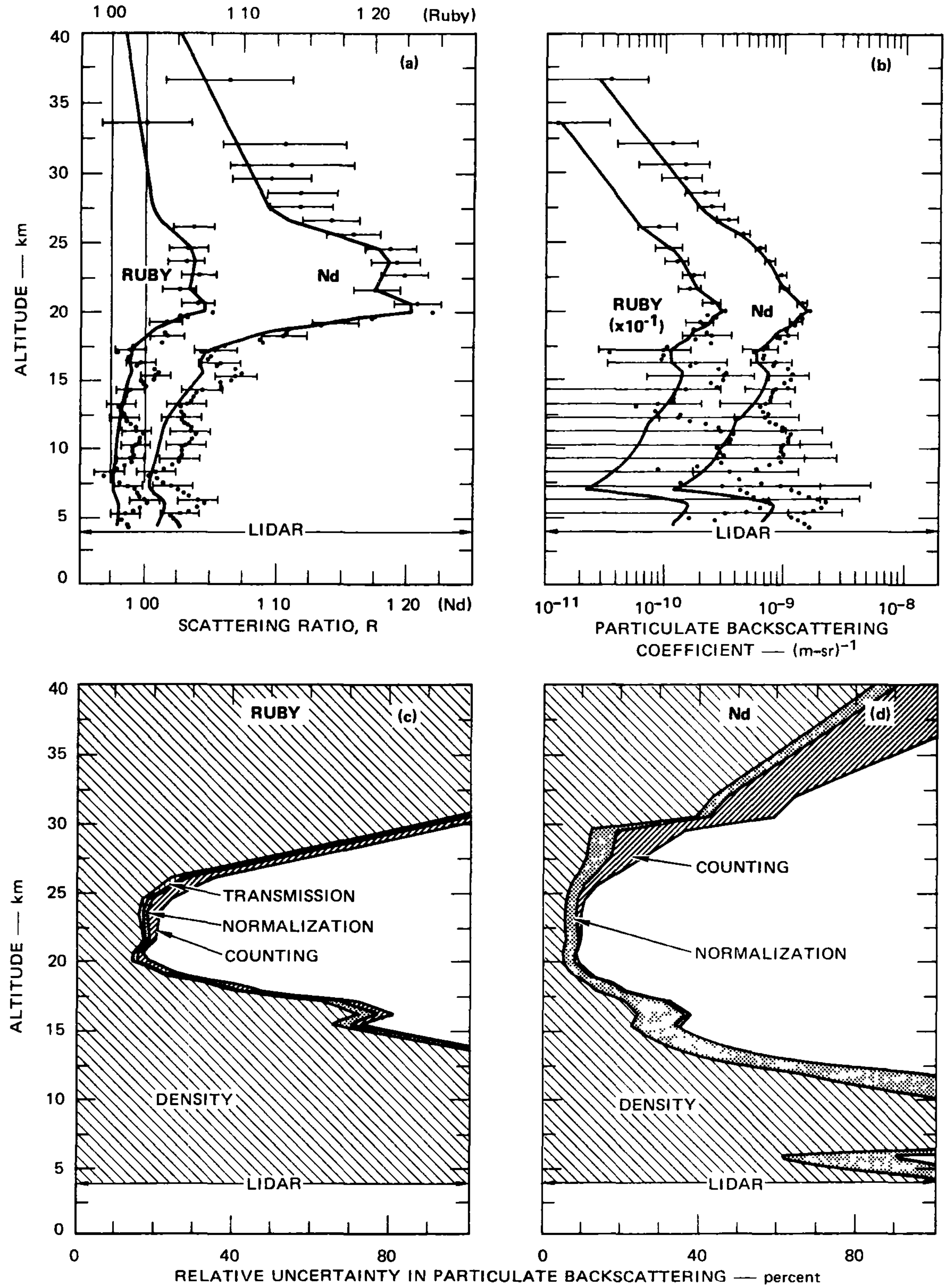

FIGURE 20 LIDAR MEASUREMENT UNCERTAINTIES AND SIMULATED MEASUREMENTS FOR THE L-3 (LONGREACH, AUSTRALIA) MODEL ATMOSPHERE

(a) Model scattering ratios, simulated measurements (dots), and expected error bars (b) Model backscattering coefficients, simulated measuremens (dots), and expected error bars (c),(d) Relative uncertainty in particulate backscattering, showing contributions by source

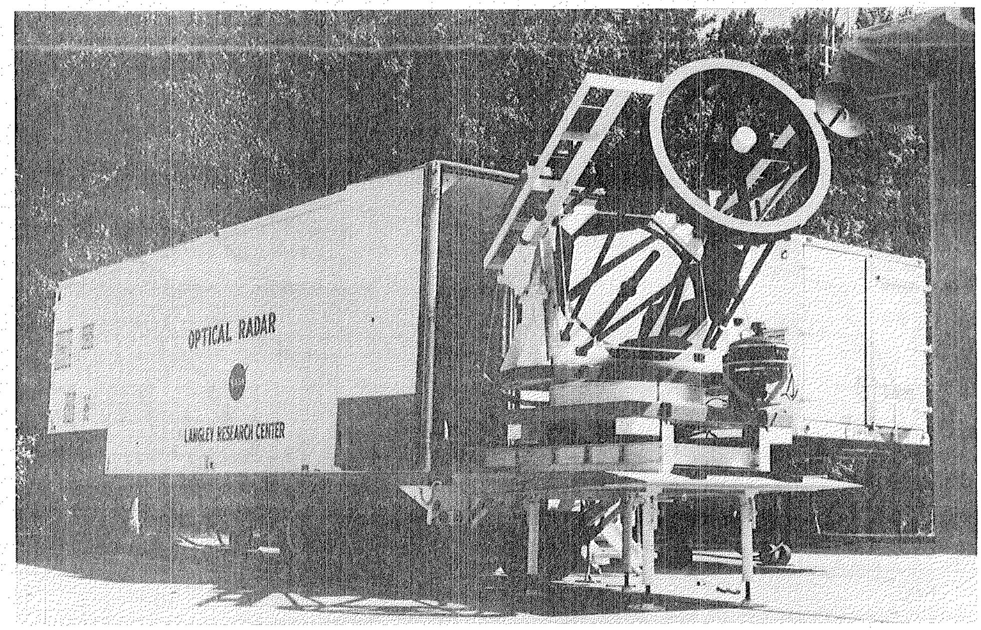

FIGURE 21 THE 48-INCH (1.22-METER) NASA LANGLEY RESEARCH CENTER LIDAR SYSTEM

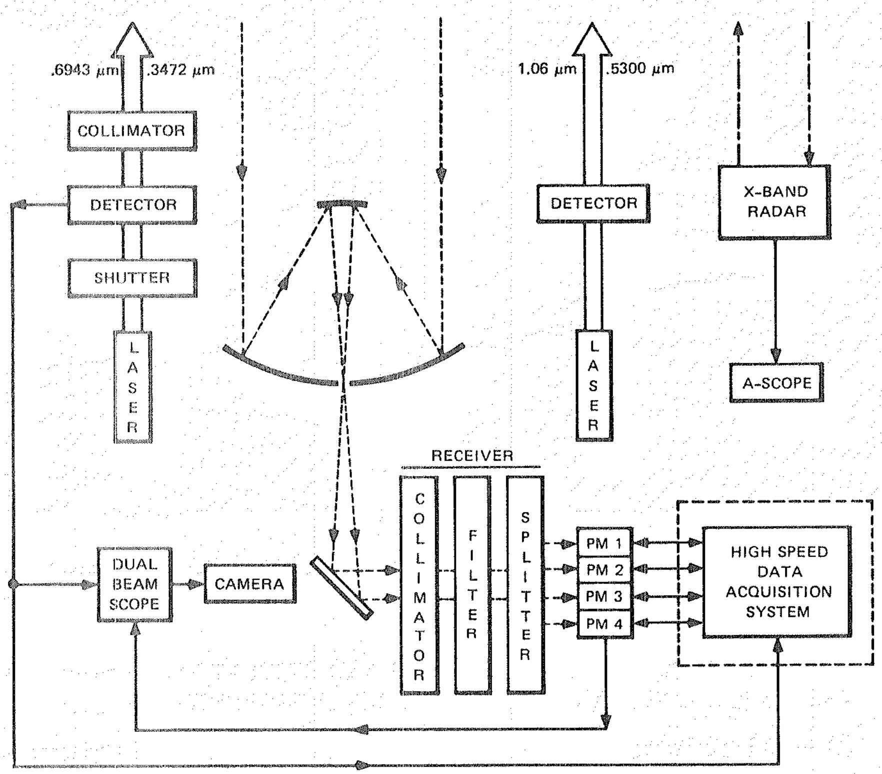

FIGURE 22 SCHEMATIC DIAGRAM OF THE 48-INCH (1.22-METER) NASA LANGLEY RESEARCH CENTER LIDAR SYSTEM

2.3.3.2. NCAR 60" Ruby Lidar System

The National Center for Atmospheric Research (NCAR) in Boulder, Colorado has a ground-based ruby lidar that has been used for stratospheric aerosol measurements at various times since about 1969 The system is built around a 60-inch-diameter searchlight mirror It has a pulse energy of 1-2 J and a pulse duration of 60 ns The system's field of view is fixed at the vertical

This system will be operated by Dr Frederick G Fernald of Denver University and Mr Charles Frush of NCAR as part of the SAGE ground truth program Specifically, it was used in the Laramie-Boulder practice comparative experiment in September 1978 and will be used in the White Sands-Boulder correlative experiment in February or March 1979 (See also Table 2 and Sections 3 1 and 3 2 4)

2.3.3.3. CNRS Heyss Island Lidar System

Dr M L Chanin of France's Centre National de la Recherche Scientifique (CNRS) will conduct a program of noctilucent cloud observations by dye lidar techniques from Heyss Island (80 5°N), where a lidar station has been established since 1975 for sodium measurements The observations, part of a joint Franco-Soviet program, are planned to start prior to the SAGE launch Dr Chanin has agreed to make available to the SAGE and SAM II ground truth programs any NLC observations that are near SAM-II or SAGE scans in both space and time

2.3.3.4. NOAA Point Barrow Dye Lidar System

Dr Ronald Fegley of the NOAA Wave Propagation Laboratory (Boulder, Colorado) is developing a dye lidar for installation at Point Barrow, Alaska (71° 20' N, 156° 38' W) as part of NOAA's Geophysical Monitoring for Climatic Change program Starting in spring 1978, observations extending into the stratosphere are planned on a weekly basis, cloud cover permitting We intend to include such data as are made available in the SAM-II and SAGE ground truth data sets when this is appropriate However, the high probability of cloud cover at Point Barrow makes the probability of data capture within the time window of a SAM-II or SAGE overflight smaller than is acceptable for a primary ground truth sensor Moreover, the short wavelength (585 nm) of the lidar yields expected errors in measured particulate backscattering of greater than ±30% throughout the stratosphere under nonvolcanic background conditions (These errors result primarily from molecular density uncertainties, see also Section 2 2 1) It is for these reasons that an airborne lidar of longer wavelength (694 or 1060 nm) has been developed specifically for SAM-II and SAGE ground truth measurements

2.3.4. Polar Nephelometer

The Georgia Tech laser polar nephelometer (Grams, et al , 1975) measures the angular scattering pattern (often called the scattering phase function) of the light scattered out of a collimated beam by aerosol particles This parameter is important for use in calculating the effect of airborne particles on the transfer of radiation in the atmosphere It can also be used to infer other physical properties of the aerosol particles, such as their size distribution or refractive index (e g , Grams, et al , 1974)

The nephelometer has been designed to operate in a pressurized aircraft cabin, using outside air ducted through an airflow tube The sample volume is the intersection of a collimated source beam and the detector field of view within the airflow tube The source is a linearly polarized laser beam The optical system defines a collimated field of view (0 5° half-angle), a photomultiplier tube is located immediately behind an aperture in the focal plane of the objective lens to measure the amount of light scattered from the laser beam A two-channel pulse counter, synchronized to the laser output, measures the photomultiplier pulse rate with the light beam both on and off The difference in these measured pulse rates is directly proportional to the intensity of the scattered light from the volume in which the laser beam and the detector field of view intersect

The nephelometer is operated under the control of a microprocessor system The light-scattering measurements can be made at angles of 15°-165° from the direction of propagation of the laser beam Intermediate angles between these extremes are obtained by selecting the angular increments desired, pulses provided by digital circuits control a stepping motor that rotates the detector sequentially by preselected angular increments (usually 5°) The synchronous photon-counting system automatically begins to measure the scattered-light intensity immediately after rotation to the new angle has been completed

2.3.5. In Situ Particle Sizing Devices

2.3.5.1. Quartz Crystal Microbalance Cascade Impactor

The quartz crystal microbalance cascade impactor (QCM) is a multistage impactor that senses the mass of suspended particles as a function of particle size The particles are drawn into the sensor and separated aerodynamically into ten size intervals ranging from 0 05 μm to 25 μm in diameter (assuming spherical particles of mass density 2 gm cm^{-3}) Figure 23 illustrates the flow through the sensor The air velocity increases as it flows from one stage of the cascade to the next because of the decreasing diameters of the entrance jets Thus, the larger particles impact on the upper stages and the smaller ones are carried with the flow to the lower stages Table 8 lists the 50-percent cut points (diameter at which the particles have 50-percent impaction efficiency) for each of the ten stages Each impactor stage contains a piezoelectric crystal microbalance that senses the mass of the particles collected by a change in oscillator frequency between a reference crystal and the sensing crystal The time response is on the order of two seconds, so that temporal or spatial variations are resolved Laboratory analysis (scanning electron microscopy) can be performed on the samples for elemental composition and morphology

This technique can provide data that are free of some of the ambiguities present in light-scattering and other remotely sensed data Information needed to expand the usefulness of satellite data for radiative transfer and associated modeling studies can be obtained

NASA Langley owns two of these QCM instruments One of them, with an improved design for high-altitude sampling, was flown aboard the NCAR Sabreliner up to an altitude of 13 km, it performed successfully in measuring the stratospheric aerosol size distribution over the Fairbanks, Alaska area in May 1977 and over the Sondrestrom, Greenland area in November 1978 as part of the SAM-II ground truth program It was also flown aboard the NCAR Queen Air over Guatemala, where, in February 1978, it successfully measured the size distribution of volcanic aerosols In addition, the instrumention was flown with the airborne lidar on the WFC P-3 during the Laramie practice comparative experiment in September 1978

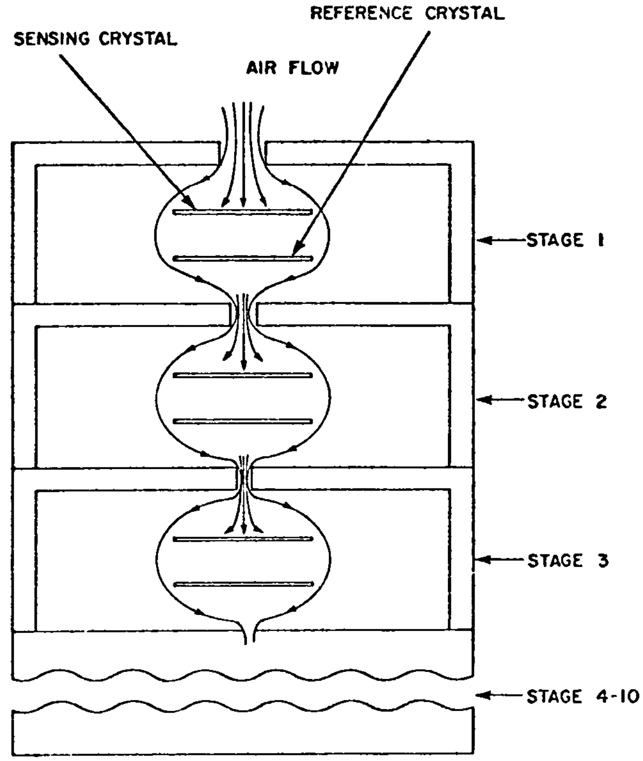

FIGURE 23 ILLUSTRATION OF AIR FLOW THROUGH THE 10-STAGE QCM CASCADE IMPACTOR

These experiments demonstrate the impactor's suitability for airborne measurements and its ability to provide useful data on atmospheric aerosols Figure 24 shows the aircraft mounting for the microbalance Listed below are the specifications relevant to aircraft operation

Cascade and Aerodynamic Housing	
External dimensions	5-inch-diameter cylinder 22 in long with hemispherical end caps
Weight	15 lbs
Control Units	
External dimensions	19-inch rack mount 7 in high 12 in deep
Weight	8 lbs
Power Requirements	
Pump Motor	28 Vdc, 2 amps
Electronics	115 Vac, 50-60 Hz, 1 amp

Table 8

50%-EFFICIENCY POINTS FOR THE CELESCO MODEL C-1000
QCM CASCADE IMPACTOR

Stage No	50%-Cut-Point Diameter* (Micrometers)
1	25 0
2	12 5
3	6 3
4	3 2
5	1 6
6	0 8
7	0 4
8	0 2
9	0 1
10	0 05

*Assuming spherical particles of mass density 2 g cm^{-3}

Major Equipment Subsystems

- Ten-stage cascade-sensing stack assembly with remote-controlled motor-driven inlet valve
- Sample-air pump
- Isokinetic air inlet
- Aerodynamic housing
- Control unit for 19-inch rack mounting (includes power supply, signal conditioning electronics, and printer)
- Interfacing cable

The current plan is to transfer this high-altitude QCM to the NASA Ames U-2 and fly it as a SAGE correlative sensor at White Sands in February or March 1979 (See Experiment 2 in Table 2)

2.3.5.2. Other In Situ Particle-Sizing Devices

It is possible that other particle-sizing devices may be employed on aircraft platforms during the SAGE ground truth program For example, a Climet single-particle optical counter was installed on the NCAR Sabreliner aircraft along with the Georgia Tech polar nephelometer and the NASA Langley quartz crystal microbalance during the November 1978 SAM II ground truth program in Sondrestrom, Greenland The principle of operation of this type of instrument[7] is similar to that of the University of Wyoming dustsonde (Section 2 3 1), i e , aerosol

[7]Counters of this type are manufactured by such companies as Bausch and Lomb, 820 Linden Avenue Rochester New York 14625 Climet Instruments Company 1240 Birchwood Drive Sunnyvale, California 94086 Particle Measuring Systems 1855 S 57th Court Boulder Colorado Royco Instruments Inc 141 Jefferson Drive, Menlo Park California 94025

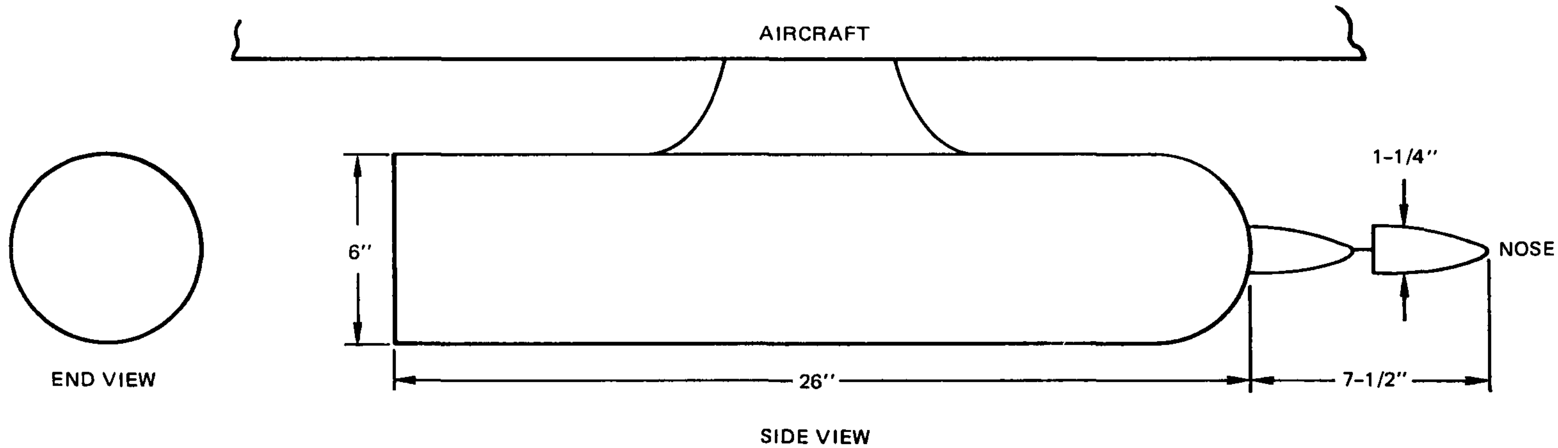

FIGURE 24 CONFIGURATION FOR EXTERNAL AIRCRAFT MOUNTING OF QUARTZ CRYSTAL MICROBALANCE

particles flow through an illuminated volume, light scattered by an individual particle into a particular solid angle is sensed photoelectrically, and the response pulses are classified according to their magnitude

Other possible techniques that could be employed for in situ measurements include the use of devices for collecting particles by impaction and then analyzing the sample in the laboratory to establish the particle size, shape, and composition by electron microscopy (e g , Ferry and Lem, 1974) In a similar fashion, Nuclepore filters with very small pore diameters might be used to collect particles to obtain samples for analysis by scanning electron microscopy (e g , Patterson and Gillette, 1977) Other techniques for sampling aerosol particles have been described by Grams and Rosen (1978) However, many of these techniques have not been employed in stratospheric sampling programs, and thus modifications of the sampling equipment would probably be required

2.3.6. Noctilucent Cloud Sightings

The International Noctilucent Cloud (NLC) Program, in cooperation with the World Meteorological Organization, records and collates observations of noctilucent clouds (particulate layers in the 73-95 km altitude region) Mr E J Truhlar of the Canadian Atmospheric Environment Service (AES) collects observations from 60 Canadian and 16 U S stations, and Dr D H McIntosh of the University of Edinburgh (UE) collects them for Western Europe We have made arrangements to receive tabulations of sightings (with about one month's delay) from the AES and UE and will attempt to make similar arrangements with others Sample tabulations, relevant correspondence, and a description of the observation characteristics are given in Appendix C

Resolution and Accuracy

Bronshten and Grishiken (1975) estimate that the height accuracy of the "best" NLC measurements is better than 1 km (see also Appendix C) Presumably the "best" measurements are those made with aligned cameras or visually with theodolites Many sightings are made with the unaided eye, and their height accuracy is probably considerably worse than 1 km Uncertainties in the size distribution and shape of NLC particles, together with the uncalibrated brightness scale of observations, make conversion of sightings to 1 0-μm extinction coefficients extremely approximate at best The purpose of the NLC sightings will be to provide time and location data for comparison with any layers detected by SAGE in the 73-95 km region Because of the paucity of other particulate data in this height region, the NLC data are considered an important source of ground truth information

2.3.7. SAM II

The Stratospheric Aerosol Measurement II (SAM II) was launched on the Nimbus 7 satellite in October 1978 SAM II is a scanning solar photometer that operates similarly to SAGE, however, it has only one optical channel--at wavelength 1 0 μm (the longest SAGE wavelength) SAM II's mission is to map vertical profiles of aerosol extinction by scanning through the atmosphere during spacecraft sunrise and sunset events Because of the Nimbus 7 orbit these vertical profiles will be restricted to two latitude bands 64°-80° N and S (See, e g , Russell et al , 1978)

Since SAGE's coverage is expected to extend from the equator to 75° N and S, there is some overlap in the coverage of the SAM II and SAGE sensors Moreover, the seasonal dependence of coverage indicates that there will be occurrences of near-coincidence in space and time between SAM II and SAGE scans When this occurs comparisons will be made--as a means of evaluating the mutual consistency of the two measurements In particular, near-coincidences are expected to occur in late spring and early fall of 1979 near Sondrestrom, Greenland SAGE Correlative Experiment 4 (see Table 2 and Section 3 2 4) aims to provide correlative ozone, aerosol, and other measurements at the time of one or more of these coincidences

2.4. NO_2 and Multiconstituent Sensors

2.4.1. Pepin Balloon-Borne Sunphotometer and Spectrometer

The University of Wyoming has developed a balloon-borne sunphotometer and spectrometer system The photometer contains a seven-channel instrument, four channels of which are spectrally equivalent to the SAGE instrument The spectral wavelengths for the instrument are

Channel #	Wavelength (μm)
1	0 39
2	0 43
3	0 45
4	0 60
5	0 82
6	0 93
7	1 00

The spectrometer scans the spectral interval between 0 37 and 1 1 μm with wavelength resolution on the order of 0 05 μm During flight both instruments on the balloon gondola lock onto the sun and view it during the sunrise or sunset event

Resolution and Accuracy

The photometer and spectrometer have the capability to measure the intensity of the sun as viewed through the atmosphere with a precision of ±0 1% of that intensity Both instruments are calibrated during the extinction balloon flight by observing the sun at high elevation angles from the balloon platform and then extrapolating the observed signal to conditions outside the atmosphere Observations are made to less than 0 01 airmass

Both the photometer and spectrometer measuring systems make use of the total solar disk, rather than the partial disk observed by the SAGE scan system Since these systems are used at balloon altitude, not at spacecraft altitude, they achieve vertical resolution of the same order as SAGE, but do not require high pointing accuracy and are less sensitive to refraction

Conversion to Particulate and Ozone Extinction Profiles

The measurements from the photometer and spectrometer systems will be converted to extinction profiles using the method outlined by Pepin (1970, 1977) The spectral intervals around the SAGE bands can be studied by using the spectrometer measurements made at spectral intervals near the SAGE observations

2.4.2. Murcray Interferometer and Spectrometer

NO_2 was first detected in the lower stratosphere by means of absorption features observed in infrared solar spectra, these features are associated with the ν_3 band in the 1618 cm^{-1} region (Murcray et al , 1968, Goldman et al , 1970) The few altitude profiles currently available for NO_2 in this wavelength region have been derived from infrared solar spectra obtained by balloons, although some recent results have been reported for the same spectral region used by SAGE (Kerr et al , 1977, Goldman et al , 1978)

In view of the small amount of data available concerning the altitude distribution of NO_2, there is no accepted measuring technique that can be applied to obtain "ground truth" data for SAGE It is rather proposed that a balloon flight be performed to obtain a vertical profile of NO_2 using the infrared solar spectral technique for comparison with the profile obtained by SAGE The spectral data required for this comparison will be obtained by means of the University of Denver balloon-borne interferometer system, which consists of an interferometer capable of obtaining solar spectra with a resolution of 0 01 cm^{-1} covering the 1600 cm^{-1} region Previous experiments have shown that this resolution is more than adequate to determine an NO_2 profile from sunset solar spectra The system includes a biaxial pointing control, a PCM telemetry system, an on-board digital magnetic tape-recording system, and power supplies for operating the various components The balloon flight will be performed as part of a series of flights for NASA and will obtain comparative data Many constituents in addition to NO_2 will also be measured

NO_2 total column data have also been obtained from ground-based visible spectra with a technique initially proposed by Brewer (1973) and used extensively by Noxon By obtaining data on the ground from the scattered sunlight after sunset (solar zenith angles > 90°) one can use an Umkehr technique to obtain some profile data The spectral resolution needed in this type of measurement is not high, the main requirement for the measurement is wide dynamic range

A balloon-borne UV-visible grating spectrometer system suitable for collecting data of this sort will be incorporated into the P3 aircraft instrumentation The advantages of operating the system from the aircraft are twofold the increased latitude range over which comparison data can be obtained and the ability to obtain data when the weather precludes doing so from the ground The spectrometer system is a 0 5-meter Czerny-Turner system that is double-passed The radiation is interrupted by a tuning-fork chopper after the first pass and the radiation is synchronously detected, which results in a significant reduction in stray light The system is capable of a 0 3A resolution, but for this application it will be degraded to ~5A Data will be recorded by means of a digital magnetic-tape recording system

2.4.3. LIMS Instrument Package

The LIMS Instrument Package (LIP) consists of a number of instruments that will provide measurements for validating the data obtained from the Limb Infrared Monitor of the Stratosphere (LIMS) experiments on Nimbus 7 This balloon-borne package is scheduled for two or three flights in support of the LIMS experiment The sensors on the LIP will measure ozone, water vapor, nitric acid, temperature, and pressure The instruments are (1) a Dasibi ozone sensor (Johnson Space Center), (2) an infrared emission radiometer (Belgium), (3) an absorbing filter sensor (NCAR), (4) a water vapor infrared radiometer (United Kingdom) and (5) an electrochemical concentration cell sonde and radiosonde (Wallops Flight Center) Maximum altitude of the LIP is approximately 35 km All LIP data, as well as other ground truth data for LIMS, are expected to be stored at NOAA/NESS in Suitland, Maryland The sensor scientists are (1) Dr Don Robbins (JSC), (2) Dr Carlos Lippens (Belgium), (3) Dr Bruce Gandrud (NCAR), (4) Dr John Harries (U K) and (5) Mr Lawrence Rossi (WFC) Mr Ed Szajna and Mr Fred Witten (GSFC) are the LIP manager and engineer, respectively

The possibility of making a LIP flight from Palestine, Texas in coincidence with a SAGE tangent scan is being explored with members of the European ad hoc ground truth group (see Table 3) In addition, a LIP flight scheduled for LIMS support in Cold Lake, Alberta, in February 1979 may be sufficiently close in space and time to a SAGE tangent scan to provide useful correlative data

2.4.4. Noxon Spectrometer

As indicated above (Section 2 4 3) NO_2 was initially detected in the stratosphere by means of absorption features observed in infrared solar spectra obtained from a balloon NO_2 also has a strong absorption band in the visible region, Noxon has used this band to obtain total column data on stratospheric NO_2 with a ground-based spectrometer system The visible region has the advantage that spectral scans of the zenith sky made at solar zenith angles $> 90°$ contain absorption features resulting from the path of solar radiation in the stratosphere Noxon's system, designed to be portable, has been used by him to obtain data over a wide range of latitudes A description of his instrumentation, data reduction procedures, and the results he has achieved is contained in a recent series of articles (Noxon et al , 1978, Noxon, 1978) It is proposed that this system be utilized as part of the ground truth obervation program scheduled for late February 1979 at White Sands Proving Ground

2.4.5. Schmeltekopf Chemiluminescent Sensor

As indicated above, the amount of data currently available on the altitude distribution of NO_2 is limited All data obtained so far are based on spectroscopic techniques and have been secured by remote sensing Schmeltekopf has developed an instrument for obtaining in situ NO_2 data that makes use of a chemiluminescent NO sensor constructed for balloon-borne operation The unit first measures NO with the chemiluminescent technique and then, using a mercury lamp, converts the NO_2 present in the atmosphere to NO by photodissociation The NO concentration is then remeasured, the increase over the preceding measurement denotes the NO_2 concentration The system has not been flown yet, but will be flown as part of the SAGE ground truth plan if it is operational by then

2.4.6. LIMS

The Limb Infrared Monitor of the Stratosphere (LIMS) experiment on the Nimbus 7 satellite is being conducted to determine global-scale vertical distributions of temperature, as well as of several gases involved in the chemistry of the ozone in the stratosphere Profiles of ozone (O_3), nitrogen dioxide (NO_2), nitric acid (HNO_3), water vapor (H_2O), and temperature are determined with fine vertical resolution from the lower stratosphere ($\simeq$10 km) to the lower mesophere ($\simeq$65 km) These data are derived by inverting measured limb radiance profiles obtained by LIMS, an infrared multispectral scanning radiometer Measurements are made in each of six spectral regions one each in the 9 6 μm O_3 band, the 6 3 μm NO_2 band, the 6 2 μm H_2O band, and the 11 3 μm HNO_3 band, and two in the 15 μm band of CO_2

This experiment is a follow-on to the successful Limb Radiance Inversion Radiometer (LRIR) experiment flown on Nimbus 6 to measure O_3, H_2O, and temperature The LIMS instrument is identical to the LRIR in many respects, but with the essential difference that two detectors were added to the focal plane array and five parameters are being measured rather than three The horizon scan rate was also decreased from one degree per second to a quarter degree per second to provide improved signal-to-noise performance These changes facilitate the measurement of constituents with small signals (e g NO_2, HNO_3) and allow extension of these measurements to lower and higher altitudes

A programmed scanning mirror in the radiometer causes the field of view of the six detectors to make coincident vertical scans across the earth's horizon The data from these scans are stored on tape for later transmission to the ground During data reduction the measured limb radiance profiles from the carbon dioxide channels are operated on by inversion algorithms to determine the vertical temperature distribution This inferred temperature profile, together with the radiance profiles in the other channels, is then used to infer the vertical distribution of the trace constituents

Comparisons of the ozone and NO_2 profiles measured by SAGE with those measured by LIMS will be made for cases in which the two measurements are in sufficient proximity In addition, the LIMS Experiment Team plans to use SAGE and SAM-II data on aerosols and thin clouds to identify any possible effects on the LIMS data (Russell and Gille, 1978)

2.4.7. SBUV/TOMS

The Solar and Backscattered Ultraviolet (SBUV) instrument on the Nimbus 7 satellite should provide ozone profiles between 30 and 45 km with a vertical resolution of 3-5 km and a precision of 5-10% In this height region the time scale for ozone changes is expected to be several days or longer Therefore, the differing local measurement times of SAGE (sunrise and sunset) and SBUV (approximately local noon) are not expected to invalidate comparisons of observed ozone profiles It is planned that comparisons will be restricted to spatial separations of $\pm$500 km Concurrent SAGE data on aerosols and on neutral density will be used to eliminate some of the uncertainties inherent in the inversion procedures for the two experiments

SAGE ozone profiles can also be compared against total ozone observations determined both by SBUV, which views an area approximately 200 km x 200 km, and by the Nimbus-7 Total Ozone Monitoring System (TOMS), which views an area approximately 50 km x 50 km Total ozone observations will be compared during SAGE and SBUV/TOMS coincidences (as defined above) Moreover, the TOMS instrument will scan across the satellite track, thus providing almost full global coverage for total ozone during a 24-hour period TOMS observations may therefore also be used to indicate spatial variability at the time of the major ground truth experiments depicted in Table 2

2.5. Temperature, Pressure, or Density Sensors

2.5.1. Balloon-Borne Radiosonde

The radiosonde[8] is a balloon-borne, battery-powered, meteorological instrument that automatically transmits to a ground receiving station radio signals relating to the pressure, temperature, and humidity of the air from the surface to a height of approximately 30 km Wind direction and speed data are calculated from the rise and horizontal drift of the radiosonde, which are measured by the ground receiving station (RAWIN Set AN/GMD)

The radiosonde system is enclosed in a plastic and paper container and is approximately 40 cm high, 17 cm wide, and 12 cm thick It weighs 392 grams without batteries Figure 25 shows the flight configuration of this instrument when attached to a standard 1200-gram Weather Service balloon

The precision of the radiosonde instrument is specified below

Atmospheric Pressure	1060 mb to 50 mb ±2 mb	50 mb to 20 mb ±0 5 mb	20 mb to 2 mb 0 25 mb
Temperature	±0 5°C		
Relative Humidity	Within ±5% at temperatures +40°C to 0°C		

Section 4 2 4 1 describes the radiosonde data, their management, distribution, and so forth

2.5.2. Super Loki Datasonde

The Super Loki datasonde is the standard rocket-launched meteorological payload used by the U S meteorological community It is used to measure vertical profiles of atmospheric temperature and wind between 70 and 20 km Figure 26 depicts this system in descent configuration suspended below its decelerator after launch by the Super Loki rocket This system is used in conjunction with a GMD set at 1680 MHz

The precision of the Super Loki datasonde system is from 1 5 to 3 5 C for temperature data, $\pm 3 \mathrm{msec}^{-1}$ for the wind data, 1 5-3% for pressure and 3-5% for density

Section 4 2 4 2 describes the data handling aspects of this instrument system

[8]Vehicles and Sensors of the UPN 607 Applications Sounding Rocket Program October 1977 Preliminary

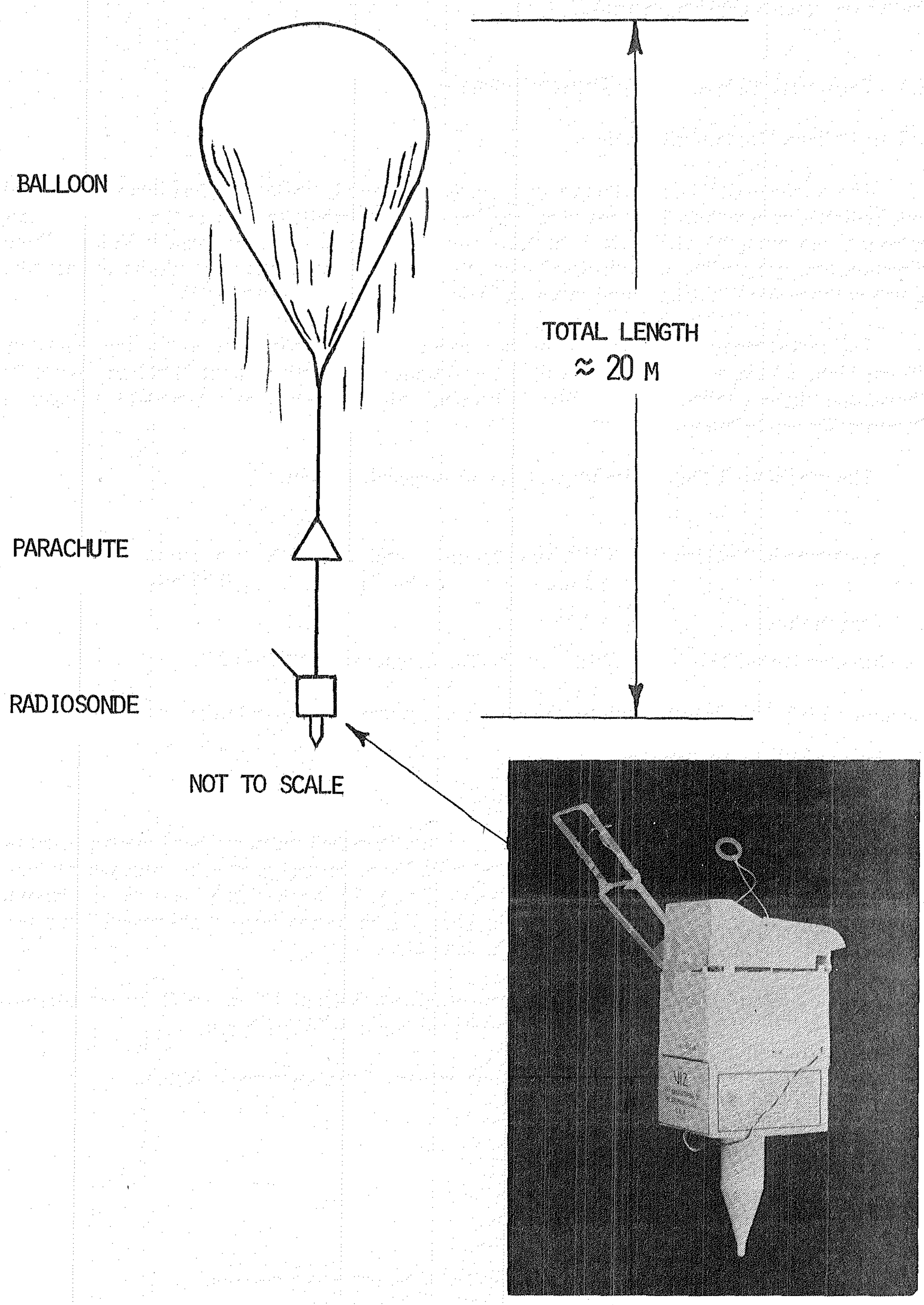

FIGURE 25 RADIOSONDE FLIGHT CONFIGURATION

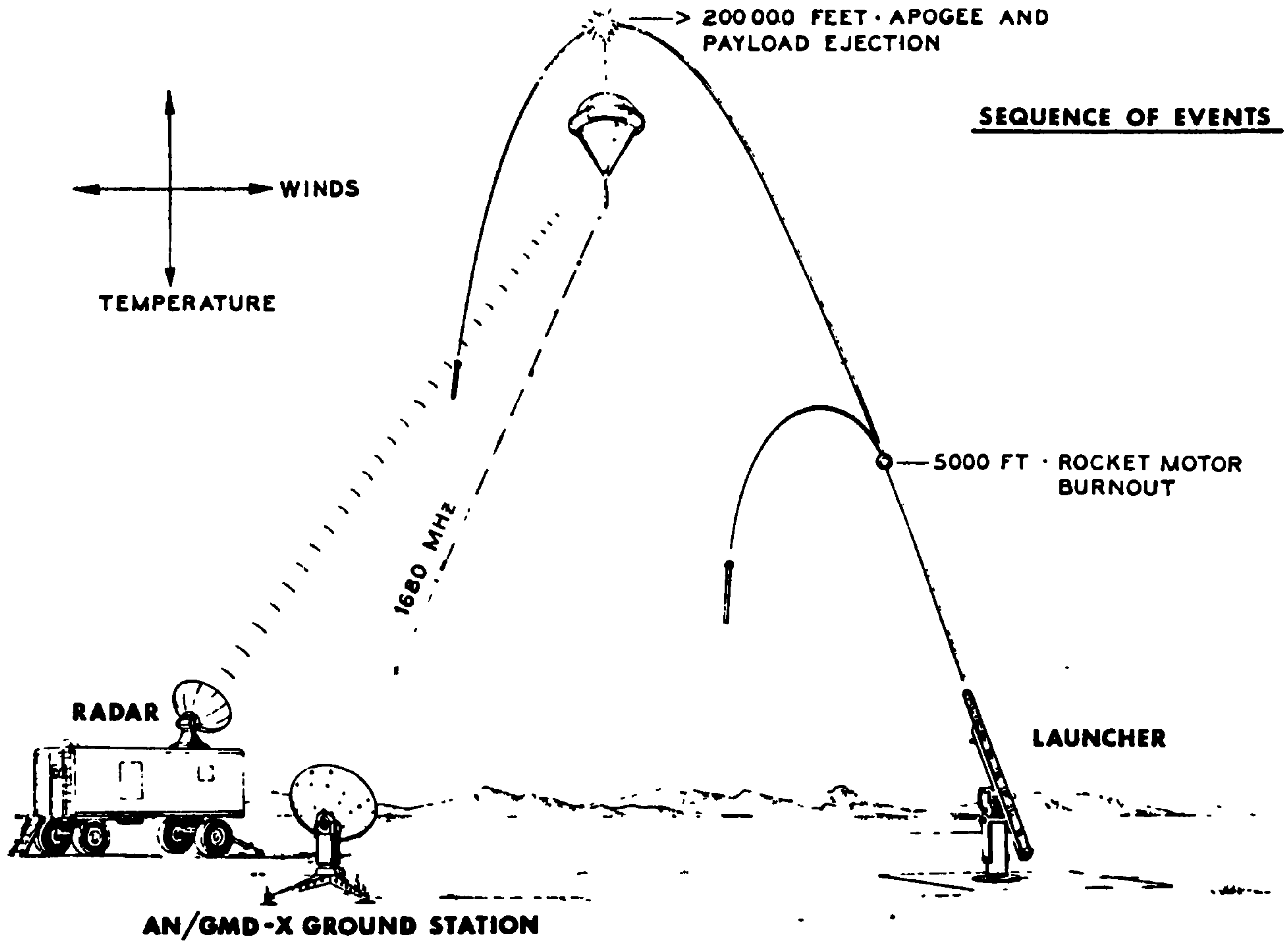

FIGURE 26 SUPER LOKI DATASONDE FLIGHT PROFILE AND GMD TRACKING SCENARIO

2.5.3. NMC Global Data Net

The National Meteorological Center (NMC) will supply SAGE with profiles of temperature, pressure-surface heights, and density inferred from the NMC upper-air data network (principally balloonsondes, rocketsondes, and satellite sensors) Procedures for deriving these profiles and the data format are described in Section 4 2 4 4

3. MEASUREMENT SITES, SCHEDULES, AND LOGISTICS

3.1. Aerosol Practice Comparative Experiment

An aerosol Practice Comparative Experiment was held on September 27, 1978 in Laramie, Wyoming It included flights by the airborne lidar and a dustsonde, as well as ground-based lidar measurements at NCAR in Boulder, Colorado (see Section 2 3 3 2) Its purpose was to develop multisensor and multiplatform coordination procedures, and also to test data reduction and comparison techniques, as mentioned previously in Section 1 2

Laramie, Wyoming, was chosen as the preferred site for the Practice Comparative Experiment because of its proximity to the University of Wyoming This was a cost-reducing factor that also simplified the logistics of the dustsonde balloon flight and maximized chances of instrument recovery Although the balloon-borne sunphotometer was unable to participate in the Practice Experiment, it is expected that both the sunphotometer and spectrometer will be available for the February 1979 ground truth experiments at White Sands

3.2. Postlaunch Measurements

3.2.1. Predicting SAGE Tangent Times and Locations

The SAGE tangent times and locations are determined by the AEM-B orbit parameters (inclination, height, and shape) and the launch time and date (which determine the relative positions of SAGE, the sun and earth surface sites) Since none of these factors can be known precisely before launch, exact predictions of tangent times and locations can be made only after launch, when orbit parameters have been accurately determined Possible variations in orbit parameters are considerable because the Scout launch rocket is less controllable than some other vehicles, and AEM-B cannot make postinsertion orbit corrections Nevertheless, as a means of preparing for postlaunch contingencies, it is useful to predict tangent occurrences for nominal orbit parameters and launch times, as well as for probable variations in these factors

Edwin F Harrison of NASA Langley Research Center has prepared such a set of parametric predictions Figure 27 shows examples of these results, as latitude-vs-longitude plots of all tangent locations for each of 12 months after launch, assuming a launch time of 1030 EST, January 25, 1979, a circular orbit with a height of 600 km, and an inclination of 55° Also shown on each plot are circles of 500-km radius each, centered on Sondrestrom, Greenland, Wallops Island, Virginia, White Sands, New Mexico, and Natal, Brazil (The circles appear as ellipses because of the map projection) These circles show at a glance the number of times that SAGE sunrise and sunset tangent scans will occur within 500 km of each site in a given month

A more detailed look at this question of tangent opportunities is given by Table 9, which focuses on the first 60 days of the mission (a time of intense ground truth activity, see Table 2) and the sites of Wallops Island, White Sands, and Natal Table 9 considers a range of launch times, two launch dates, and two orbit shapes A list of prioritized requirements for SAGE tangent locations and times is given in Table 10 In view of Table 9, it appears that a launch time of about 1030 EST would yield the greatest probabilty of satisfying the requirements of Table 10

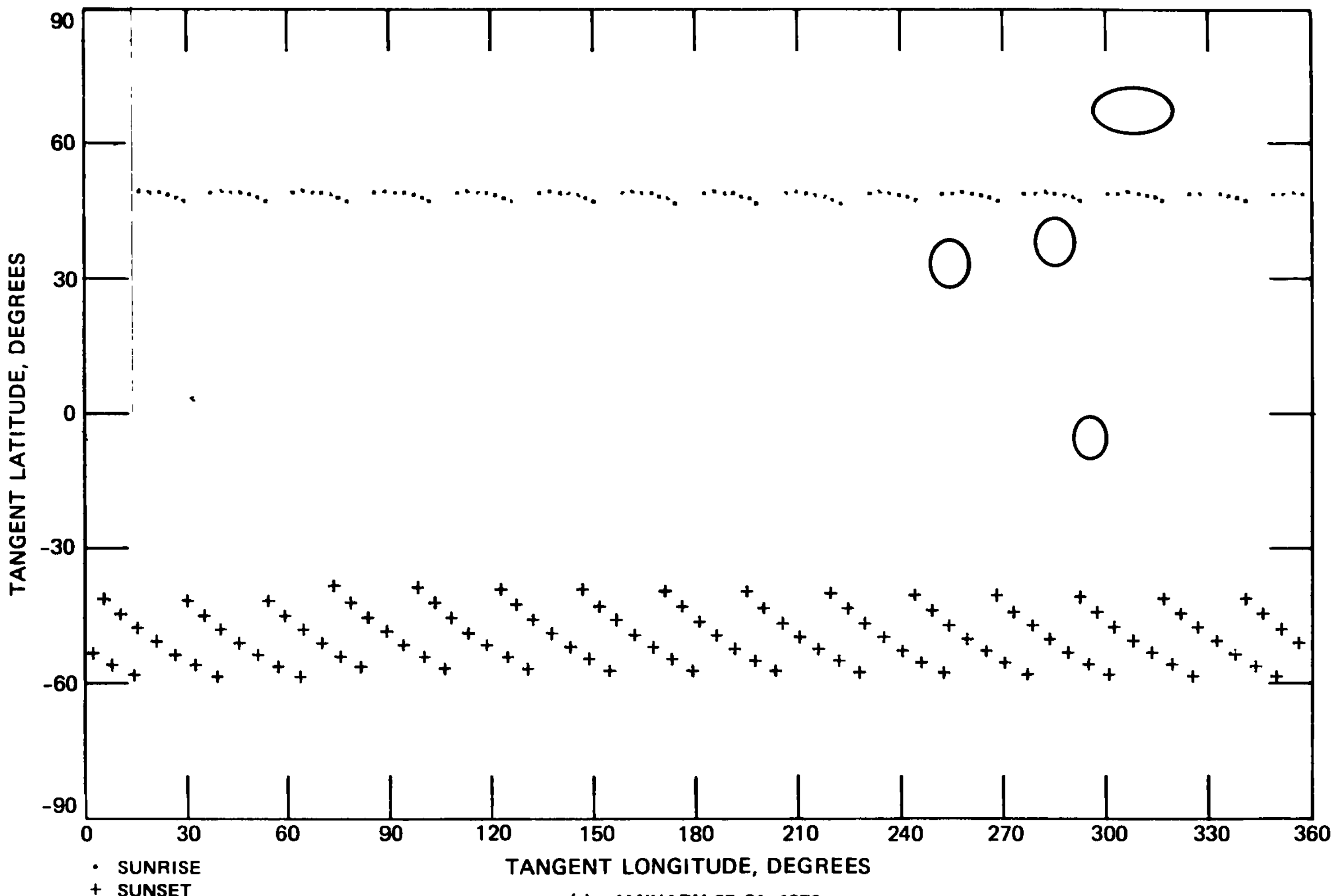

(a) JANUARY 25–31, 1979

FIGURE 27 SAGE SUNRISE AND SUNSET TANGENT LOCATIONS FOR SELECTED TIME PERIODS

Calculations assume $i = 55°$, $k = 600$ km, launch time = 1030 EST, 25 January 1979 Ellipses have 500-km radius and are centered at Sondrestrom, Wallops Island, White Sands, and Natal

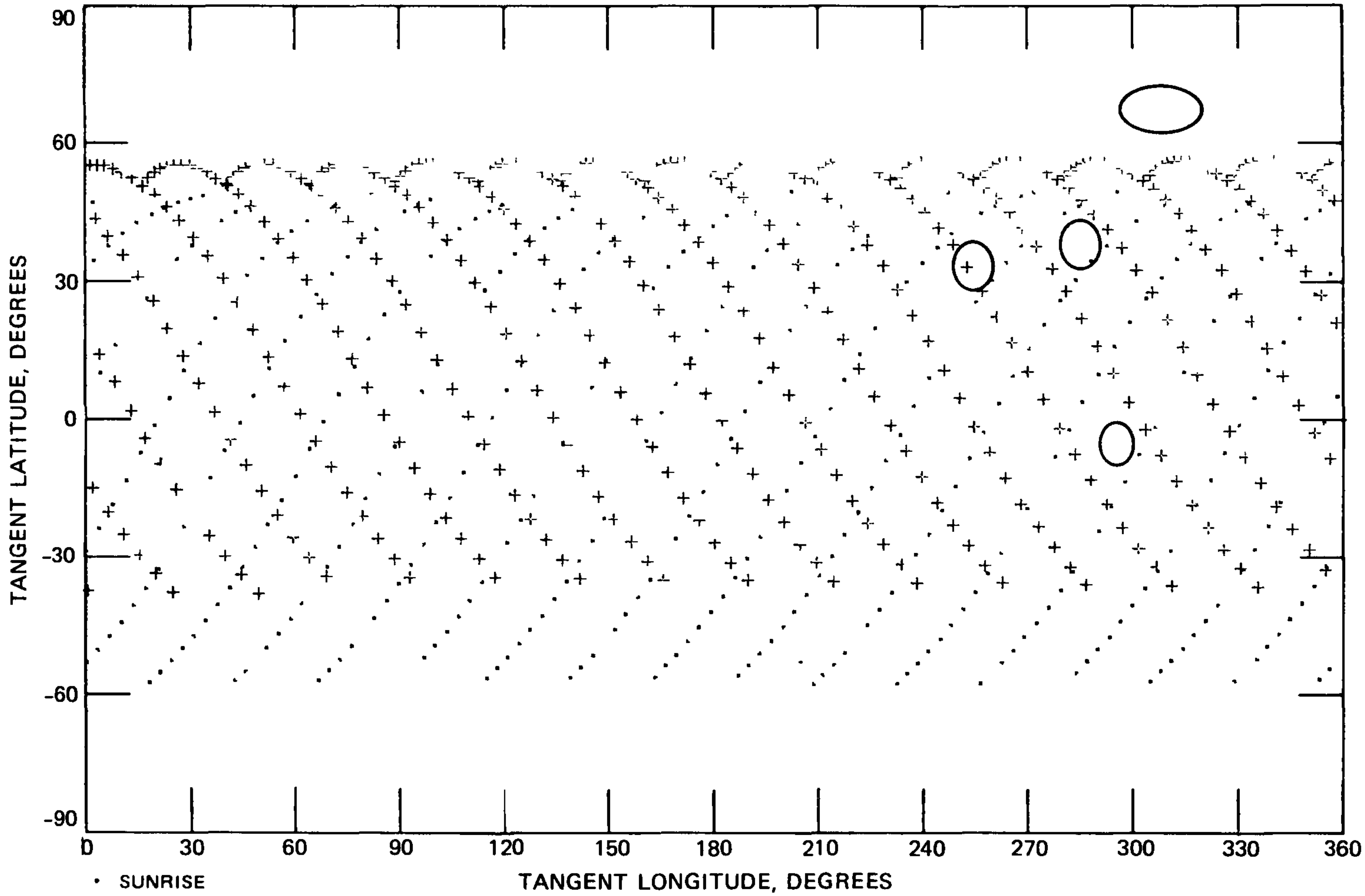

(b) FEBRUARY 1979

FIGURE 27 SAGE SUNRISE AND SUNSET TANGENT LOCATIONS FOR SELECTED TIME PERIODS (Continued)

Calculations assume i = 55°, k = 600 km, launch time = 1030 EST, 25 January 1979 Ellipses have 500-km radius and are centered at Sondrestrom, Wallops Island, White Sands, and Natal

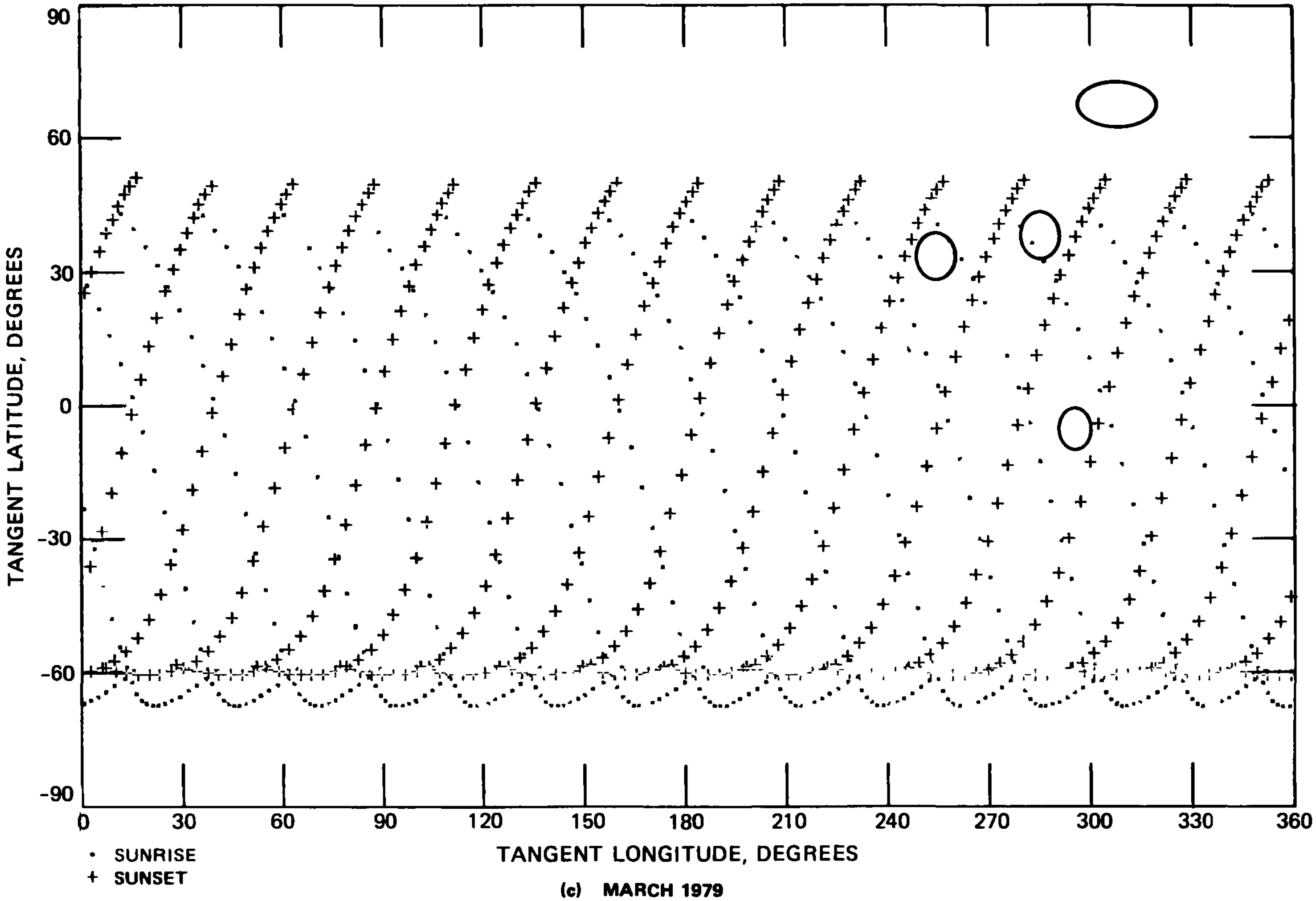

(c) MARCH 1979

FIGURE 27 SAGE SUNRISE AND SUNSET TANGENT LOCATIONS FOR SELECTED TIME PERIODS (Continued)

Calculations assume $i = 55°$, $k = 600$ km, launch time = 1030 EST, 25 January 1979 Ellipses have 500-km radius and are centered at Sondrestrom, Wallops Island, White Sands, and Natal

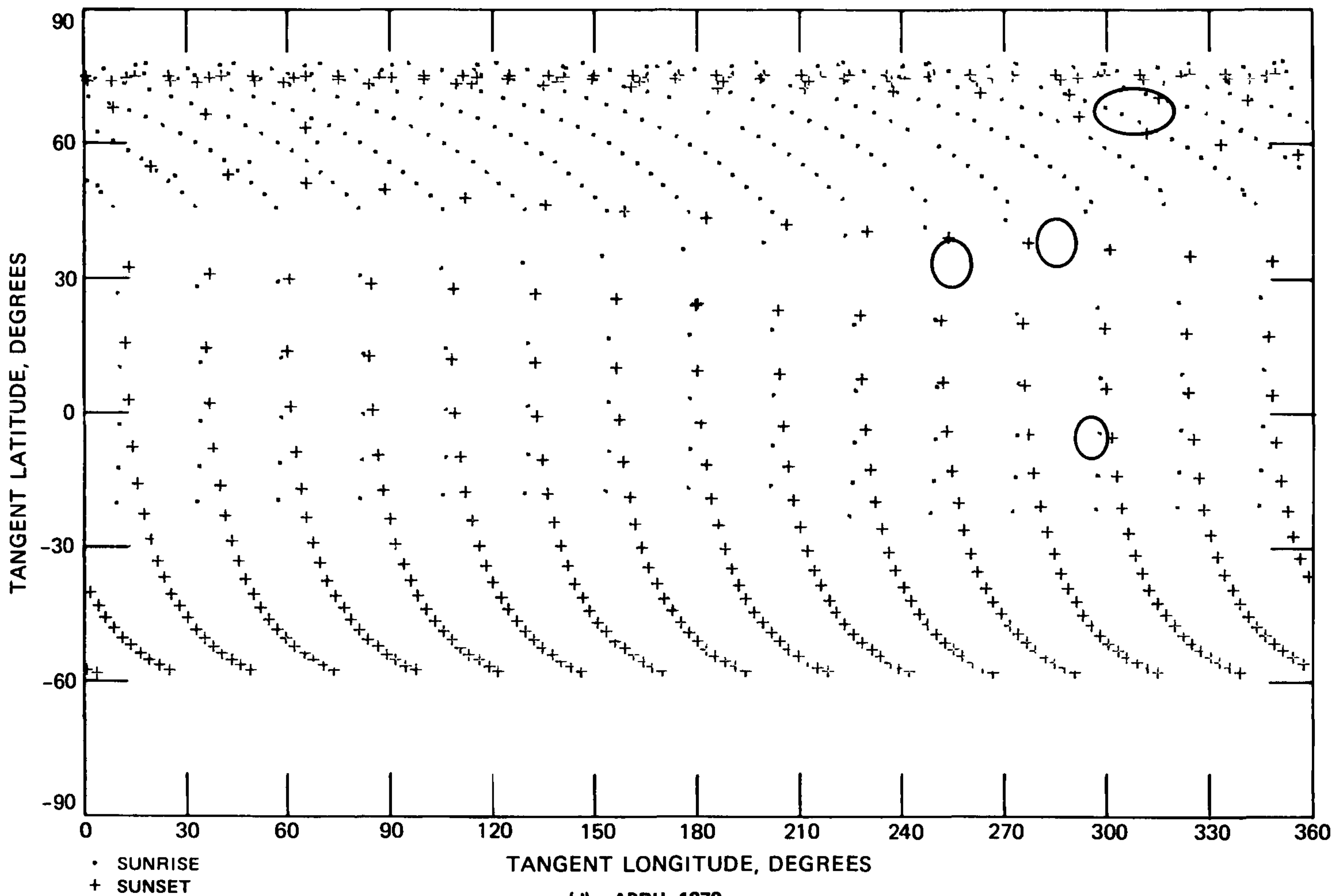

(d) APRIL 1979

FIGURE 27 SAGE SUNRISE AND SUNSET TANGENT LOCATIONS FOR SELECTED TIME PERIODS (Continued)

Calculations assume i = 55°, k = 600 km, launch time = 1030 EST, 25 January 1979 Ellipses have 500-km radius and are centered at Sondrestrom, Wallops Island, White Sands, and Natal

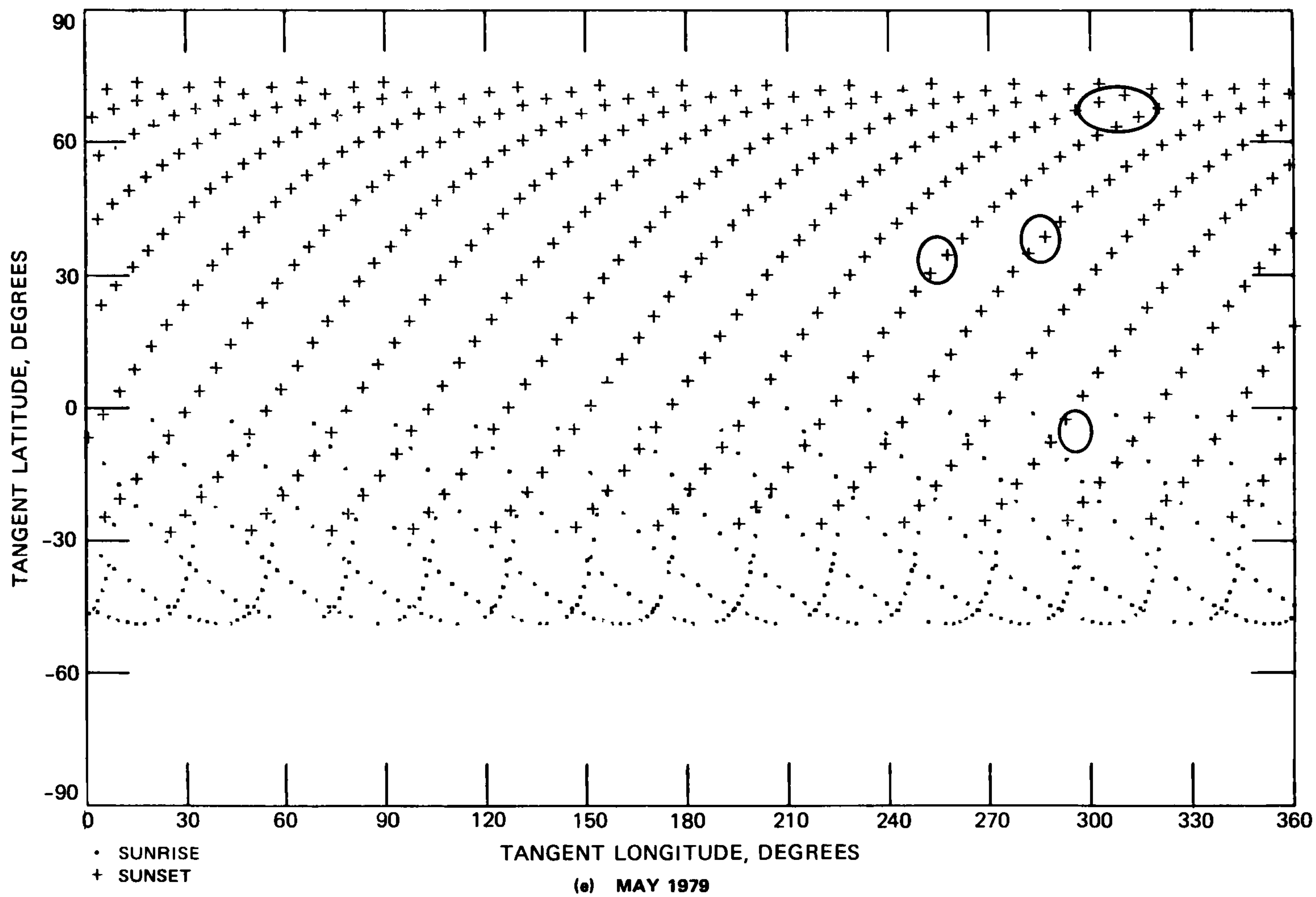

(e) MAY 1979

FIGURE 27 SAGE SUNRISE AND SUNSET TANGENT LOCATIONS FOR SELECTED TIME PERIODS (Continued)

Calculations assume $i = 55°$, $k = 600$ km, launch time = 1030 EST, 25 January 1979 Ellipses have 500-km radius and are centered at Sondrestrom, Wallops Island, White Sands, and Natal

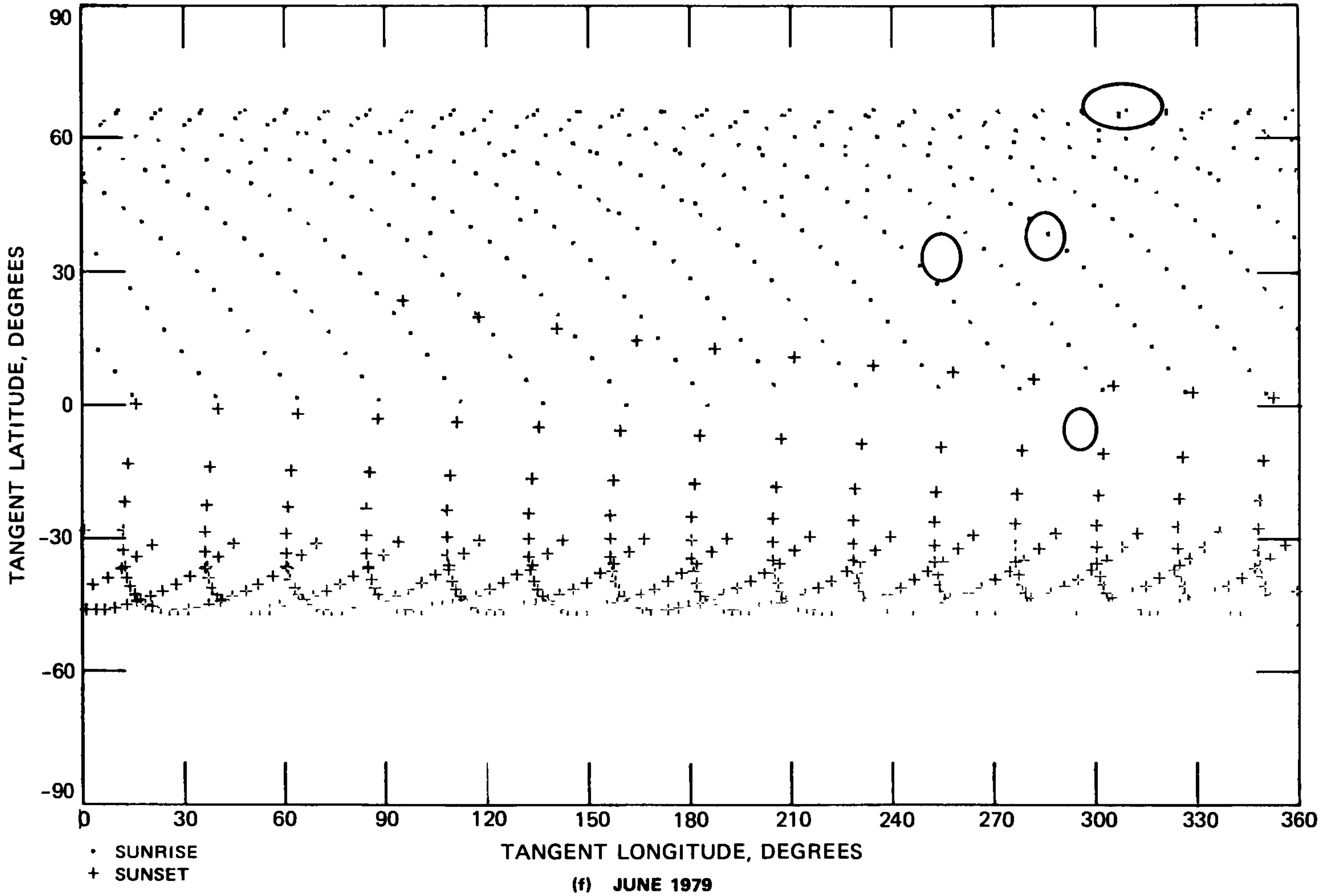

(f) JUNE 1979

FIGURE 27 SAGE SUNRISE AND SUNSET TANGENT LOCATIONS FOR SELECTED TIME PERIODS (Continued)

Calculations assume ı = 55°, k = 600 km, launch time = 1030 EST, 25 January 1979 Ellipses have 500-km radius and are centered at Sondrestrom, Wallops Island, White Sands, and Natal

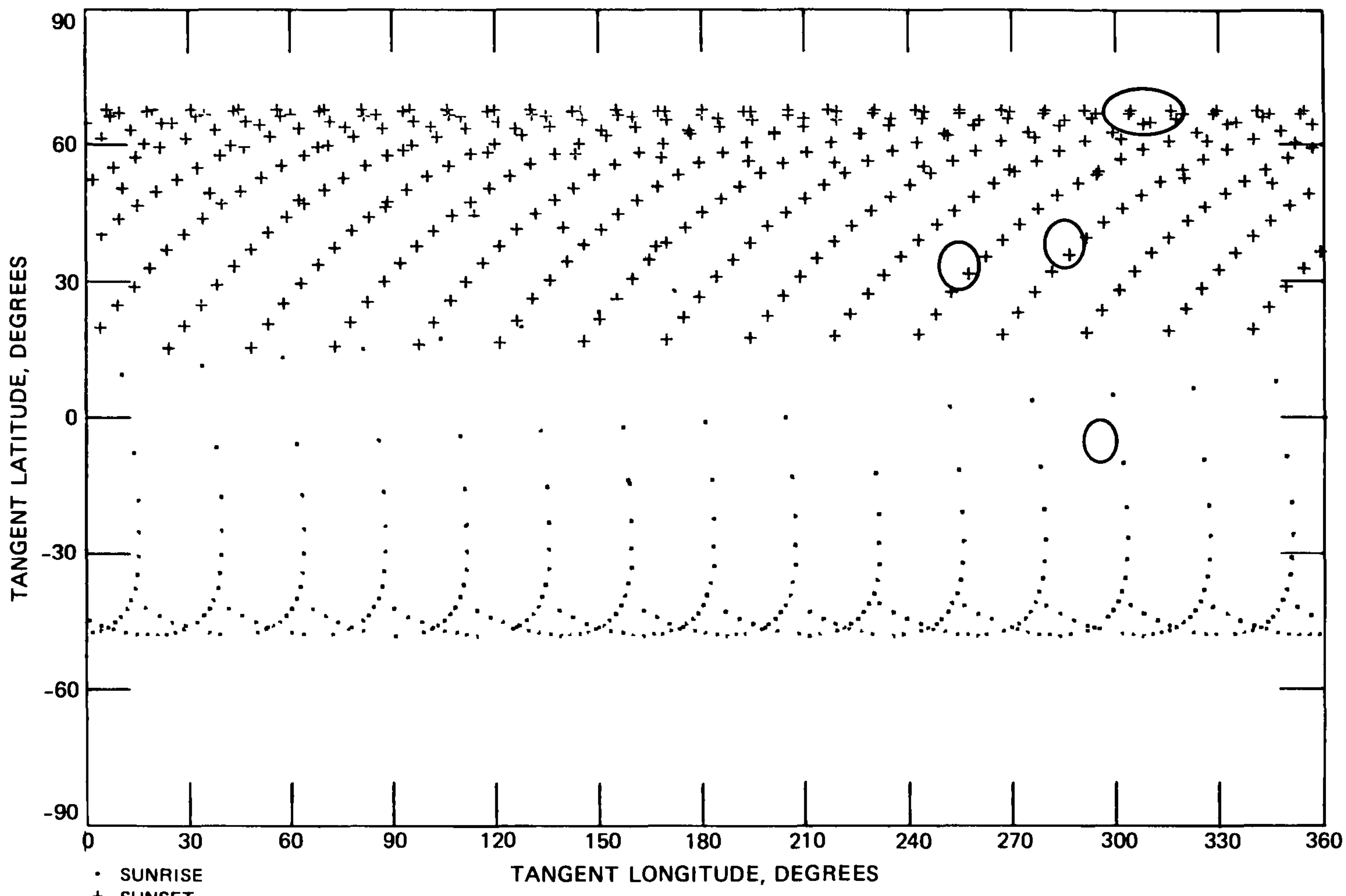

(g) JULY 1979

FIGURE 27 SAGE SUNRISE AND SUNSET TANGENT LOCATIONS FOR SELECTED TIME PERIODS (Continued)

Calculations assume $i = 55°$, $k = 600$ km, launch time = 1030 EST, 25 January 1979 Ellipses have 500-km radius and are centered at Sondrestrom, Wallops Island, White Sands, and Natal

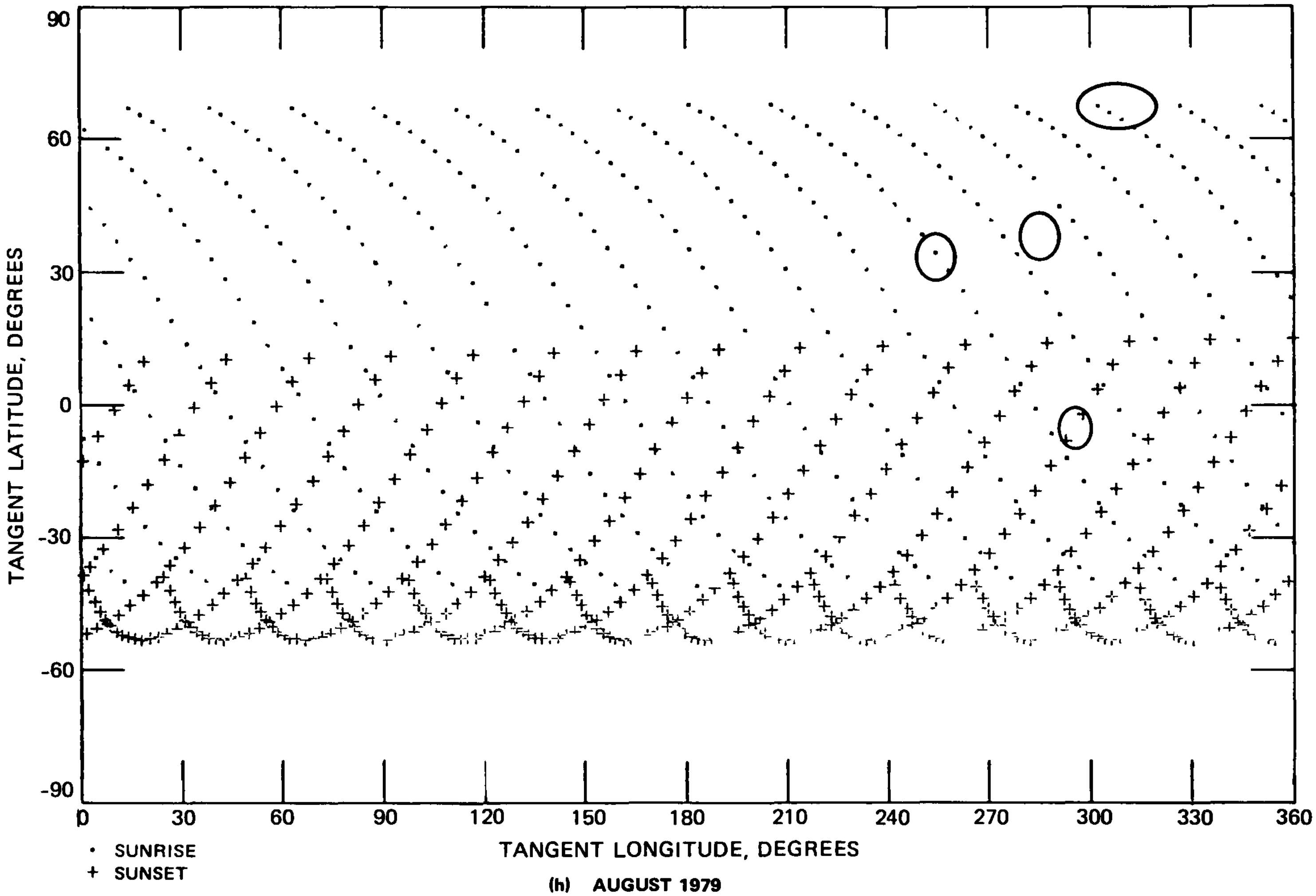

(h) AUGUST 1979

FIGURE 27 SAGE SUNRISE AND SUNSET TANGENT LOCATIONS FOR SELECTED TIME PERIODS (Continued)

Calculations assume ι = 55°, k = 600 km, launch time = 1030 EST, 25 January 1979 Ellipses have 500-km radius and are centered at Sondrestrom, Wallops Island, White Sands, and Natal

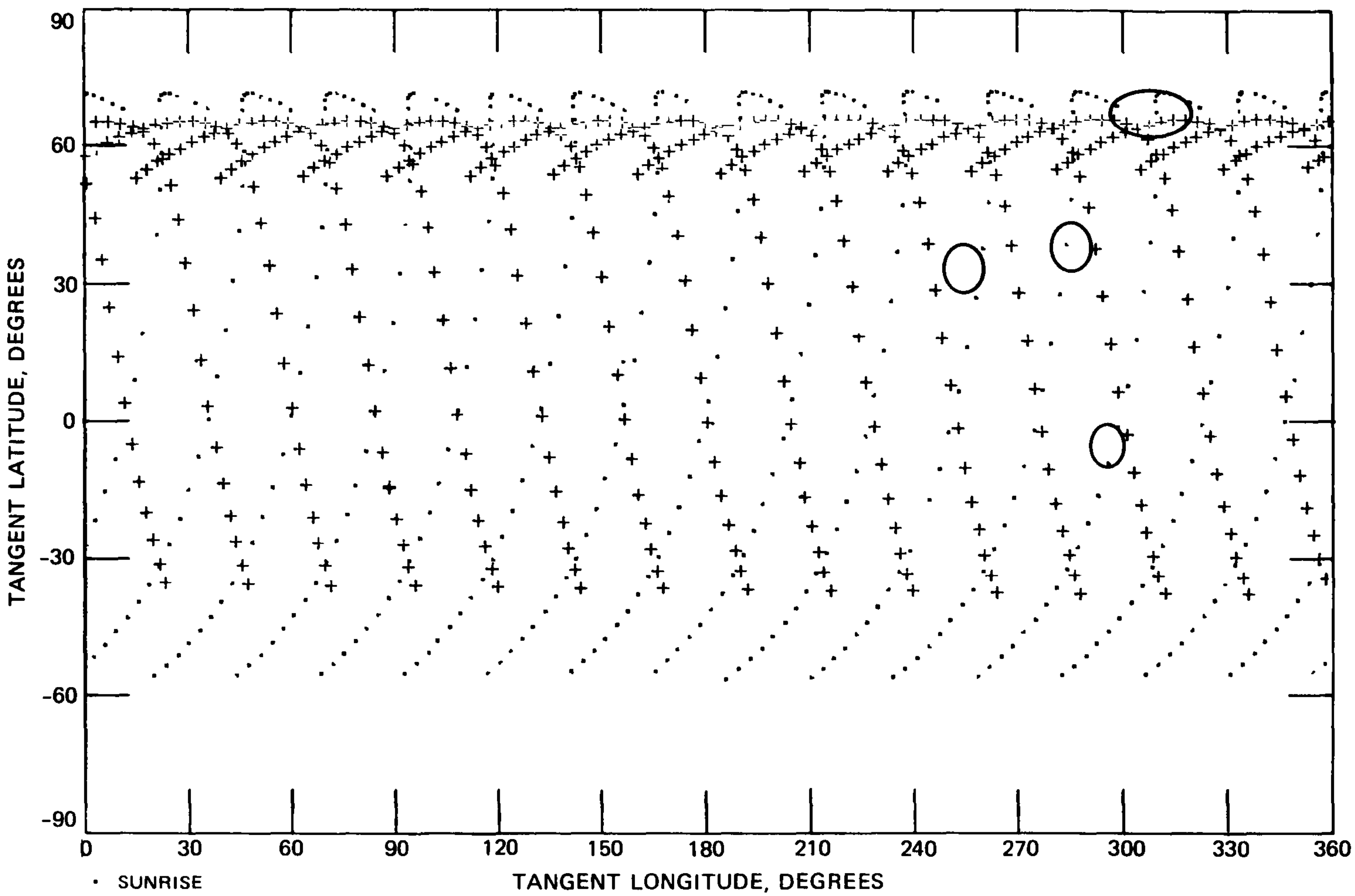

(i) SEPTEMBER 1979

FIGURE 27 SAGE SUNRISE AND SUNSET TANGENT LOCATIONS FOR SELECTED TIME PERIODS (Continued)

Calculations assume i = 55°, k = 600 km, launch time = 1030 EST, 25 January 1979 Ellipses have 500-km radius and are centered at Sondrestrom, Wallops Island, White Sands, and Natal

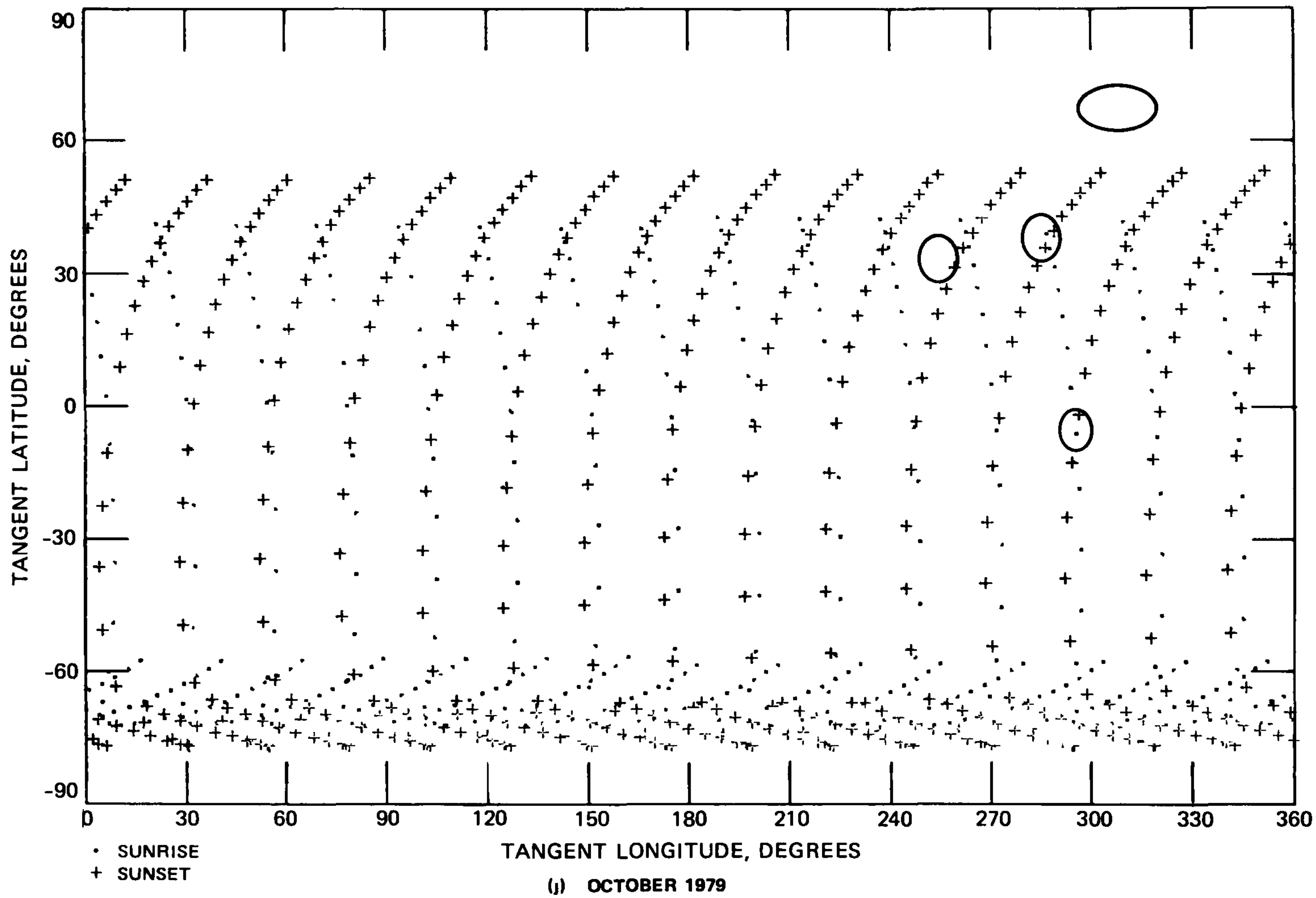

(j) OCTOBER 1979

FIGURE 27 SAGE SUNRISE AND SUNSET TANGENT LOCATIONS FOR SELECTED TIME PERIODS (Continued)

Calculations assume i = 55°, k = 600 km, launch time = 1030 EST, 25 January 1979 Ellipses have 500-km radius and are centered at Sondrestrom, Wallops Island, White Sands, and Natal

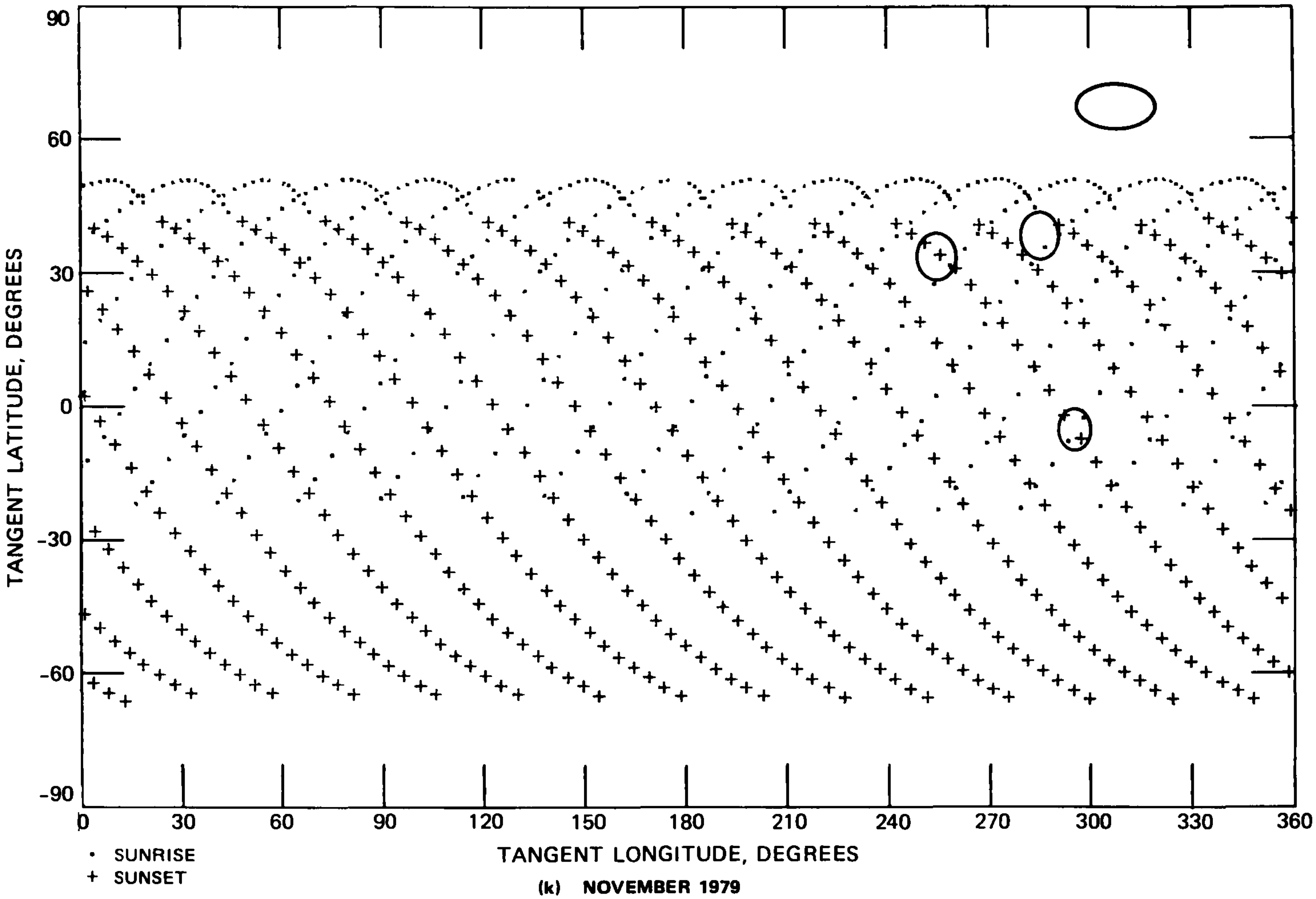

(k) NOVEMBER 1979

FIGURE 27 SAGE SUNRISE AND SUNSET TANGENT LOCATIONS FOR SELECTED TIME PERIODS (Continued)

Calculations assume $i = 55°$, $k = 600$ km, launch time = 1030 EST, 25 January 1979 Ellipses have 500-km radius and are centered at Sondrestrom, Wallops Island, White Sands, and Natal

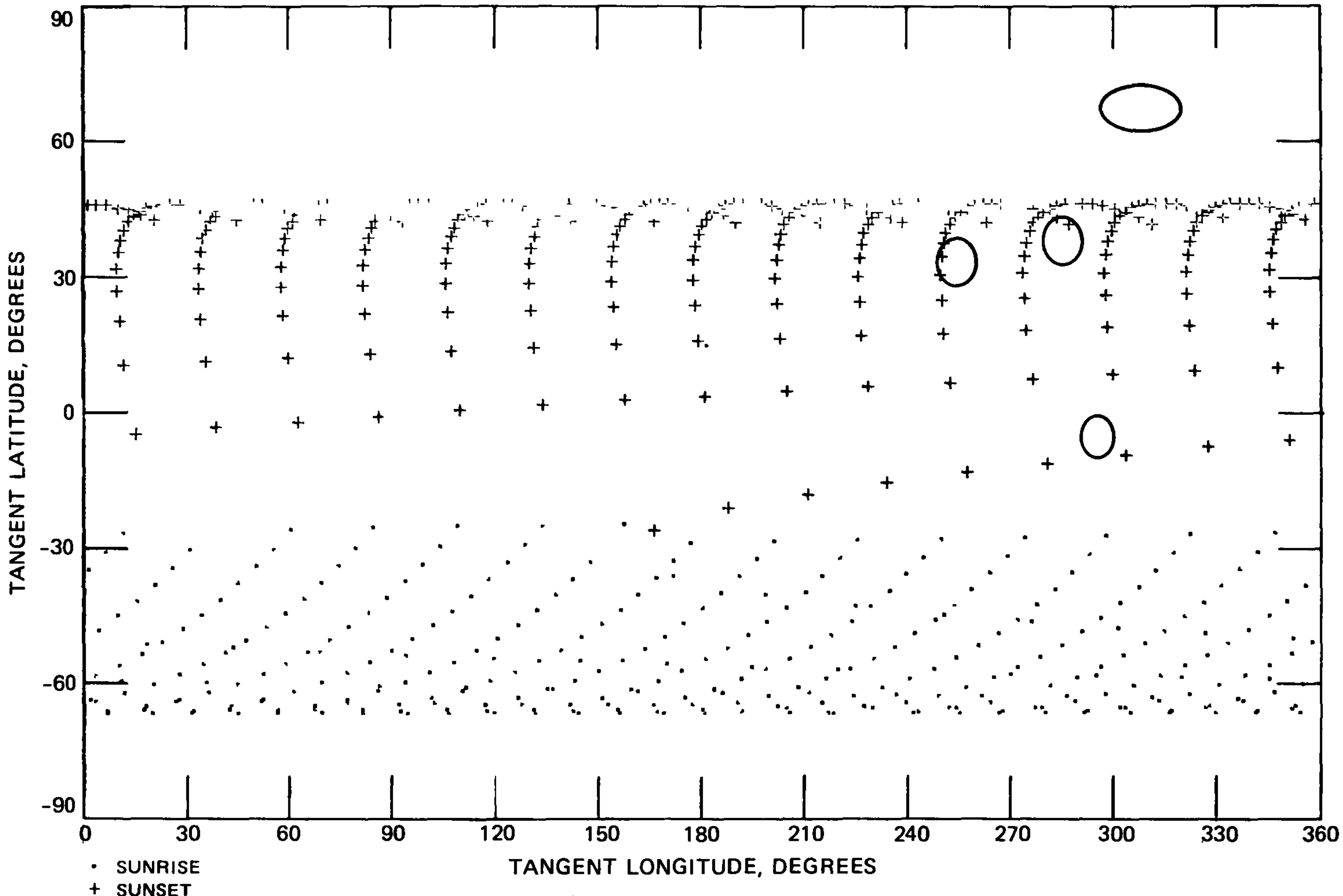

(l) DECEMBER 1979

FIGURE 27 SAGE SUNRISE AND SUNSET TANGENT LOCATIONS FOR SELECTED TIME PERIODS (Continued)

Calculations assume i = 55°, k = 600 km, launch time = 1030 EST, 25 January 1979 Ellipses have 500-km radius and are centered at Sondrestrom, Wallops Island, White Sands, and Natal

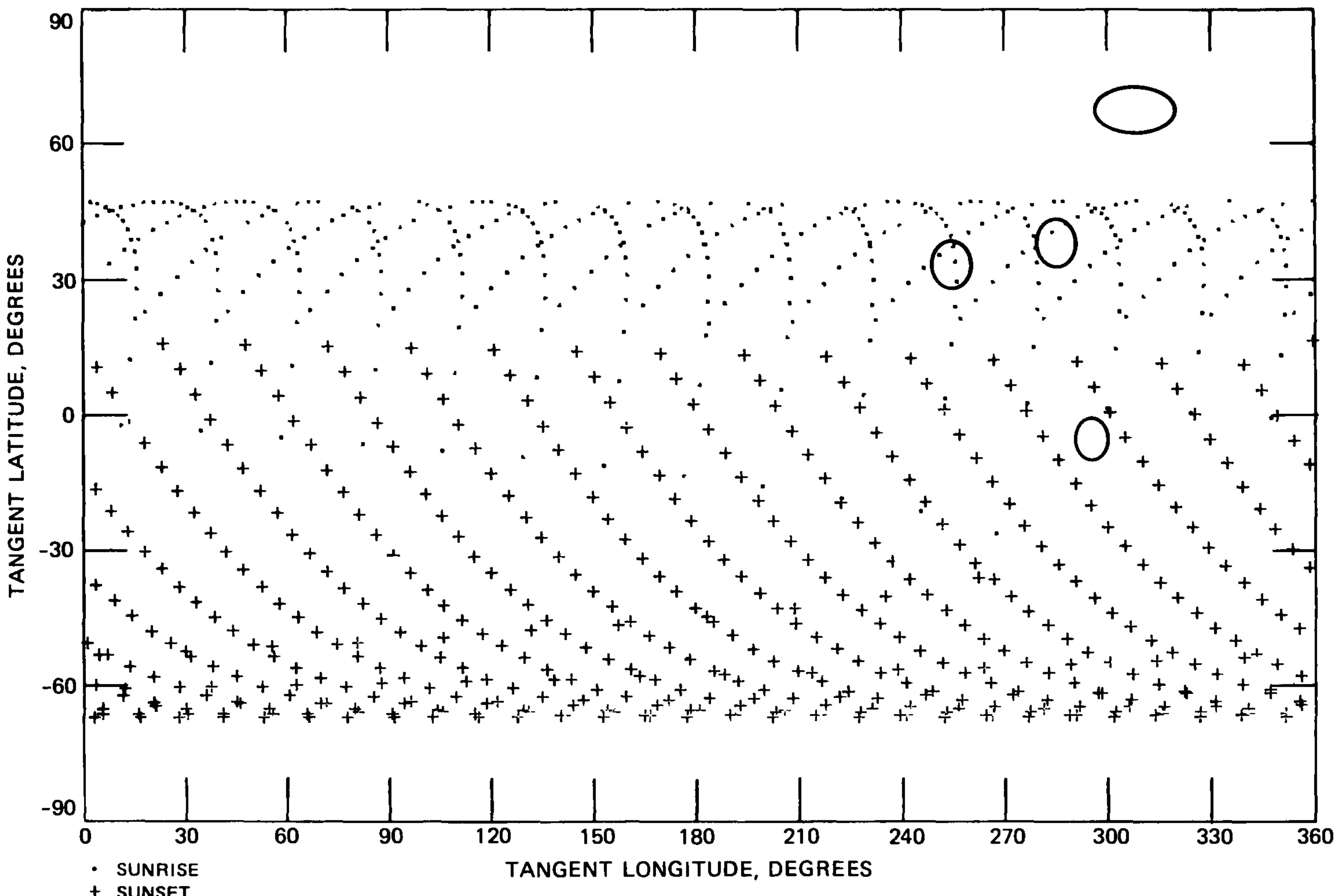

(m) JANUARY 1980

FIGURE 27 SAGE SUNRISE AND SUNSET TANGENT LOCATIONS FOR SELECTED TIME PERIODS (Concluded)

Calculations assume i = 55°, k = 600 km, launch time = 1030 EST, 25 January 1979 Ellipses have 500-km radius and are centered at Sondrestrom, Wallops Island, White Sands, and Natal

Table 9

SAGE GROUND TRUTH OPPORTUNITIES AS A FUNCTION OF LAUNCH TIME

Sage Launch (EST)	OPPORTUNITIES WITHIN 500 km RADIUS					
	Wallops Island (37 85 N, 75 48 W)		White Sands (32 38 N, 106 48 W)		Natal, Brazil (5 87 S, 35 32 W)	
	Mission Days	Distance, km	Mission Days	Distance, km	Mission Days	Distance, km
0900†	40 3	138 8	13 9	373 4	10 2 *	225 0
			17 4 *	253 5	47 2 *	223 6
			41 4 *	198 4	55 7	380 5
0930†	12 8	464 0	17 4 *	443 9	12 2 *	460 9
	19 3 *	336 9	43 4 *	447 0	21 7	489 5
1000†	14 8	388 7	12 9	439 2	–	–
	21 3 *	482 0	19 4 *	417 5		
			45 4 *	495 3		
1030†	16 8	278 9	17 9	466 4	–	–
	22 2 *	411 9	21 4 *	369 1		
1100†	18 8	158 6	19 9	379 6	–	–
	45 2 *	432 1				
	46 3 *	460 0				
1130†	20 8	36 1	21 8	340 5	28 6	419 3
	24 2 *	435 5	48 3 *	370 1		
	47 2 *	383 0				
	48 2 *	471 1				
0900‡	17 3 *	376 3	57 9	269 9	10 2 *	96 0
	18 3 *	424 8	58 9	329 4	18 7	411 5
	37 3 *	370 7				
	38 3 *	167 7				
	59 8	448 1				
0930‡	10 9	432 3	59 9	364 1	11 2 *	340 3
	11 8	371 0			19 7	393 6
	18 3 *	302 3			20 7	358 1
	19 3 *	280 5				
	39 3 *	46 6				
1000‡	12 8	366 5	19 4 *	294 8	21 7	391 6
	13 8	93 6			22 7	434 9
	14 8	424 4			48 2 *	342 2
	20 3 *	215 5			57 2 *	489 4
	21 3 *	363 6				
	41 3 *	249 0				
1030‡	14 8	321 6	20 3 *	190 3	23 7	483 6
	15 8	158 8	21 3 *	407 5	49 2 *	364 2
	22 3 *	377 1	43 3 *	456 0	56 7	193 7
	43 3 *	456 9				

inc = 55°, launch date = February 1, 1979
*Sunset
†h = (600 X 750) km
‡h = (450 X 700) km

Table 9 (Concluded)

Sage Launch (EST)	OPPORTUNITIES WITHIN 500 km RADIUS					
	Wallops Island (37 85 N, 75 48 W)		White Sands (32 38 N, 106 48 W)		Natal, Brazil (5 87 S, 35 32 W)	
	Mission Days	Distance, km	Mission Days	Distance, km	Mission Days	Distance, km
0900†	17 32 *	331 1	39 4 *	413 2	–	–
	60 8	463 4	40 4 *	405 2		
0930†	12 8	337 4	14 9	368 3	11 2 *	367 0
	13 9	426 5	17 4 *	104 7	20 2	305 3
					47 2 *	341 1
1000†	20 3 *	88 1	42 4 *	374 2	–	–
	41 3 *	402 9	43 4 *	202 1		
1030†	15 8	427 3	17 9	200 8	14 2 *	466 1
	16 8	143 0	20 3 *	167 0	15 2 *	424 7
					24 2 *	256 3
					58 7	324 2
1100†	23 2 *	175 3	45 3 *	462 8	–	–
	44 3 *	240 0	46 3 *	127 8		
	45 3 *	395 3				
0900‡	9 9	370 8	17 4 *	318 8	–	–
			39 4 *	458 3		
0930‡	12 8	499 4	17 4 *	388 4	11 2 *	426 6
			18 4 *	483 3	20 7	216 4
					47 2 *	303 8
					55 7	493 9
1000‡	12 8	374 1	14 9	423 6	–	–
	20 3 *	367 3	42 4 *	343 7		
			43 4 *	310 2		
1030‡	15 8	437 0	17 9	420 2	15 2 *	375 0
	16 8	450 7	20 3 *	434 0	23 7	446 3
			21 4 *	394 5	24 7	363 3
					50 2 *	350 3
					58 7	272 2
1100‡	15 8	450 0	17 9	414 7	–	–
	16 8	404 4	45 3 *	365 5		
	23 2 *	188 8	46 3 *	164 6		
	24 2 *	429 8				
	44 3 *	313 8				
	100 km=1 11°lat =0 87°long		100 km=1 07°lat =0 86°long		100 km=0 91°lat =0 86°long	

inc = 55°, h = 600 km
*Sunset
† Launch date = February 1, 1979
‡ Launch date = January 25, 1979

Table 10

PRIORITY OF SAGE SATELLITE COINCIDENCE SITES
FOR GROUND TRUTH MEASUREMENTS

1st	No unocculted period during first two months to avoid interference with initial ground truth experiments (listed below)
2nd	Sunrise *and* sunset satellite profiles occurring within a 5-day period at White Sands, NM (32°23' N, 106°29' W) during mid-February to early March 1979
	— or —
	Sunrise profile at White Sands
	— or —
	Sunset profile at White Sands
3rd	Sunrise and/or sunset satellite profile at Wallops Island, Virginia (37°51' N, 75°29' W) during mid-February to early March 1979
4th	Sunrise or sunset satellite profile at Natal, Brazil (5°52' S, 35°19' W) during mid-to-late March 1979

The results shown in Figure 27 and in Tables 9 and 10 have been taken into account in choosing the experiment sites and schedule shown in Table 2 Definitive tangent locations and times will be recomputed after launch, when more precise orbit data are available These results will be made available to all correlative sensor scientists, including those on the ad hoc ground truth teams and others outside the United States

3.2.2. Required Proximity of SAGE and Correlative Measurements

The required proximity of SAGE tangent scans and correlative measurements is determined by the typical variability of the measured constituents On the scales of interest (several hundred km and several hours) this variability is difficult to assess because of the very small number of appropriate measurements that have been made During nonvolcanic conditions lidar measurements of stratospheric aerosols have frequently shown that, within the layer of maximum aerosol content (~16-24 km), profile shape and magnitude were typically preserved throughout a night of observations, when stratospheric wind velocities were about 10 $msec^{-1}$ Assuming an observation time of about eight hours, this converts to a spatially uniform region of about 300 km or more Furthermore, occasional comparisons have been drawn between stratospheric lidar measurements made on the same night at locations separated by 1500-2400 km (17-27° of longitude and 2-5° of latitude, the locations included Menlo Park, California, Laramie, Wyoming, Boulder, Colorado, and Kansas City, Missouri) On these occasions, which were 8 or more months after any noticeable volcanic injections, approximate spatial uniformity was also observed

In view of these results, it appears that a proximity of ±500 km and ±2 hr between SAGE and correlative *aerosol* measurements would be satisfactory during times not appreciably perturbed by volcanic activity Conditions can be expected to be more variable during the very interesting period just after a volcanic injection However, flights by the P-3 lidar will be made to document any spatial variations in aerosol structure between the SAGE tangent location and the site of any balloon flights

Diurnal changes in *ozone* concentration caused by changes in solar irradiance should be primarily confined to altitudes above 50 km, which are above the range of SAGE measurements Between 50 and 25 km, ozone changes are related both to temperature-induced chemical changes and to transport variations Below 25 km, where ozone variations are related almost entirely to transport variations, extremely large ozone variations occur, the vertical distribution found on one day may bear little similarity to that of the previous day These low-altitude changes are primarily responsible for the variations in total ozone from day to day and, although these variations are difficult to predict, a high correlation is found between total ozone and changes of the 100-mb height field The day-to-day change in maximum ozone concentration is about 20%, and the altitude of the peak may change by as much as 4 km

In view of this temporal variability, correlative ozone measurements should be taken as close in time to the SAGE measurements as possible, probably within ±2 hours of the tangent scan It is difficult to translate the temporal variations described above into their spatial counterparts However, the spatial variations can be expected to be meteorology-dependent and possibly significant For this reason the LIMS Correlative Measurements Plan specifies a desirable proximity between LIMS scans and correlative sensors of ±0 5° latitude and ±1° longitude, with maximum separations of ±2° latitude and longitude At the SAGE ground truth sites, 1° of latitude or longitude is roughly 100 km (to within ±14%, except at Sondrestrom, where 1° of longitude is only about 40 km) Thus, the LIMS plan specifies maximum separations of about ±200 km From Figure 27 and Table 9 it can be seen that, within any given month, the probability of a SAGE tangent scan's falling within 200 km of a ground truth site is very small Thus, it would be unrealistic to specify such a small coincidence requirement for SAGE correlative measurements Nevertheless, because of the variabilities mentioned above, it is important that each SAGE correlative experiment attempt to characterize the local spatial variability near the time of the experiment This will be done by making ozone profile measurements several days and hours before and after SAGE tangent scans, as well as during the scans (See Sections 3 2 4 and 3 2 5)

3.2.3. Cluster Concept

Because of the need to measure multiple constituents (hence, to use multiple sensors) and the desire to take advantage of existing capabilities, the SAGE Ground Truth Plan was built around measurement facilities that formed natural clusters These clusters are described in more detail in Table 3 (Section 1 2) Within some of the clusters simultaneous aerosol or ozone measurements can be made from different sites Such simultaneous measurements will be useful in characterizing spatial variability in the region of SAGE tangent scans

3.2.4. Northern Hemisphere Measurements

3.2.4.1. Experiment 1--Wallops Island/Hampton, April 1979

The sensors to be included in this experiment have been listed in Table 2 Figure 28 shows a typical measurement sequence for the correlative sensors that are launched within a few hours of the SAGE tangent scan

3.2.4.2. Experiment 2--Holloman/White Sands, March 1979

Sensors are listed in Table 2 and more information is presented in Table 11 A typical time sequence both for sunrise and for sunset scans is shown in Figure 29

3.2.4.3. Experiment 4--Sondrestrom or Poker Flats, Spring or Summer 1979

Sensors are listed in Table 2 A typical measurement sequence both for SAGE sunrise and for SAGE sunset scans is shown in Figure 30 Note that, because of its retrograde orbit, SAM II views a sunset while SAGE and earthbound observers view a sunrise, conversely, SAM II views a sunrise while SAGE and earthbound observers view a sunset

3.2.4.4. Experiment 5--Wallops Island/Hampton, Fall 1979

Sensors are listed in Table 2 The measurement sequence is as shown in Figure 28

3.2.4.5. Experiment 6--Wallops Island/Hampton, Winter 1979-80

Sensors are listed in Table 2 The measurement sequence is as shown in Figure 28

3.2.4.6. Other Northern Hemisphere Measurements

It is expected that other northern hemisphere measurements will be scheduled by the European and Japanese ad hoc ground truth groups (See Section 2 1, Tables 4 and 5, and Figure 3) The SAGE Experiment Team will furnish predictions of SAGE tangent locations and times to these groups The correlative sensor scientists will then schedule observations on the basis of these opportunities and their own constraints

3.2.5. Southern Hemisphere Measurements

3.2.5.1. Experiment 3--Foraleza/Natal, April 1979

Sensors are listed in Table 2 The measurement sequence will be as shown in Figure 28, with the addition of a dustsonde sequence as in Figure 29

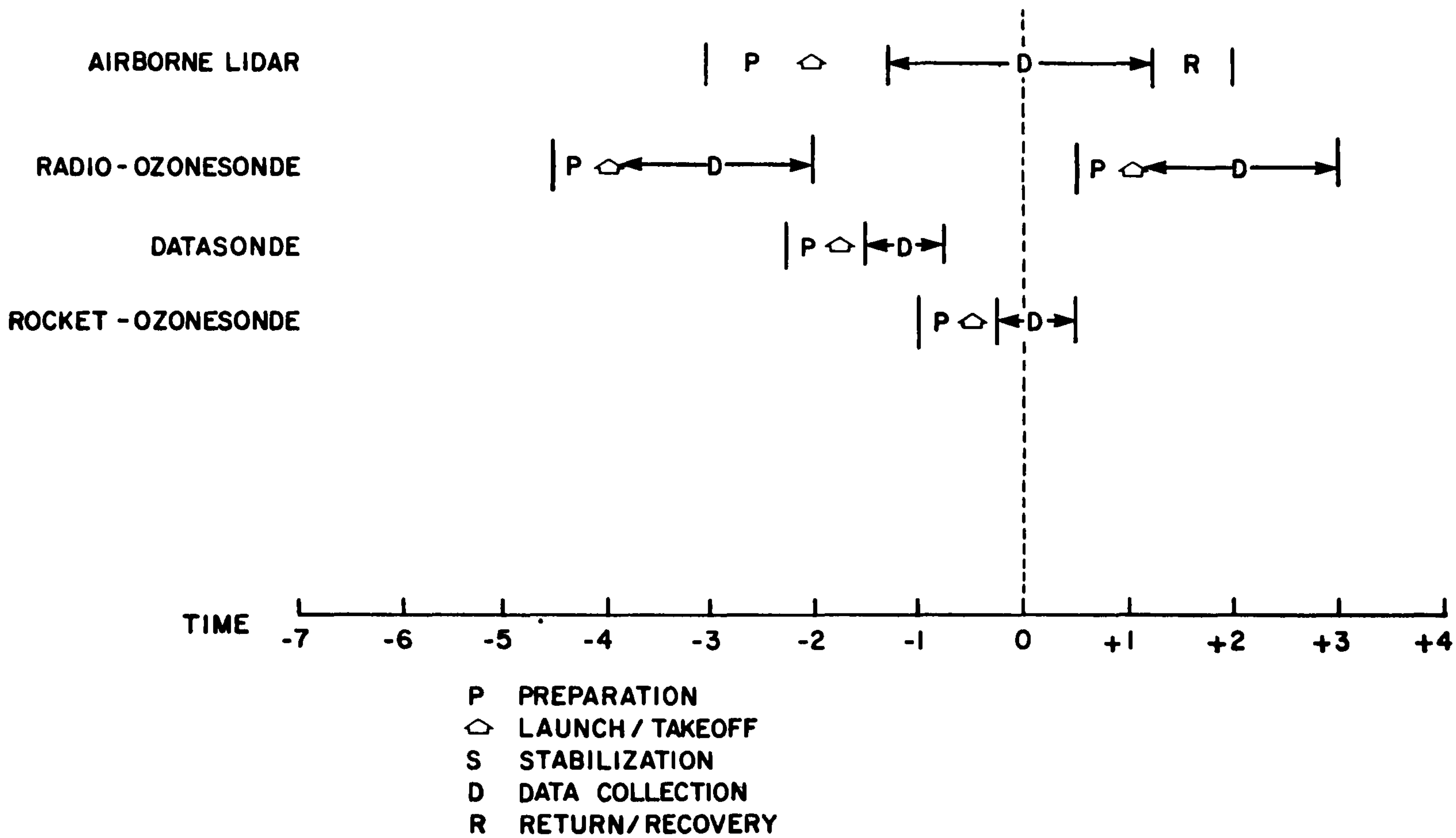

FIGURE 28 TYPICAL CORRELATIVE MEASUREMENT SEQUENCE FOR SAGE SUNRISE OR SUNSET PROFILE AT WALLOPS ISLAND

Table 11

PRELIMINARY DESCRIPTION OF SAGE GROUND TRUTH EXPERIMENTS AT HOLLOMAN AFB, NM

Measurement	Measurement Coordinator(s)	Flight Schedule	Flight Duration	Maximum Altitude	Maximum Diameter	Load Train Length	Transmitter and Payload Weight
Airborne Lidar	W H Fuller (NASA-LaRC)	5 flts (1 flt/day)	4 hrs	16,000 ft			
Dustsonde	D T Hoffman (U of Wyoming) J M Rosen (U of Wyoming)	1 flt	3 hrs	100,000 ft	50 ft	320 ft	20 lbs
Balloon Sunphotometer	T J Pepin (U of Wyoming)	1 flt	9 hrs	100,000 ft	60 ft	20 ft	150 lbs
Rocket Ozonesonde	T Perry D Bruton (NASA-WFC)	2 flts	2 hrs	250,000 ft	16 ft	18 ft	2 lbs
Balloon Ozonesonde	T Perry D Bruton (NASA-WFC)	4 flts	2 hrs	100,000 ft	9 ft	50 ft	4 lbs
Balloon Interferometer	D G Murcray (U of Denver)	1 flt	5 hrs	120,000 ft	275 ft	200 ft	1400 lbs
U-2 $O sub 3 $, NO, T Sensor	M Lowenstein T Starr (NASA-ARC)						
U-2 Wire Impactor	N Farlow, G Ferry (NASA-ARC)	2 flts	6 hrs	70,000 ft			
U-2 Quartz Crystal Microbalance	M P McCormick (NASA-LaRC) D C Woods (NASA-LaRC)	2 flts	6 hrs	70,000 ft			
U-2 Multifilter Package	A Lazrus (NCAR)	2 flts	6 hrs	70,000 ft			
U-2 Glass Collector	R Charlson (U of Washington)	2 flts	6 hrs	70,000 ft			

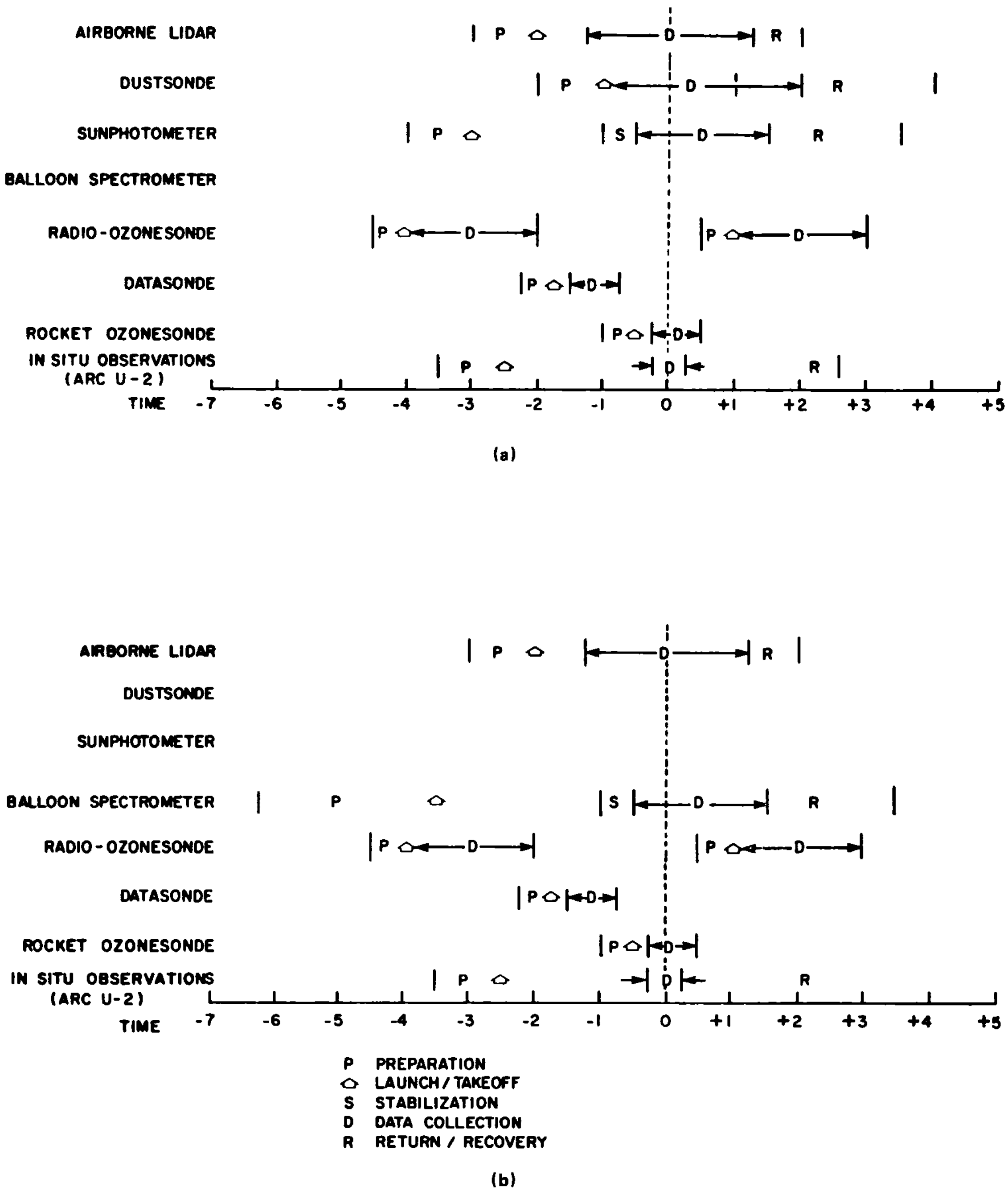

FIGURE 29 TYPICAL CORRELATIVE MEASUREMENT SEQUENCE FOR SAGE SUNRISE AND SUNSET PROFILE AT HOLLOMAN-WHITE SANDS IN FEBRUARY 1979

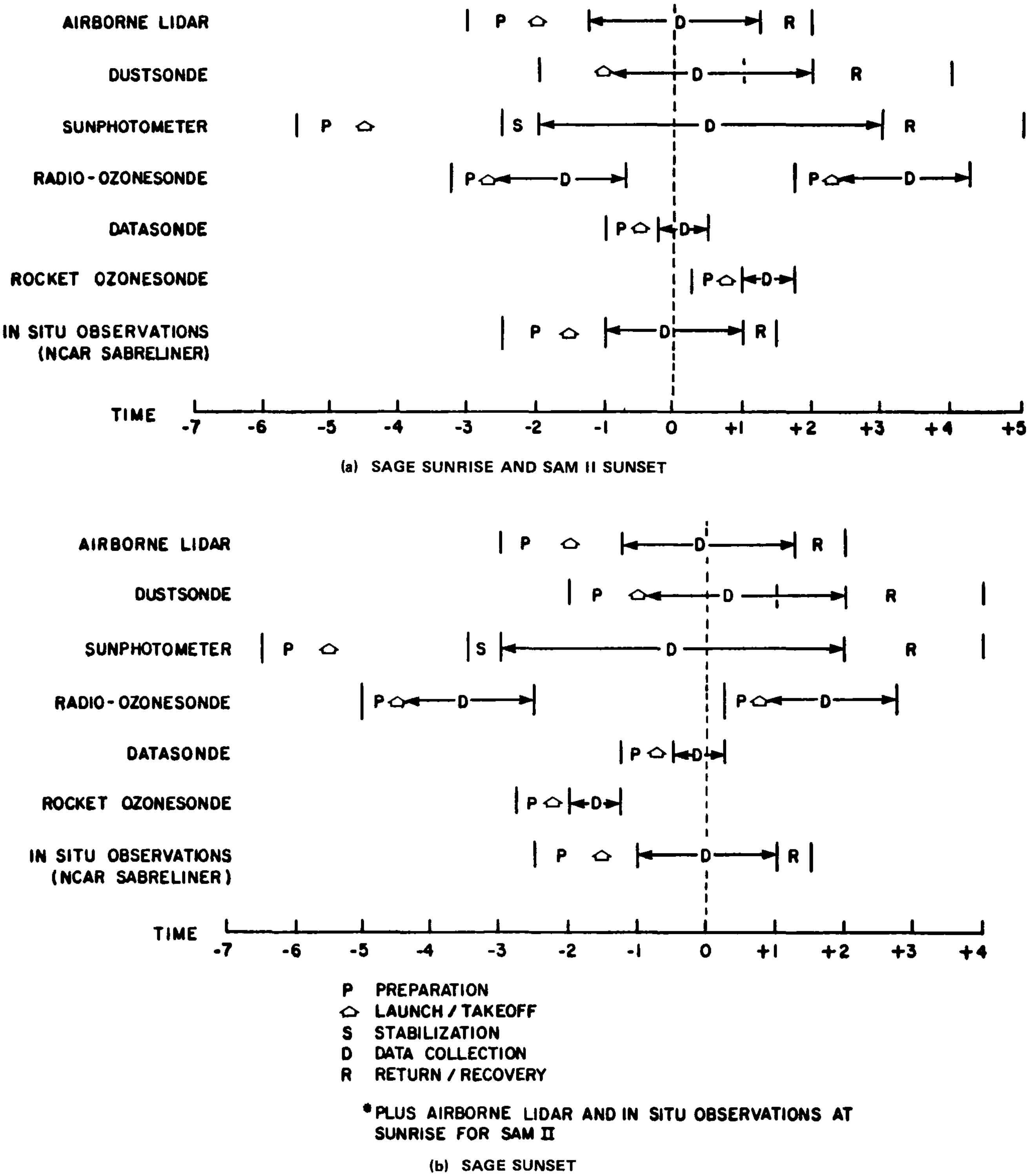

FIGURE 30 TYPICAL CORRELATIVE MEASUREMENT SEQUENCE FOR SAGE SUNRISE AND SAM-II SUNSET PROFILE AND FOR SAGE SUNSET PROFILE AT SONDERSTROM IN SUMMER 1979

3.2.5.2. Other Southern Hemisphere Measurements

It is hoped that other southern hemisphere measurements will be scheduled by CSIRO in Australia and INPE in Brazil (See Appendix B, Table B-1) In particular, Dr John Gras of CSIRO is planning balloon-borne measurements of aerosol concentration for several size cutoffs

4. DATA PROCESSING

Procedures for reducing ground truth data to formats that are readily comparable to SAGE extinction and number profiles will be established and tested prior to launch, so that data comparisons can be carried out in the shortest time possible

4.1. Ancillary Data

Both the lidar and sunphotometer data require a molecular density profile for separation of gaseous from particulate optical coefficients In addition, the lidar data (especially ruby data) require an estimated ozone and particulate extinction profile A two-step process will be used to incorporate these ancillary data into the data analysis

4.1.1. Model Atmospheres

Prior to launch, model profiles of atmospheric density and of ozone and particulate extinction (at the lidar wavelengths) will be developed for the location and month of each ground truth site (see Table 2) These profiles will be stored on cards or another medium that can be computer-read as input to the lidar and sunphotometer data reduction algorithms (see Section 4 2) They will be used for initial reduction of the lidar and balloon photometer data

4.1.2. Measured Atmospheres

Each ground truth experiment will include at least one measurement of the local temperature and pressure profiles (These will be provided by standard radiosonde, by radiosonde packages on the ozone balloonsondes, by the rocket-launched datasondes, and by the dustsondes, which measure temperature and pressure in addition to the aerosol data See also Section 4 2 4) These profiles will be converted to density profiles and stored in the same format as the model density profiles, so that they can be readily substituted for the model profiles in the data reduction In addition, as a routine part of SAGE data reduction, density profiles for the time and location of each SAGE scan will be derivYd from the SAGE data These SAGE density profiles will be extracted from the SAGE data tapes and stored in the same format as the model and sonde-measured density profiles Model, sonde-measured, and SAGE-measured density profiles will be plotted for each ground truth experiment when available In this manner differences in density profiles can be highlighted and, by using each profile sequentially in the data analysis, effects of density differences on derived constituent profiles (both SAGE and correlative) can be explored and understood

Carefully chosen model ozone profiles are probably adequate for lidar data reduction (certainly for Nd lidar), nevertheless, measured ozone profiles near the time and location of lidar flights will be compared to the model profiles and, if necessary, substituted Likewise, particulate extinction profiles (at the lidar wavelength) derived from the lidar and SAGE measurements will be compared to the model profiles and iteratively substituted whenever appropriate

4.2. Production of Data Products for Comparison to SAGE Data

4.2.1 Ozone Data

4.2.1.1. Dobson Spectrophotometer

Dobson spectrophotometer observations will normally be made three times daily (morning, near local noon, and afternoon) The observational procedures that will be followed are outlined in the Weather Service Observer's Manual [9] The Dobson dial readings and other pertinent data are entered by hand on the NOAA observation form, NWS form B-35b (3-73) shown in Figure 31a Instructions regarding the use of this form are provided on the reverse side (Figure 31b) The total ozone overburden above each site is derived by applying the appropriate correction factors and the air mass data pertinent to that site Sample results obtained by both manual and computer data processing are shown in Figures 32 and 33

4.2.1.2. Canterbury Spectrometer

The Canterbury spectrometer will conduct basically the same type of observations, with similar data output and data delivery schedules as for the Dobson spectrophotometer

4.2.1.3 Balloon ECC Ozonesonde

The data measured as the ECC ozonesonde rises consist of a vertical profile of ozone However, since the ozonesonde is attached to a standard radiosonde, atmospheric pressure, temperature, and relative humidity data are also measured (See Section 4 2 4) The ozone data are fed to the telemetry unit in the radiosonde and transmitted in flight to an AN/GMD, where they are automatically recorded along with the pressure, temperature, and humidity data on a TMQ-5 recorder The GMD antenna angles are recorded on a control recorder Figure 34 depicts the acquisition and flow of ozone data These are subsequently digitized and inputted to the Wallops ozone computer program, where they are merged with associated calibration data The calibration data are obtained from the ozonesonde's preflight calibration process and the radiosonde's preflight baseline checks The ozone data are then outputted as tables (Figure 35) and charts (Figure 36) Typically, the final data for flights launched from Wallops will be available within 1-2 weeks Final data from launches away from Wallops (allowing for transmittal from the field site to Wallops) will be available within 3-4 weeks These data will also be provided on magnetic tape Standard card and plotting formats for comparisons of SAGE and correlative profile data are described in Section 4 2 5

4.2.1.4. Super Loki Optical and Super Arcas Chemiluminescent Ozone Payloads

Both these systems are launched on rockets and are ejected at apogee to descend on a decelerator The ozone measurements are made during the descent phase Figure 37 shows the data flow for these systems The measured data are transmitted to an AN/GMD which is modified to allow it to receive and record an 8-bit PCM telemetry signal from these payloads The frequency is the standard AN/GMD 1680 MHz In addition, to obtain accurate position data of the ozone sensor during descent, radar tracking is required All the rocket systems

[9] Observer's Manual, Dobson Ozone Spectrometer revised November 1 1972 U S Department of Commerce National Weather Service

WB FORM B-35b (3-73)

U.S. DEPARTMENT OF COMMERCE
NATIONAL OCEANIC AND ATMOSPHERIC ADMINISTRATION
NATIONAL WEATHER SERVICE

OZONE OBSERVATIONS

Station: WSSF, WALLOPS ISL. VA. BLDG. X 85

Instrument No: 72

											PUNCH CARD COLUMNS FOR USE IN PREPARING FORM 610-15C
OBSERVATIONS	R_A or R_C	•	878	736	106.1		936	73.0	981		
		•	875	736	106.4		981	73.2	997		
		•	875	73.6	106.8		92.8	73.6	100.3		
	R_D or R_C'	•	33.2	29.0	39.3		34.7	28.2	36.2		
		•	33.4	29.0	39.1		34.5	28.4	36.5		
COMPUTED DATA	Mean R_A or R_C		87.6	73.6	106.4		93.2	73.3	99.4		
	Mean R_D or R_C		33.3	29.0	39.2		34.6	28.3	36.4		
	DO NOT PUNCH ABOVE THIS LINE										
	N_A or N_C										13 to 18
	N_D or N_C										20 to 26
	Declination = δ										29 to 36
	Greenwich Hr Angle = GHA										38 to 45
CODED DATA	Type of Observation	•	AD DSGQP	AD DSGQP	AD DSGQP		AD DSGQP	AD DSGQP	AD DSGQP		47 to 50
	Day of the Month	•	1	1	1		2	2	2		52 and 53
	Time of Observation	•	1000·55	1217 35	1456.00		0945 20	1216·25	1446·00		55 to 58
	Month and Year	•	4-78	4-78	4-78		4-78	4-78	4-78		60 to 63
	Instrument and Station		72								66 to 71
	Computer Project										72 to 80
	DO NOT PUNCH BELOW THIS LINE										
OUTPUT ENTRIES	μ										
	N_A−N_D N_C−N_D or N_C										Δ N_A = ____
	Δ N_C										Δ N_C = ____
	δ (Δ N_C)										Δ N_C = ____
	Corrected N_C										Δ N_D = ____
	x cm										
	Δx or MF										
	Corrected x cm										Date of N Tables
NOTES	Blue Sky C H VH	•	C	C			C	C			
	Cloudy Zenith: Height L M H	•			H				H		
	Cloudy Zenith: Thickness TN M TK	•			TN				TN		
	Cloudy Zenith: Texture U V P	•			V				V		
											Computed by
											Checked by
Observer's Initials			WRL	WRL	AB		WRC	WRC	AB		

WB FORM B-35b 3-73

(a) FORM

FIGURE 31 DOBSON OZONE OBSERVATION FORM AND INSTRUCTIONS

INSTRUCTIONS

1. GENERAL

The arrangement of WS Form B – 35b is dictated by computer programming and punch card requirements. Observational data should be entered only in the rows marked with an asterisk, and should be recorded in successive columns, except that blank columns should be used to separate data obtained on different days.

2. ENTRY OF DATA

a. **Station** - Enter the name of the station.

b. **Instrument Number** - Record the serial number of the Dobson Ozone Spectrophotometer employed.

c. **Observations** - Enter the spectrophotometer dial readings to the nearest tenth of a degree. Observational procedures are outlined in the Observers' Handbook Dobson Ozone Spectrophotometer.

d. **Coded Data**

(1) **Type of Observation** - Indicate the type of observation made, according to the code in the following table

Code	Wavelengths Used	Light Source
ADDSGQP	A and D	Direct Sun, Using GQP
CDDSGQP	C and D	Direct Sun, Using GQP
ADZB	A and D	Blue Zenith
CC'ZB	C and C'	Blue Zenith
ADZC	A and D	Cloudy Zenith
CC'ZC	C and C'	Cloudy Zenith

Specially trained observers may at times be required to make the following additional types of measurements

Code	Wavelengths Used	Light Source
CDDSFI	C and D	Focussed Image of Sun
ADRMFI	A and D	Focussed Image of Moon
CDRMFI	C and D	Focussed Image of Moon

(2) **Day of the Month** - Enter the day of the month, local standard time (LST), corresponding to the time of observation, e.g., 02 for the second day of the month.

(3) **Time of Observation** - Enter local standard time of observation, in 24-hour clock time, to the nearest hour, minute and second, e.g., 16 20 07 for an observation made 07 seconds after 4 20 P M.

(4) **Month and Year** - Use two figures to designate the month, followed by a blank and two figures to designate the year, e.g., 07 67 for July, 1967.

e. **Notes**

(1) **Description of Blue Sky** - When an observation is made on direct sun (or moon) or on the blue zenith, indicate the state of clarity of sky in the vicinity of the sun (or moon) or the zenith according to the following code

C - Clear	H - Hazy	VH - Very Hazy

(2) **Description of the Cloudy Zenith** - When an observation is made on the cloudy zenith, indicate the cloud height, thickness and texture in the vicinity of the zenith according to the code in the following table

Cloud Height	Cloud Thickness	Cloud Texture
L - Low	TN - Thin	U - Uniform
M - Middle	M - Medium	V - Variable
H - High	TK - Thick	P - Patchy

Space is provided under "Notes" for recording additional information pertaining to the accuracy of an observation, e.g., indicate the presence of fog, smoke etc.

f. **Observer's Initials** - The observer should initial the observational data for which he is responsible.

WS FORM B-35b 3-73

* U.S. GOVERNMENT PRINTING OFFICE: 1973 768-076

(b) INSTRUCTIONS

FIGURE 31 DOBSON OZONE OBSERVATION FORM AND INSTRUCTIONS (Concluded)

OZONE DATA REDUCTION FORM

Manual Data Reduction from AD or CD Direct Sun Measurements by Dobson Spectrophotometer

COL #	NAME OR OPERATION	WSSF, WALLOPS FLIGHT CTR, VA.		
1	DATE	4-1-78		
2	TIME	1501	1718	1956
3	WAVELENGTH	AD	AD	AD
4	R_A or R_C	87.6	73.6	106.4
5	R_o	87	73	106
6	ΔR	.6	.6	.4
7	N_o	955	828	112.8
8	ΔN	.5	.5	.4
9	$N_{A,C}$=(7)+(8)	960	83.3	113.2
10	R_D	33.3	29.0	39.2
11	R_o	33	29	39
12	ΔR	.3	0	.2
13	N_o	34.4	30.4	40.4
14	ΔN	.3	0	.2
15	N_D=(13)+(14)	34.7	30.4	40.6
16	(9)-(15)	61.3+0.3= 61.6	52.9+0.3= 53.2	72.6+0.3= 72.9
17	T_o	1500	1718	1954
18	ΔT=(2)-(17)	1	0	2
19	μ_o	1.384	1.196	1.569
20	$\Delta\mu$	-0.020	0	0.035
21	$\Delta T * \Delta\mu/6$	-0.003	0	0.012
22	μ=(19)+(21)	1.381	1.196	1.581
23	C_1* (16)	44.4	38.3	52.5
24	(23)/μ	32.1	32.0	33.2
25	(24)-C_2	31.2	31.1	32.3
26	X=(25)/100	.312	.311	.323

	AD	CD
C_1	.7205	2.037
C_2	0.9	1.2

INTERPOLATION TABLE FOR ΔN

ΔR	.9	1.0	1.1
.1	.1	.1	.1
.2	.2	.2	.2
.3	.3	.3	.3
.4	.4	.4	.4
.5	.4	.5	.6
.6	.5	.6	.7
.7	.6	.7	.8
.8	.7	.8	.9
.9	.8	.9	1.0

FIGURE 32 MANUAL WORKUP FOR DOBSON TOTAL OZONE OVERBURDEN

** TOTAL OZONE REDUCTION PROGRAM **

STATION	INSTRUMENT	DAY	DATE	DECLINATION	D/DT (DEC)	EPHEMERIS TRANSIT	D/DT (EPH)
WALLOPS ISLAND	DOBSN1	TUESDAY	10 4 77	-4.13. 3.7	-1388.3	11.48.44.53	-18.14

WEATHER, COMMENTS...INTERCOMPARISON DATA TAKEN BY DICK BRADFORD ET AL, TEST RUN FOR HIM,

	TIME	AIRMAS	1/AMAS	ATTN A	ATTN C	ATTN D	OZN A	OZN C	OZN D	OZN AC	OZN AD	OZN CD	COMMENTS
1	952.00	1.5625	0.6400	0.8545	0.	0.1749	0.3129	0.	0.3109	0.	0.3134	0.	TEST SET
2	958.00	1.5389	0.6498	0.8370	0.	0.1645	0.3111	0.	0.2970	0.	0.3148	0.	
3	1003.00	1.5206	0.6576	0.8318	0.	0.1665	0.3129	0.	0.3041	0.	0.3152	0.	
4	1059.00	1.3851	0.7220	0.7524	0.	0.1458	0.3107	0.	0.2924	0.	0.3155	0.	
5	1103.00	1.3795	0.7249	0.7476	0.	0.1434	0.3100	0.	0.2887	0.	0.3155	0.	
6	1146.00	1.3491	0.7412	0.7329	0.	0.1375	0.3108	0.	0.2832	0.	0.3180	0.	

END OF PROCESSING FOR DOBSN1 ON 10 4 77 AT WALLOPS ISLAND RAW DATA IS LISTED BELOW

RAW DATA	TIME	DATA 1	DATA 2	DATA 3	DATA 4	DATA 5	DATA 6	COMMENTS
1	952.00	99.60	0.	36.20	0.	0.	0.	TEST SET
2	958.00	97.40	0.	34.90	0.	0.	0.	
3	1003.00	96.60	0.	34.90	0.	0.	0.	
4	1059.00	86.20	0.	31.40	0.	0.	0.	
5	1103.00	85.60	0.	31.10	0.	0.	0.	
6	1146.00	83.60	0.	30.20	0.	0.	0.	

END OF RAW DATA FOR DOBSN1 ON 10 4 77 AT WALLOPS ISLAND

FIGURE 33 COMPUTER WORKUP FOR DOBSON TOTAL OZONE OVERBURDEN

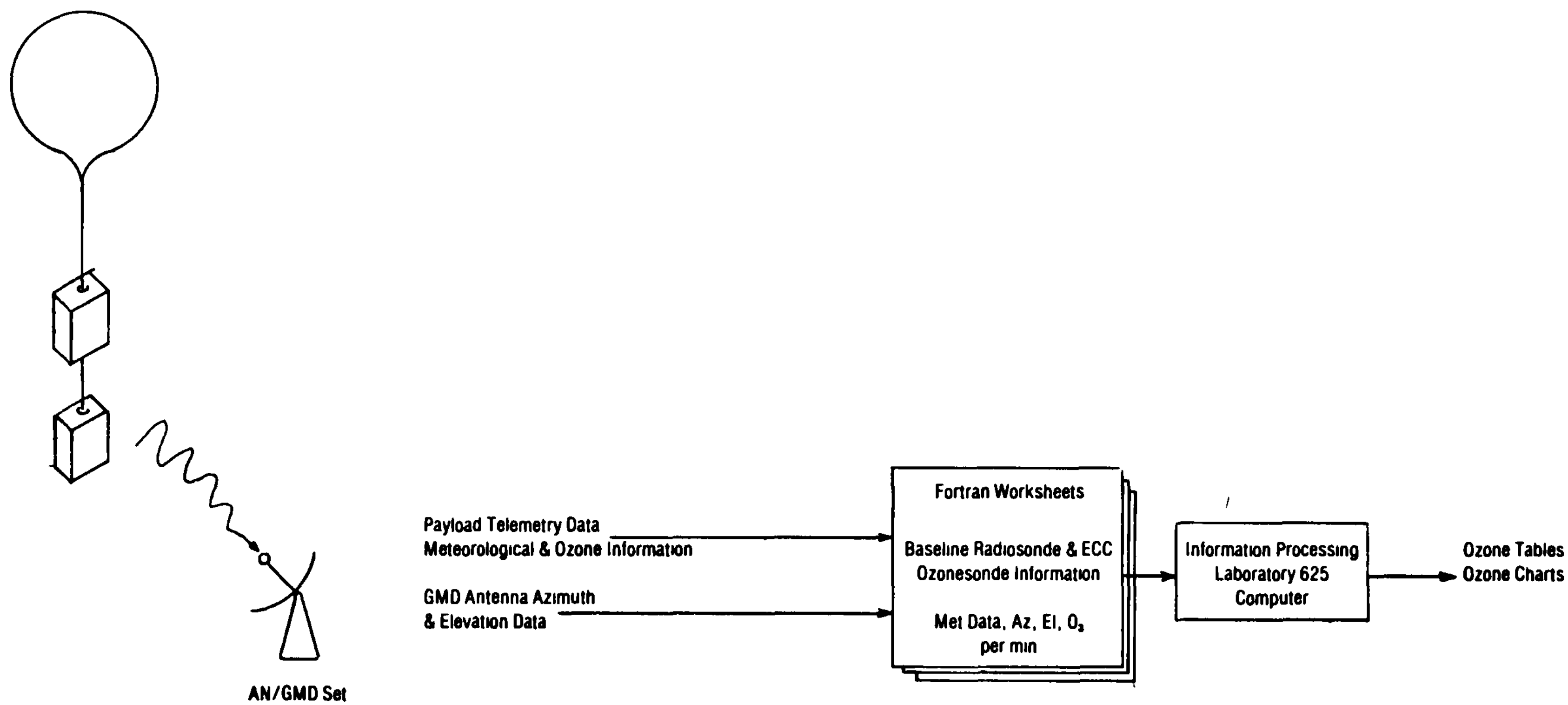

FIGURE 34 DATA FLOW FOR BALLOONBORNE ECC OZONESONDE PAYLOAD

STATION WALLOPS IS   LAUNCH DATE 72277   LAUNCH ZULU 317   ECC SONDE 3A-174X

SURFACE CONDITIONS   PRESS 1011.3 MB   TEMP 299.9 DEG K   HUMIDITY 49.0 PRCNT

TO CAL 30.0 DEG C AT 73.5 ORD   OO3= 39.2 OIZ= 38.5 OZC= 64.7 IO=0.140 PS= 29.2

BASELINE CAL TEMP 30.0 DEG C AT 73.3 DIV   HUMIDITY 62.0 PRCNT AT 46.0 ORD

TIME MIN	ALT GM MT	OZONE MICMB	OZTEN GAMMA	TOTOZ ATMCM	PRESS MB	TEMP DEG K	HUMTY PRCNT	DEWPT DEG K	LOG PRESS	PTEMP DEG K	MIXRT MICGG	SPD MPS	DIR DEG	NS MPS	EW MPS	TV DEG K	SPECIF HUMTY
0	4	[illegible]	115.9	0.	1011.3	299.5	63.6	292.2	3.0049	298.5	0.10	4.0	300.0	-2.0	3.5	301.92	0.0133
1	203	63.0	122.4	0.00100	989.0	297.4	63.8	290.2	2.9952	298.3	0.11	8.5	307.0	-5.2	6.7	299.54	0.0120
2	470	65.9	127.7	0.00265	959.0	297.8	62.5	290.3	2.9818	301.4	0.11	12.9	305.8	-7.5	10.4	300.09	0.0125
3	720	[illegible]	129.5	0.00414	932.0	296.9	56.7	287.9	2.9694	302.9	0.12	14.5	295.8	-6.3	13.1	298.89	0.0110
4	976	58.3	109.9	0.00557	905.0	295.5	54.0	285.8	2.9566	304.1	0.10	14.3	288.6	-4.6	13.5	297.32	0.0099
5	1239	55.2	108.4	0.00690	878.0	294.0	61.3	286.3	2.9435	305.1	0.10	11.8	283.8	-2.8	11.4	295.87	0.0106
6	1498	63.9	124.9	0.00809	856.0	292.9	60.7	285.2	2.9325	306.2	0.12	11.4	279.0	-1.8	11.3	294.68	0.0101
7	1733	57.8	111.6	0.00955	829.0	291.0	62.7	283.9	2.9186	307.0	0.12	11.0	280.2	-1.9	10.9	292.67	0.0095
8	1994	57.7	[illegible]	0.01107	804.0	289.3	62.3	282.2	2.9053	307.9	0.12	9.1	281.9	-1.9	8.9	290.88	0.0088
9	2251	56.0	116.4	0.01246	783.0	287.7	63.4	280.9	2.8921	308.9	0.12	8.1	281.9	-1.7	7.9	289.18	0.0083
10	[illegible]	55.0	111.2	0.01397	754.0	285.6	62.9	278.8	2.8774	309.6	0.12	8.6	277.4	-1.1	8.5	286.88	0.0074
11	[illegible]	51.1	109.1	0.01532	730.0	283.5	61.9	276.6	2.8637	310.2	0.12	10.7	271.7	-0.3	10.7	284.65	0.0066
12	3119	50.3	103.3	0.01683	703.0	281.0	70.7	276.0	2.8470	310.7	0.12	10.8	268.1	0.4	10.8	282.10	0.0066
13	3417	47.6	97.3	0.01823	678.0	279.2	74.4	275.0	2.8312	312.0	0.12	9.6	273.3	-0.5	9.6	280.29	0.0064
14	3711	54.6	118.7	[illegible]	654.0	277.0	80.5	273.9	2.8156	312.7	0.14	9.4	279.5	-1.6	9.2	278.01	0.0061
15	3963	62.1	136.3	0.02111	634.0	275.1	96.3	274.6	2.8021	313.4	0.16	9.4	279.9	-1.6	9.2	276.26	0.0066
16	4247	53.6	[illegible]	0.02272	612.0	273.4	99.8	273.3	2.7868	314.5	0.15	9.3	284.3	-2.3	9.0	274.40	0.0062
17	4510	[illegible]	[illegible]	0.02419	590.0	271.9	100.0	271.9	2.7709	316.2	0.14	9.1	269.2	-3.0	8.5	272.89	0.0058
18	4842	17.9	[illegible]	0.02553	568.0	270.2	100.0	270.2	2.7543	317.6	0.14	8.7	293.1	-3.4	8.0	271.08	0.0053
19	5139	43.6	94.0	0.02699	547.0	268.1	79.0	264.9	2.7380	318.5	0.13	6.1	302.4	-3.3	5.2	268.66	0.0037
20	5417	46.3	99.8	0.02824	528.0	266.1	62.2	261.9	2.7226	321.7	0.15	6.0	300.1	-3.0	5.2	266.55	0.0030
21	5756	46.0	99.7	0.02987	505.0	266.4	86.6	264.5	2.7031	323.8	0.15	8.9	282.3	-1.9	8.7	267.04	0.0039
22	6030	44.6	97.3	0.03131	485.0	264.5	97.1	264.1	2.6857	325.2	0.15	10.8	273.9	-0.7	10.8	265.12	0.0039
23	6415	42.4	93.0	0.03276	465.0	262.9	94.4	262.1	2.6675	327.2	0.15	10.9	270.6	-0.1	10.9	263.46	0.0035
24	6708	40.9	90.4	0.03405	447.0	261.3	82.9	258.9	2.6503	328.9	0.15	10.5	268.5	0.3	10.5	261.77	0.0028
25	7004	39.5	87.6	0.03528	430.0	260.0	79.2	257.1	2.6335	331.0	0.15	9.4	271.3	-0.2	9.4	260.45	0.0025
26	7310	37.8	84.8	0.03651	413.0	257.5	79.8	254.8	2.6160	331.6	0.15	8.5	279.0	-1.3	8.4	257.88	0.0022
27	7606	36.4	[illegible]	0.03774	394.0	255.8	77.5	252.7	2.5977	333.3	0.15	9.3	285.8	-2.5	8.9	256.05	0.0019
28	7992	36.2	[illegible]	0.03915	377.0	253.2	76.2	249.9	2.5763	334.6	0.16	9.1	290.4	-3.2	8.5	253.42	0.0016
29	8312	36.0	[illegible]	0.04038	361.0	250.6	73.0	247.0	2.5574	335.3	0.17	8.9	305.5	-5.2	7.3	250.83	0.0012
30	8685	32.2	71.9	0.04176	345.0	247.8	75.3	244.6	2.5351	336.5	0.16	9.3	317.5	-6.9	6.3	248.01	0.0011
31	[illegible]	31.3	[illegible]	0.04289	328.0	245.6	69.7	241.6	2.5159	337.7	0.16	9.6	318.6	-7.2	6.3	245.73	0.0008
32	9343	29.7	70.5	0.04401	313.0	243.5	66.1	239.0	2.4954	339.3	0.16	9.8	311.6	-6.5	7.3	243.59	0.0007
33	9643	31.2	71.9	0.04503	300.0	240.7	58.1	235.1	2.4771	339.5	0.17	10.7	302.5	-5.7	9.0	240.79	0.0005

FIGURE 35   EXAMPLE OF COMPUTERIZED BALLOON OZONE DATA PRINTOUT

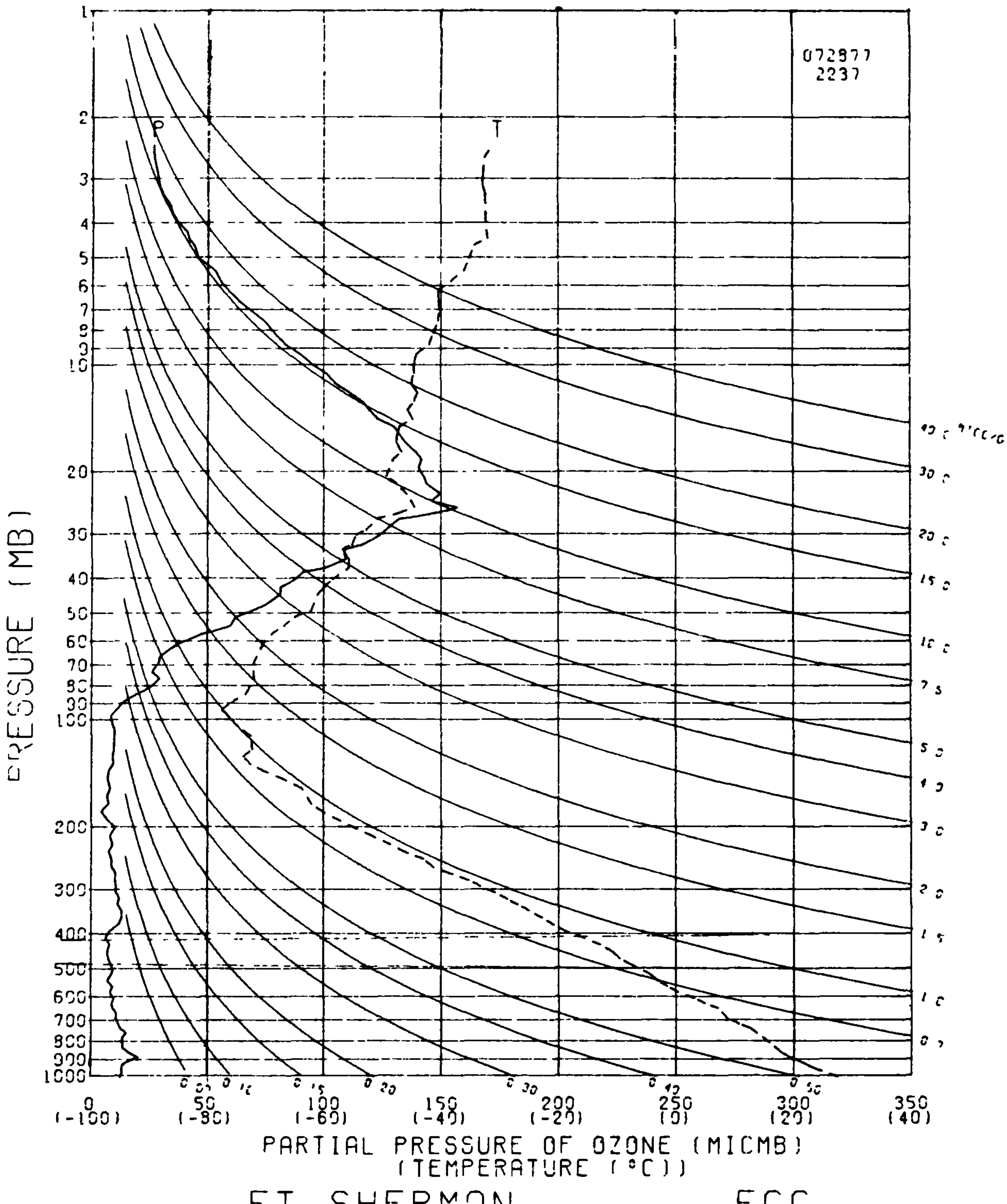

FIGURE 36 BALLOON OZONE DATA CHART

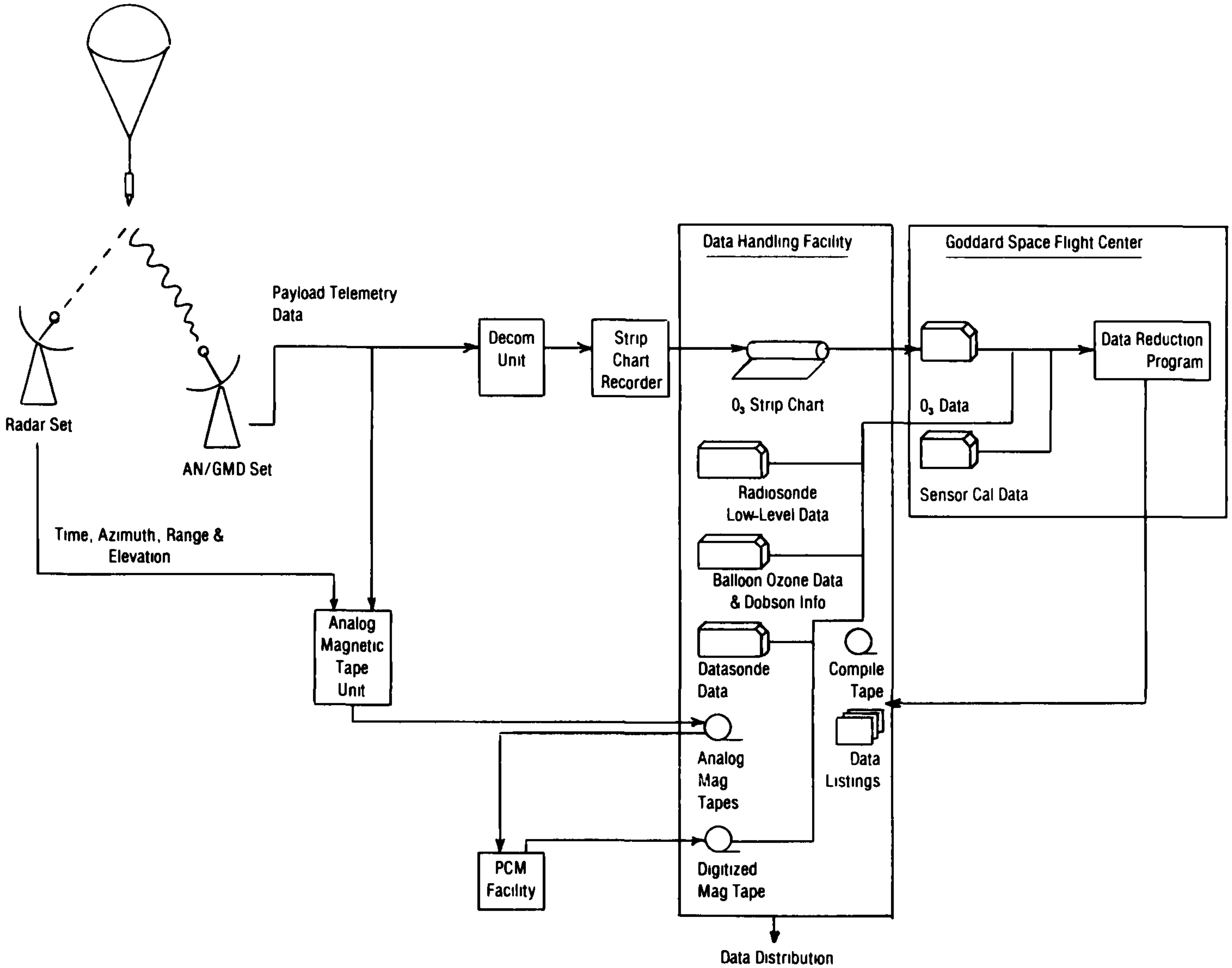

FIGURE 37 DATA FLOW FOR SUPER LOKI OPTICAL OR SUPER ARCAS CHEMILUMINESCENT OZONE PAYLOAD

planned for the SAGE ground truth program will be launched from sites at which support is provided from both AN/GMD and radar systems The ozone data are recorded on an analog tape Wallops will provide an analog magnetic recording system for recording the ozone data to interface with the AN/GMD at other sites The radar installations will record radar data on a digital magnetic tape Both the ozone and radar magnetic tapes, as well as the associated paper records, will be forwarded to Wallops along with the data from the supporting balloon radiosondes (Section 4 2 4), the ECC ozonesondes, and the Super Loki datasondes The rocket ozonesonde data are digitized at Wallops The rocket ozonesonde and radar data, along with the lower-level balloon radiosonde, ECC ozonesonde, and the upper-level Super Loki Datasonde data (temperature/winds), are then forwarded to Goddard Space Flight Center These data and the calibration data associated with the respective rocket ozonesonde are then merged and reduced to form the final data product In the case of the Super Loki Optical Ozonesonde, the data are reduced by computer and plotter The final products are an ozone data table, as shown in Figure 38, and plots of ozone density and the ozone mixing ratio, as shown in Figures 38 and 39, respectively In the case of the Super Arcas chemiluminescent ozonesonde, the data reduction is performed with a desk-top minicomputer and the final product is an ozone data table as shown in Figure 40

After reduction, the data for both types of rocket system are forwarded to the Wallops ASRP office for packaging and distribution Typically, the data will be ready for distribution within eight weeks following the sounding

Standard card and plotting formats for comparisons of SAGE and correlative profile data are described in Section 4 2 5

4.2.2. Aerosol Data

4.2.2.1. Airborne Lidar

The lidar data will be reduced to vertical profiles of the particulate backscattering coefficient (at the lidar wavelength) by using data reduction techniques similar to those routinely employed by SRI and NASA Langley in many previous measurements (See, e g Russell et al , 1976a, b) The reduction algorithm will automatically compute error bars that include uncertainties in (1) signal measurement, (2) density estimation, (3) transmission estimation, and (4) normalization (See Figure 41) In addition, scattering ratio profiles will be normalized to make the minimum scattering ratio equal the value expected on the basis of previous dustsonde measurements and optical models (e g , Russell et al , 1976b), rather than the value of unity that has customarily been assumed in the past This procedure has the effect of symmetrizing the expected normalization error and reducing it by about half

Lidar-measured particulate backscattering coefficients can be converted to particulate 1 0 μm extinction coefficients by using an assumed refractive index and particle size distribution Figure 42 shows the dependence of the conversion ratio on optical model properties (cf Figure 13 and accompanying discussion) (The size distributions and compositions shown have been derived from measurements by various investigators -- e g Hofmann et al , 1975, Pinnick et al , 1976, Shettle and Fenn, 1976, Deirmendjian, 1969, Toon and Pollack, 1976, Harris and Rosen, 1976, Swissler and Harris, 1976) In a given lidar measurement the optical model can in general only be estimated on the basis of previous or simultaneous (e g dustsonde) measurements Numerous dustsonde measurements have shown a preferred height dependence for the channel ratio, N_{15}/N_{25} (defined in Section 2 3 1) Specifically, for nonvolcanic conditions,

ROCKET OZONE DATA

Flight No 139 | Location Wallops Island | Rocket Total Ozone Above 18 5 km

Equals .214

Date 11/17/76 | Experimenter A. Krueger | Balloon Residual Ozone Below 18.5 km

Equals 103

GMT Time 1621Z | Payload No 209 | Total Ozone = .317

Sec Z = 1.831

= 1.836 | Scale Height = 3.85 | Dobson Total Ozone = .293 @ 1540

= 1.836 | | .296 @ 1739

Ht km	Δx/Δh atm-cm/km	Probable Error %	x(h) atm-cm	E(h) mol/cm³	Mixing Ratio µgm/gm	O_3 Partial Pressure µmb	Air Temp °C	Air Pressure mb	Ratio E(h) to Model
60									
59									
58									
57									
56	.00003	46	.00012	8.06x10^9	1.6	.30	-8	.31	0.05
55	00005	41	.00015	1.34x10^10	2.3	.49	-11	.36	
54	.00006	29	.00020	1.61	2.4	.59	-11	.40	0.63
53	.00008	29	.00026	2.15	2.8	.79	-8	.46	
52	00011	19	.00034	2.96	3.5	1.10	-6	.52	0.77
51	.00013	17	.00045	3.49	3.6	1.31	-4	.59	
50	.00017	10	.00058	4.57	4.2	1.71	-5	67	0.69
49	.00021	09	.00075	5.64	4.6	2.10	-6	.76	
48	.00028	07	.00096	7.53	5.3	2.79	-7	.86	0.73
47	.00035	09	.00124	9.41	5.8	3.46	-9	.98	
46	.00044	07	.00159	1.18x10^11	6.3	4.25	-15	1.11	0.70
45	.00058	05	.00203	1.56	7.2	5.58	-16	1.27	
44	.00080	05	.00261	2.15	8.6	7.55	-21	1.44	0.78
43	.00110	05	.00341	2.96	10.3	10.3	-22	1.65	
42	.00132	07	.00451	3.55	10.8	12.4	-22	1.89	0.89
41	.00165	10	.00583	4.44	11.3	14.9	-32	2.16	
40	00209	09	.00748	5 62	12.4	18.8	-33	2.49	0.93
39	.00269	08	.00957	7.23	13.7	23.9	-36	2.87	
38	.00306	08	.0123	8.23	13.3	26.8	-39	3.31	0.94
37	00386	22	.0153	1.04x10^12	14.4	33.5	-41	3 82	
36	.00435	21	.0192	1.17	13.8	37.1	-45	4.42	0.96
35	00503	18	.0235	1.35	13 5	42.4	-48	5.13	
34	.00567	14	.0286	1.52	13.0	47.1	-51	5.97	0.96
33	.00606	16	.0342	1.63	11.6	49.2	-56	6.96	
32	00708	11	.0403	1.90	11.7	58.1	-54	8.13	0.94
31	.00803	10	.0474	2.16	11.3	64.9	-57	9.49	
30	.00866	11	.0554	2.33	10.2	69.1	-60	11.1	0.92
29	00991	10	.0641	2.66	10.0	79.0	-60	13.0	
28	0110	08	.0740	2.96	9.4	87.3	-61	15.3	0.91
27	.0119	10	.0850	3.20	8.8	95.8	-58	17.9	
26	.0136	07	.0969	3.66	8 4	107.	-62	21.0	0.91
25	.0158	07	.110	4.25	8.5	127.	-58	24.6	
24	.0162	08	.126	4.35	7.4	130.	-59	28.8	0.96
23	.0159	10	.142	4.27	6.3	129.	-57	33.7	
22	.0158	08	.158	4.25	5.3	127.	-58	39.5	0.87
21	.0143	14	174	3.84	4.0	113.	-61	46.1	
20	.0131	10	.188	3.52	3.1	103.	-63	54.0	0.74
19	.0122	11	.202	3.28	2.5	96 4	-62	63.4	
			.214						

Air Temp, Pressure Density, Data Source

for 24056 k.m. used the datasonde for 11/17/76 at 1715Z at Wallops Island, VA, for 19-23 k m., used the balloonsonde for 11/18/76 at 1726Z at Wallops Island, VA

FIGURE 38 EXAMPLE OF ROCKET OZONE DATA

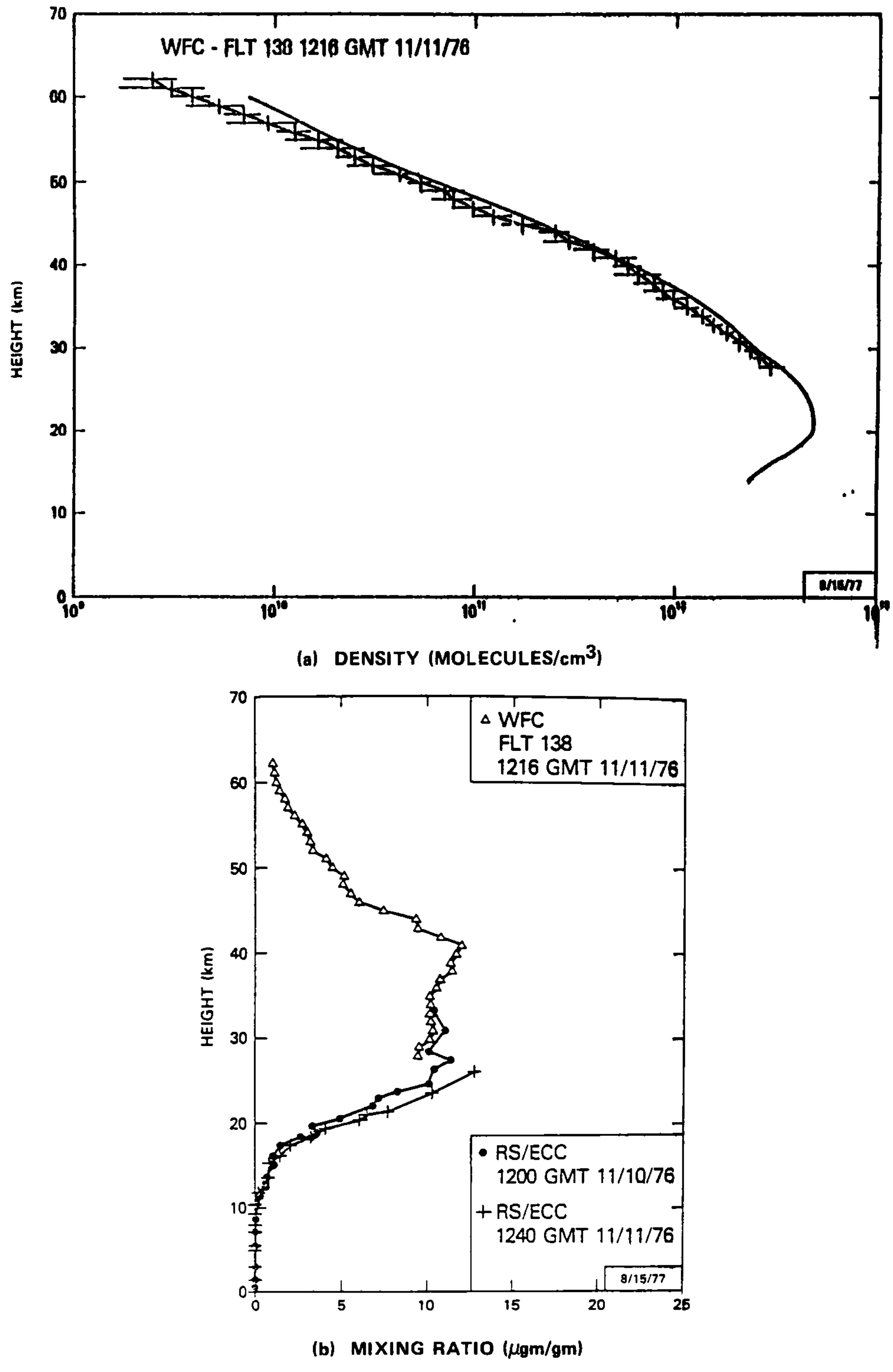

FIGURE 39 EXAMPLES OF OZONE CONCENTRATION PROFILE MEASURED BY OPTICAL ROCKETSONDE

Poker Flat, Alaska   September 25, 1976   0756Z

Alt.	Temp. (°K)	P(mb)	ρ air (g/m^3)	O_3 (ug/gm)	$\rho\ O_3$ (mol/cm^3)
70	221	.041	.069		
69	223	.048	.077	7.0	6.7×10^9
68	224	.056	.086	6.6	7.1
67	227	.064	.098	6.2	7.6
66	231	.075	.11	5.6	7.7
65	233	.086	.13	4.8	7.8
64	234	.10	.15	4.6	8.6
63	237	.11	.16	4.5	9.0
62	240	.13	.18	4.3	9.7
61	243	.15	.21	4.0	1.1×10^{10}
60	245	.17	.24	3.9	1.2
59	247	.21	.29	3.9	1.4
58	247	.23	.33	3.8	1.6
57	248	.27	.37	3.9	1.8
56	248	.31	.43	4.2	2.3
55	249	.35	.49	4.5	2.8
54	252	.40	.56	4.8	3.4
53	255	.46	.63	4.9	3.9
52	258	.52	.71	5.2	4.6
51	258	.60	.80	5.5	5.5
50	256	.68	.93	6.2	7.2
49	254	.78	1.1	6.6	9.1
48	254	.89	1.2	6.8	1.0×10^{11}
47	252	1.01	1.4	7.1	1.2
46	250	1.16	1.6	7.7	1.5
45	249	1.33	1.9	9.0	2.1
44	246	1.52	2.1	9.8	2.6
43	242	1.75	2.5	10.5	2.9
42	240	2.0	2.9	10.6	3.8
41	238	2.31	3.4	10.8	4.6
40	237	2.67	3.9	11.2	5.5
34	226	6.42	9.9	10.6	1.3
33	225	7.46	11.6	10.3	1.5
32	223	8.68	13.6	10.0	1.7
31	221	10.11	15.9	9.7	1.9
30	219	11.80	18.8	9.5	2.2
29	219	13.78	22.0	9.4	2.6
28	210	16.09	25.7	9.4	3.0
27	218	18.80	30.0	9.4	3.5
26	219	21.96	35.0		
25	219	25.65	40.9		
24	219	29.97	47.7		
23	219	35.00	55.7		
22	220				

FIGURE 40   EXAMPLE OF SUPER ARCAS CHEMILUMINESCENT OZONE DATA

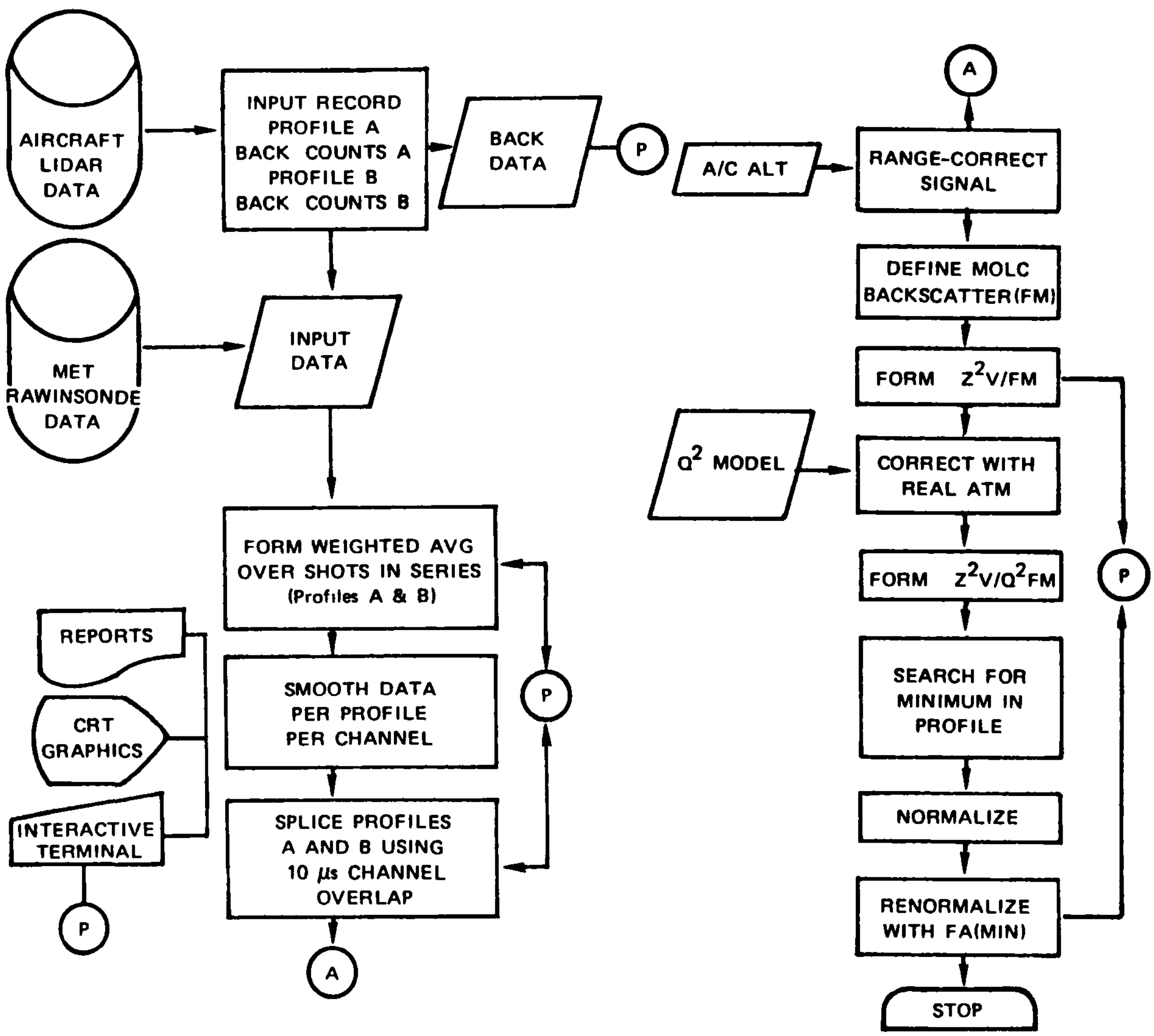

FIGURE 41 AIRBORNE LIDAR DATA-PROCESSING FLOW

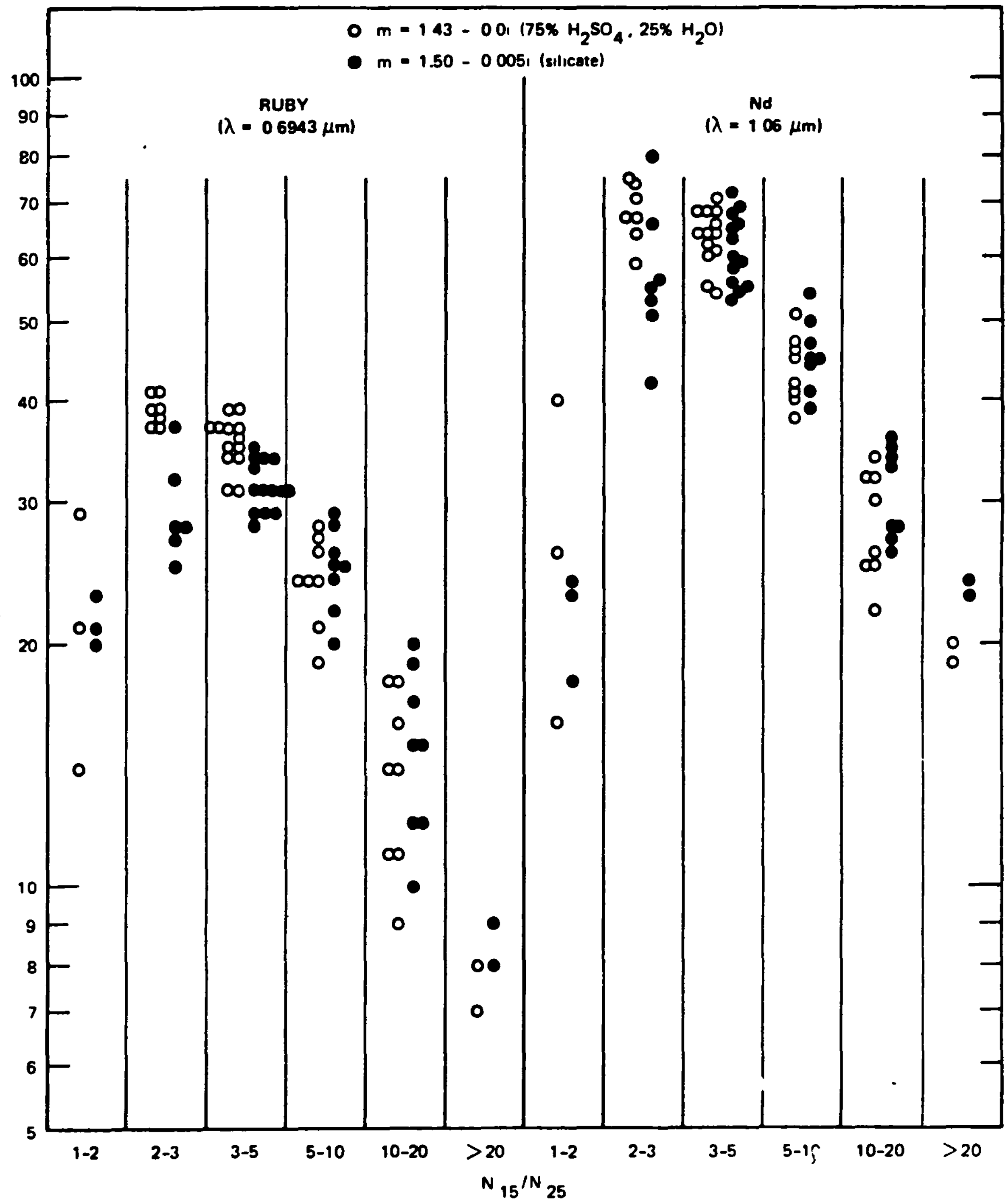

FIGURE 42 EXTINCTION-TO-BACKSCATTER RATIOS, E(1.0μm)/B(λ), COMPUTED FOR RUBY AND Nd WAVELENGTHS λ, SILICATE AND AQUEOUS SULFURIC ACID COMPOSITIONS, AND A WIDE RANGE OF SIZE DISTRIBUTIONS

Size distributions are grouped according to their value of the integral number ratio N_{15}/N_{25}. See Table 6 and text for discussion of observed regions and frequency of N_{15}/N_{25} values

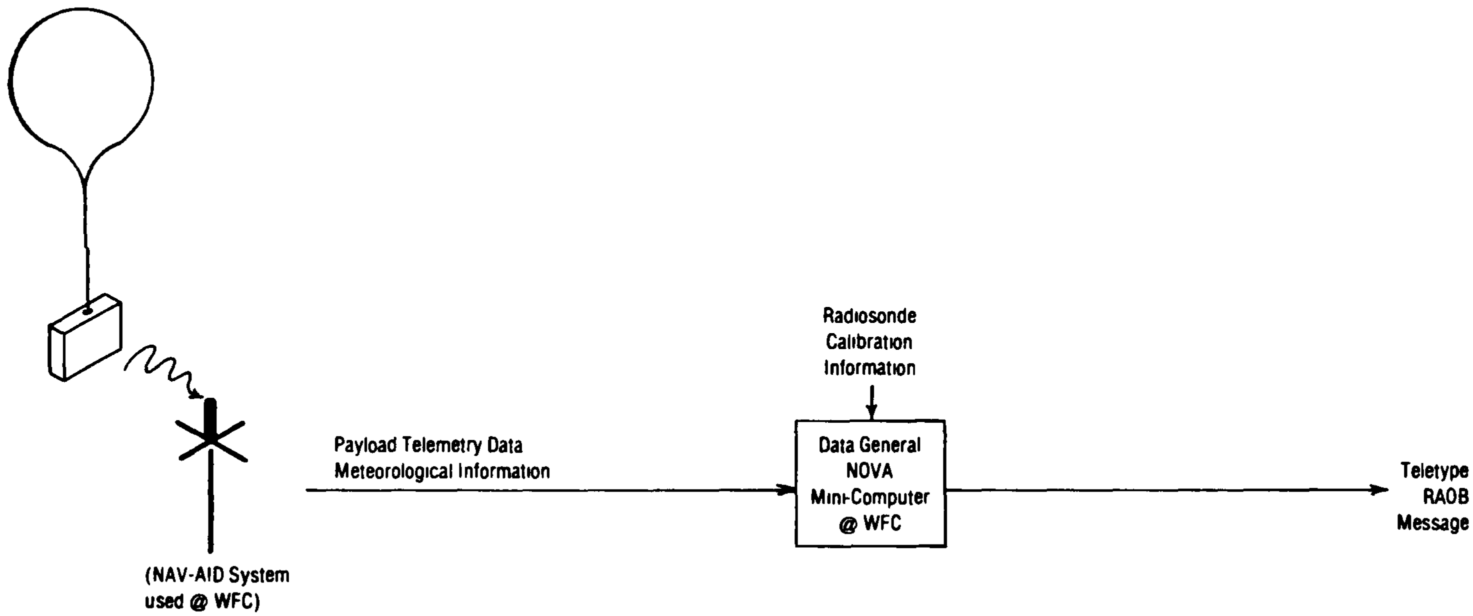

FIGURE 43 DATA FLOW FOR BALLOON-BORNE RADIOSONDE PAYLOAD

N_{15}/N_{25} values within the major aerosol mixing-ratio peak are usually between 3 and 5 (Hofmann et al , 1975) Thus the uncertainty in conversion ratio is given by the vertical spread of data points in Figure 42 above the appropriate range of N_{15}/N_{25} values The mean and standard deviation of appropriate subsets of conversion ratios is shown in Table 12

Figure 42 and Table 12 show that when recent or nearby dustsonde measurements, or other measurements, indicate that N_{15}/N_{25} falls in the range 3-5, the uncertainty (standard deviation) in the conversion ratio is about $\pm 10\%$ for both ruby (λ=0 694 μm) and Nd(λ=1 06 μm) measurements The slightly larger uncertainty for ruby measurements shown in Table 12 arises from uncertainty in particle composition (aqueous sulfuric acid or silicate), to which the Nd conversion ratio is not so sensitive (presumably because the Nd wavelength is close to 1 0 μm) If the particle composition can be ascertained by some other measurement(s), then the uncertainty in the ruby conversion ratio is reduced slightly--to about $\pm 8\%$, which is about equal to the uncertainty in the Nd ratio

The derived profiles of particulate backscattering coefficient will be converted to profiles of 1 0-μm extinction coefficient by using an appropriate conversion factor from Figure 42 Extinction error bars will also be computed, based on the particulate backscattering error bars and the uncertainty in the conversion factor

Both the backscattering and extinction profiles will be plotted on standard scales and stored on standard-format punched cards, as described in Section 4 2 5

The lidar-measured backscattering coefficient profile will be superimposed on the SAGE extinction coefficient profile to derive a cross-wavelength extinction-to-backscatter ratio (which may be height-dependent) Conversion ratios derived in this manner will be compared with the values in Figure 42 to facilitate the selection of appropriate optical models and subsequent aspects of data validation and reduction

4.2.2.2. Dustsondes

The dustsonde data will be reduced to vertical profiles of N_{15} and N_{15}/N_{25} by means of the data reduction techniques the University of Wyoming has routinely employed for many years (N_x is the number of particles with radius > $x\mu$m, cf Figure 12) The derived profiles of N_{15} and N_{15}/N_{25} will be converted to profiles of 1 0-μm extinction coefficient by using an appropriate conversion factor from Figure 13 or 14 Extinction error bars, based on the uncertainties in N_{15}/N_{25} and in the conversion ratio, will also be computed

Number and extinction profiles derived from the balloon data will be plotted on the standard scales described in Section 4 2 5 The extinction will be compared directly with the corresponding lidar and SAGE results In addition, the particle number profile will be used to derive an extinction-to-number ratio, possibly height-dependent, for comparison with Figure 13--and will be directly compared with the particle number profile derived from the SAGE extinction profile

4.2.2.3. Balloon-borne Sunphotometer

The sunphotometer data, using algorithms now being developed by T Pepin at the University of Wyoming, will be reduced to vertical profiles of particulate 1 0 μm extinction

Table 12

MEAN AND STANDARD DEVIATION OF EXTINCTION-TO-BACKSCATTER RATIO, E(1 0μm)/B(λ), FOR TWO LIDAR WAVELENGTHS λ AND VARIOUS GROUPS OF SIZE DISTRIBUTIONS

Composition	Lidar	Ruby (λ=0 6943 μm)							Nd-YAG (λ=1 06 μm)						
	N_{15}/N_{25}	1-2	2-3	3-5	3 5-4 5	5-10	10-20	>20	1-2	2-3	3-5	3 5-4 5	5-10	10-20	>20
75% H_2SO_4-25% H_2O	Mean (sr)	30	38	35	35	23	14	8	44	70	63	63	43	28	21
	σ/Mean	33%	6%	8%	5%	21%	24%	25%	46%	9%	8%	3%	18%	14%	13%
Silicate	Mean (sr)	23	29	31	32	23	15	9	32	61	61	61	45	31	23
	σ/Mean	22%	13%	8%	6%	20%	24%	12%	51%	22%	10%	6%	18%	12%	5%
Both	Mean (sr)	26	34	33	33	23	14	8	38	65	62	62	44	29	22
	σ/Mean	31%	16%	10%	7%	21%	24%	20%	50%	17%	9%	5%	18%	14%	12%

These results will be plotted on the standard scales and punched in the standard format Error bars will be provided at 1-km intervals

4.2.2.4. Polar Nephelometer

The nephelometer records data on the scattering phase function for an aerosol Measurements of the light scattered from the laser beam at the wavelength (633 nm) of the helium-neon laser used in the instrument are recorded in 5-degree steps at angles between 15 and 165 degrees When the nephelometer is used on an aircraft platform such as the NCAR Sabreliner, phase function measurements can be obtained at some three to five altitudes along SAGE tangent paths For data validation, analysis can be made of other in situ data obtained simultaneously on the same aircraft with the quartz crystal microbalance, single-particle optical counter, and particle collection devices to determine particle size distribution, shape, and composition In this way an effective value of the complex refractive index of the particles can be established by means of least-squares curve-fitting techniques similar to those described by Grams et al (1974) These results, together with the aerosol number density profiles obtained by the dustsonde, the backscattering profiles obtained with the airborne lidar, and the extinction profiles obtained with the SAM II and SAGE sensors, will be used to improve the optical model

In addition, the intercomparisons among all the above measurements will allow inferences to be drawn regarding the radiative properties of the stratospheric aerosol layer These results, combined with the SAM II and SAGE data on the spatial and seasonal variability of the stratospheric aerosol layer, can then be used by the experiment team members in a variety of SAM II and SAGE data-use investigations Of particular interest for these investigations will be the so-called asymmetry factor, single-scattering albedo, and extinction coefficient for use in climate theories involving two-stream radiative transfer approximations (see, e g , Chylek and Coakley, 1974) Estimates of these parameters will be based on analysis of the scattering data (obtained with the polar nephelometer and the lidar) and the extinction coefficients measured by the SAGE instrument

4.2.3. NO_2 and Multiconstituent Data

4.2.4. Temperature, Pressure, and Density Data

4.2.4.1. Balloon-borne Radiosonde

The data measured as the radiosonde balloon rises consist of vertical profiles of atmospheric pressure, temperature, and relative humidity The data are transmitted in flight to a standard ground-based AN/GMD (see Figure 26),[10] where they are automatically recorded on a TMQ-5 recorder The GMD antenna azimuth and elevation angles are recorded on a control recorder At sites without computer support an observer transcribes the TMQ-5 and control recorder's chart data onto standard plot forms Measurements of pressure are made in millibars, temperature in Celsius, and moisture in percent of relative humidity Wind direction and speed are also determined in this process Figure 43 illustrates the flow of the radiosonde data Figures 44, 45, and 46 comprise samples of the standard NOAA Weather Service Charts (Forms MF3-31A, B, C) used in compiling the basic raw data, while Figure 47 is a computerized reduction of the data These data, whether from the manual or the computerized reduction, are

[10]Federal Meteorological Handbook No 3 Radiosonde Observations U S Department of Commerce U S Department of Defense Change #4, January 1 1974

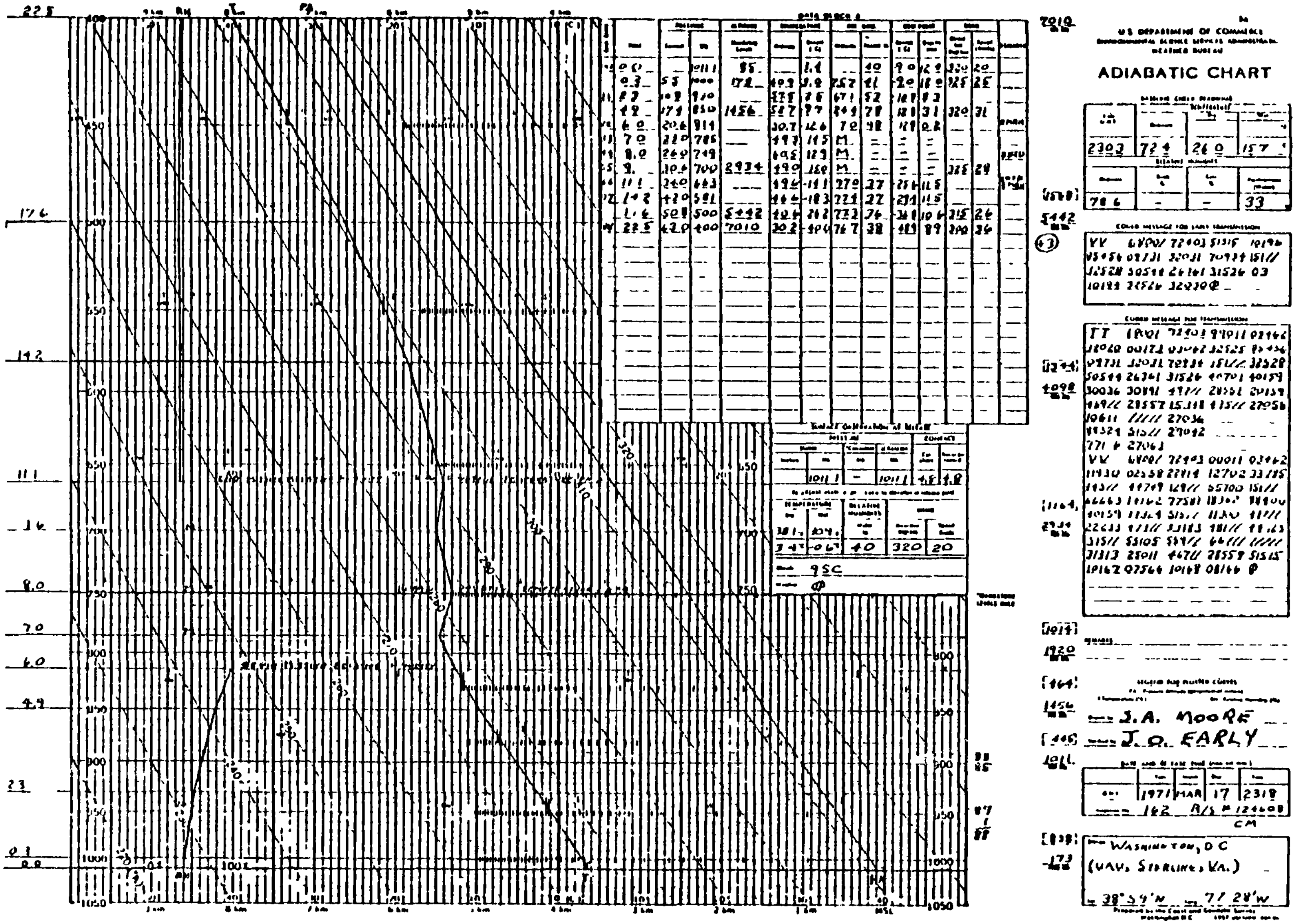

FIGURE 44 SAMPLE FORM MF3-31A

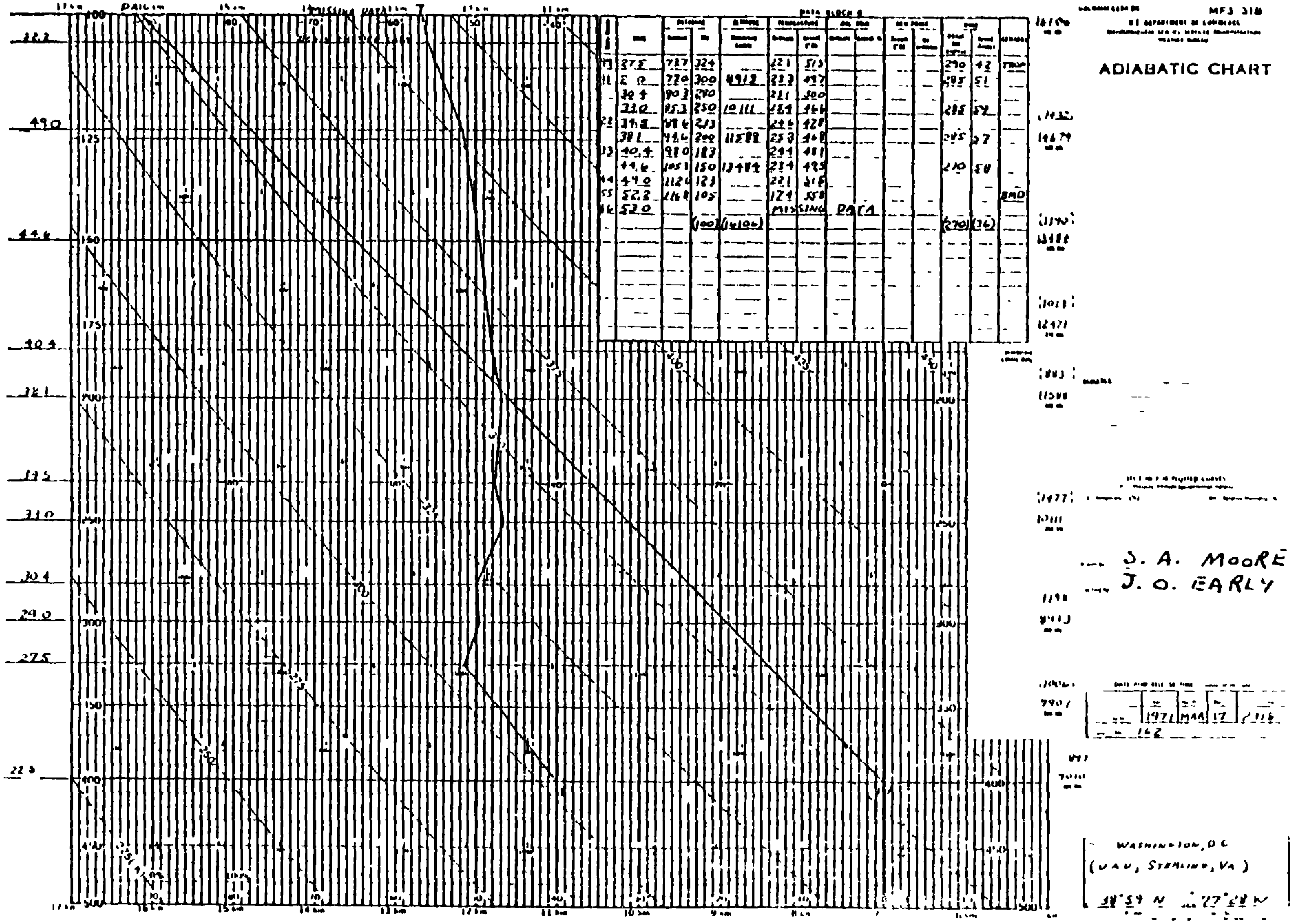

FIGURE 45 SAMPLE FORM MF3-31B

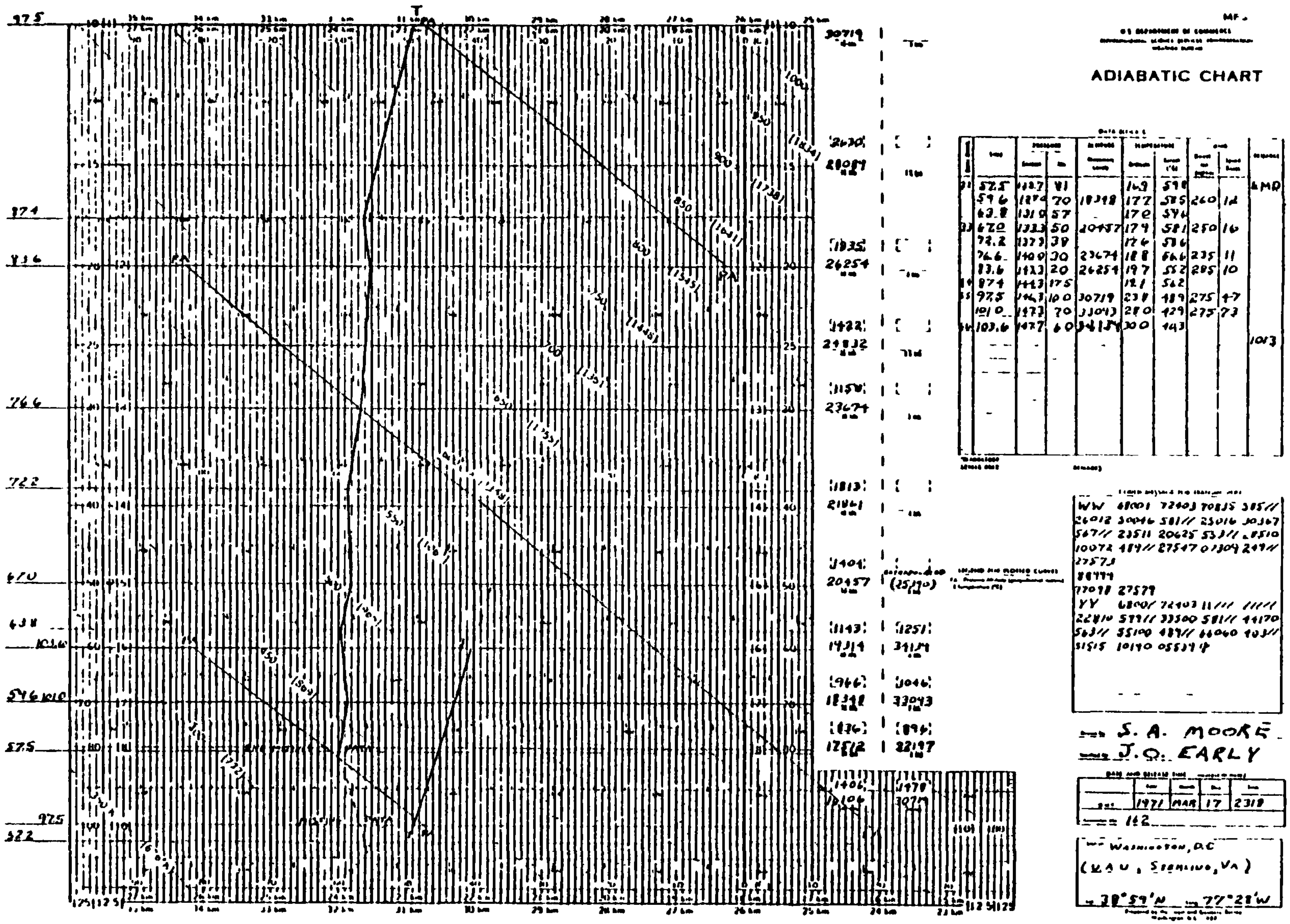

FIGURE 46 SAMPLE FORM MF3-31C

DATE	.TIME.	A.NM	F.EQ	STATION
770707	12	375	1343.2	72402

TIME	PRESS	H-MSL	TEMP	DP-DEP
0.000	1009.0	4	26.7	3.1
0.100	1000.0	84	26.5	3.3
1.200	976.0	300	28.7	8.1
5.000	882.0	1196	24.2	10.7
6.400	850.0	1518	21.9	8.8
8.000	797.0	2074	17.0	6.2
10.500	754.0	2545	14.6	11.5
12.900	700.0	3169	10.0	4.6
15.200	647.0	3820	5.4	10.8
17.100	610.0	4298	1.4	1.3
19.600	560.0	4984	-1.8	11.4
20.400	545.0	5199	-3.2	11.5
21.200	529.0	5435	-4.0	3.3
22.700	505.0	5801	-5.0	9.9
23.000	500.0	5879	-5.5	7.4
24.000	482.0	6166	-7.3	4.6
27.900	424.0	7158	-11.6	16.1
29.600	400.0	7601	-15.3	13.7
31.200	376.0	8067	-17.7	30.0
37.300	300.0	9713	-30.8	5.3
39.300	275.0	10325	-35.9	6.5
40.200	265.0	10581	-38.3	5.1
40.800	258.0	10764	-40.1	6.7
41.500	250.0	10979	-42.0	9999.0
47.000	200.0	12448	-54.6	9999.0
48.700	184.0	12976	-59.4	9999.0
52.600	150.0	14239	-64.8	9999.0
55.800	126.0	15285	-72.1	9999.0
60.200	100.0	16656	-69.1	9999.0
64.400	81.0	17929	-64.8	9999.0
66.000	75.0	18404	-59.4	9999.0
67.400	70.0	19835	-60.4	9999.0
74.000	50.0	20951	-56.6	9999.0
83.400	30.0	24242	-49.8	9999.0
87.600	24.0	25717	-45.1	9999.0
90.100	20.0	26935	-45.6	9999.0
96.300	13.5	29572	-43.4	9999.0
100.600	10.0	31621	-36.5	9999.0
102.200	8.8	32510	-35.0	9999.0

MIN	M-AS	DIR	S-KTS	FT-
0	0	260	5	1.
1	242	287	10	806
2	484	314	14	1602
3	720	324	17	2376
4	956	327	19	3149
5	1192	318	20	3922
6	1422	312	17	4679
7	1653	305	17	5437
8	1885	299	19	6196
9	2125	304	23	6985
10	2403	305	27	7896
11	2671	305	30	8778
12	2931	302	27	9631
13	3194	300	28	10491
14	3476	299	31	11418
15	3759	302	35	12346
16	4017	302	34	13192
17	4269	304	32	14018
18	4541	300	27	14911
19	4815	298	28	15810
20	5087	302	30	16704
21	5372	310	28	17637
22	5626	311	23	18471
23	5875	300	17	19288
24	6162	299	17	20230
25	6416	309	21	21064
26	6671	305	25	21898
27	6925	299	21	22732
28	7180	285	15	23569
29	7441	281	12	24425
30	7714	278	9	25320
31	8004	274	7	26274
32	8279	270	4	27173
33	8548	285	5	28059
34	8818	299	7	28945
35	9088	314	8	29830
36	9358	312	8	30716
37	9623	310	9	31602
38	9923	323	11	32569
39	10229	336	14	33572
40	10520	349	16	34527
41	10822	354	17	35516
42	11109	359	18	36457
43	11375	5	18	37333

FIGURE 47 EXAMPLE OF COMPUTERIZED RADIOSONDE DATA

summarized in a teletype radiosonde observation (RAOB) message This message contains the meteorological and wind data at standard pressure levels (surface, 1000, 850, 700, 500, 400, 300, 200, 150, 100, 70, 50, 30, 20, 10, 7, 5, 3, 2 and 1 millibar) and other levels as required by a particular mission These data are routinely sent to the World Data Center at Asheville, N C , for the SAGE project, however, copies of appropriate radiosonde data will also be sent to the Wallops Flight Center ASRP for distribution and archiving Typically, these data should be available at WFC within ten calendar days after acquisition for further handling and input into final data packages

Standard card and plotting formats for comparisons of SAGE and correlative profile data are described in Section 4 2 5

4.2.4.2. Super Loki Datasonde

The Super Loki datasonde[11] is a rocket payload launched in support of the rocket ozone systems, primarily to provide temperature, pressure, and wind profiles The Datasonde payload is ejected at apogee to descend on a decelerator Temperature measurements are made between 70 and 20 km during the descent phase Figure 48 shows the data flow at Wallops for this system The payload is tracked by an AN/GMD for the temperature/pressure data and by radar for positional data Both tracking systems at Wallops will digitize their data during the track The data flow at sites away from Wallops may be slightly different in that the AN/GMD data may not be digitized but may be a TMQ-5 paper strip chart The radar data may also be in analog form

The digitized AN/GMD and radar data from Wallops, along with datasonde calibration data and lower-level balloon radiosonde data are inputted to the METROC-K computer program for data reduction Atmospheric density is computed by using the temperature data, a base-level pressure, the hydrostatic equation, the equation of state, and a standard baseline temperature Atmospheric pressure is also computed from this information, and winds are derived from the radar data Figure 49 is a typical set of datasonde data Figure 50 (the portion above the 26-28 km level) is a typical chart presentation of the datasonde temperature/altitude data That portion below 26 km is radiosonde data

For those cases in which the AN/GMD and/or radar data from other sites arrive at Wallops in analog form, a different approach is used The TMQ-5 meteorological data will be extracted manually and put through a FORTRAN formatting process The radar data will be digitized and then inputted together with the meteorological data to the Hypso-2 computer program at Wallops

The meteorological data products from either the METROC-K or Hypso-2 programs are provided (as shown in Figure 51) as part of the supporting data required for processing the ozone data from the Super Loki and Super Arcas ozonesondes

A standard card and plotting format for comparisons of SAGE and correlative data is described in Section 4 2 5

---

[11] Federal Meteorological Handbook No 10, Meteorological Rocket Observations, NASA, U S Department of Commerce, U S Department of Defense Change #1 May 1, 1977

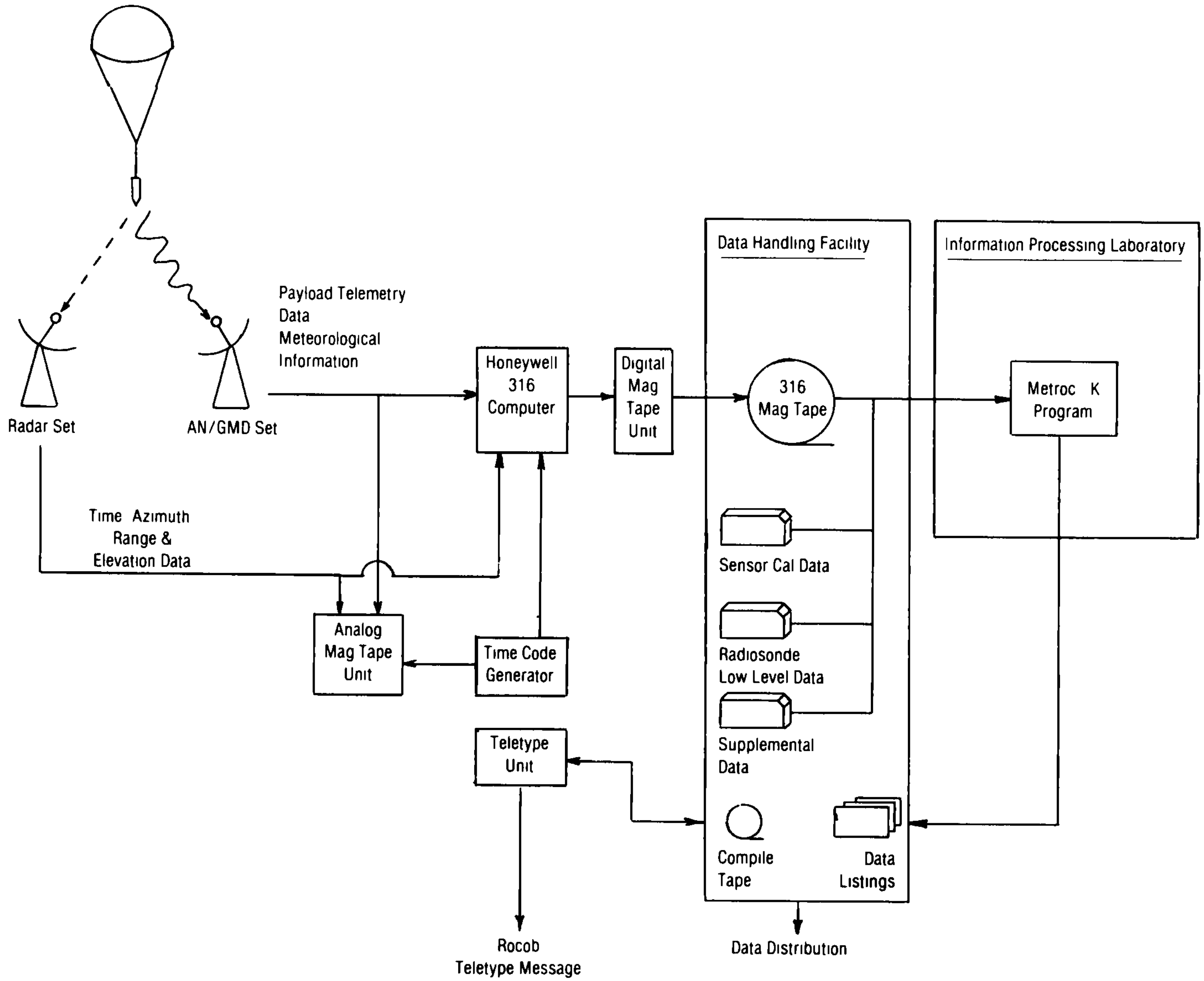

FIGURE 48 DATA FLOW FOR SUPER LOKI DATASONDE PAYLOAD

72402
WALLOPS ISLAND, VA.
3778N 07548

Y	M	D	GMT	TR	WE	TS	AC	BC	RO	TO
77	08	29	1754	-109	DBL	810				

11-9134

QUESTIONABLE DATA

BASE DATA

GEOM HGT 2106 DECAMTRS WNT WHB THT TWB SQ SWT SHB RT RP
PRESSURE 50.00 MBS
TEMP -37.7 DEGC 01 00

SOUNDING (HGT IN GEOMETRIC DECAMTRS)

HGT	WIND POLAR DEG	WIND POLAR MPS	COMPONENT N-S	COMPONENT E-W	MR MAX	TEMP DEGC	TC	PRES MB	DENSITY G M-3	SOS MPS	SRC A	SPC B
07600	321	041	-032	026	239	999	99	9999999	9999999	999		
07500	320	035	-027	022	236	999	99	9999999	9999999	999		
07400	320	030	-023	019	231	999	99	9999999	9999999	999		
07300	323	025	-020	015	225	999	99	9999999	9999999	999		
07200	329	022	-019	012	216	999	99	9999999	9999999	999		
07100	338	020	-019	007	206	-058	-40	5,322-2	8,618-2	294		
06900	351	018	-018	003	196	-054	-34	6,207-2	9,852-2	297		
06800	007	017	-017	-002	184	-051	-29	7,220-2	1,130-1	299		
06700	025	017	-015	-007	172	-049	-25	8,384-2	1,300-1	300		
06600	042	018	-013	-012	159	-046	-21	9,721-2	1,490-1	302		
06500	053	020	-012	-016	145	-043	-17	1,125-1	1,706-1	304		
06400	057	021	-011	-018	132	-041	-14	1,301-1	1,950-1	306		
06300	054	021	-012	-017	120	-039	-11	1,501-1	2,230-1	307		
06200	049	019	-012	-014	110	-039	-10	1,734-1	2,576-1	307		
06100	053	016	-009	-013	102	-036	-08	1,999-1	2,938-1	309		
06000	082	015	-002	-015	098	-031	-06	2,299-1	3,301-1	312		
05900	113	022	009	-020	091	-028	-06	2,637-1	3,746-1	314		
05800	125	031	018	-025	086	-024	-05	3,020-1	4,228-1	316		
05700	126	038	022	-030	081	-020	-04	3,452-1	4,758-1	319		
05600	123	040	022	-034	078	-019	-04	3,940-1	5,390-1	320		
05500	120	040	020	-034	071	-016	-04	4,492-1	6,093-1	321		
05400	121	039	020	-033	066	-015	-03	5,117-1	6,896-1	322		
05300	124	039	021	-032	061	-009	-02	5,820-1	7,673-1	326		
05200	119	037	018	-033	057	-009	-03	6,607-1	8,704-1	326		
05100	107	035	010	-034	053	-012	-03	7,507-1	1,000+0	324		
05000	096	034	003	-033	051	-012	-02	8,536-1	1,139+0	324		
04900	091	030	001	-030	048	-009	-03	9,697-1	1,278+0	326		
04800	091	026	001	-025	045	-009	-02	1,101+0	1,452+0	326		
04700	090	022	000	-022	042	-011	-02	1,251+0	1,665+0	324		
04600	093	019	001	-019	039	-009	-01	1,422+0	1,878+0	326		
04500	100	019	003	-019	037	-011	-01	1,616+0	2,149+0	324		
04400	105	023	005	-023	034	-009	-02	1,836+0	2,421+0	326		
04300	100	028	005	-028	033	-013	-02	2,084+0	2,791+0	324		
04200	095	029	003	-029	031	-018	-02	2,378+0	3,252+0	320		
04100	090	029	000	-029	029	-022	-01	2,717+0	3,762+0	318		
04000	088	020	-001	-020	026	-025	-01	3,111+0	4,374+0	316		
03900	091	016	000	-016	024	-029	-01	3,567+0	5,098+0	313		
03800	094	013	001	-013	022	-033	-01	4,101+0	5,950+0	311		
03700	099	011	002	-011	022	-029	-01	4,715+0	6,721+0	313		
03600	104	010	003	-010	020	-026	-01	5,409+0	7,636+0	315		
03500	108	011	004	-011	017	-030	-01	6,209+0	8,899+0	313		
03400	107	013	004	-012	016	-035	-01	7,144+0	1,043+1	310		
03300	100	014	003	-014	016	-040	-01	8,245+0	1,232+1	306		
03200	094	015	001	-015	015	-039	-01	9,533+0	1,421+1	306		
03100	090	016	-000	-016	013	-042	-01	1,103+1	1,664+1	305		
03000	090	015	000	-015	012	-046	-01	1,278+1	1,960+1	302		
02900	092	014	000	-014	011	-047	-01	1,484+1	2,287+1	301		
02800	094	012	001	-012	010	-047	-01	1,722+1	2,648+1	302		
02700	099	013	002	-013	009	-048	-01	2,002+1	3,100+1	301		
02600	105	016	004	-015	009	-051	-01	2,328+1	3,647+1	299		
02500	102	015	003	-015	008	-053	-01	2,715+1	4,299+1	297		

FIGURE 49 EXAMPLE OF ROCKET DATASONDE DATA

SOUNDING CONSTANT PRESSURE LEVELS (HGT IN GEOPOTENTIAL DECAMTRS)

06750	003	017	-017	-001	-031	7,000-2	1,099-1	299
06515	045	019	-013	-013	-069	1,000-1	1,529-1	303
06042	043	016	-012	-011	-076	2,000-1	2,939-1	309
05753	126	032	019	-026	-025	3,000-1	4,203-1	316
05541	122	041	022	-035	-018	4,000-1	5,466-1	320
05374	120	039	019	-034	-015	5,000-1	6,745-1	322
05213	116	038	016	-034	-010	7,000-1	9,271-1	325
04840	093	030	002	-030	-009	1,000+0	1,318+0	326
04400	103	027	006	-026	-011	2,000+0	2,663+0	324
04003	085	019	-002	-017	-024	3,000+0	4,202+0	316
03638	099	010	001	-009	-028	5,000+0	7,096+0	314
03498	108	012	004	-012	-034	7,000+0	1,019+1	310
03253	090	016	000	-016	-040	1,000+1	1,497+1	306
02689	098	012	002	-012	-048	2,000+1	3,097+1	301

RAWINSONDE (HGT IN GEOPOTENTIAL DECAMETRS)

03292					000	-036	9,500+0	
03156	095	019	002	-019	000	-038	1,000+1	
02692	105	012	003	-012	000	-046	2,000+1	
02420	090	013	000	-013	000	-052	3,000+1	
02099	100	011	002	-011	000	-058	5,000+1	
01888	145	004	003	-002	000	-090	7,000+1	
01668	120	009	004	-005	000	-066	1,000+2	
01528	160	012	011	-004	000	-070	1,280+2	
01325	170	019	018	-003	000	-065	1,500+2	
01242	165	019	018	-005	000	-055	2,000+2	
01100	175	012	012	-001	000	-046	2,500+2	
01030	190	007	007	001	014	-040	2,770+2	
00975	200	008	007	003	030	-035	3,000+2	
00768	210	009	008	004	030	-020	4,000+2	
00598	325	004	-003	003	030	-006	5,000+2	
00327	275	004	-000	004	030	011	7,000+2	
00162	145	002	002	-001	030	017	8,500+2	
00022	200	004	004	001	003	024	1,000+3	
00000	175	004	004	-000	003	026	1,025+3	

4848

SUPPLEMENTAL DATA

RADAR TYPE- FPS-16 GROUND EQUIP, - GMD-1B
LAUNCH SITE CLOUD DATA; TOTAL SKY COVER (TENTHS)- 2
CLOUD LAYERS (TYPE AND TENTHS) ASCENDING ORDER-
1, 2 01 2, 3,
4, 5, 6,
REDUCTION METHOD- ELEC, COMPUTER
WIND DATA - ELEC, COMPUTER
THERMODYNAMIC DATA - ELEC, COMPUTER
REMARKS -

FIGURE 49 EXAMPLE OF ROCKET DATASONDE DATA (Concluded)

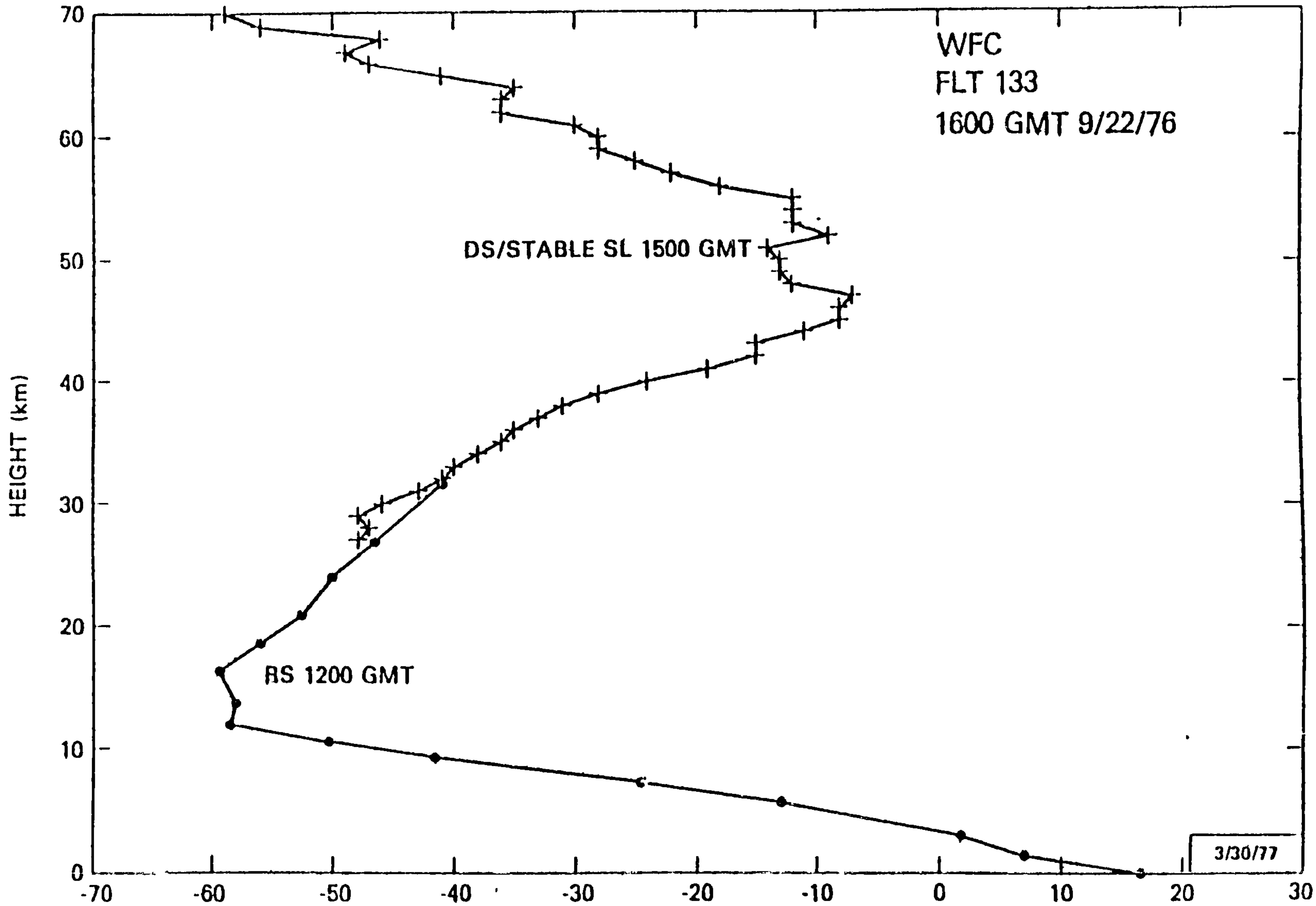

FIGURE 50 EXAMPLE OF TEMPERATURE PROFILE ASSEMBLED FROM RADIOSONDE AND DATASONDE DATA

```
72402                                   Y  M  D  GMT  TR  WS  TS  AC  BC  WC  TC
WALLOPS ISLAND, VA,
 37,8N 075,5W                          78-01-18 1552 -197 031 010            TI-9268

                                   QUESTIONABLE DATA
 BASE DATA
 GEOM HGT   2358 DECAMTRS   WHT  WHB  THT  THB SQ  SHT  SHB  RT  RP
  PRESSURF  30,00 MBS
  TEMP      -62,5 DEGC                                     01   00

SOUNDING                     (HGT IN GEOMETRIC DECAMTRS)
```

HGT	WIND POLAR DEG	WIND POLAR MPS	COMPONENT N-S	COMPONENT E-W	FV MPS	TEMP DEGC	TC	PRES MB	DENSITY G M^{-3}	SOS MPS	SPC A	SPC B
06900	261	084	012	083	189	-049	-20	5,646-2	8,784-2	300		
06800	261	090	014	089	185	-046	-25	6,547-2	1,003-1	302		
06700	260	096	016	094	178	-042	-23	7,576-2	1,144-1	304		
06600	260	101	018	100	170	-040	-20	8,750-2	1,305-1	306		
06500	259	107	020	105	160	-038	-18	1,009-1	1,492-1	308		
06400	258	112	023	110	149	-036	-16	1,162-1	1,704-1	309		
06300	258	117	025	115	137	-033	-13	1,337-1	1,942-1	311		
06200	256	120	029	116	125	-025	-08	1,534-1	2,155-1	316		
06100	254	117	033	113	114	-017	-07	1,752-1	2,382-1	321		
06000	249	109	039	102	104	-017	-09	1,995-1	2,710-1	321		
05900	243	099	044	088	096	-021	-08	2,277-1	3,147-1	318		
05800	238	090	047	076	090	-023	-07	2,602-1	3,617-1	317		
05700	236	084	047	069	084	-021	-05	2,975-1	4,115-1	318		
05600	235	081	046	067	079	-019	-05	3,396-1	4,661-1	319		
05500	236	081	045	067	074	-014	-04	3,870-1	5,210-1	322		
05400	240	081	041	069	070	-016	-04	4,407-1	5,981-1	321		
05300	246	082	033	075	065	-015	-03	5,023-1	6,774-1	322		
05200	252	088	027	084	062	-012	-03	5,716-1	7,614-1	324		
05100	254	096	027	092	058	-017	-03	6,510-1	8,855-1	321		
05000	252	101	031	096	055	-019	-02	7,409-1	9,777-1	326		
04900	251	102	034	096	052	-003	-02	8,402-1	1,083+0	330		
04800	249	101	036	095	047	-014	-02	9,552-1	1,282+0	323		
04700	249	100	036	093	044	-011	-01	1,086+0	1,445+0	324		
04600	248	097	036	090	041	-003	-01	1,233+0	1,590+0	329		
04500	247	093	037	086	038	-007	-02	1,397+0	1,828+0	327		
04400	244	089	039	080	036	-009	-01	1,587+0	2,093+0	326		
04300	242	083	039	073	034	-006	-01	1,802+0	2,352+0	327		
04200	243	075	034	066	033	-001	-01	2,042+0	2,610+0	331		
04100	249	069	025	064	032	-002	-01	2,312+0	2,968+0	330		
04000	256	069	017	067	030	-007	-01	2,619+0	3,429+0	327		
03900	260	071	013	070	027	-011	-01	2,975+0	3,958+0	324		
03800	259	068	013	067	024	-015	-01	3,388+0	4,566+0	322		
03700	258	063	014	061	021	-023	-01	3,868+0	5,394+0	317		
03600	256	059	014	057	021	-024	-01	4,428+0	6,203+0	316		
03500	256	058	014	057	020	-032	-01	5,079+0	7,329+0	311		
03400	257	059	013	057	018	-037	-01	5,850+0	8,630+0	308		
03300	256	058	014	057	016	-045	-01	6,767+0	1,032+1	303		
03200	255	056	014	054	015	-050	-01	7,851+0	1,224+1	300		
03100	255	052	013	051	014	-055	-01	9,149+0	1,461+1	296		
03000	256	047	011	046	012	-056	-01	1,068+1	1,713+1	295		
02900	258	042	009	042	011	-060	-01	1,249+1	2,039+1	293		
02800	260	037	006	037	010	-064	-01	1,467+1	2,447+1	290		
02700	260	032	006	032	009	-064	-01	1,724+1	2,873+1	290		

FIGURE 51   EXAMPLE OF METROC-K OR HYPSO-2 DATA

SOUNDING CONSTANT PRESSURE LEVELS(HGT IN GEOPOTENTIAL! DECAMTRS)

06686	261	092	015	091	-044	7.000-2	1.065-1	303
06442	259	107	020	105	-038	1.000-1	1.479-1	308
05943	250	110	038	103	-017	2.000-1	2.717-1	321
05644	235	082	047	067	-021	3.000-1	4.148-1	318
05430	235	082	047	067	-015	4.000-1	5.397-1	322
05261	247	079	031	073	-015	5.000-1	6.744-1	322
05006	253	101	029	096	-013	7.000-1	9.357-1	323
04731	249	101	036	095	-013	1.000+0	1.338+0	323
04190	240	075	038	065	-002	2.000+0	2.565+0	330
03871	260	073	012	072	-012	3.000+0	3.995+0	324
03493	257	059	014	057	-031	5.000+0	7.192+0	312
03262	256	058	014	057	-046	7.000+0	1.074+1	302
03030	255	050	012	048	-056	1.000+1	1.601+1	296

RAWINSONDE (HGT IN GEOPOTENTIAL DECAMETRS)

03115					100	-051	8.800+0
03032	255	043	011	041	100	-055	1.000+1
02599	255	010	003	010	100	-063	2.000+1
02349	260	018	003	018	100	-063	3.000+1
02039	250	018	006	017	100	-067	5.000+1
01836	240	024	012	021	100	-067	7.000+1
01618	255	030	008	029	100	-063	1.000+2
01364	245	039	017	036	100	-053	1.500+2
	255	035	009	034	100	-048	2.000+2
01029	255	041	011	040	100	-047	2.500+2
00908	250	040	014	038	100	-048	3.000+2
00713	250	031	011	029	030	-035	4.000+2
00553	260	027	005	027	030	-021	5.000+2
00295	270	021	-000	021	030	-004	7.000+2
00142	265	013	001	013	006	000	8.500+2
00011	285	009	-002	009	001	001	1.000+3
00000	285	006	-002	006	002	003	1.013+3

8080

SUPPLEMENTAL DATA

RADAR TYPE- FPS-16 GROUND EQUIP.- GMD-1B
LAUNCH SITE CLOUD DATA, TOTAL SKY COVER (TENTHS)- 2
CLOUD LAYERS (TYPE AND TENTHS) ASCENDING ORDER-
1. 2 ST 2. 3.
4. 5. 6.
REDUCTION METHOD- ELEC. COMPUTER
WIND DATA - ELEC. COMPUTER
THERMODYNAMIC DATA - ELEC. COMPUTER
REMARKS -

FIGURE 51 EXAMPLE OF METROC-K OR HYPSO-2 DATA (Concluded)

4 2.4 3. Upper-Air Synoptic Analysis for 5-, 2-, 1- and 0.4-Millibar Surfaces

Meteorological rocketsonde and satellite radiance data are used to generate high-altitude synoptic charts Broad-scale analyses for the Northern Hemisphere at 5-, 2-, 1-, and 0 4-mb levels are prepared by NOAA routinely on a weekly basis The WFC ASRP Office will coordinate the specific requirements for these charts with NOAA

4 2 4 4. NMC Meteorological Data Products Provided Regularly for SAGE

In addition to the above data provided by specific ground truth experiments, the Upper Air Branch (UAB) of the National Meteorological Center (NMC) will provide for each SAGE tangent location and time meteorological data profiles interpolated from NMC gridded global data sets, as well as profiles at the nearest radiosonde location Tapes containing these data will be sent regularly by NMC to NASA Langley Research Center for use in SAGE data validation or in routine data processing

The starting point for deriving the profiles at SAGE tangent locations and times is an archive tape of gridded global height and temperature fields at constant pressure levels Each file on this tape contains one calendar week of fields in the format specified by NMC Office Note 84 Although these gridded archive fields are created weekly, they will be distributed on multifile tape in 2- to 4-week batches Figure 52 is an example of the log that accompanies each weekly archive file Note that 80 fields are currently available, in the vertical sequence shown in Figure 52, for each of the seven days The log serves only as a guide, since each available tape field can be identified through its unique 12-word label A more detailed description of tape and field formats is available from NMC on request Interpolations within these fields are the source of all density-height profiles at SAGE tangent locations and times

Figure 53 shows the four analysis programs that generate fields saved on the UAB archive tapes Input parameters to these various systems of analysis are also shown Within the next several months the transition from NOAA-5 (VTPR) satellite radiance data to TIROS-N (TOVS) data will affect all products at all levels A significant amount of work remains to be done in integrating TOVS data into the analysis schemes and profile error estimates

The links between SAGE events, analyzed fields, density/height profiles, error estimates, and radiosonde data are diagrammed in Figure 54 The entire system of Figure 54 must run in quasi-real time (within ten days of the earliest SAGE event to be profiled in a given batch), since radiosonde data are available only for a limited time The profile-generation program will be run once each week (between Sunday and Wednesday) and will process batches of input information from the previous calendar week Figure 54 also shows input functions and provides a general summary of the content of the output profile information, which will also be distributed in weekly batches

Figures 55 and 56 and Table 13 depict specific processing of SAGE events, error estimates, and profile information, respectively Figure 55 indicates that an input tape of SAGE event cards will be accepted by UAB covering any length of time from several hours to several weeks, although the latter is preferred Each batch of SAGE events, as well as each event within a batch, is expected to be in chronological sequence The format of UAB's analysis and data archives dictates the creation of profile information in calendar-week batches As in the

ARCHIVE LOG FOR 5/17/78 THRU 5/23/78 (1=FLD AVBLE, **=FLD MSG)

	DAY 1	DAY 2	DAY 3	DAY 4	DAY 5	DAY 6	DAY 7
1000MB H NHEM	1	1	1	1	1	1	1
850MB H NHEM	1	1	1	1	1	1	1
700MB H NHEM	1	1	1	1	1	1	1
500MB H NHEM	1	1	1	1	1	1	1
400MB H NHEM	1	1	1	1	1	1	1
300MB H NHEM	1	1	1	1	1	1	1
250MB H NHEM	1	1	1	1	1	1	1
200MB H NHEM	1	1	1	1	1	1	1
150MB H NHEM	1	1	1	1	1	1	1
100MB H NHEM	1	1	1	1	1	1	1
70MB H NHEM	1	1	1	1	1	1	1
50MB H NHEM	1	1	1	1	1	1	1
30MB H NHEM	1	1	1	1	1	1	1
10MB H NHEM	1	1	1	1	1	1	1
5MB H NHEM	1	1	1	**	1	1	1
2MB H NHEM	1	1	1	**	1	1	1
1MB H NHEM	1	1	1	**	1	1	1
0.4MB H NHEM	1	1	1	**	1	1	1
1000MB T NHEM	1	1	1	1	1	1	1
850MB T NHEM	1	1	1	1	1	1	1
700MB T NHEM	1	1	1	1	1	1	1
500MB T NHEM	1	1	1	1	1	1	1
400MB T NHEM	1	1	1	1	1	1	1
300MB T NHEM	1	1	1	1	1	1	1
250MB T NHEM	1	1	1	1	1	1	1
200MB T NHEM	1	1	1	1	1	1	1
150MB T NHEM	1	1	1	1	1	1	1
100MB T NHEM	1	1	1	1	1	1	1
70MB T NHEM	1	1	1	1	1	1	1
50MB T NHEM	1	1	1	1	1	1	1
30MB T NHEM	1	1	1	1	1	1	1
10MB T NHEM	1	1	1	1	1	1	1
5MB T NHEM	1	1	1	**	1	1	1
2MB T NHEM	1	1	1	**	1	1	1
1MB T NHEM	1	1	1	**	1	1	1
0.4MB T NHEM	1	1	1	**	1	1	1
VTPR C1 NHEM	1	1	1	**	1	1	1
VTPR C2 NHEM	1	1	1	**	1	1	1
1000MB H SHEM	1	1	1	1	1	1	1
850MB H SHEM	1	1	1	1	1	1	1
700MB H SHEM	1	1	1	1	1	1	1
500MB H SHEM	1	1	1	1	1	1	1
400MB H SHEM	1	1	1	1	1	1	1
300MB H SHEM	1	1	1	1	1	1	1
250MB H SHEM	1	1	1	1	1	1	1
200MB H SHEM	1	1	1	1	1	1	1
150MB H SHEM	1	1	1	1	1	1	1
100MB H SHEM	1	1	1	1	1	1	1
70MB H SHEM	1	1	1	**	1	1	1
50MB H SHEM	1	1	1	**	1	1	1
30MB H SHEM	1	1	1	**	1	1	1
10MB H SHEM	1	1	1	**	1	1	1
5MB H SHEM	1	1	1	**	1	1	1
2MB H SHEM	1	1	1	**	1	1	1
1MB H SHEM	1	1	1	**	1	1	1
0.4MB H SHEM	1	1	1	**	1	1	1
1000MB T SHEM	1	1	1	1	1	1	1
850MB T SHEM	1	1	1	1	1	1	1
700MB T SHEM	1	1	1	1	1	1	1
500MB T SHEM	1	1	1	1	1	1	1
400MB T SHEM	1	1	1	1	1	1	1
300MB T SHEM	1	1	1	1	1	1	1
250MB T SHEM	1	1	1	1	1	1	1
200MB T SHEM	1	1	1	1	1	1	1
150MB T SHEM	1	1	1	1	1	1	1
100MB T SHEM	1	1	1	1	1	1	1
70MB T SHEM	1	1	1	**	1	1	1
50MB T SHEM	1	1	1	**	1	1	1
30MB T SHEM	1	1	1	**	1	1	1
10MB T SHEM	1	1	1	**	1	1	1
5MB T SHEM	1	1	1	**	1	1	1
2MB T SHEM	1	1	1	**	1	1	1
1MB T SHEM	1	1	1	**	1	1	1
0.4MB T SHEM	1	1	1	**	1	1	1
VTPR C1 SHEM	1	1	1	**	1	1	1
VTPR C2 SHEM	1	1	1	**	1	1	1

THE FILE HAS 504 RECORDS AND USES APPROX. 255.15 FT OF TAPE

*Note that final format will have four additional lines (for a total of 80) Northern Hemisphere tropopause temperature and pressure, and Southern Hemisphere tropopause temperature and pressure

FIGURE 52 EXAMPLE OF ARCHIVE LOG FOR TAPE FILE OF NMC GRIDDED GLOBAL DATA

LEVEL	NORTHERN HEMISPHERE	SOUTHERN HEMISPHERE
0.4 mb 5 mb	CRESSMAN VTPR RADIANCES (CHAN 1, 2) + ROCKET/RADIANCE REGRESSIONS	
10 mb 70 mb	CRESSMAN HEIGHT, TEMPERATURE, WIND	CRESSMAN TEMPERATURE ONLY (HYDROSTATIC BUILDUP)
100 mb 1000 mb	OPTIMUM INTERPOLATION NMC 127 FINAL CYCLE GLOBAL TEMPERATURE, WIND	

FIGURE 53 NMC ANALYSIS ARCHIVE SOURCES AND THEIR INPUT

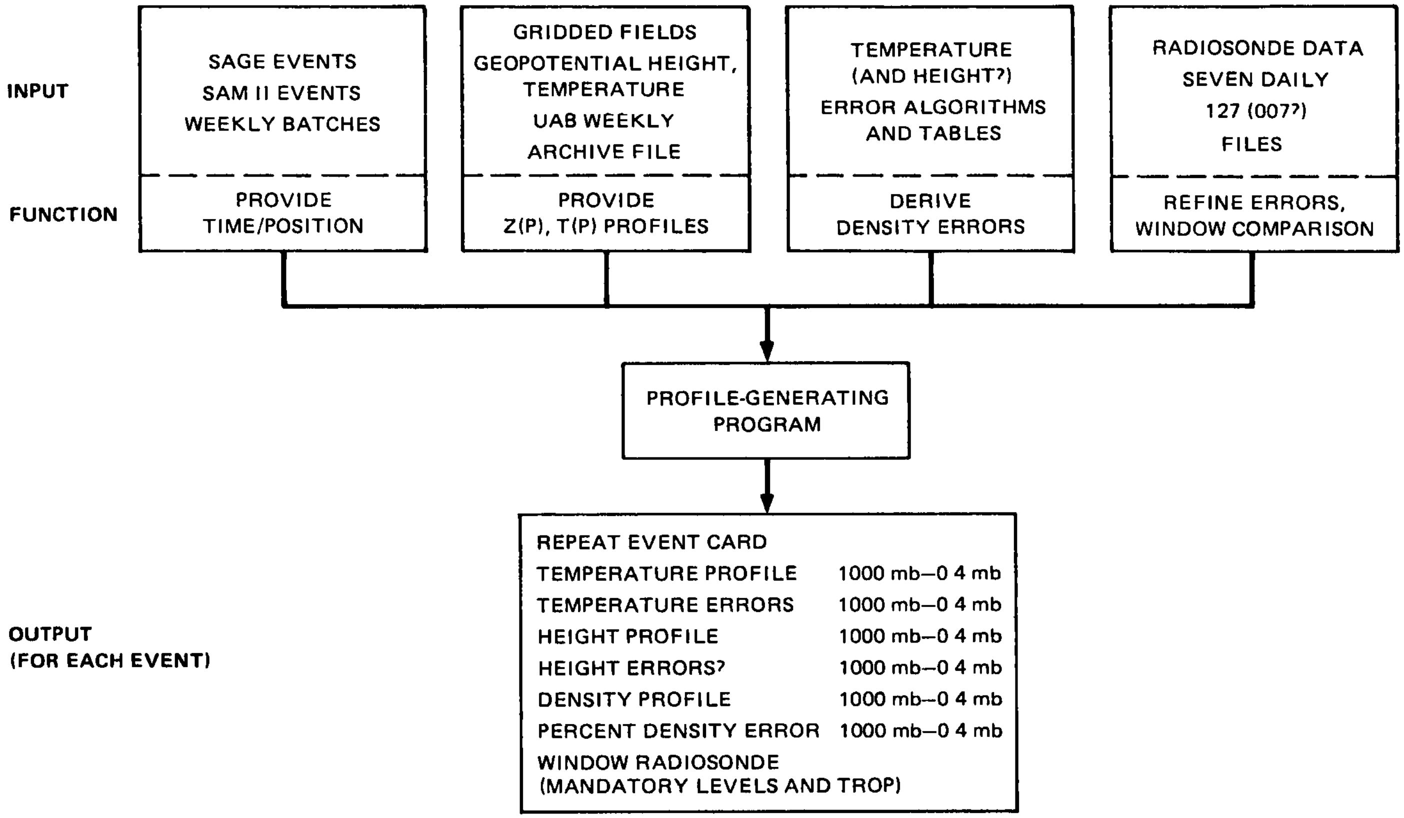

FIGURE 54 INPUTS AND OUTPUTS OF NMC PROFILE-GENERATING PROGRAM

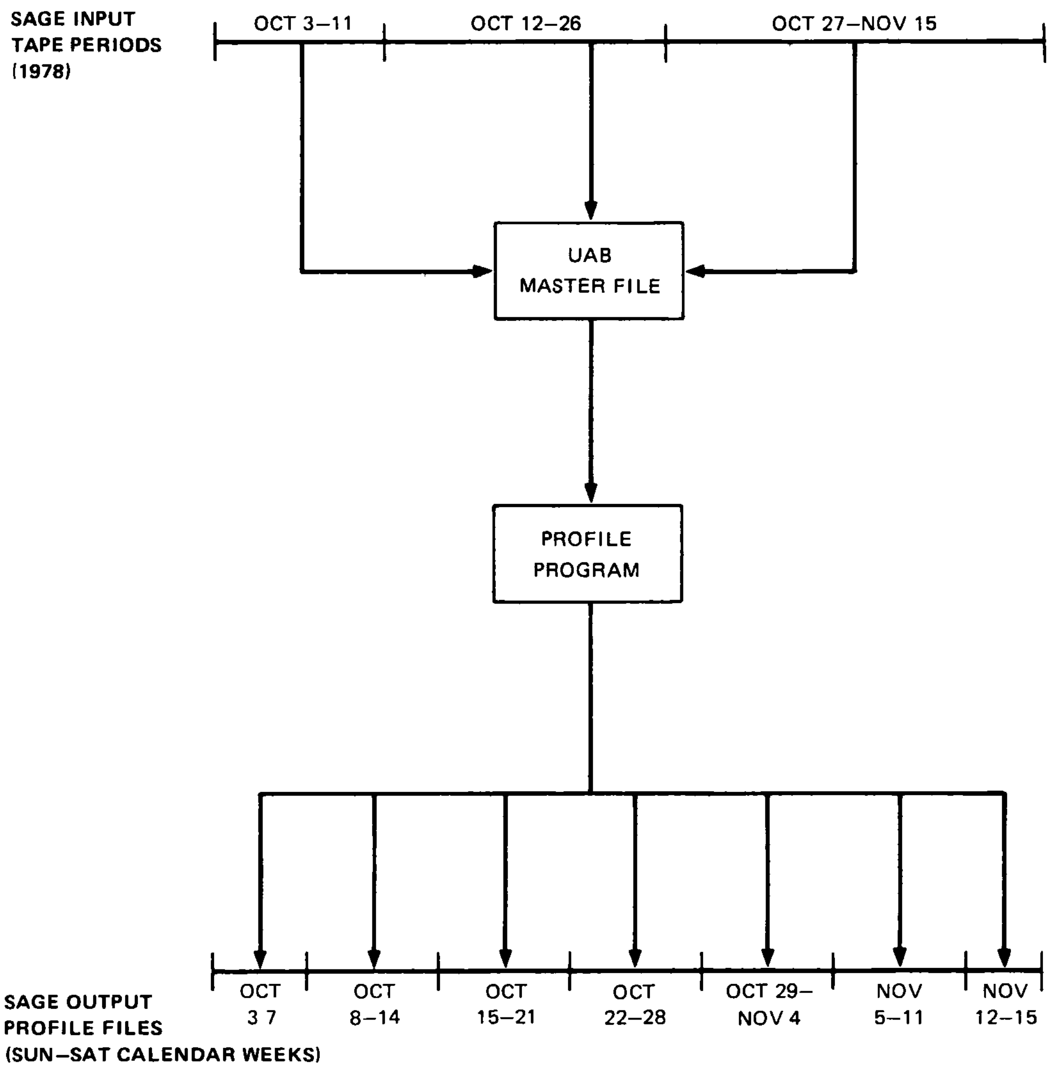

FIGURE 55 EXAMPLE OF NMC PROCESSING FOR SAGE EVENTS

LEVEL	PROFILE ERROR (ϵ_o)	
	NORTHERN HEMISPHERE	SOUTHERN HEMISPHERE
1 mb	±9° C	±9° C
	±8° C	±8° C
5 mb	±6° C	±6° C
10 mb – 70 mb	±1–3° C	±2–3° C
100 mb – 500 mb	±1–3° C	±2–3° C

A FUNCTION OF DATA COVERAGE

*Additional errors required for time interpolation

FIGURE 56 TEMPERATURE PROFILE ERRORS FOR 12Z EVENTS

Table 13

TENTATIVE FORMAT FOR NMC PROFILE OUTPUT

Fourteen 80-character records are written for each event – all values can be read as integers or characters

Parameter	Units	Fortran Format	Remarks/Sample Element
Event	–	(80A1)	Original event card
1000-10MB Temp	Tenths °K	(14I5,10X)	$\vert\wedge 2732\vert$ = 273 2°K ≈ 0°C
5-0 4MB Temp	Tenths °K	(4I5,60X)	$\vert\wedge 2732\vert$ = 273 2°K ≈ 0°C
1000-0 4MB T_{ERR}	Tenths °K	(18I4,8X)	$\vert\wedge\wedge 56\vert$ = ±5 6°C error
1000-10MB HGT	Meters	(14I5,10X)	$\vert\wedge 1580\vert$ = 500MB geopotential height
5-0 4MB HGT	Meters	(4I5,60X)	$\vert 42412\vert$ = 2MB geopotential height
1000-0 4MB H_{ERR}	Meters	(18I4,8X)	$\vert 9999\vert$ = missing
1000-10MB Density	gm/m^3	(14(I4,I1),10X)	$\vert 5369\vert 2\vert = 5369 \times 10^{-2}$ = 53 69 gm/m^3
5-0 4MB Density	gm/m^3	(4(I4,I1),60X)	$\vert 5112\vert 4\vert = 5112 \times 10^{-4}$ = 5112 gm/m^3
1000-0 4MB % Density ERR	–	(18I4,8X)	$\vert\wedge\wedge 30\vert$ = 3 0%
Radiosonde Ident, Tropopause		(5I7, 3I5)	If available Stn, Date, Time, Lat, Lon, T, H, P
1000-10MB $T_{R/S}$	Tenths °K	(14I5,10X)	See above
1000-10MB $H_{R/S}$	Meters	(14I5,10X)	See above
Miscellaneous	–	–	–

case of the gridded archive field files, profile information files will be distributed on multifile tapes containing several weeks of profiles

Figure 56 gives an abbreviated depiction of the current estimates of temperature profile errors (ϵ_o) at mandatory pressure levels, assuming that events occur at 12Z Additional errors result from time interpolation for event profiles between 12Z analysis cycles The equation $\epsilon = \epsilon_o(1 + \alpha|\sin \pi T/24|)$ supplies this adjustment error where α is 1 from 500-100 mb, α is a function of season from 70 mb through 10 mb, and α is 0 above 10 mb This scheme is presented in greater detail in Appendix D For the present, UAB is assuming that the relative error in density is nearly equal to the relative error in temperature In most cases the pressure error contribution to the density error is smaller than the temperature error contribution as defined above If the pressure error effect is determined to be significant, UAB may convert this error to an additional probable temperature profile error A slot is being allotted for reporting height errors if they are later determined to be useful

A tentative format has been chosen for the SAGE event profiles and accompanying information Table 13 describes the proposed content of fourteen 80-character records that will be produced for each SAGE event (Note that more than 14 records may be used in the final format) This record count per event will remain constant, and any missing information will be filled in with an appropriate number of 9s Ample room has been left for revisions and additions to the profile information Once format and content are agreed upon, such changes will be kept to a minimum to allow for a consistent data set

4.3. Standard Card and Plotting Formats for Data Exchange

To facilitate comparison the following standard formats are recommended for correlative profile data

4.3.1. Punched Cards

In general, punched cards are preferred over magnetic tapes as a data exchange medium, because of the possible problems entailed in reading tapes on one computer that have been written on another Because of the limited number of correlative profiles to be measured by any single investigator, the bulk of cards necessary for data exchange is not expected to be excessive Two types of card format are acceptable one with a single height, but with many parameters, per card and one with many heights, but with a single parameter, per card These alternative formats are described in Sections 4 3 1 2 and 4 3 1 3 Cards in either format must be preceded by main-deck header cards, as described in Section 4 3 1 1

4.3.1.1. Main-Deck Header Cards

The first two main-deck header cards are in (nAx) format and contain the following information

1 Instrument name (cols 1-20), location name (21-40), date and Greenwich Mean Time (41-60), investigator's serial number, etc (61-80)

2 Beginning latitude and longitude (1-20), end latitude and longitude (21-40), investigator (41-60), institution (61-80)

The third main-deck header card is in (I5) format and gives the number of altitudes for which data will follow

4.3.1.2. Data Cards: Single Height and Many Parameters per Card

This type of format was used in the first SAM II ground truth experiment in Sondrestrom, Greenland, November 1978 It lends itself readily to cases with a limited number of measured parameters that can be anticipated sufficiently in advance

For *aerosol data* the standard FORTRAN coding format is

(I5,F6 2, F6 1, F5 1, F4 1, 1PE9 3, OPF6 3*U*F4 3,F6 3*U*F4 3,F6 3*U*F4 3, 2F6 3)

The allocation of fields to parameters is as follows

Columns	Format	Parameter	Typical Sensor
1-5	I5	Card Number	
6-11	F6 2	Altitude (km)	Many
12-17	F6 1	Pressure (mb)	Balloonsonde, rocketsonde, aircraft
18-22	F5 1	Temperature (C)	Balloonsonde,, rocketsonde aircraft
23-26	F4 1	Dew-Point Depression (C)	Balloonsonde rocketsonde, aircraft
27-35	1PE9 3	Neutral Gas Density (g/cm^3)	Balloonsonde, rocketsonde, aircraft
36-41	OPF6 3	180° Scattering Ratio*	Lidar
42	*U*	Delimiter	
43-46	F4 3	Absolute Uncertainty (1 σ) in Preceding Parameter	
47-52	F6 3	25° Scattering Ratio*	Polar nephelometer
53	*U*	Delimiter	
54-57	F4 3	Absolute Uncertainty (1 σ) in Preceding Parameter	
58-63	F6 3	Extinction Ratio*	SAGE, SAM II balloon photometer
64	*U*	Delimiter	
65-68	F4 3	Absolute Uncertainty (1 σ) in Preceding Parameter	
69-74	F6 3	Number Mixing Ratio, r $\geqslant$ 0 15 μm (mg^{-1})	Dustsonde
75-80	F6 3	Number Mixing Ratio, r $\geqslant$ 0 25 μm (mg^{-1})	Dustsonde

* At wavelength specified in header cards

Fields for parameters not measured in a particular correlative experiment will be left blank The rationale for specifying ratio data (rather than absolute concentrations) is that this avoids using an E format and saves space on the cards By using the molecular density provided on the cards, the computer can readily convert to absolute concentrations

For *ozone and nitrogen dioxide data* the standard FORTRAN coding format is

(I5, F6 2, F6 1, F5 1, F4 1, 1PE9 3, 0PF6 3*R*F4 2, F6 3*R*F4 2)

The allocation of fields to parameters is as follows

Columns	Format	Parameter	Typical Sensor
1-35		Same as for aerosol cards	
36-41	OPF6 3	O_3 Mass Mixing Ratio ($\mu g/g$)	Balloonsonde, rocketsonde, photometer
42	*R*	Delimiter	
43-46	F4 2	Relative Uncertainty (1σ) in Preceding Parameter	
47-52	F6 3	NO_2 Mass Mixing Ratio ($m\mu g/g$)	interferometer, spectrometer
53	*R*	Delimiter	
54-57	F4 2	Relative Uncertainty ($1\ \sigma$) in Preceding Parameter	

We anticipate correlative data that will not fit into the above formats For example, aerosol number data may have different size cutoffs, and extinction or scattering data may be measured at more than the allotted number of wavelengths For data that do not fit into the above format the following more general format is recommended

4.3.1.3. Data Cards: Many Heights and Single Parameter per Card

In this format each parameter has its own header card and data subdeck The complete set of subdecks follows the three header cards described in Section 4 2 5 1 1 The parameter header cards and data subdecks are as follows

Altitudes

Altitude header card Format (nAx) Example

ALTITUDE (MSL) --- KM

Altitude data cards Format (8F10 x)

First Parameter

First parameter header card Format (nAx) Example

PARTICLE NUMBER GT 0 3 UM RADIUS --- CM**(-3)

First parameter data cards Format (8E10 x) or (8F10 x)

First Parameter Uncertainty (if available)

First parameter uncertainty header card Format (nAx) Example

ABS UNC , PARTICLE NUMBER GT 0 3 UM RADIUS --- CM**(-3)

First parameter uncertainty data cards Format (8E10 x) or (8F10 x)

Header cards and data subdecks for other parameters measured at the same altitudes follow the first-parameter subdeck in similar format Parameters measured at different altitudes must be preceded by three new header cards (as described in Section 4 2 5 1 1), plus a new altitude header card and altitude data subdeck

Note that *all* height and parameter data described in this section can be read by the *single* FORMAT specification (8F10 x) or by the single specification (8E10 x) Thus, a plotting program with either of these input formats can read any data prepared in the format described in this section Such a program will be available at NASA Langley Research Center for plotting SAGE and correlative results on matching axes for rapid comparisons (See Section 4 4)

4.3.1.4. Other Formats

It is to be expected that some correlative data will not fit into any of the formats described above (One example would be repeated measurements made at one altitude, but in varying horizontal positions) If this is the case, an appropriate format can be chosen by the correlative sensor scientist Cards in such nonstandard formats should be accompanied by FORMAT cards suitable for reading the data Brief instructions or a sample FORTRAN card-reading program would also be desirable

4.3.2. Plotting Axes

The following standard plotting axes are recommended semilogarithmic, 7 inch (17 78 cm) x 10 inch (25 4 cm), four orders of magnitude (logarithmic) on the 10-inch dimension, and 7 major divisions on the 7-inch dimension The logarithmic axis is for constituent concentration or mixing ratio data, and the linear axis is for height data. The standard height ranges are

Ozone Data	10-45 km	Nitrogen Dioxide Data	15-50 km
Aerosol Data	5-40 km	Total Density Data	10-45 km

Any limits and units can be used on the logarithmic scale Comparisons will be made by overlapping plots and by sliding the logarithmic scales to obtain overlap

As regards the plots, it is preferred that constituent data be expressed in absolute units (not mixing ratios), plots of mixing ratio, however, in addition to absolute concentration plots, will be welcome and useful

Correlative sensor scientists (especially those outside of the U S) who are unable to obtain the proper graph paper can request it from Mr Leonard McMaster, the SAGE Science Manager, at Mail Stop 234, NASA Langley Research Center, Hampton, Virginia 23365

4.4. Joint Evaluations and Visits to Langley Research Center

The SAGE Experiment Team (SET) feels that cooperative efforts by correlative and SAGE scientists are required to obtain the best scientific judgment of data validity This cooperative evaluation must be based on a thorough comprehension of the error sources in the correlative measurements Hence, a writeup explaining these sources and their effects should be furnished the SET as part of the joint evaluation. The most useful way of expressing these effects is to include error bars on the correlative data points

Communication would also be facilitated by having correlative and SAGE sensor scientists work together at a common location Toward this end, NASA plans to make space and faclities available at the Langley Research Center (LRC) for visiting scientists to analyze and evaluate SAGE and correlative sensor data Correlative sensor scientists are encouraged to visit LRC and take advantage of this opportunity to exchange information (Any such visits must be coordinated with NASA International Affairs Division, Code 21C-17, Washington, D C 20546)

REFERENCES

Brewer, A W , C T McElroy and J B Kerr, 1973 Nitrogen dioxide concentrations in the atmosphere *Nature,* **246,** 129-133

Bronshten, V A , and N I Grishin, 1975 *Noctilucent Clouds,* Jerusalem, Keter Publications, 288 pp

Chu, W P , T J Swissler, and M P McCormick, 1977 Theoretical analysis of the retrieval of stratospheric aerosol vertical profiles from spacecraft measurements of solar extinction in the 0 3-1 0-μm region *Proc Symp Rad in Atmos*, pp 138-140, H J Bolle, Ed , Princeton, Science Press

Chu, W P , and M P McCormick, 1979 Inversion of stratospheric aerosol and gaseous constituents from spacecraft solar extinction data in the 0 38-1 0-micrometer wavelength region *Appl Opt*, **18,** in press (May issue)

Chylek, P , and J Coakley, 1974 Aerosols and Climate, *Science,* **183,** 75-77

Deirmendjian, D , 1969 *Electromagnetic Scattering on Spherical Polydispersions,* New York, Elsevier, 290 pp

Evans, W E , 1977 Design of an airborne lidar for stratospheric aerosol measurements Final Report 5557, SRI International, Contract NAS1-14520, May 1977, to NASA Langley Research Center, Hampton, Virginia 23665, 94 pp

Evans, W E , 1978 Evaluation of a near-infrared photomultiplier for airborne lidar applications Final Report 6919, SRI International, Contract NAS1-15114, March 1978, to NASA Langley Research Center, Hampton, Virginia 23665

Ferry, G N , and H Y Lem, 1974 Aerosols in the stratosphere *Proc 3rd Conf Climatic Impact Assessment Program* (February 26-March 1, 1974), A J Broderick and T M Hard, Eds , U S Dept of Transportation, DOT-TSC-OST-74-15, 310-317

Fuller, W H , T J Swissler, and M P McCormick, 1976 Comparative analysis of red-blue lidar and rawinsonde data Paper TuC2 of *Atmospheric Aerosols Their Optical Properties and Effects* NASA CP-2004, available from NASA Langley Research Center, Hampton, Virginia 23665

Goldman, A , D G Murcray, F H Murcray, W J Williams, and F S Bonomo, 1970 Identification of the $\nu_3 NO_2$ band in the solar spectrum observed from a balloon-borne spectrometer *Nature,* **225,** 443-444

Goldman, A , F G Fernald, W J Williams, and D G Murcray, 1978 Vertical distribution of NO_2 in the stratosphere as determined from balloon measurements of solar spectra in t 4500-Å region *Geophys Res Lett*, 257-260

Grams, G W , I H Blifford, Jr , D A Gillette, and P B Russell, 1974 Complex refractive index of airborne soil particles, *J Appl Meteor*, **13,** 459-471

Grams, G W , A J Dascher, and C M Wyman, 1975 Airborne laser polar nephelometer for airborne measurements of aerosol optical properties, *Opt Eng*, **14,** 85-90

Grams, G W , and J M Rosen, 1978 Instrumentation for in situ measurements of the optical properties of stratospheric aerosol particles, *Atmos Technology,* **9,** 35-54

GSFC, 1975, 1976 Nimbus Observation Processing System (NOPS) design study report, main volume and Appendix D NASA Goddard Space Flight Center, Greenbelt, Maryland 20771, October 1975 and January 1976

Harris, F G , and J M Rosen, 1976 Measured and analytic distributions of stratospheric aerosols A review and commentary *Atmospheric Aerosols Their Optical Properties and Effects* NASA CP-2004, pp MA2-1 to MA2-4 National Aeronautics and Space Administration, Langley Research Center, Hampton, Virginia 23665

Hofmann, D J , J M Rosen, T J Pepin, and R G Pinnick, 1975 Stratospheric aerosol measurements I time variations at northern mid-latitudes *J Atmos Sci*, **32,** 1446-1456

Hofmann, D J and J M Rosen, 1977 Balloon observations of the time development of the stratospheric aerosol event of 1974-1975 *J Geophys Res*, **82,** 1435-1440

Hoxit, L R , and R M Henry, 1973 Diurnal and annual temperature variations in the 30-60-km region as indicated by statistical analysis of rocketsonde temperature data *J Atmos Sci*, **30,** 922-933

Kerr, J B , W F J Evans and J C Connell, 1977 The effects of NO_2 changes at twilight on tangent-ray NO_2 measurements *Geophys Res Lett*, **4,** 557-579

Lenhard, R W , 1973 A revised assessment of radiosonde accuracy *Bull Amer Meteor Soc*, **54,** 691-693

McCormick, M P , H B Edwards, L E Mauldin, III, and L R McMaster, 1976 Satellite solar occultation measurements SAM-II and SAGE *Atmospheric Aerosols. Their Optical Properties and Effects,* NASA CP-2004, pp TuB2-1 to TuB2-4 Available from National Aeronautics and Space Administration, Langley Research Center, Hampton, Virginia 23665

Megie, G , J Y Allain, M L Chanin, and J E Blamont, 1977 Vertical profile of stratospheric O_3 (18-28 km) by lidar sounding from the ground *Nature* (submitted August 1977)

Miller, D E , ed , 1979 *SAGE european ground truth plan* In preparation

Murcray, D G , T G Kyle, F H Murcray and W J Williams, 1968 Nitric acid and nitric oxide in the lower stratosphere *Nature,* **218,** 78-79

Noxon, J F , E C Whipple, Jr and R S Hyde, 1978 Stratospheric NO_2 I Observational method and behavior at midlatitude *J Geophys Res*, submitted for publication

Noxon, J F , 1978 Stratospheric NO_2 II Global behavior *J Geophys Res*, submitted for publication

Patterson, E M , and D A Gillette, 1977 Commonalities in measured size distribution for aerosols having a soil-derived component, *J Geophys Res*, **82,** 2074-2082

Pinnick, R G and D J Hofmann, 1973 Efficiency of light-scattering aerosol particle counters *Appl Opt*, **12,** 2593-2597

Pinnick, R G., J M Rosen, and D J Hofmann, 1976 Stratospheric aerosol measurements III optical model calculations *J Atmos Sci*, **33,** 304-314

Pepin, T J , 1970 The use of extinction from high-altitude balloons as a probe of the atmospheric aerosols Ph D thesis, Part II, Dept of Physics and Astronomy, University of Minnesota

Pepin, T J , 1977 Inversion of solar extinction data from the Apollo-Soyuz Test Project Stratospheric Aerosol Measurement (ASTP/SAM) *Inversion Methods in Atmospheric Remote Sounding,* NASA CP-2004, available from NTIS, Springfield, Virginia 22151, 620 pp

Pepin, T J , and T A Cerni, 1977 Definition of model atmospheres for application in preliminary studies of the Stratospheric Aerosol Experiment (SAM-II) aboard the Nimbus-G spacecraft Report APP-11, Dept of Physics and Astronomy, University of Wyoming

Pepin, T J and T A Cerni, 1978 High-latitude model atmospheres for application to the SAM-II experiment, SAGE experiment, and associated ground truth measurements Report APP-20, Dept of Physics and Astronomy, University of Wyoming, Laramie 82070, 137 pp

Rosen, J M , 1964 The vertical distribution of dust to 30 km *J Geophys. Res*, **69,** 4673-4676

Rosen, J M , D J Hofmann, and J Laby, 1975 Stratospheric aerosol measurements II the worldwide distribution *J Atmos Sci*, **32,** 1457-1462

Russell, J M , and J C Gille, 1978 The Limb Infrared Monitor of the Stratosphere (LIMS) Experiment Section 4 of *The Nimbus 7 Users' Guide,* Edited by C R Madrid Goddard Space Flight Center, National Aeronautics and Space Administration, Greenbelt, Maryland, 263 pp

Russell, P B , and R D Hake, 1977 The post-Fuego stratospheric aerosol lidar observations, with radiative and thermal implications *J Atmos Sci*, **34,** 163-177

Russell, P B , W Viezee, R D Hake, Jr , and R T H Collis, 1976a Lidar measurements of the stratospheric aerosol California, October 1972-February 1974 *Quart J Roy Meteor Soc*, **102,** 675-695

Russell, P B., W Viezee, R D Hake, Jr , and R T H Collis, 1976b Lidar measurements of the stratospheric aerosol summary of results and a calibration error assessment *Proc Fourth Conf Climatic Impact Assessment Prog*, U S Dept of Transportation Report DOT-TSC-OST-75-38, August 1976, Available from NTIS, Springfield, Virginia 22151, 554 pp

Russell, P B , M P McCormick, L R McMaster, T J Pepin, W P Chu, and T J Swissler, 1978 *SAM-II Ground Truth Plan* NASA TM78747, June 1978 Available from National Technical Information Service, Springfield, Virginia

Shettle, E S , and R W Fenn, 1976 Models of atmospheric aerosols and their optical properties *Proc AGARD Conf Optical Propagation in the Atmosphere,* GP-183, pp 2-1 to 2-16

Swissler, T J , and F S Harris, Jr , 1976 Comparison of extinction and backscattering coefficients for measured and analytic stratospheric aerosol size distributions *Atmospheric Aerosols: Their Optical Properties and Effects,* NASA CP-2004, MC11-1 to MC11-4, available from NASA Langley Reseach Center, Hampton, Virginia 23665

Toon, O B , and J B Pollack, 1976 A global average model of atmospheric aerosols for radiative transfer calculations *J Appl Meteor ,* **15,** 225-246

Wu, M -F , 1973· Observation and analysis of trace constituents in the stratosphere Report No ERT P-93 DOT-TST-74-7, Available from NTIS, Springfield, Virginia 22151, 218 pp

Appendix A

THE SAGE INSTRUMENT AND EXPECTED MEASUREMENT ERRORS

Appendix A

THE SAGE INSTRUMENT AND EXPECTED MEASUREMENT ERRORS

The SAGE sensor is a four-spectral-channel radiometer that measures the extinction of solar radiation during solar occultation As the conveying spacecraft emerges from the earth's shadow during each orbit, the sensor will acquire the sun and measure solar intensity in four wavelength bands centered at 0 385 μm, 0 45 μm, 0 60 μm, and 1 0 μm As the spacecraft continues in orbit, the line of sight from the spacecraft to the rising sun will scan the earth's atmosphere, resulting in a measurement of the attenuated solar intensity at different atmospheric layers The procedure will then be repeated in a reverse sense during spacecraft sunset

Each sunrise and sunset event will be monitored from the top of the clouds to approximately 150 km above the earth's surface The sensor will have an instantaneous field of view of approximately 0 5-arc minutes in elevation, which corresponds to approximately 0 5 km measured at the horizon for a 600 km orbit The total field of view is 360° in azimuth and -14° to -30° in elevation The dynamic range of each radiometric channel is approximately 3000 and the uncertainty in any radiometric measurement is specified to be less than 0 1% of the unattenuated solar intensity The sensor is partially self-calibrating, as a measurement of the unattenuated solar intensity is made prior to each spacecraft sunset and following each spacecraft sunrise Figure A-2 shows the orbit and viewing geometry of the SAGE instrument in orbit

The instrument module (Figures A-2 and A-3) consists of optical and sensor subassemblies mounted side by side The optical subassembly consists of a flat scanning mirror, Cassegrain optics, and a detector package The entire optical subassembly is gimballed in azimuth The azimuth servo employs sun sensors driven to null on the center of the sun to a tolerance of ± 45-arc seconds At the beginning of a sunrise or sunset event, the instrument slews in azimuth to a position for acquiring the sun Upon acquisition in azimuth the mirror servo scans in elevation until the sun is acquired The scan range is then constrained to scan back and forth across the solar image only

The solar input is reflected from the scan mirror through the Cassegrain telescope, which produces a solar image at the science detector aperture This image is scanned across the aperture by the motion of the scan mirror The radiation through the aperture is dispersed by a holographic grating and the four beams representing the four wavelength bands are then collected and applied to silicon PIN diode detectors The outputs of the detectors are fed to signal-conditioning amplifiers whose outputs go to the PCM encoder

After multiplexing and digitizing the signals, the PCM encoder transfers the digital data to the AEM-B data system The radiometric data for each wavelength channel will be sampled 64 times per second or approximately four times per km of tangent altitude, and digitized to 12 bits (3072 bps), these data, plus science-supporting data and instrument module housekeeping data, total 5440 bps

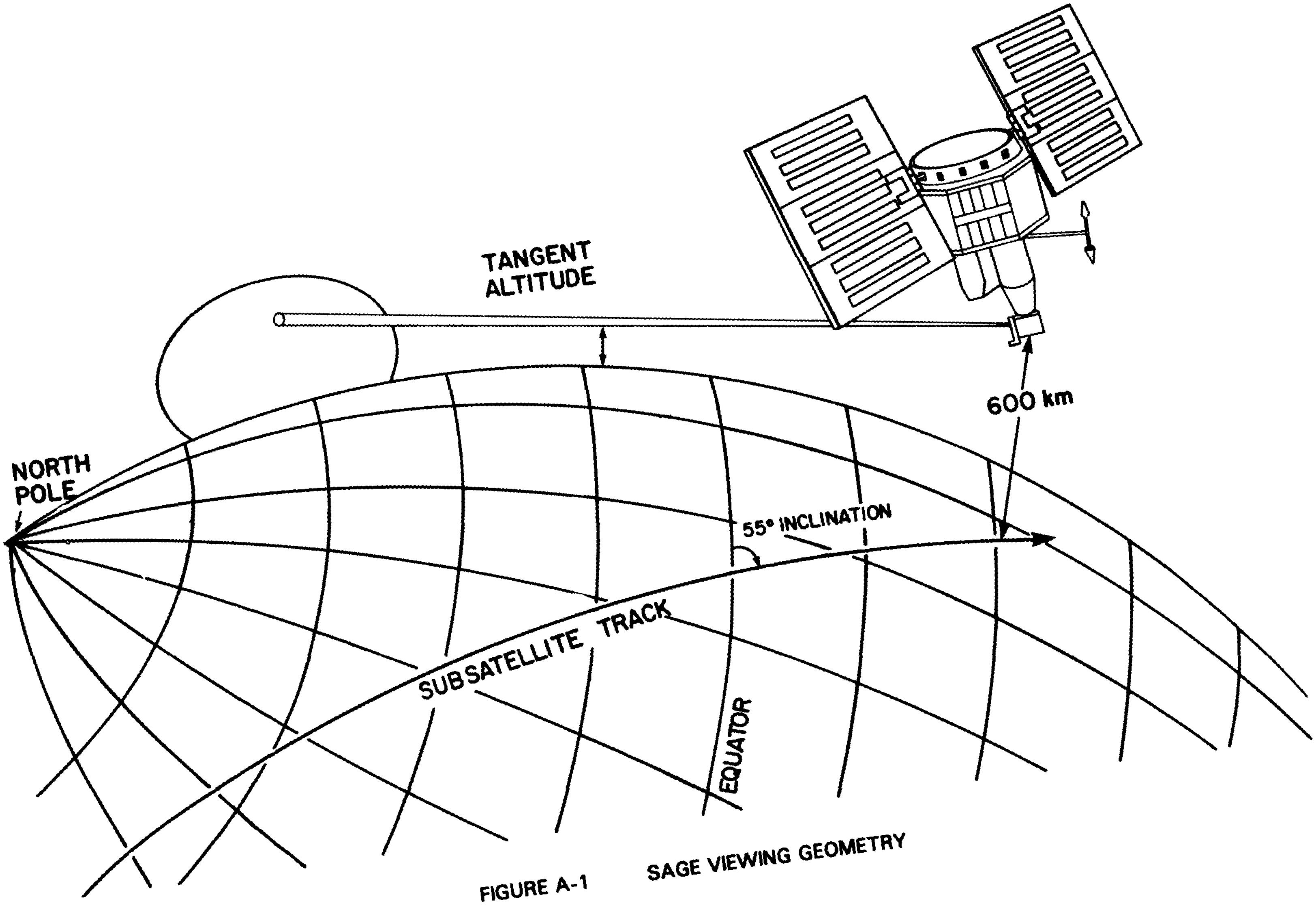

FIGURE A-1 SAGE VIEWING GEOMETRY

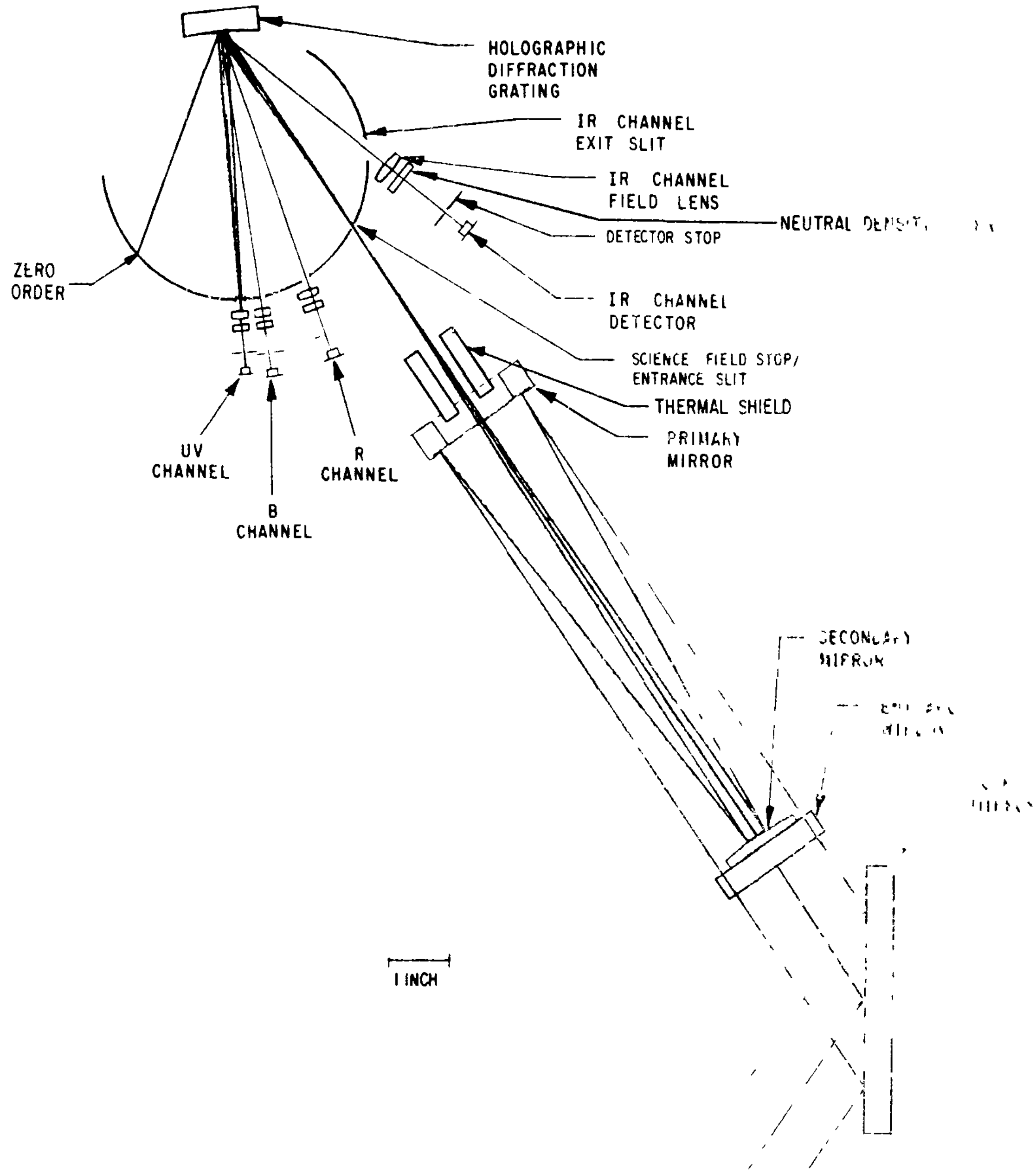

FIGURE A-2 SAGE OPTICAL SYSTEM

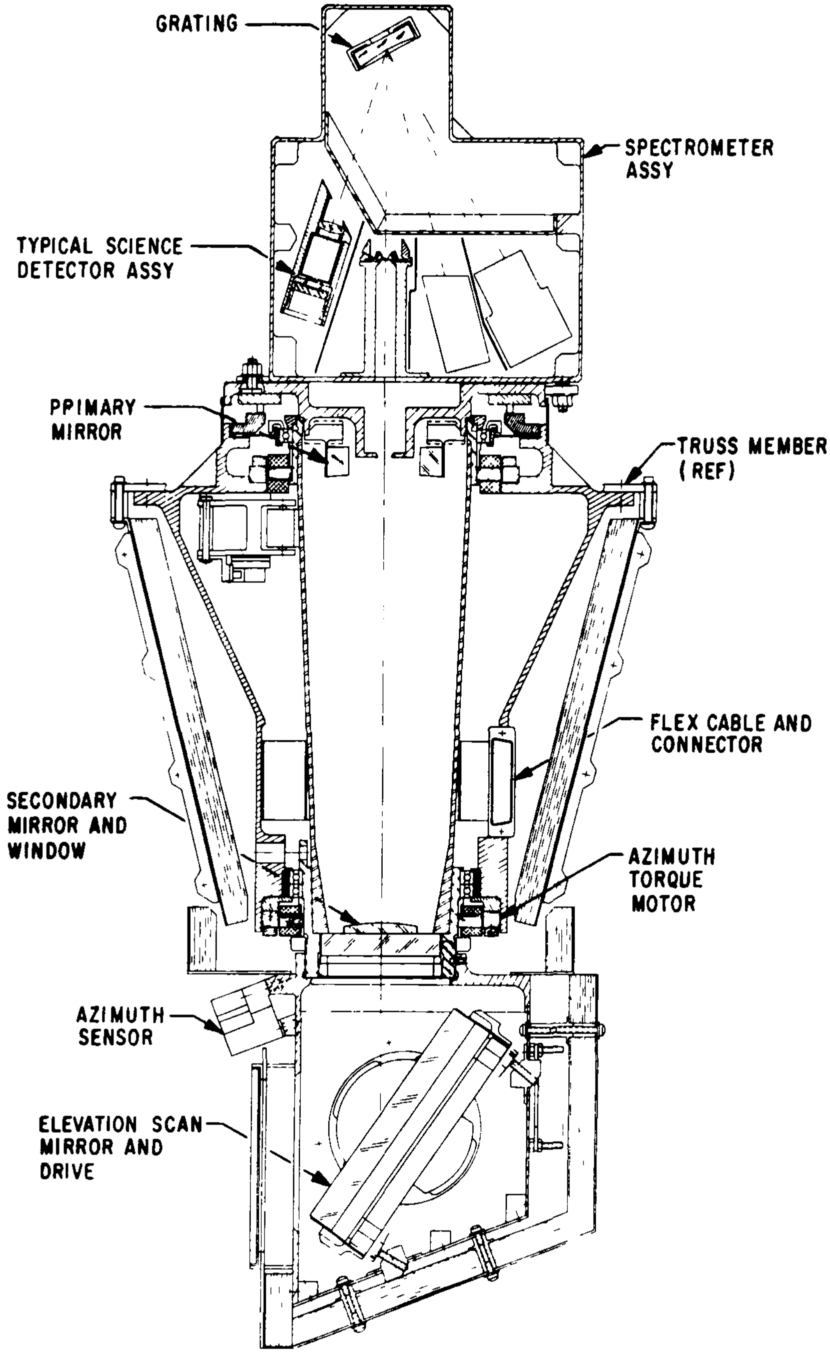

FIGURE A-3 SAGE SENSOR SYSTEM

Appendix B

SURVEY OF POTENTIAL GROUND TRUTH SUPPLIERS

Appendix B

SURVEY OF POTENTIAL GROUND TRUTH SUPPLIERS

In February 1978 a letter and questionnaire (reproduced on the following pages) were composed to aid in locating established teams that might be able to provide correlative measurements for SAGE data validation Responses describing potentially useful measurements are summarized in Table B-1 Many of the teams listed are now being integrated into the European, Japanese, or United States SAGE ground truth groups As an aid in the scheduling of correlative measurements, all teams on this list will be provided with updated information on SAGE coverage and the activities of the established ground truth groups

The Stratospheric Aerosol and Gas Experiment (SAGE) is scheduled for launch in February 1979 aboard the National Aeronautics and Space Administration's AEM-B satellite. The purpose of SAGE is to map vertical profiles of ozone, aerosol, nitrogen dioxide, and Rayleigh molecular extinction. We expect that the ozone data will extend from about 10-45 km, the aerosol data from cloud tops to about 35 km plus occasional strong layers in the mesosphere, the nitrogen dioxide data from about 25-40 km; and the Rayleigh molecular extinction from about 15-40 km.

SAGE is a 4-channel photometer that measures the intensity of sunlight (centered at wavelengths 0.385, 0.45, 0.60 and 1.0 μm) traversing the earth's limb during spacecraft sunrise and sunset events. In this manner it will measure vertical profiles of 4-wavelength extinction, at the rate of about 30 profiles per day Spatial coverage will extend from about 75° N to 75° S latitude (with some seasonal dependence) and thus will complement the coverage (64° - 80° N and S) of the SAM-II stratospheric aerosol sensor to be flown on the Nimbus G Satellite.

SAGE's four-channel extinction measurements will be numerically inverted to yield vertical profiles of aerosol extinction (and inferred number density), ozone concentration, nitrogen dioxide concentration, and total molecular density (When available, molecular density may be derived from the rawinsonde network and other sources and used as an input to the 4-channel inversion process, if this improves the accuracy of the other derived parameters) The derived data will be archived and made available to the scientific community for use in a variety of studies

A very important step in making these data available to the scientific community is to validate them by making comparisons between the SAGE measurements and other aerosol, ozone, nitrogen dioxide, and density measurements made nearby in space and time This validation is a primary function of the SAGE Experiment Team [M P McCormick (Team

Leader), R. A. Craig, D. E. Cunnold, G. W. Grams, B M Herman, D E Miller, D. G. Murcray, T. J. Pepin, W. G. Planet, and P. B. Russell]. One of our first actions is to identify those data available from other measurements that can be used for validation purposes. Not only aerosol, ozone, nitrogen dioxide, and density measurements per se, but also related information, such as volcanic eruption and noctilucent cloud observations, will be useful to us.

We would appreciate your assistance by filling out the enclosed questionnaire and returning it at your earliest convenience. Attached to the questionnaire are guidelines for the type of information required for our planning. Even if you do not plan to make correlative measurements during the SAGE validation period, please answer Part I regarding possible data use, as this will aid us in our efforts to accelerate data utilization. If, by returning Part II, you indicate an intention to make correlative measurements, we will contact you to discuss SAGE intercept times and dates for your sensor location(s).

We look forward to your support of this very important phase of a major stratospheric research endeavor.

Sincerely,

Richard A. Craig Walter G. Planet Philip B. Russell

Richard A. Craig
Department of Meteorology
Florida State University
Tallahassee, FL 32306

Walter G. Planet, S321B
National Environmental Satellite Service
NOAA
Washington, D.C. 20233

Philip B. Russell
Atmospheric Sciences Laboratory
SRI International
Menlo Park, CA 94025

(SAGE DATA VALIDATION GROUP)

PART I   POTENTIAL APPLICATIONS OF SAGE DATA

I would like to use SAGE data in the following scientific studies

(Check as many as are appropriate)

- [ ] Ozone Climatology
- [ ] Radiative Transfer
- [ ] Earth Radiation Balance and Climate
- [ ] Pollution Background
- [ ] Pollution Sources and Sinks
- [ ] Atmospheric Chemistry
- [ ] Absorption of Solar Radiation
- [ ] Atmospheric Dynamics and Transport
- [ ] Mesospheric Aerosols and/or Noctilucent Clouds
- [ ] Aerosol Optical and Physical Models
- [ ] Aerosol Effects on Passive Sensors
- [ ] Other (Please Specify) ______________________________

Date ______________________________

Name ______________________________

Address ______________________________

____

____

Return to

Dr. Philip B Russell K2056
Atmospheric Sciences Laboratory
SRI International
Menlo Park, CA 94025

PART II: AVAILABILITY OF DATA TO VALIDATE SAGE MEASUREMENTS

The following measurements or observations, relevant to SAGE validation, are contemplated: (See sample responses on following page)

1. Parameter to be measured:
2. Accuracy of measurement:
3. Altitude region:
4. Altitude resolution:
5. Observation period:
6. Frequency of observation:
7. Measurement technique:
8. Instrument type:
9. Measurement platform:
10. Type of data product:
11. Funding authority:
12. Measurement program:
13. Status of prime instrument:
14. Assurance of instrument availability in Jan. 1979-July 1979:
15. Location of measurement:
16. Experimental limitations:
17. Instrumental physical characteristics:
18. Experimenter operation experience:

Date: ______________________________ Return to:

Prepared by: ________________________

Address: ___________________________

____

____

Dr. Philip B. Russell, K2056
Atmospheric Sciences Laboratory
SRI International
Menlo Park, CA 94025

Guidelines for Part II

The following guidelines are to assist you in supplying the necessary information for Part II of the questionnaire.

	Required Parameter	Example of Responses
1.	Parameter to be measured:	Aerosol particle number: Ozone concentration; noctilucent cloud occurrence
2.	Accuracy of measurement:	%, $\pm$ a $m^{-1}sr^{-1}$
3.	Altitude region:	a km to b km
4.	Altitude resolution:	c km
5.	Observation period:	June-August 1979
6.	Frequency of observation:	single flight weekly
7.	Measurement technique:	in situ, remote
8.	Instrument type:	lidar, sampler
9.	Measurement platform:	RB-57 at 20 km altitude
10.	Type of data product:	direct, analysis
11.	Funding authority:	FAA, COVOS
12.	Measurement program:	Atmospheric radiation studies, part of WWW, flight test for specific instrument development, etc.
13.	Status of prime instrument:	x years of use, demonstration planned for_____: research stage
14.	Assurance of instrument of availability, Jan 1979-July 1979	% probability
15.	Location of measurement:	Siberia; Fairbanks, Alaska
16.	Experimental limitations:	day-night, duration
17.	Instrumental physical characteristics	weight, size, power requirements
18.	Experimenter operation experience:	10 flights in RB-57

Table B-1

CORRELATIVE MEASUREMENT CAPABILITIES DESCRIBED BY QUESTIONNAIRE RESPONSES

Part A Ground-Based

Team	Objective	Instrument	Site
CSIRO, Aspendale (R Kulkarni)	1 Total O_3	1 Dobson spectrophotometer	Aspendale
	2 O_3 profiles	2 Dobson Umkehr observations	Vairns Brisbane Perth Hobart Macquarie Island
NCAR (C Frush)	Aerosol profiles	Ruby lidar* (λ=0 6943 μm)	Boulder, Colorado
INPE, São Paulo (B Clemesha)	Aerosol profiles	Dye lidar (λ= 0 5893 μm)	São Paulo, Brazil (23 S, 46 W)
U of West Indies (G Kent)	Aerosol profiles	Ruby lidar (λ= 0 6934 μm)	Kingston Jamaica
Hebrew U of Israel (A Cohen)	Aerosol profiles	Ruby lidar	Jerusalem, Israel
Atmos Env Serv (J Kerr)	Total NO_2 above 14 km	Twilight spectrophotometer	Downsview, Ontario (44 N, 79 W)
U of Arizona, (R Schotland)	O_3 profiles	Dye lidar	Tucson, AZ (32 N, 110 W)

Part B Airplane-Borne

Team	Objective	Instrument	Site
NASA Ames (M Lowenstein)	O_3,NO_2 concentration	Chemiluminescent sensor on U-2 or other aircraft*	U-2 routes, based at Mountain View, CA (37 N, 122 W)
NASA Ames (N Farlow, G Ferry)	Aerosol size distribution, concentration, composition	Impactor on U-2,* Lear jet, or balloon	California, Alaska Panama, Hawaii
LASL (W Sedlacek)	Aerosol concentration and composition, 4 altitudes 12-20 km	Filter sampler and A N counter on WB-57F	0-75 N Panama-Houston-Seattle-Alaska
NASA Lewis (D Briehl)	Aerosol concentration and size distribution, 6-14 km	Forward-scattering counter on commercial B-747's (GASP)	United and Pan/Am airline routes

*Already included in the U S ground truth experiment schedule See Table 2

Table B-1 (Concluded)

Part C Balloon-Borne

Team	Objective	Instrument	Site
U of Koln* (A Ghazi)	O_3, H_2O profiles, 0-35 km	Optical sonde	Koln, W Germany
CSIRO, Aspendale (R Kulkarni)	O_3 profiles	Mast sonde	Aspendale
CSIRO, Aspendale (I Galbally, with Canadian AES and York U)	O_3 ,NO_2 , NO profiles, 10-35 km	Chemiluminescent and infrared spectrometer	Mildura (34 S) Alice Springs (23 S)
U of Wyoming† (J Rosen)	Aerosol, H_2O,O_3,CN profiles, 0-30 km	Optical particle counter (plus others)	Laramie, WY (41 N, 105 W) Arctic, Antarctic, Equatorial
AES, Ontario (W Evans)	O_3 ,NO_2 ,NO HNO_3, Aerosol H_2O profiles 10-36 km	Stratoprobe Payload (Several instruments assembled for LIMS/Nimbus G rendezvous)	Cold Lake, Alberta (55 N, 110 W) February 1979*
JPL (C Farmer)	O_3 ,NO_2,other profiles, tropopause-42 km	Fourier spectrometer	Palestine, Texas, Alice Springs, Australia

*This team has recently joined the SAGE European ad hoc ground truth group

†Already included in U S ground truth experiment schedule See Table 2

Appendix C

INFORMATION ON NOCTILUCENT CLOUD OBSERVATIONS

Table C1

DESCRIPTION OF GROUND-BASED PASSIVE NOCTILUCENT CLOUD OBSERVATIONS

1. Parameter to be measured: Noctilucent cloud occurrences; time of display, intensity; forms; extent of azimuth; extent in elevation.

2. Accuracy of measurement: Several degrees in azimuth and elevation.

3. Altitude region: $\sim 83 \pm 10$ km

4. Altitude resolution: Not actually measured, but see attached Fig. C1 from "Noctilucent Clouds" by V.A. Bronshten and N.I. Grishin, Keter Publ., Jerusalem.

5. Observation period: March 1 - October 31, annually.

6. Frequency of observation: Daily

7. Measurement technique: Visual estimation (supplemented by theodolites at some locations); photographic recording of displays at 6 stations.

8. Instrument type: Human eye; 35 mm camera

9. Measurement platform: Surface of the earth.

10. Type of data product: Direct, recorded on forms for punching onto cards; printed in annual publication

11. Funding authority: Atmospheric Environment Service (Canada)

12. Measurement program: International NLC program in cooperation with World Meteorological Organization

13. Status of prime instrument: Operational for many years

14. Assurance of instrument availability in Aug. 1978-Sept. 1979: 100%

15. Location of measurement: 60 stations in Canada; 16, in U.S.A.

16. Experimental limitations: Observations made during pre-sunrise and post-sunset periods when sun's depressional angle is between 6° and 18°.

17. Instrumental physical characteristics: Normal as to class

18. Experimenter operation experience: Annual regular observations since 1964

Prepared by: Mr. E. J. Truhlar

Address. Atmospheric Environment Service
4905 Dufferin Street
Downsview, Ontario, Canada M3H 5T4

Date: May 18, 1977

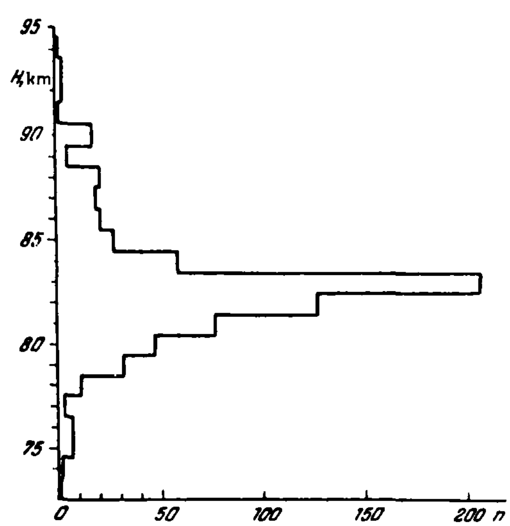

FIGURE C-1 DISTRIBUTION OF NOCTILUCENT CLOUD HEIGHTS FROM 695 MEASUREMENTS BETWEEN 1887 AND 1964

Your file Votre dossier

Our file Notre dossier 8061-2 (ARPD)

Environment Canada Environnement Canada

Atmospheric Environment Environnement atmospherique
4905 Dufferin Street
Downsview, Ontario
M3H 5T4

May 5, 1977

Dr. P.B. Russell
Science Coordinator for Ground Truth
SAM-II Nimbus G Experiment Team
Stanford Research Institute
Menlo Park. Calif. 94025
U.S.A.

Dear Dr. Russell:

This letter will confirm preliminary arrangements made during your recent discussion with Mr. E.J. Truhlar concerning the provision of noctilucent cloud (NLC) observations in support of SAM-II measurements of mesospheric aerosols. Observations of NLC data will be forwarded to you after they have been received from the stations, transferred to cards, processed by computer for quality and listed in tabular format. (See attachment for an example of a regular listing of such data, including the explanatory legend). About a one-month delay should be expected before a listing for a particular data-month is received by your institute.

The following table shows the average monthly distribution of station-night sightings of NLC during the period 1964-1976 inclusive.

MAR	APR	MAY	JUN	JUL	AUG	SEP	OCT
0.6	0.8	2.6	40	71	24.5	1.2	0.6

Most occurrences are in the months of June to August, with a peak in July; very fewoccur from March to May or in September or October. No NLC are observed from November to February during the fall and winter when the sun's elevation is too low to allow the clouds to be illuminated in the pre-sunrise and post-sunset twilight periods.

We would appreciate receiving information on the progress of the arrangements to implement the SAM-II project.

Yours sincerely

B.W.Boville, Director
Atmospheric Processes Research Branch

Table C2

EXAMPLE OF LISTING OF NLC SIGHTING DATA PROVIDED BY ENVIRONMENT CANADA

[illegible] INFORMATION ON THE NLC SIGHTINGS REPORTED FROM ALASKA,
CANADA, GREENLAND AND ICELAND

DATE	STATION	CODE	LAT.	LONG.	GMT	LST	SOA	I	FORM	AZ.	[illegible]	
730727	FORT CHIPEWYAN	YPY	58.8	111.1	9.3	1.8	9.0	4	25	350-100	15 50	A
730727	FORT CHIPEWYAN	YPY	58.8	111.1	9.5	2.0	9.0	3	12	360 [illegible]	20 50	A
730727	FORT CHIPEWYAN	YPY	58.8	111.1	9.8	2.3	7.0	2	12	360 [illegible]	[illegible] 60	A
730727	FORT RELIANCE	YFL	62.7	109.2	7.5	0.1	8.0	4	23	300 050	35 90	[illegible]
730727	FORT RELIANCE	YFL	62.7	109.2	7.8	0.4	8.0	3	23	290 [illegible]	40 70	B
730727	FORT RELIANCE	YFL	62.7	109.2	8.1	0.7	7.5	3	23	300 075	[illegible]	[illegible]
730727	FORT RELIANCE	YFL	62.7	109.2	8.3	0.9	7.0	3	34	310-[illegible]	[illegible]	B
730727	FORT RELIANCE	YFL	62.7	109.2	8.5	1.1	7.0	1	13	225 [illegible]	20 45	B
730727	FORT RELIANCE	YFL	62.7	109.2	8.8	1.4	6.0	2	12	270 030	20 40	B
730727	FORT RELIANCE	YFL	62.7	109.2	9.0	1.6	5.5	2	12	275 090	[illegible]	B
730728	FORT SMITH	YSM	60.0	11[illegible].0	7.0	23.4	10.5	3	13	330 040	10 45	B
730728	FORT SMITH	YSM	60.0	11[illegible].0	8.0	0.4	10.5	3	13	330 040	10-45	A
730728	FORT SMITH	YSM	60.0	11[illegible].0	9.0	1.4	9.0	3	12	330-040	15 60	A
730729	WATSON LAKE	YQH	60.1	128.8	8.0	23.3	10.5	2	2	-348	11-	C
730729	WATSON LAKE	YQH	60.1	128.8	8.3	23.6	11.0	2	12	309-	-12	B
730729	WATSON LAKE	YQH	60.1	128.8	8.5	23.8	11.0	2	12	-360	10-	B
730729	WATSON LAKE	YQH	60.1	128.8	8.8	0.1	11.0	1	12	334-357	11	B
730729	WATSON LAKE	YQH	60.1	128.8	9.0	0.3	11.0	1	12	335-357	-12	B
730729	WHITEHORSE	YXY	60.7	135.1	8.0	22.9	9.0	2	1	360-015	20 40	C
730729	ENNADAI LAKE	YEI	61.1	10[illegible].9	6.5	23.7	10.0	3	4	330-010	15 30	B
730727	ENNADAI LAKE	YEI	61.1	10[illegible].9	6.8	24.0	10.0	4	24	335-010	15-30	B
730729	FORT RELIANCE	YFL	62.7	109.2	6.0	22.6	6.5	2	12	340-070	10 50	B
730729	FORT RELIANCE	YFL	62.7	109.2	6.3	22.9	7.5	3	12	360-060	10-40	B
730729	FORT RELIANCE	YFL	62.7	109.2	6.5	23.1	7.5	3	12	010 060	15-[illegible]	B
730729	FORT RELIANCE	YFL	62.7	109.2	6.8	23.4	8.0	3	12	350-070	10 [illegible]	[illegible]
730729	FORT RELIANCE	YFL	62.7	109.2	7.0	23.6	8.0	3	2	350-060	10-65	B
730729	FORT RELIANCE	YFL	62.7	109.2	7.3	23.9	8.5	2	2	340-050	15-60	B
730729	FORT RELIANCE	YFL	62.7	109.2	7.5	0.1	8.5	2	23	360 080	10 70	B
730729	FORT RELIANCE	YFL	62.7	109.2	7.8	0.4	8.0	3	23	010-080	10-75	B
730729	FORT RELIANCE	YFL	62.7	109.2	8.0	0.6	8.0	3	3	350-070	20-75	B
730729	FORT RELIANCE	YFL	62.7	109.2	8.3	0.9	7.5	3	3	350-070	10-[illegible]	B
730729	FORT RELIANCE	YFL	62.7	109.2	8.5	1.1	7.5	2	2	340-070	10-90	B
730729	FORT RELIANCE	YFL	62.7	109.2	8.8	1.4	6.5	1	2	320-085	40-90	B
730730	FORT RELIANCE	YFL	62.7	109.2	6.3	22.9	7.5	1	1	290-040	40-65	B
730730	FORT RELIANCE	YFL	62.7	109.2	6.5	23.1	8.0	1	1	310-070	50-60	B
730730	BAKER LAKE	YBK	64.3	96.0	6.0	23.5	7.0	2	2	300-070	40-90	A
730730	BAKER LAKE	YBK	64.3	96.0	7.0	0.5	7.0	2	2	270-030	50 90	A
730802	GRANDE PRAIRIE	YQU	55.2	11[illegible].9	10.0	2.0	12.5	1	2	340-042	25-40	A
730802	GRANDE PRAIRIE	YQU	55.2	11[illegible].9	10.3	2.3	11.5	1	2	340-042	25-40	A
730803	YELLOWKNIFE	YZF	62.5	114.5	7.0	23.3	9.5	2	2	330-015	10-25	A
730803	YELLOWKNIFE	YZF	62.5	114.5	7.5	23.8	9.5	2	2	330 015	05-25	A
730803	YELLOWKNIFE	YZF	62.5	114.5	8.0	0.3	9.5	2	2	330-015	10-25	A
730803	YELLOWKNIFE	YZF	62.5	114.5	8.5	0.8	9.5	2	12	330-030	10-30	A
730803	YELLOWKNIFE	YZF	62.5	114.5	9.0	1.3	8.5	2	123	330-060	10 55	A
730803	FORT RELIANCE	YFL	62.7	109.2	6.0	22.6	8.0	2	1	300 030	10 20	B
730803	FORT RELIANCE	YFL	62.7	109.2	6.3	22.9	8.5	2	1	290-030	05 20	B
730803	FORT RELIANCE	YFL	62.7	109.2	6.5	23.1	9.0	2	1	270 030	05-25	B
730803	FORT RELIANCE	YFL	62.7	109.2	6.8	23.4	9.5	2	1	270-015	05-15	B
730803	FORT RELIANCE	YFL	62.7	109.2	7.0	23.6	9.5	2	1	290-015	05-15	B
730803	FORT RELIANCE	YFL	62.7	109.2	7.3	23.9	9.5	2	1	290 320	10-15	B
730803	FORT RELIANCE	YFL	62.7	109.2	7.5	0.1	9.5	1	1	300-320	15-20	B
730803	NORMAN WELLS	YVQ	65.3	126.8	8.8	0.2	7.0	2	23	270-120	30-90	A
730803	NORMAN WELLS	YVQ	65.3	126.8	9.0	0.4	7.0	2	23	320-130	30-90	A
730803	NORMAN WELLS	YVQ	65.3	126.8	9.3	0.7	6.5	2	23	270-100	20-90	A
730803	NORMAN WELLS	YVQ	65.3	126.8	9.5	0.9	6.5	2	12	200-080	80-90	A
730803	NORMAN WELLS	YVQ	65.3	126.8	9.8	1.2	6.0	3	12	200-070	80-90	A
730803	NORMAN WELLS	YVQ	65.3	126.8	10.0	1.4	5.5	3	1	140-110	-90	A

(See next page for key to column headings.)

Table C2.
(continued)

KEY TO COLUMN HEADINGS

DATE	- Year, month, night
STATION	- Station
CODE	- Station Identifier
LAT.	- Latitude
LONG.	- Longitude
GMT	- Greenwich Mean Time
LST	- Local Solar Time (or Local Apparent Time)
SDA	- Solar depression angle at time or sighting
I	- NLC intensity on 5-point scale, from very weak to extremely bright
FORM	- Structural forms: 1 veils; 2-bands; 3-billows; 4-whirls; 5-amorphous
AZ	- Azimuthal extend of NLC, relative to geographic North
EL	- Extent of NLC in elevation, relative to the horizon
CL	- Tropospheric cloud cover in twilight section of sky· A-clear; B-scattered; C-broken; D-overcast

HEAD OF DEPARTMENT
D H McINTOSH, B Sc, M A, D Sc, F R S E
TEL 031-667 1081 Ext 2920

Universitу of Edinburgh

DEPARTMENT OF METEOROLOGY
THE UNIVERSITY
JAMES CLERK MAXWELL BUILDIN(
KING'S BUILDINGS
EDINBURGH EH9 3JZ

7th October 1977

Dr. P.B. Russell,
Science Coordinator for Ground Truth,
SAM-II Nimbus Experiment Team,
Stanford Research Institute,
Menlo Park,
California 94024,
U.S.A.

Dear Dr. Russell,

Thank you for your letter of 3rd October expressing interest in data relating to noctilucent clouds.

We shall of course be pleased to cooperate with you in any way we can be sending you our data. Observations made here or reported to us are in large measure confined to June and July; only exceptionally are the clouds seen by 'our' observers in August (or May). It seems likely then that our first reports of interest to you will be for 1979.

The latitude belt you refer to (64° - 80°) is a good deal poleward of our most northerly observers. We shall make enquiries as to how far poleward we may be able to extend our network, perhaps obtaining the cooperation of other observers in Scandinavia or Iceland.

Yours sincerely,

D. H. McIntosh

D.H. McIntosh.

Appendix D

GROUND TRUTH PLANS FOR SAGE

Appendix D

APPROACH FOR ESTIMATING ERRORS IN DENSITY PROFILES

We describe here briefly the rationale for estimating errors in the temperature profiles to be required by SAGE and enumerate these errors for specials sets of conditions Constant-pressure synoptic maps will serve as the basis for the profiles The maps themselves are subject to several types of errors, viz, instrument errors, first-guess errors, and analysis-system errors It is known, in a general way, how these errors vary with geographical location, instrument type, altitude, and density of data It is also known approximately what errors are induced by interpolating between map times (errors due to moving weather systems between observations)

The numerical values given here as error estimates result from long experience on the part of the Upper Air Branch staff in dealing with problems of instrument accuracy and data compatibility A complete rationale for these estimates is much too complicated for inclusion in a brief document, but this may be found in the papers cited among the references to this appendix

The Upper Air Branch (UAB) of the National Meteorological Center (NMC) will provide atmospheric temperature profiles and associated error estimates for any point on the globe in support of SAGE operations All mandatory levels between 500 and 1 mb (~ 5 to ~ 48 km) are to be included in the profiles

The principal systems of upper air observations for direct use in this support are rawinsonde and satellite (Rocketsonde data comprise an essential contribution to the derivation of satellite profiles, however, besides providing "ground truth" for high-level radiosonde observations) Since spatial and temporal separations between the data points are large for all these systems, it is necessary to use methods of interpolation, in both space and time, to derive the required temperature profiles The synoptic meteorological charts indicating temperature, wind and geopotential heights for constant-pressure surface areas serve as the basis for this interpolation

The procedure for supplying temperature profiles may be outlined as follows

(1) The SAGE team notifies UAB of its need for a temperature profile and temporal-geographical coordinates (τ, ϕ, λ), where τ = time, ϕ = latitude, and λ = longitude

(2) The UAB consults all constant-pressure charts from 500 mb to 1 mb valid for the map time τ_1 prior to the given time τ, as well as the map times τ_2 subsequent to τ The charts provide the best estimates of temperatures for times τ_1 and τ_2, i e , for (τ_1, ϕ, and λ) and (τ_2, ϕ, and λ) Linear interpolation in time is then used to obtain the profiles for (τ, ϕ, and λ) Admittedly, there are errors associated with this profile, such errors are functions of time and pressure level

(3) The UAB attaches "error bars" to the temperature profiles in accordance with the procedure outlined in the following paragraphs

When error estimates are made, the atmosphere between 500 mb and 1 mb is stratified in the vertical according to circulation regimes and measurement techniques The upper troposphere, because of its dynamic features and the fact that it is monitored quite well by rawinsondes, is taken here as a distinctive layer (500-100 mb) The lower stratosphere (50-10 mb) is the next highest layer, taken as distinct from the layer below because of its thermodynamic structure (Staff, Upper Air Branch, 1967, 1969) The upper stratosphere (5-1 mb) is the third layer, regaded as distinctive primarily because of the different techniques used for its measurement (Staff, Upper Air Branch, 1975)

Figure D-1 is a flow diagram that shows how errors in a given tropospheric temperature profile may be deduced for the Northern Hemisphere The first consideration is whether the number of rawinsonde or satellite data points within a distance a (radius of the scan circle A) exceeds a critical value x that depends on a If the answer is "yes," A is considered to be a data-rich area and, as the figure shows, the combination of radiosonde/satellite data determines the error characteristics—since any analysis system presently used would provide an analysis faithful to the mean values within a data-rich area Similarly, if the answer is "no," A is considered to be a data-poor region, and any errors would depend more on the analysis system used (including first-guess fields) than on current data

The standard error of the temperature estimate at any point in space-time will thus depend on instrument accuracy and quality of analysis, as well as the time-interval t which separates the instant for which the profile is required from the time of the map on which the estimate is based The standard error ϵ_o at time t = 0 is known from various studies of instrument performance and data compatibility (McInturff and Finger, 1968, Finger et al , 1973, McInturff, 1978) The empirical formula

$$\epsilon = \epsilon_o \left(1 + \alpha \left| \sin \frac{\pi t}{24} \right| \right) ,$$

where α = constant for a specified latitude, geographical area, and season, relates the sandard error at zero time to the standard error at an earlier or later time (the time-interval t is measured in hours) (Bengtsson, 1969) The choice of $\alpha = 1$ for the layer 500-100 mb is based on the observation that the error approximately doubles in 12 hours under the average conditions of variability that characterize the troposphere

Figure D-2 is a flow diagram that shows how errors in Northern Hemisphere profiles between 70 mb and 10 mb may be deduced The situation for the Northern Hemisphere is simpler in this case, because VTPR data are not presently being used in the analysis (although satellite data, which will form the basis for such Southern Hemisphere analyses, may be used for these levels in the Northern Hemisphere as well) The standard errors vary seasonally more than in the troposphere, because the contrast between summer and winter is greater in the stratosphere As can be seen from the formulas, time interpolation should not pose much of a problem for the stratosphere in summer The wintertime stratosphere, however, is as variable as the wintertime troposphere, and this fact is reflected in assigning $\alpha = 1$ for winter

Even though there are in situ data available for the layer from 5 to 1 mb (primarily rocketsonde data), they cannot be depended upon for present purposes as they are very sparse both

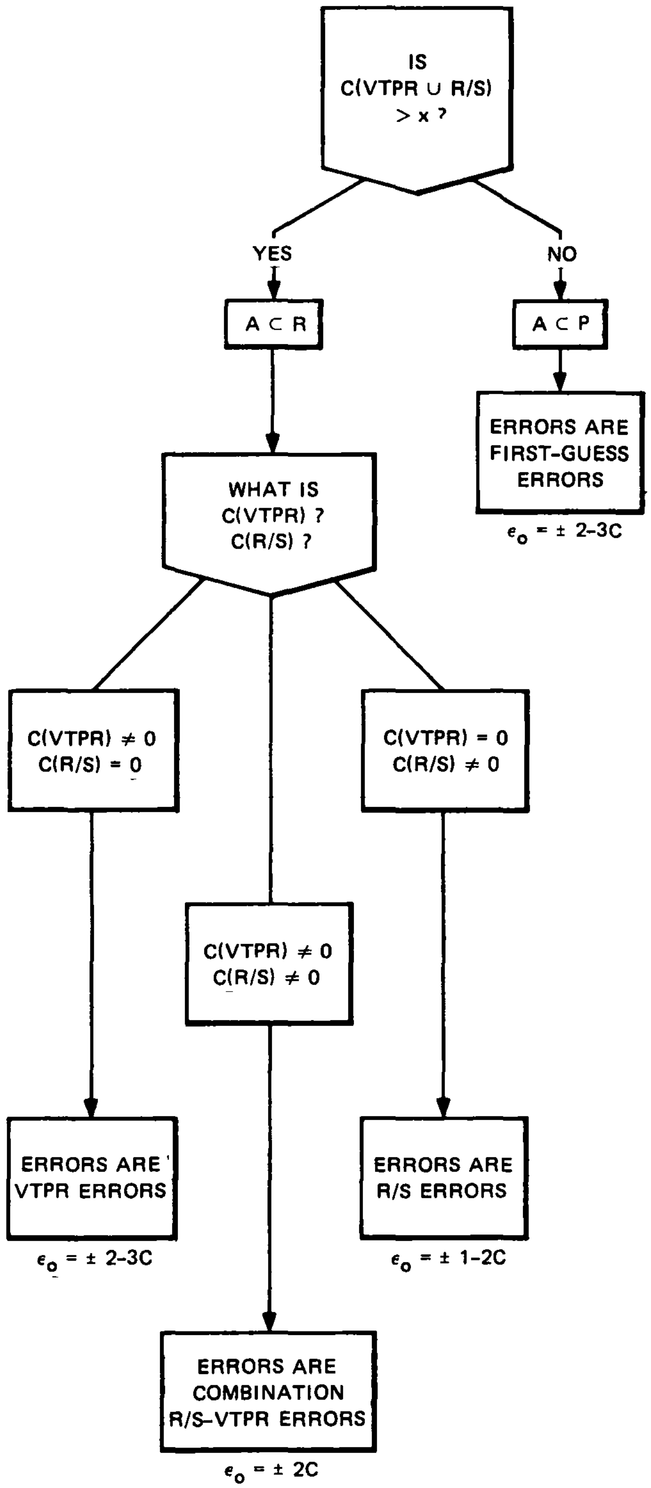

$$\epsilon = \epsilon_o \left(1 + \left|\sin \frac{\pi t}{24}\right|\right)$$

KEY

ϵ = STANDARD ERROR AT TIME t

ϵ_o = STANDARD ERROR AT t = 0

t = DIFFERENCE BETWEEN TIME OF SATELLITE SOUNDING AND MAP TIME (in hours)

R/S RADIOSONDE

C(VTPR) COUNT OF VTPR REPORTS WITHIN SCAN REGION A

C(R/S) COUNT OF RADIOSONDE POINTS WITHIN SCAN AREA A

(VTPR ∪ R/S) COLLECTION OF VTPR AND R/S POINTS

C(VTPR ∪ R/S) COUNT OF VTPR AND R/S POINTS WITHIN REGION A

A CIRCULAR SCAN REGION OF REGION a

P DATA-POOR REGION

R DATA-RICH REGION

x INTEGER DEPENDENT ON a

A ⊂ R "REGION A IS INDLUDED IN REGION R"

A ⊂ P "REGION A IS INCLUDED IN REGION P"

FIGURE D-1 FLOW DIAGRAM OF ERROR-CALCULATION PROCEDURE FOR THE NORTHERN HEMISPHERE, 500- to 100-mb HEIGHTS

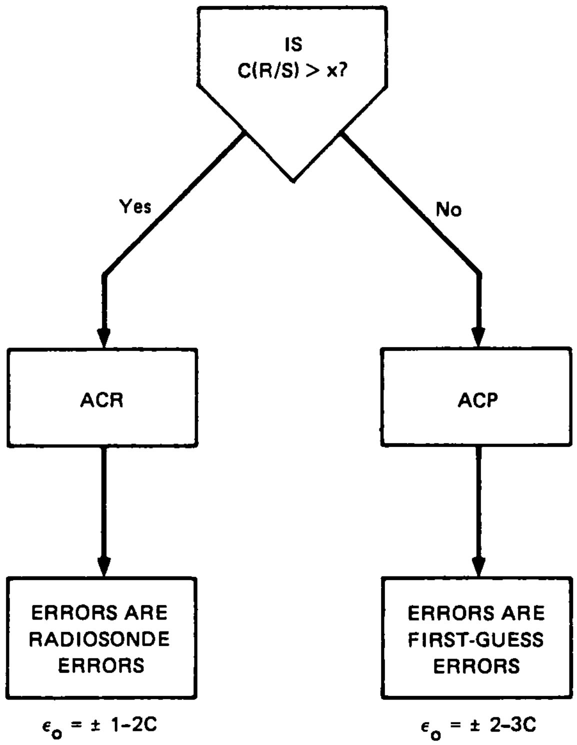

$\epsilon = \epsilon_o(1 + \alpha|\sin \pi t/24|)$

α = 0 4 in summer (May–September)

α = 0 5 in April and October

α = 0 5 in winter (November–March) south of 30° N

α = 1 0 in winter (November–March) north of 30° N

FIGURE D-2 FLOW DIAGRAM OF ERROR-CALCULATION PROCEDURE FOR THE NORTHERN HEMISPHERE, 70- to 10-mb HEIGHTS in space and time Thus, satellite data derived with a currently used system will form the basis for producing temperature profiles Estimates of these errors are as follows

At 5 mb, $\epsilon \sim \pm 6C$
At 2 mb, $\epsilon \sim \pm 8C$
At 1 mb, $\epsilon \sim \pm 9C$

No time dependence is indicated—not because it does not exist, but rather because it is not known (It is believed that the error due to off-time data may commonly be as great with t = 1 hour as with t = 10 hours, cf Miller and Schmidlin, 1971)

As is well known, TIROS N is expected to supersede VTPR in the near future as the NOAA operational satellite For this reason we have included Figure D-3, which shows temperature standard errors in TIROS N simulations, both with and without noise It will be necessary to study the actual TIROS N data before Figures D-1 and D-2 or the estimates of temperature errors given above can be modified to take the TIROS N contribution into account

Most regions of the Southern Hemisphere (S H) may be considered data-poor, except for the availability of satellite data The dearth of either S H rawinsonde or rocketsonde data makes calibration of satellite data difficult Consequently, error estimates for the S H are questionable The following summarizes the best current error estimates for S H profiles

Time dependence

$$\epsilon = \epsilon_o \left(1 + \alpha \left| \sin \frac{\pi t}{24} \right| \right)$$

where ϵ_o = error estimate for t = o
t = interval separating map time from time for which profile is required (in hours)
α = constant for a given altitude and geographic area

Values of ϵ_o

ϵ_o = $\pm$2-3°C for 500-10 mb
ϵ_o = $\pm$6°C at 5 mb
$\pm$8°C at 2 mb
$\pm$9°C at 1 mb

Values of α

For 500-100 mb
α = 1 0

For 70-10 mb
α = 0 4 in summer (November-March)
α = 0 5 in April and October
α = 0 5 in winter (May-September), equatorward of 30°S
α = 1 0 in winter, poleward of 30°S

For 5-1 mb
α = 0 (time dependence unknown)

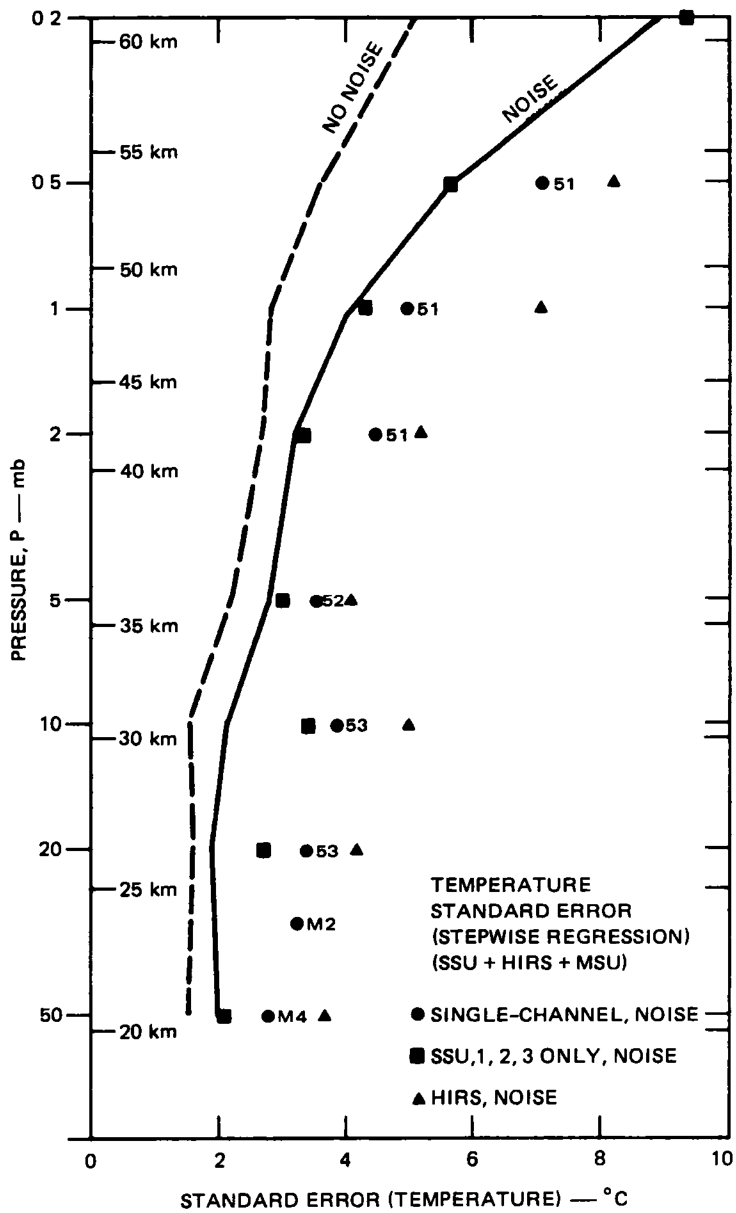

FIGURE D-3 TEMPERATURE STANDARD ERRORS IN TIROS-N SIMULATIONS

REFERENCES — APPENDIX D

Bengtsson, L , 1969 Numerical prediction of upper winds and temperatures, and presentation of the numerical forecasts for aeronautical purposes *Aeronautical Meteorology*, Technical Note No 95, World Meteorological Organization, Geneva, Switzerland, pp. 197-210.

Finger, F. G , K W Johnson, M E Gelman, and R M McInturff, 1973 Compatibility of radiosionde and Nimbus 4 SIR-derived data at stratospheric constant-pressure surfaces *Monthly Weather Review*, **101**, 244-251

McInturff, R M , 1978 A comparison of temperatures and winds reported by the Concorde SST with data obtained from rawinsonde and satellite Fourth Symposium of Meteorological Observations and Instrumentation, April 10-14, 1978, Denver, Colorado

McInturff, R M and F G Finger, 1968 *The Compatibility of Radiosonde Data at Stratospheric Levels Over The Northern Hemisphere* ESSA Tech Memo WBTM-DATAC 2, U.S Weather Bureau

Miller, A J and F J Schmidlin, 1971 Rocketsonde repeatability and stratospheric variability *Journal of Applied Meteorology*, **10**, 320-327

Staff, Upper Air Branch, 1967, 1969 *Monthly Mean 100-, 50-, 30-, and 10-Millibar Charts for 1964, 1965, 1966, 1967* ESSA Tech Reps WB-1 and WB-11, National Weather Service

Staff, Upper Air Branch, 1975 *Weekly Synoptic Analyses, 5-, 2-, and 0 4-Mb Surfaces for January 1972 through June 1973* NASA SP-3091

End of Document